Water quality of the Loopspruit, North-West Province: A geospatial, physico-chemical and microbiological analysis

L Bredenhann

orcid.org 0000-0003-2700-3167

Dissertation accepted in fulfilment of the requirements for the degree *Master of Science in Microbiology* at the North-West University

Supervisor:	Prof CC Bezuidenhout
Co-supervisor:	Dr D La Grange
Assistant-supervisor:	Dr L Molale-Tom

Graduation December 2020

25083945

ABSTRACT

In the North West Province, surface water is polluted from sources such as surface runoff from agricultural settings, storm-water runoff as well as sewage from urban locations, and mining. This study aimed to evaluate the water quality of the Loopspruit River by analysing the physico-chemical and microbiological aspects of the Loopspruit River. Six objectives were set to achieve this. The first objective focussed to identify sampling sites using Geographic Information Systems (GIS) and aerial photographs to ensure. The second and third objectives set out to determine the water quality of two wet seasons and two dry seasons (2018 to 2019) and to analyse the historic data. The fourth was the isolation and identification of possible faecal associated micro-organisms, including *Clostridium*, presumptive *E. coli* and *Enterococci* species. Objectives five and six were to create predictive physico-chemical and microbiological point source contamination visual representation with historic data and data obtained from this study and to compare the outcomes. These isolated bacterial species (objective 4) were used to create a faecal point source pollution visual representation with their associated land-use contributions that were deposited within the Loopspruit River. Historic data were used to develop a predictive geospatial visual representation of the physico-chemical parameters to illustrate the land-use contributions to possible pollution in the Loopspruit River. The historic and current water quality data were visually represented using GIS software for water quantity. The results visually indicated that high magnesium (±41.30 mg/L) levels are prominent in mining and urban areas and pH levels (±9.49) are high in the dam area - all above normal levels. Antibiotic profiles indicated an increase in Multiple Antibiotic Resistances (MAR) with increased urban activities. Genes associated with antibiotic resistance were also detected. These included the *intI1* integrase gene and the *FOX* AmpC β-lactamase gene. The LC/MS analyses revealed an excess amount of Ampicillin in the Loopspruit River with a risk value of 637.95 where the predicted no-effect concentration is 75. The bacterial diversity showed the highest diversity at less polluted areas whereas, in contrast, more pollution-prone areas showed less bacterial diversity. Dominating at all the sites were *Proteobacteria*, followed by *Bacteroidetes*, *Cyanobacteria, Actinobacteria* and *Verrucomicrobia,* having a broad variation to the total contribution from sample to sample. Finally, the predicted metagenome analysis revealed a correlation between the physico-chemical parameters and the observed taxonomic units (OTU). The temperature had negative correlations with *Patescibacteria, Nanoarchaeaeota* and *Firmicutes* ($p<0.05$). The negative correlation was strongest with *Patescibacteria*. SO_4 showed the best correlation with *Fusobacteria* ($p<0.05$). The metabolic activity of the species diversity showed that 24.6% of the total OTUs used the ammonia oxidizer metabolic pathway, followed by dehalogenation with 20.2%. The sulphate-reducing bacteria, sulphide oxidizers, nitrite reducers and nitrogen fixation were also abundant in the

predicted metabolic pathways that were used. Analysing and visually representing the water quality of the Loopspruit River demonstrated the value of combining geospatial and microbiological components for a holistic understanding of environmental health risks and management strategies.

Keywords: Antibiotics, Bacterial diversity, Faecal indicator organisms, GIS, LC/MS, Visual representation, Water Quality

ACKNOWLEDGEMENTS

All glory and praise go to the Heavenly Father YHWH (יהוה) my Elohim, for giving me the opportunity, talents and blessings to pursue my Master's degree and everything it encompasses. May this dissertation only glorify and magnify your Holy Name, YHWH (יהוה).

To my Father Hennie, the wise one. Just being grateful is an understatement. Thank you for all the love, advice and financial support. Thank you for giving different perspectives when I am challenged with an obstacle, whether it was mentally or physically. Thank you for being there even though I did not know I needed it. You are the best father any son could ask for!

To my Mother Riana, the strong one, words cannot express how privileged I am to be your son. You supported me when I needed emotional comfort and always helped me consider things outside of my narrow focus. Thank you for being an excellent example of being a kind and gentle person. I would not be the person I am today if it was not for you.

Prof. Carlos Bezuidenhout, my supervisor, thank you for all the guidance and support in steering and panel beating this dissertation. You did not only supervise but also taught me how to be a better researcher and will carry these insights with me always. You did more for me as a researcher than you know. Thank you.

Dr Danie la Grange, even though you are on the other side of the planet, you always had time to give me advice and help me write this dissertation. Your critique and suggestions made me a better writer, and I have you to thank.

Dr Jaco Bezuidenhout and Dr Charlotte Mienie, thank you for your open-door policy and making time to see any student in need of your guidance. Thank you for allowing me to sit and listen to your morning coffee discussions. It made my day all the better.

Thank you, Dr Lesego Molale-Tom, for all the guidance you gave me through the final stages of this dissertation. Thank you for the financial support you provided during this dissertation. I am honoured to have had you as one of my supervisors and all that I have learned from you.

Funding acknowledgement for this project goes to the National Research Foundation (NRF) through a grant holder bursary (TTK170518231376) from Dr Molale-Tom, and grant UID 113824. The opinions expressed in this dissertation, and conclusions arrived at are those of the author and are not necessarily to be attributed to the funders.

Chané de Bruyn, thank you for being you. You kept my year interesting with all the late-night talks on politics, religion and conspiracy theories, tolerating my spicy foods (and not saying it was too hot with tears in your eyes). I could not have asked for a better friend. Your friendship reinforces my belief that true friendship will last forever. You are #SlickApproved.

To my friends Ilzé, Gerhard, Rohan and Schalk, thank you for all the coffee trip we made, laughter turned to tears and talking about the latest movies, series and games. Thank you for all the abrupt coffee breaks. Thank you for all the memories made, they are the best.

Leani, my on-again-off-again mentor. Thank you for all the comments, critique and support you showed me during my studies. You are a true inspiration as someone to look up to as a researcher.

To my far long friend Franciska Heystek. Thank you for all the unexpected and random phone calls that last over two hours. Thank you for also reassuring me that there are job opportunities for me after this dissertation is finished.

Maricélle Botes, my oldest friend. Thank you for all the last-minute scheduling, and proofreading advice you gave me during the last stretch of the dissertation. Thank you for always thinking of me and sending me messages of wisdom and encouragement. These always made my day a lot better. Your friendship means the world to me, and I will forever cherish that. Thank you.

TABLE OF CONTENTS

LIST OF TABLES

LIST OF FIGURES

LIST OF EQUATIONS

LIST OF ABBREVIATIONS

MISCELLANEOUS	
°C	Degrees Celsius
µg	Microgram
µm	Micrometre
A	
ABE	Acetone-butanol-ethanol
AMD	Acid mine drainage
ARG	Antibiotic-resistant genes
B	
BOD	Biochemical oxygen demand
BRICS	Brazil, Russia, India, China and South Africa
C	
Ca	Calcium
$Ca_5(PO_4)_3(OH, F, Cl)$	Apatite
$CaMg(CO_3)_2$	Dolomites
CFU	Colony-forming units
CO_2	Carbon dioxide
COD	Chemical Oxygen Demand
D	
DEM	Digital Elevation Model
DO	Dissolved Oxygen
DWAF	The Department of Water Affairs and Forestry
E	
EC	Electrical Conductivity
eDNA	Environmental DNA
EHEC	Enterohemorrhagic E. coli
ESRI	Environmental Systems Research Institute
EUCAST	European Committee on Antimicrobial Susceptibility Testing
F	
FDT	Fung double tube
FeS_2	Pyrite
FIO	Faecal indicator organisms
G	
GIS	Geographic Information Systems
H	
H_2O	Water
H_2O_2	Hydrogen peroxide
H_2S	Hydrogen sulphide
H_2SO_4	Sulphuric acid
HGT	Horizontal Gene Transfer
HPC	Heterotrophic Plate Count
I	
IDW	Inverse Distance Weight
IS	Internal standards
K	
K	Potassium
km^2	Square kilometres
L	
L	Litre
LC	Liquid chromatography

LOD	Limit of detection
LOQ	Limit of quantification
M	
m/z	mass-to-charge ratio
m^3	Cubic meters
MAE	Mean absolute error
MAP	Mean annual precipitation
MAR	Multiple Antibiotic Resistance
MEC	Measured environmental cencentration
Mg	Magnesium
mg/L	Milligrams per litre
min	Minutes
mL	Millilitre
mm	Millimetre
mM	micromolar
mm/a	Millimetre per annum
MS	Mass spectrometry
mS/m	Milli-siemens per meter
N	
N	Nitrogen
N_2	Atmospheric nitrogen
Na	Sodium
NaCl	Sodium chloride
ng	Nanogram
NGS	Next Generation Sequencing
NH_2CONH_2	Urea
NH_3	Ammonia
NH_4	Ammonium
NO_2	Nitrite
NO_3	Nitrate
O	
O_2	Oxygen
OS	Organic sulphur
OTU	Operational taxonomic units
P	
P	Phosphorus
PCR	Polymerase Chain Reaction
pmol	Picomole
PNEC	Predicted no effect concentration
PO_4	Orthophosphate
P-values	Parametric values
Q	
Q-TOF/MS	Quadrupole time of flight mass spectrometer
R	
rDNA	Ribosomal deoxyribonucleic acid
RNA	Ribonucleic acid
rpm	Revolutions per minute
RQ	Risk selecton index
rRNA	Ribosomal ribonucleic acid
RWQO	Resource Water Quality Objectives
S	
S_2^-	Sulphide
SO_3	Sulphide
SO_4	Sulphates

SRC	Sulphite-reducing *Clostridium*
T	
TDS	Total dissolved solids
TNTC	Too numerous to count
TP	Total phosphorus
TSC	Tryptose sulphite cycloserine
TSI	Triple Sugar Iron
TTC	Triphenyltetrazolium chloride
U	
UHPLC	Ultra-high-pressure liquid chromatography
US-EPA	United States Environmental Protection Agency
V	
V	Volts
W	
W	Watt
WASP	Water Quality Analysis Simulation Program
WHO	World Health Organisation
WWTP	Wastewater Treatment Plant

CHAPTER 1: GENERAL INTRODUCTION

1.1 Introduction

Natural resources such as fertile soils, water, and oxygen are privileges we receive from earth (Liu, 2019). Mismanagement of these natural resources has led to severe problems without immediate solutions. One primary natural resource of all life on earth is dependent on water. Water is of paramount importance to ensure the continuation of the livelihoods of all species. The number of countries that face economic and social development challenges as a result of water-related issues are progressively increasing (Adler *et al.*, 2007; Holmatov *et al.*, 2017; Kisakye & Van der Bruggen, 2018). The impacts of floods, water shortages, and water quality deterioration are only some of the problems that require extensive attention and action. Water is essential for life and should be managed properly.

South Africa is a water-scarce country and is classified as one of the mining capitals of the world. Although mines contribute to the economy of South Africa, they also require water and have a substantial impact on the environment. This makes sustainable water resource management in South Africa essential for the development and prosperity of the country. An article by von Bormann and Gulati (2016) stated that mining activities have a considerable impact on water quality, even to the extent to where it is unfit for other uses. According to Ashton (2002) the availability of water can have a significant effect on disease, hunger and poverty in specific areas.

Water quality is defined as the physical, chemical, biological and aesthetic properties of water over a spectrum of uses (Bui *et al.*, 2019; DWAF, 1996c; Li *et al.*, 2016). This includes the protection of water as a sustainable water resource. Some properties commonly found in water include either suspended or dissolved physical, chemical or biological compounds (DWAF, 1996b). Some examples are nutrients such as calcium and sodium, temperature and bacterial indicators of faecal pollution.

In the environment, water polluted with faecal matter appears to be the most significant vector for contamination (Hamiwe *et al.*, 2019). Surface runoff carries faecal matter from agriculture (treated crops and animals) to larger reservoirs like dams and river systems. Faecal indicator bacteria (FIB) reside in the gastrointestinal tracts of humans and animals. Various indicator organism levels are used to distinguish between faecal pollution of humans and animal origin during the wet and dry seasons (Sankararamakrishnan & Guo, 2005). Ghaju Shrestha *et al.* (2017) emphasized that testing water for the presence of indicators and health-threatening contaminants may be an indication of the presence of pathogens and that negative testing for the presence of indicators does not necessarily imply the absence of pathogens.

Faecal bacteria can survive in the environment for weeks or months, depending upon the microbial species and the environmental temperature. Intestinal bacteria like *E. coli* and *Enterococci* are quickly disseminated in different ecosystems through water, thus these bacteria are intensively used as indicator species for faecal pollution. *E. coli* is best suited for identifying faecal pollution in drinking water. *Enterococc*i have a vast range of environmental resistances, such as antibiotic resistance and posing threats to human and animal (Molale & Bezuidenhout, 2016). Both *E. coli* and *Enterococci* account for aerobes but there are also some anaerobes such as *Clostridium perfringens*. *Clostridium* spp. are the most dominant of all the anaerobes in the gastrointestinal tract of humans and warm-blooded mammals. *C. perfringens* can serve as a long term faecal indicator because of the organism's ability to produce spores (Fourie, 2017). These spores are extremely resistant to harsh environmental conditions such as pH and temperature extremes and UV radiation, and most importantly, disinfection treatment processes

Pathogenic bacteria are dangerous to people, animals and even plant life, and the risk of these bacterial infections is increasing the spectrum of infectious diseases (Radhouani *et al.*, 2014). A surveillance report from the World Health Organization (WHO, 2014) showed that there is strong resistance worldwide in *Escherichia coli*, *Staphylococcus aureus* and enteric bacteria, including *Klebsiella pneumoniae* and *Shigella spp*. It is already widely known that the overuse of antibiotics in both human and veterinary medicine, as well as in agriculture, contributes to the spread of antimicrobial resistance. According to Allen *et al.* (2010), antibiotics given to animals orally fail to fully metabolise in the digestive tract, with the result that they are excreted into the environment. This may be a contributing factor to antibacterial resistance in the environment (Kora *et al.*, 2017). The dung/manure of farm animals is often used by farmers to fertilise the soil for better crop production. This practice contributes to the spread of antibiotic resistance in vegetation (Wright, 2010).

Monitoring the prevalence of faecal indicator bacteria such as *E. coli* and *Enterococci and Clostridium* sp. in different environments will provide data on faecal contamination in the environment and on the prevalence of antibiotic resistance. This would aid in the detection of transfer methods of resistant bacteria or resistant genes from animals to human beings and vice-versa (Dolejska & Papagiannitsis, 2018; Martel *et al.*, 2001).

The portrayal and visual presentation of the effects of such pollution in a specific study area can be performed with geospatial software such as Geographic Information Systems (GIS). GIS enables the user to observe locations of interest by using geospatial data to create maps. This can be executed through even more specific data manipulation, to show for example the spread of microbial resistance in certain areas.

Few interdisciplinary studies have been done in the field of aquatic ecosystems using geospatial analysis to explain microbiological events. Kim *et al.* (2011) used GIS to predict and map the microbial diversity of a forest area between Yongcheon and Seorak in South Korea. The current study intends to accurately depict the study area and to represent historical data and visualise possible future contamination patterns relating to the study area. The use of GIS in biological fields such as ecology, microbiology, zoology and botany, gains the added element of space-time, making it the ideal tool for monitoring (Stoner *et al.*, 2001). The establishment of the extent of microbiological diversity through the agency of GIS is a technique yet in its infancy. Researchers can, by using this tool, account for historical and future changes in certain areas and monitor the changes that arise in ecological regions, whether they are natural or artificial.

1.2 Problem statement

Water scarcity and water quality are both research themes that need constant attention. Water quality is a very broad and dynamic subject. Some of the aspects of water quality are the physico-chemical parameters of the water body, the use of the bacterial community to evaluate the health of the water body and the antibiotic resistance of the bacterial consortia in the environment. The physico-chemical and microbiological parameters need to be monitored to ensure that any elevated levels do not cause harm to humans, animals and the environment. The use of antibiotics in agriculture on South African farms contributes to resistant organisms and genes remaining in circulation. Middle-income countries such as South Africa are very susceptible to the spreading of antibiotic-resistant bacteria because of the lack of adequate sanitation and clean water in rural areas. Another predicament to consider is the extent to which water quality is affected by agricultural activities, specifically cattle and chicken farms, with surface runoff that carries faecal material into river systems. Moreover, there are feedlots on farms which contain chemical constituents that can contribute to microbial and or faecal contamination. With this in mind, physico-chemical and microbiological data are usually presented separately in the form of figures and tables. Finally, there is the use of GIS. GIS utilises geospatial data that represents a specific area of interest in the form of a geographical map. Wrublack *et al.* (2018) listed some examples such as land use and occupancy, watershed delineation which are important to evaluate environmental impacts and its sources. A need, therefore, arises to combine these databases in a uniform dataset to generate a comprehensive and entirely accurate study and altogether represent these datasets on a geospatial and visual manner.

1.3 Research aim and objectives

This study aims to evaluate the water quality of the Loopspruit River from a physico-chemical and microbiological perspective to see how the current data are different from the historical data. The aim of the study is underpinned by six objectives which are:

I. To identify sampling sites using GIS and aerial photographs.
II. To test the water quality during two dry and two wet seasons.
III. To analyse the historical water quality data.
IV. To isolate, identify and characterise *Clostridium* sp., presumptive *E. coli* and *Enterococcus* sp. from the Loopspruit River.
V. To determine whether faecal pollution in the Loopspruit River is the result of anthropogenic factors.
VI. To create a geospatial representation of possible point- and non-point contamination using GIS approaches.

CHAPTER 2: LITERATURE REVIEW

2.1 Water scarcity and availability

One of the major concerns in modern society is the availability of water. This problem encompasses the concern of the populace on a global, regional and local scale. Rijsberman (2006) defines water scarcity as a lack of access to safe and affordable water for daily use. Water scarcity has a direct correlation to water availability, which has a profound impact on population health, economic growth and activity, geophysical processes and ecosystem functionality (Milly *et al.*, 2005). Given the current trend of urbanization, there is an increased demand for sustainable water and food productions which threatens water and food security (Kookana *et al.*, 2020).

South Africa is classified as a semi-arid country. It has an estimated average rainfall of 450 mm per year (mm/a) in comparison to the global annual rainfall average of 860 mm/a (DWAF, 2004). Water scarcity is an ever-present concern that can adversely affect all water-dependent sectors, especially agriculture (Gerten *et al.*, 2011). This creates an urgent need for sustainable water resource management for development and prosperity in South Africa. There is a negative effect on the availability of water when pollution and resource depletion are present. According to Ashton (2002), the availability of water can have a significant impact on the prevalence of disease, hunger and poverty in a specific area. The water availability in South Africa is estimated at 1100 m^3 per person for one year (Binns *et al.*, 2001; StatsSA, 2010).

The North West Province has a surface area of 116 320 km^2, with its geology comprising volcanic igneous and sedimentary rock (Serumaga-Zake & Arnab, 2012). Noteworthy water reservoirs in the North West Province are dams (Potchefstroom Dam and Klipdrift Dam), rivers (Mooi River, Crocodile River and Marico River) and wetlands (DWAF, 2009). Despite these water systems, very little research has been done on the Loopspruit River. The North West Province is still considered water-scarce, which limits economic development of the province. According to NWREAD (2014), the water resources in the North West Province are used mostly for mining activities, agriculture, domestic and industrial purposes.

The use of these resources eventually leads to various point source pollution factors, from activities like mining that generate acid mine drainage, or sewage effluent generated from residential and industrial areas. Non-point source pollution generated through agriculture and surface runoff during a precipitation event should also be considered.

2.2 Loopspruit River

The Loopspruit River is part of three major sub-catchments of the Mooi River Catchment, which include the Wonderfonteinspruit River (north-eastern reach), the Mooi River proper (northern reach), and the Loopspruit River (eastern reach) (van der Walt *et al.*, 2002). One of the major dams through which the Loopspruit River flows is the Klipdrift Dam. The Loopspruit River flows through the C21J and C21K quaternary catchments, which has a combined surface area of 1286.2 km^2. Some descriptions of the area include the Mean Annual Precipitation (MAP) with values of 604 mm and 620 mm for C21J and C21K respectively and a population of 25528 and 1605, respectively (DWAF, 2009). These populations are expected to increase annually, as these populations are specifically to the C21J and C21K quaternary catchments.

The land use surrounding the Loopspruit River is primarily agricultural (crop farming and grazing) together with gold mining activities (Van der Walt *et al.*, 2002). A more detailed site description is discussed in Section 4.1.1.

2.3 Anthropogenic, agricultural and industrial water use

Three main sectors contribute to water use in South Africa, namely the urban sector, agriculture and industry. Water in urban and domestic areas is typically collected from surface runoff systems or underground reservoirs such as groundwater aquifers. The water can be used for household activities, hygiene or recreation. Lükenga (2015) explains that wastewater generated from domestic use is dispersed through the sewer network in underground pipelines, where on occasion faulty pipelines lead to leakage causing pollution in that area. Wastewater is treated at wastewater treatment plants and recirculated into surface waters whereby, by extension, it recharges aquifers.

The agricultural sector is the largest consumer of water in South Africa (DWAF, 1996a). Irrigation water is used to water vegetation that may be treated with pesticides or insecticides to preserve crops before harvesting or to wet fertilised soils (Olad *et al.*, 2018). There is also the use of fertiliser for crop production. Some fertilisers are organic manures, which are used to improve organic material in soils. Inorganic fertilisers include nitrogen-phosphorous-potassium (NPK) supplements (Senna & Botaro, 2017).

South Africa is known worldwide for its abundance of its mineral resources, such as gold in the Witwatersrand region (Naicker *et al.*, 2003). The gold mining industry in South Africa plays a

central role in the country's social, political and especially the economic environments (Adler *et al.*, 2007). One of these gold mining activities is located upstream of the Loopspruit River.

Mining operations use water to cool their machinery and to wash out the waste rock and dust particulates containing sulphide minerals such as pyrite (FeS_2), which are also found on mine tailing dump sites. These may be oxidised in the presence of water during precipitation, leading to acid mine drainage (Masindi *et al.*, 2015). Mining can affect water quality of surrounding surface water systems. In the study, there are mining activities present near the Loopspruit. However, there are other mining activities upstream of the study area but these are outside the scope of this study.

2.4 Factors influencing water quality

Water quality is defined as the physical, chemical, and biological characteristics used to indicate whether water can sustain and maintain good quality to the benefit of society (Ji, 2008). Surface water typically contains calcium (Ca), magnesium (Mg), sodium (Na) and potassium (K), depending on different weathering regimes (Andrews *et al.*, 2004). According to Ji (2008) and Zhu *et al.* (2018), hydrodynamics is a control mechanism which regulates the transport of algae, dissolved oxygen (DO), and nutrients. These authors further explain that the nutrients in the water are of paramount importance for living organisms in and around the water source. There are two nutrients listed by Álvarez *et al.* (2017) that are problematic in an aquatic environment, viz. nitrogen and phosphorous. In their dissolved inorganic forms, the nitrogen in nitrite (NO_2), nitrate (NO_3) and ammonium (NH_3) contribute to eutrophication (Ji, 2008), while orthophosphate (PO_4) contributes to algal blooms, giving rise to the identification of algae as the new predatory species in aquatic ecosystems (Khatri & Tyagi, 2015).

Many sources contribute to the occurrence of these nutrients, but in this instance, the focus will be on the biological, agricultural and geological sources. In general, the soil is rich in nitrogen. Through hydrolysis nitrogenous trace gases like urea (NH_2CONH_2), which is present in animal urine, generate nitrogen compounds in soils (Andrews *et al.*, 2004). During hydrolysis, urea is converted into ammonia (NH_3) and carbon dioxide (CO_2) as shown in Equation 2.1:

$$\boldsymbol{NH_3CONH_{2(aq)} + H_2O_{(l)} \rightarrow 2NH_{3(g)} + CO_{2(g)}} \quad (2.1)$$

This chemical reaction (Equation 2-1) takes place during anaerobic digestion, which is the first step of four during the digestive process (Chen *et al.*, 2008; Watson-Craik & Stams, 1995; Zhang

et al., 2007), which include hydrolysis, acidogenesis, acetogenesis and methanogenesis. These biological processes are performed by the anaerobic bacteria, such as *Clostridium,* and aerobic bacteria such as *Bacillus* and *E. coli* (Bajpai, 2017).

Animal waste (high concentrations include livestock faecal matter, feedlot runoff, bedding and livestock feed) in an agricultural setting with livestock has a high ammonia (NH_3) nitrogen concentration (Chen *et al.*, 2008). These waste sources can have a substantial impact on water quality by contributing to non-point source pollution, affecting water sources like rivers, dams and lakes. Many agricultural irrigation schemes surrounding the Loopspruit River make use of the Loopspruit River and water from boreholes for domestic purposes.

Finally, weathering geology delivering excess nutrients and soils into the environment can be a principal contributor to environmental contamination and pollution. The Loopspruit catchment may have dolomite ($CaMg(CO_3)_2$) in the headwaters which may contribute to the increased availability of macronutrients such as magnesium (Mg). Some areas are dominated by minerals containing Apatite [$Ca_5(PO_4)_3(OH, F, Cl)$], which give rise to phosphorus (Khatri & Tyagi, 2015).

2.5 Contaminant movements

Surface water and groundwater are hydraulically connected in most areas, making surface water bodies an integral part of groundwater flow systems (Han, 2010; Ji, 2008). Surface water can seep through unsaturated zones and still act to recharge groundwater. The primary transport method of contaminants from a source towards a resource such as a river is through advection (contaminants moving with the groundwater) and diffusion (contaminants moving with random motion) (Socolofsky & Jirka, 2002). This interchange between surface and groundwater allows pollutants to be transported from a groundwater source, moving through aquifers and surfacing in discharge areas like dams and rivers (Ji, 2008). The movement from groundwater to surface and vice versa, according to Sophocleous (2002), is directly related to the geology and topography of the specific area, where the climate, precipitation and vegetation affect the distribution of water on the surface.

From an agricultural perspective, the factors influencing water quality mentioned in Section 2.4 need to take into consideration the principle of surface runoff. The surface runoff carries all the contaminants that reside on the agricultural surface and to water reservoirs like the Loopspruit River. During a precipitation event, the stormwater seeps into the soils with all the contaminants picked up, until the soil is saturated when the water finally ends up in water reservoirs (Lee *et al.*, 2020).

2.6 Physical and chemical parameters of water systems

The technique of measuring the physico-chemical parameters of environmental water indicates the water quality and, by extension, the productivity and sustainability of that water body (Sagar *et al.*, 2015). Concerning the physico-chemical properties, any changes provide valuable information on the water quality and indicate the impacts that the water may have on functions and biodiversity (Adeyemo *et al.*, 2013; Patil *et al.*, 2012). As a result of the increase in the size of the human population, there is also an increase in industrialisation and the use of fertilisers, and in anthropogenic activities that may contribute to the pollution of the environment with harmful contaminants (Patil *et al.*, 2012). The physical parameters involved are listed as temperature, pH, electrical conductivity (EC) and total dissolved solids (TDS). Chemical parameters include sulphides (SO_3), sulphates (SO_4), nitrites (NO_2), nitrates (NO_3), phosphates (PO_4) and chemical oxygen demand (COD) (Gorde & Jadhav, 2013).

2.6.1 Temperature

Temperature is a necessary parameter to measure because of the effect it has on plants and animals, and according to Sagar *et al.* (2015), it is the most critical environmental parameter. Yang *et al.* (2018) pointed out that temperature is a leading ecological environmental indicator that can lead to an understanding of various factors of water quality. Temperature is used to indicate the physical, chemical and biological properties during seasonal temperature changes (Han, 2010). According to Dharmappa *et al.* (1998) temperature is indicative of biochemical activities that occur in water systems such as metabolism, growth and reproduction. Temperature affects the growth of river organisms (Mbuh *et al.*, 2019). Temperature also contributes to the release of chemical constituents during warmer seasons, which is a consequence of geological erosion and anthropogenic activities (WHO, 2011).

2.6.2 pH

pH is the measurement of how acidic or alkaline soil or water is (Sagar *et al.*, 2015). In a mathematical approach to pH, this refers to the negative logarithm of the total proton [H^+] concentration. As a result, when the pH value ranges from 1 – 6.9, the pH is considered as acidic, whereas a pH value ranging from 8.1 – 14 is considered as alkaline, and a pH of 7 is neutral. The pH range of polluted water ranges from 6.5 – 8.5 (WHO, 2011). As the pH decreases the acidity of the area increases, and as a result, heavy metals and other pollutants are released from their respective parent rocks (Dannhauser, 2016). Under favourable conditions, the bacteria in surface waters increase rapidly with environmental conditions such as temperature and pH (Mhlongo *et*

al., 2018). One of the reasons that the Mooi River catchment's pH is considered more alkaline, can be attributed to the dolomitic waters (van der Walt *et al.*, 2002). The Mooi River catchment comprises the Mooi River Proper sub-catchment, Wonderfonteinspruit sub-catchment, and the Loopspruit River sub-catchment. The study took place within the Loopspruit sub-catchment.

2.6.3 Electrical conductivity

Electrical conductivity is the measurement of electrical energy carried by the available ions in an aqueous solution in mili-siemens per metre (mS/m) (Sagar *et al.*, 2015; Sophocleous *et al.*, 2020). With an increased number of ions, there is a direct correlation with a higher EC (Andrews *et al.*, 2004). According to Howard *et al.* (2004), there are some health effects when the EC exceeds 370 mS/m. These include disturbance of the water and salt balance in children as well as an increase in blood pressure. Renal and laxative patients may have some discomfort that may occur with high sulphate concentrations. EC can be managed (Aguado *et al.*, 2006) by increasing the pH of the water with the addition of alkaline products such as lime, sodium hydroxide or sodium carbonates. Alternatively, the pH can be decreased with acidic reagents such as sulphuric or hydrochloric acid or through the addition of carbon dioxide. This results in the formation of carbonic acid when it combines with water (Maurer & Gujer, 1995).

2.6.4 Total dissolved solids

Total Dissolved Solids (TDS) are the summation of mobile charged ions, minerals, salts or metal dissolved in a volume of water in mg/L. Examples include dissolved inorganic salts such as magnesium, sodium, calcium, potassium, bicarbonates, sulphates and chlorides (Heydari & Bidgoli, 2012; WHO, 2011). By using TDS, it is also possible to determine the EC by measuring the salinity of a water source. It is also convenient and acceptable to use the salinity measurement to determine the conductivity to give an estimation of the total dissolved solids (WHO, 2011). The EC has a direct correlation with TDS with an average conversion factor of 6.5 for most waters and is calculated as follows: EC (mS/m at 25°C) x 6.5 = TDS (mg/L) (DWAF, 1996b). At mine land uses, the acid mine drainage can explain the elevated levels of TDS, sulphates and heavy metals (Mhlongo *et al.*, 2018).

2.6.5 Sulphides and sulphates

Sulphur (S) is used as a critical ingredient in proteins, amino acids and the B vitamins of all living organisms (Han, 2015). After the death of plants and animals, bacteria make use of the sulphur cycle to convert organic sulphur (OS) to hydrogen sulphide (H_2S) (Willey *et al.*, 2011a).

South Africa is known worldwide for its abundance of mineral resources. During mining operations, and sometimes after these operations have stopped, sulphide minerals such as pyrite (FeS_2) can become oxidised in the presence of water. As a result of this oxidation, sulphuric acid (H_2SO_4) is formed, which is referred to as acid mine drainage (AMD) (Masindi *et al.*, 2015; Mhlongo *et al.*, 2018). When the dissolution of the sulphide-bearing minerals occurs, insoluble heavy metals contribute to environmental deterioration. AMD can contaminate surrounding bodies of water, such as groundwater, rivers or lakes, which can lead to the death of wildlife and make the water unsuitable for human consumption (Caraballo *et al.*, 2016; Jennings *et al.*, 2008).

The reactions which take place during the formation of AMD also leave the water with a high sulphate level. Even after the water is neutralised and the pH has returned to normal, the sulphates will remain at these high levels. Sulphates also increase the salinity of the water, which can make it unusable for agricultural, domestic or industrial use (McCarthy, 2011).

2.6.6 Nitrites and nitrates

The atmosphere of the earth contains 80% nitrogen (Gorde & Jadhav, 2013). Nitrogen (N) is used during biosynthesis to produce the basic building blocks of various fauna, flora and other life forms on a molecular scale to create nucleotides for DNA and RNA as well as amino acids for proteins (Han, 2015). Atmospheric nitrogen (N_2) is used in the nitrogen cycle, where various forms of nitrogen are generated through processes like nitrogen fixating, ammonification, nitrification and denitrification (Han, 2015). Dallas and Day (2004) provide a detailed explanation of how nitrogen is fixed from atmospheric nitrogen to produce ammonia (NH_3). Micro-organisms can convert ammonia (NH_3) to ammonium (NH_4) through ammonification. In an agricultural setting where fertiliser is applied, nitrification contributes to an increase in ammonia. When it is released, the oxidation of ammonia (NH_3) and nitrate (NO_2) occurs naturally in the environment as an inorganic ion (Sagar *et al.*, 2015). Finally, denitrification occurs when nitrates are reduced back to atmospheric nitrogen (N_2). Panigrahi *et al.* (2018) explained that in most aquacultures, the bacteria communities need 20 units of carbon to assimilate one unit of nitrogen. This is referred to as the carbon:nitrogen (C:N) ratio.

Dallas and Day (2004) state that nitrification (together with denitrification) is used to remove nitrogen from municipal wastewater, making it essential for wastewater treatment to be done. The amount of agricultural and industrial nitrogen inputs into the environment, exceeded the inputs from natural nitrogen (Han, 2015). Human activities such as fossil fuel combustion, the use of artificial nitrogen fertilisers, and the release of nitrogen in wastewater have dramatically altered the global nitrogen cycle (Lükenga, 2015).

2.6.7 Phosphates

Phosphorous (P), like sulphur and nitrogen, help make up the molecular structures of nucleic acids (DNA and RNA) and energy molecules (ATP) (Dallas & Day, 2004). Phosphorous mainly originates from soils and weathered rock and is then carried either by the wind or surface runoff to other surfaces or rivers and dams (Han, 2015). Plants and animals need phosphorus as an essential nutrient in ion form; however, it is limited to aquatic organisms (Gorde & Jadhav, 2013). The most significant source of phosphates is the oxygenated phosphorus on agriculturally fertilised soils, giving an increased concentration that may leach into groundwater reservoirs and with surface runoff eventually end up in water systems (Dallas & Day, 2004). In aquatic ecosystems, when phosphorus is in the form of phosphates (PO_4^{3-}), this limiting nutrient can lead to eutrophication as a result of over-fertilised aquatic plants through agricultural runoff or untreated sewage effluent (Lükenga, 2015). Microorganisms have an essential role in P mobilization in soil. The microbial biomass is one of the critical components for ensuring soil fertility through the recycling of C, N and P (Chen *et al.*, 2019).

2.6.8 Chemical oxygen demand

Chemical Oxygen Demand (COD) can be defined as the amount of oxygen that is needed to oxidise organic compounds such as carbon dioxide, ammonia and water. COD also is one of the main parameters used to determine the water quality of wastewater treatment plants (Cazaudehore *et al.*, 2019). According to Sagar (2015), establishing the COD is a testing procedure to determine the amount of the chemical decomposition of organic and inorganic contaminants that are dissolved and suspended in water. Patil *et al.* (2012) point out that COD is an indication of the environmental health of surface water.

COD sources that originate from agricultural and wastewater treatment plant WWTP are stored in soils as organic material that have aromatic carbon content. When the organic material is introduced into aquatic systems through surface runoff or leaching from urban and agricultural developments, COD increases gradually (Choi *et al.*, 2019).

2.7 Microbial parameters

Microbial parameters serve as an indication of how polluted a water source is with faecal contamination and may also indicate a possible source in terms of the microbial intensities if an analysis is done.

2.7.1 Indicator organisms

“Indicator organism” is a term used by water quality testers, researchers and experts, which describes a factor in microbiological testing that indicates the presence of faecal bacteria. The U.S. Environmental Protection Agency (USEPA) recommended organisms such as *E. coli* and *Enterococci* for identifying surface water contamination. In aquatic ecosystems, these indicator bacteria are dependent on external factors such as; temperature, nutrient availability and COD (Gregory *et al.*, 2017). The bacterial agar media that was used is listed in Appendix A, Table A.1 as a quick reference to explain in detail the metabolic compounds needed for optimal bacterial growth.

These tests show how contaminated the water is with faecal material, be it from agricultural runoff or anthropogenic activities such as WWTP. According to Medema *et al.* (2003) and Payment *et al.* (2003), faecal indicator bacteria reside in the gastrointestinal tracts of warm-blooded animals, including human beings. The screening and testing for indicator organisms is a precautionary measure where the presence of indicator organisms shows the presence of faecal contamination which may include possible pathogenic organisms (Tallon *et al.*, 2005).

The Department of Water Affairs and Forestry (DWAF) lists the criteria that indicator organisms should meet. The following list is provided by DWAF (DWAF, 1996a):

- indicator organisms should be suitable for all types of water;
- they should be present in sewage and polluted waters whenever pathogens are present;
- they should be present in numbers that correlate with the degree of pollution;
- they should be present in numbers higher than those of pathogens;
- they should not multiply in the aquatic environment and should survive in the environment for at least as long as pathogens;
- they should be absent from unpolluted water;
- they should be detectable by practical and reliable methods;
- and they should not be pathogenic and should be safe to work within the laboratory.

However, not all the indicator organisms comply with these requirements because most bacteria do not survive, but *E. coli* is resistant to changes, making it prone to not meeting the criteria provided above.

Payment *et al.* (2003) list examples that also need to be considered regarding indicator organisms. These include heterotrophic plate count bacteria, total coliform bacteria, faecal coliform bacteria (*E. coli*), faecal streptococci and bacteriophages. That said, routine water monitoring programs should be used to accommodate combinations of indicator tests to determine the compliance of these indicator organisms. Monitoring programmes are generally used to test for indicator organisms in surface and groundwater systems and possibly detect opportunistic pathogens.

2.7.2 Total coliforms

Total coliforms are the collective term used for coliform organisms which can be used to provide the necessary information on source water quality. Total coliforms are commonly found in environmental soil and vegetation. These organisms have been used widely to measure water quality and to detect and enumerate microbes in water (Gregory *et al.*, 2017; Medema *et al.*, 2003). The coliform group comprises bacteria that have biochemical characteristics related to faecal contaminants in water sources. This group of bacteria, according to DWAF (1996a), Payment *et al.* (2003), Tallon *et al.* (2005) and WHO (2011) can be defined as "facultative anaerobic, Gram-negative, non-spore forming, oxidase-negative, rod-shaped bacteria that ferment lactose to acid and gas within 48 hours at 35°C or members of *Enterobacteriaceae* which are β-galactosidase positive."

The group of total coliforms consists of the genera *Escherichia, Citrobacter, Enterobacter*, and *Klebsiella* (Kora *et al.*, 2017; WHO, 2011). With this holistic view of the group making it heterogeneous, this group can also include lactose fermenting bacteria (*Enterobacter cloacae* and *Citrobacter freundii*), both found in faeces and environmental conditions (Medema *et al.*, 2003). On the other hand, total coliforms are not as reliable in terms of their origins because of their ability to survive in the environment and water sources (Tallon *et al.*, 2005). According to Payment *et al.* (2003), total coliforms usually inhabit the intestine organisms and other faecal sources, and in the environment, they are used as a faecal pollution indicator.

In the South African Water Quality Guidelines for Domestic use (DWAF, 1996c), total coliforms are used as an indication of microbial water quality, and they are routinely used for the analysis of drinking water. The target water quality range, in terms of total coliforms for drinking water, according to DWAF, (1996c) is 0 – 5 CFU/100 mL and ≤10 CFU/100 mL according to SANS 241

(2015) and WHO (2011). Since this study focuses on surface water quality and not drinking water quality, all the relevant water quality ranges and levels will be referred to as the resource water quality objectives.

With high total coliform values, the risk of waterborne pathogens increases. Clarke *et al.* (2017) state that total coliforms in the environment are generally harmless, but some exceptions like pathogenic *E. coli* and *Clostridium perfringens* cause symptoms like nausea, vomiting, and diarrhoea.

To isolate and determine the presence of total coliforms in water sources, the membrane filtration method can be applied and thereafter place the membrane on m-Endo agar and incubated. Total coliforms will produce colonies with a metallic green sheen (DWAF, 1996c).

2.7.3 Faecal coliforms

Faecal coliform bacteria are a subgroup of the total coliform group that exists in the intestine of both human beings and animals. It includes thermotolerant coliforms that can grow at temperatures of 35 – 44.5°C (Tallon *et al.*, 2005). It was initially believed that organisms that could grow at these temperatures were mainly of faecal origin, and they were therefore referred to as "faecal" coliforms (Hachich *et al.*, 2012). Recently researchers have been supporting the use of the term "thermotolerant coliforms" instead of "faecal coliforms", as it is a more accurate description of the group (Paruch & Mæhlum, 2012; WHO, 2011). Some examples of thermotolerant coliforms are *E. coli*, *Klebsiella* spp., *Enterobacter* spp. and *Citrobacter* spp. However, testing for these bacteria will not give a definitive answer to actual faecal contamination (Mahmud *et al.*, 2019; Paruch & Mæhlum, 2012). The resource water quality objectives set the faecal coliforms at 10 – 130 CFU/100 mL (DWAF, 2009)

Ramos *et al.* (2006) did a study which illustrated a strong relationship between surface runoff and faecal coliforms' transportation to water. They explain that the risk of faecal pollution in water sources increases in wet seasons (Tranmer *et al.*, 2018). *E. coli* is one of the micro-organisms listed by the World Health Organization to be one of the most reliable organisms to associate with faecal pollution (WHO, 2006). At present, *E. coli* appears to deliver the best result when testing for faecal pollution in drinking water. Tallon *et al.* (2005) base these statements on the prevalence of thermotolerant (faecal) coliforms in temperate environments as compared to the rare incidence *of E. coli*. The testing of *E. coli* in human and animal faeces as compared to other thermotolerant coliforms makes it easier, affordable, fast, sensitive, specific and easy-to-perform detection methods for *E. coli*.

Baudišová (1997) also found that other thermotolerant and total coliforms can grow in non-polluted river water while *E. coli* cannot, and therefore supports the recommendation that *E. coli* be used as the sole indicator bacterium for faecal contamination. In order to check if faecal coliforms are present in water sources, the membrane filtration method can be used, with the membrane placed on m-FC agar. After the incubation process, all the faecal coliform bacteria can be identified through the growth of a blue colony (DWAF, 1996c).

2.7.4 Enterococci

Faecal enterococci are members of a subgroup of faecal streptococci, consisting of species in the *Streptococcus* genus (WHO, 2011). The reason why faecal enterococci were sub-grouped is that they are rather specific indicators of faecal pollution and have a tendency to survive longer in water environments than other coliform bacteria (DWAF, 1996c). Using enterococci as a faecal indicator can be problematic because of their ability to survive in human and animal faeces and longer still in environmental sources such as soils (including beach sand) and plant surfaces (Boehm & Sassoubre, 2014; Hamiwe *et al.*, 2019).

Faecal enterococci (faecal streptococci) can be characterised as Gram-positive, facultative anaerobic cocci. They are catalase-negative (Medema *et al.*, 2003) relatively tolerant to sodium chloride (NaCl) and alkaline pH environments and are presents as pairs or as short chains (DWAF, 1996a; WHO, 2011).

Boehm and Sassoubre (2014); Hamiwe *et al.* (2019); and Radhouani *et al.* (2014), studied faecal enterococci and suggest that *Enterococcus faecium* and *Enterococcus faecalis* have higher prevalence in human faeces than other enterococci species, whereas *Enterococcus casseliflavus* and *Enterococcus mundtii* have more significant numbers in environmental reservoirs.

With the diversity of enterococci in mind, there are health concerns regarding the bacterial resistance of enterococci to antibiotics. Studies were done on enterococcal antibiotic resistance by Ali *et al.* (2016) and showed that *Enterococcus faecalis* are resistant to oxytetracycline (OXY), chloramphenicol (CHL), and erythromycin (ERY), and these resistances increase in the presence of increased levels of nitrogen and phosphorus. Enterococci species have also gained an increased resistance to vancomycin (VRE) and a steady increase in resistance to penicillin (Hamiwe *et al.*, 2019; Higuita Agudelo & Huycke, 2014).

These resistant bacteria pose a health threat, especially in health care facilities. Higuita Agudelo and Huycke (2014) list and elaborate on the health risks associated with enterococci like endocarditis, bacteraemia and urinary tract infections.

2.7.5 Heterotrophic plate count bacteria

Heterotrophic plate count (HPC) bacteria are a standard indicator of microbiological water quality (Francisque *et al.*, 2009; WHO, 2011). HPC bacteria are a means of expanding on the microbiological diversities in water sources that utilise organic nutrients to grow (DWAF, 1996c). Depending on nutrient concentrations, they may result in the inhibition of other bacterial communities and make it impossible to determine the entire microbiological content of any water source (DWAF, 1996b; WHO, 2006). HPC bacteria provide a baseline record of the concentrations of these bacteria in food, water and water filtration systems (Edberg & Allen, 2004). HPC bacteria may also contribute to the effectiveness and sensitivity of other methods to enumerate indicator organisms (Allen *et al.*, 2004). An increased number of HPC bacteria lead to the suppression of indicator and coliform bacteria or even inhibition on selective media (Gregory *et al.*, 2017).

According to Allen *et al.* (2004), there are two means of incubation that must be considered. The first is to make a spread plate of the water sample on R2A agar at a higher incubation temperature (35 – 37°C) with a short incubation time (34 – 48 hours), which favours bacterial growth from animal and human sources. The second is to prepare a spread plate of the water sample on R2A agar but with lower temperature incubation (20 – 28°C) and longer incubation time (5 – 7 days), which favours water-based bacterial growth.

Some reasons given by Allen *et al.* (2004) as to why they use HPC bacteria screening methods, are that some HPC genera are considered as opportunistic pathogens (*Aeromonas, Klebsiella*, *Pseudomonas* and *Mycobacterium).* HPC bacteria can also indicate a spectrum of organisms that are resistant to disinfectants, spore-forming microorganisms and organisms that rapidly proliferate in treated water systems without disinfectants (WHO, 2011).

Finally, the microbial diversity that the HPC method provides makes it possible to create an antibiotic resistance profile of the given water reservoir. It also creates an opportunity to see which prominent organisms are resistant to antibiotics, if they are opportunistic pathogens, and also where these organisms might cause harm in the environment based on their nutrient uptake.

2.7.6 Clostridia

Clostridium spp. are described as anaerobic bacteria that are sulphate-reducing, Gram-positive bacilli (WHO, 2011). *Clostridium* sp. can also produce spores that are resistant to extreme pH, temperatures and disinfection (chlorination) (DWAF, 1996c). Species such as *Clostridium perfringens* can be used as a faecal pollution indicator because it can be found in the gastrointestinal tract of humans and warm-blooded animals (Desmarais *et al.*, 2002; Tallon *et al.*,

2005). Clostridia are also present in wastewaters and stable environmental water reservoirs (Romanazzi *et al.*, 2016).

Clostridium sp. has other uses in the industry. For example; *Clostridium beijerinckii* can perform acetone-butanol-ethanol (ABE) fermentation to produce biofuel (Sangavai & Chellapandi, 2017). *Clostridium butyricum* used in the medical industry has shown potential in the treatment of cancer patients (Staedtke *et al.*, 2016) and finally, it is used in the cosmetic industry to create Botox from a diluted form of the botulinum toxin produced by *Clostridium botulinum* (Awan, 2017).

Clostridia are anaerobic by nature, and therefore tryptose sulphite cycloserine (TSC) agar is the best for enumeration purposes (Barrios *et al.*, 2013). TSC agar can be reduced from sulphite (SO_3^{2-}) to sulphide (S^{2-}) by anaerobic sulphite-reducing *Clostridium* (SRC) species (Barrios *et al.*, 2013). Tryptose, yeast extract and soy peptone serve as a food source for the SRC species to grow. Furthermore, sulphite-reducing indicators such as ferric ammonium citrate and sodium metabisulphite result in distinct black SRC colonies (Doyle *et al.*, 2018). Adding D-cycloserine, it allows the inhibition of other facultative anaerobes (Harmon *et al.*, 1971).

Developed in 1980, the Fung double tube (FDT) test allows for culturing and enumerating obligate anaerobes such as *Clostridium* species (Barrios *et al.*, 2013). Vijayavel *et al.* (2009) describe the FDT as two tubes, one inside the other (Figure 2.1). The first has a small diameter. This is inserted into a larger, screw-capped test tube. This unique method accommodates for anaerobiosis without any additional atmospheric generators or chambers (Barrios *et al.*, 2013). The FDT, in combination with TSC agar (Figure 2.2), has shown to be a very reliable method for use in isolating an enumeration *Clostridium* species from surface water and sediment (Vijayavel *et al.*, 2009).

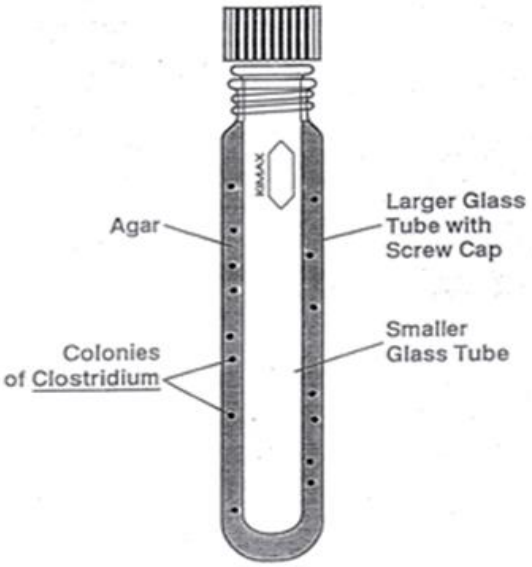

Figure 2.1: A sketch of the Fung double tube setup to create anaerobic conditions.

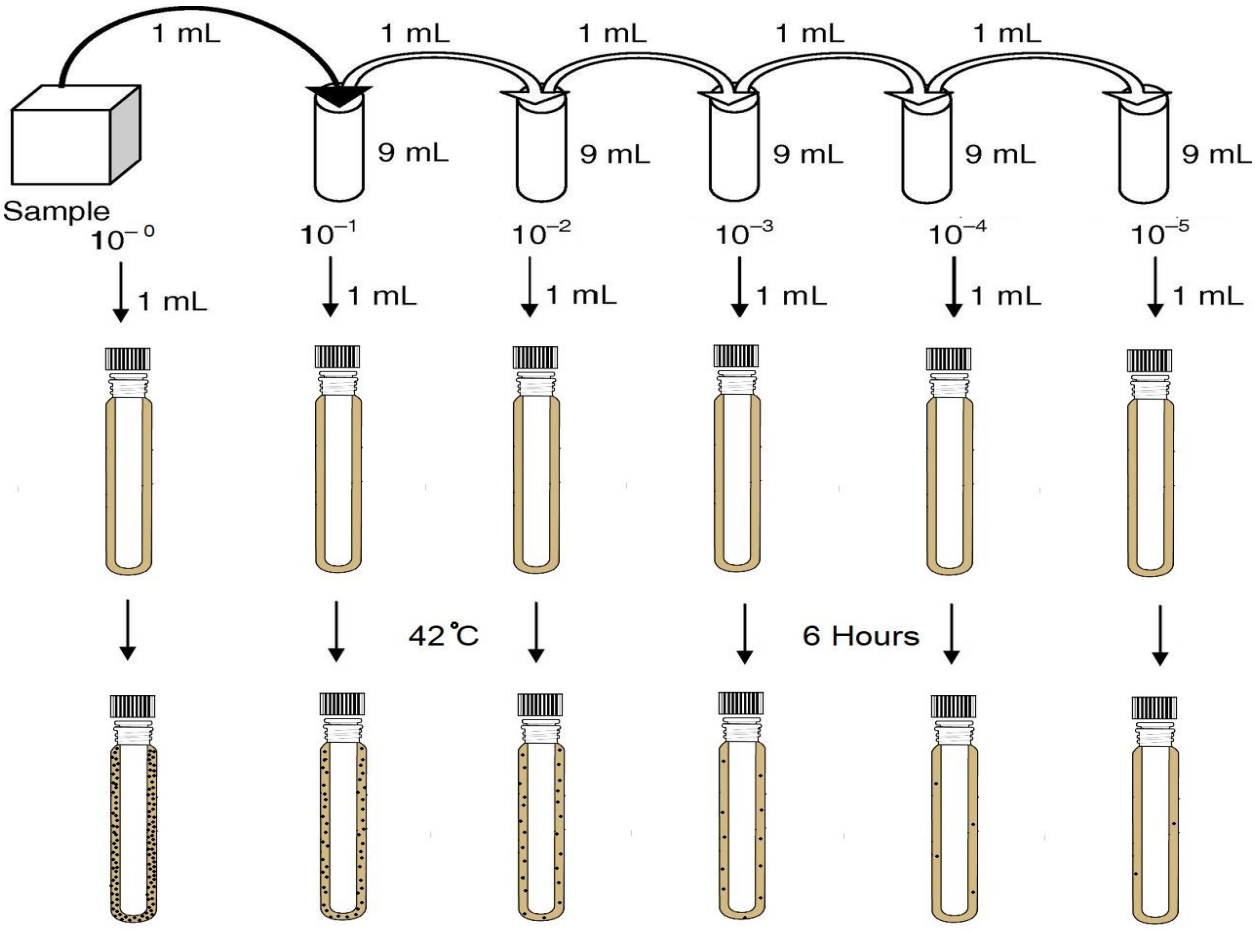

Figure 2.2: The Fung double tube technique when applying a dilution series with TSC agar.

2.8 Biochemical identification of *E. coli*, enterococci and *Clostridium*

In the traditional sense, the identification of bacterial species depends on studying the molecular and physiological characteristics (Fisher & Phillips, 2009). That said, enterococci need specific conditions to grow by utilising certain biochemical characteristics.

2.8.1 Gram staining

The Gram stain is used to differentiate between two classifications of bacterial cells and serves as the primary taxonomical tool (Beveridge, 2001). The Gram stain uses dyes to stain the bacterial cells to show whether they are to be classified as Gram-negative or Gram-positive (Willey *et al.*, 2011b). When observed under a light microscope, these bacterial cells show either a prominent purple colour, which indicates a Gram-positive stain, or a pink colour, which indicates a Gram-negative stain (Willey *et al.*, 2011b). These changes in stain colour are a result of the bacteria's morphology and arrangement. According to Thairu *et al.* (2014), the difference in cell membrane assemblage and permeability shows how Gram-positive and Gram-negative can be differentiated.

2.8.2 Identifying presumptive *E. coli* with the triple sugar iron test

Biochemical testing procedures used to identify presumptive *E. coli* can be done with the Triple Sugar Iron (TSI) test. The TSI test is a means of distinguishing among members of the family *Enterobacteriaceae,* namely *E. coli* and other intestinal bacteria (Harley & Prescott, 2002). Enteric organisms like *E. coli* can catabolise glucose, lactose, or sucrose, and release sulphides from ammonium sulphate or sodium thiosulfate as a by-product (Willey *et al.*, 2011b). The TSI test can be applied by inoculating a TSI test tube slant and incubating at 35°C for 24 hours. Notable results include a colour change of the slant and gas production. If the organisms cannot catabolise the sugars, they are not of the *Enterobacteriaceae* family (Harley & Prescott, 2002; Willey *et al.*, 2011b).

2.8.3 Testing for catalase activity in enterococci

The catalase activity of an organism is a biochemical reaction where a ubiquitous antioxidant enzyme degrades hydrogen peroxide (H_2O_2) to water (H_2O) and oxygen (O_2) (Iwase *et al.*, 2013; Painter *et al.*, 2017). Hydrogen peroxide can inactivate enzymes and also cause damage to cell DNA, and therefore catalase is a protective enzyme that halts the hydrogen peroxide degradation of cell components (Switala & Loewen, 2002).

As previously mentioned (Section 2.7.4), enterococci form a sub-group of streptococci and can be hard to distinguish from each other. On the other hand, they are both catalase-negative and

can be distinguished from morphologically similar organisms such as staphylococci, which are catalase-positive (Fisher & Phillips, 2009).

2.8.4 Identifying potential *Clostridium* species

It is difficult to perform any other phenotypical or biochemical tests as a result of the *Clostridium* species' being anaerobic (Brazier *et al.*, 2002). According to Gajdács *et al.* (2017), *Clostridium* is a Gram-positive rod-shaped bacillus that can produce endospore. All pure *Clostridium* isolates were Gram-stained, and then an endospore stain was performed to check for the presence of endospores. These characteristics are what make *Clostridium* spp. so resilient in the environment. *Clostridium* spp. are Gram-positive, meaning that they have a thicker cell wall, and their endospores can withstand a plethora of environmental changes.

2.9 Molecular identification of faecal coliforms and *Clostridium*

The Polymerase Chain Reaction (PCR) is a method used to amplify specific DNA sequences and make clones of these amplified sequences (Allison, 2007; Joshi & Deshpande, 2011; Willey *et al.*, 2011b). The PCR consists of three steps: i) the denaturation of DNA into single-stranded DNA through heating; ii) the annealing of target-specific single stand DNA primers and iii) the elongation of primers through application with a thermostable DNA polymerase. The DNA polymerase (Taq) from *Thermus aquaticus* is often used (Joshi & Deshpande, 2011; Lim *et al.*, 2018). Taq DNA polymerase is used as a heat-resistant DNA polymerase to ensure the reliability and accuracy of the PCR process, because DNA denatures at high temperatures and reanneals at lower temperatures (Allison, 2007). These steps need to be repeated between 28 and 35 cycles to ensure that enough product is synthesised.

In order to determine or confirm the identity of the unknown organism, the 16S rDNA gene is amplified because it is universally present in bacteria (Woo *et al.*, 2008). Using the 16S rDNA gene is arguably a more objective, accurate and reliable means of genotypic identification of microorganisms (Clarridge, 2004). The 16S rDNA gene of unidentified organisms can be verified from various established databases (DeSantis *et al.*, 2006).

2.10 Antibiotic resistance

There is a gross overuse of antibiotics in the anthropogenic and agricultural sectors. Antibiotics are used for various reasons, ranging from treating bacterial infections or the prevention thereof in patients with a compromised immune system or ensuring agricultural crop health (Ben *et al.*, 2019). When antibiotics are administered to livestock or human beings, the antibiotics are not completely metabolised, leaving some small quantities unused (Le *et al.*, 2018). Antibiotics have been shown to alter the microbiome of the individual taking them. People excrete unused antibiotics, and the antibiotics end up in wastewater treatment plants, exposing the microbes used for water treatment purposes. With continuous exposure, these organisms become resistant to the antibiotic (Huang *et al.*, 2019; Zhou *et al.*, 2018). According to Garner *et al.* (2017), faecal matter from livestock becomes part of the topsoils, and these excrements may contain the non-metabolised antibiotics, which may get filtered through the soil surfaces and move to water reservoirs through surface runoff. All these are factors which contribute to microbes becoming resistant to antibiotics in natural environments (Figure 2.3).

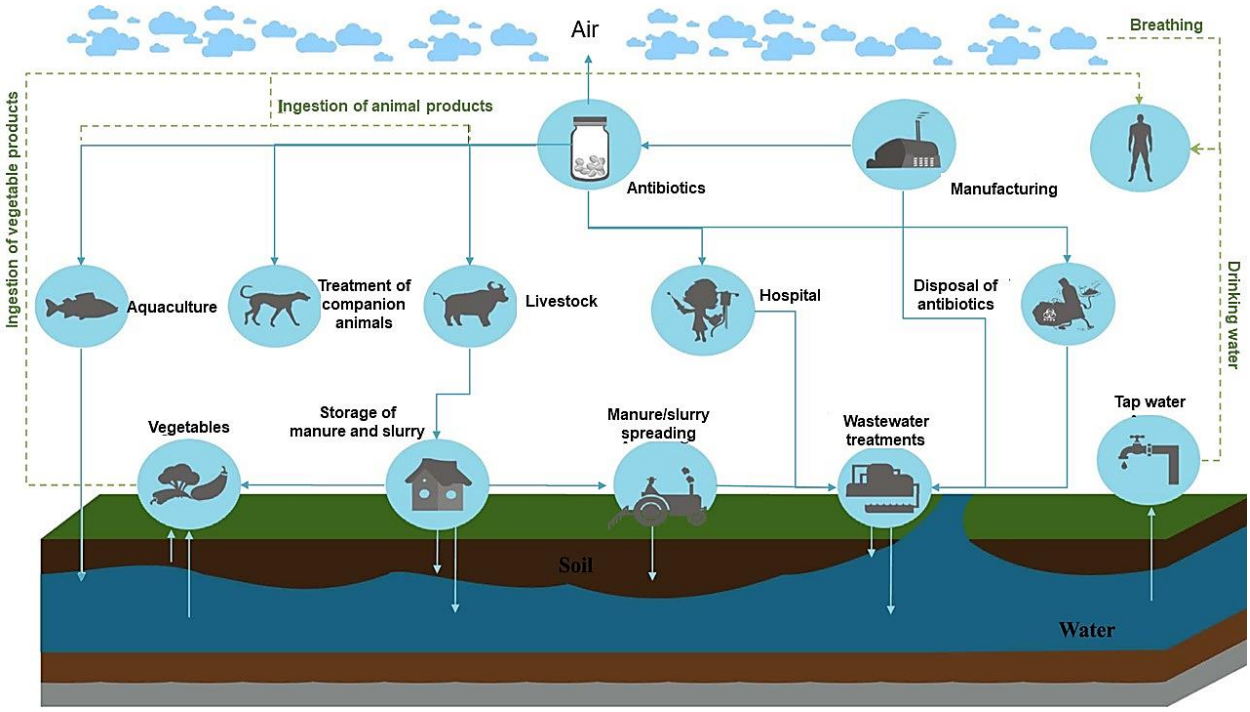

Figure 2.3: A graphic illustration of how antibiotic resistance can spread. It shows the exposure to both humans and the environment (Ben *et al.*, 2019).

That having been said, this creates a new conundrum for researchers who need to select better suited antibiotics and better manage antibiotics in both anthropogenic and agricultural situations. This goes beyond bacteria growing in antibiotic-dominated areas; as Ali *et al.* (2016) and Jia *et*

al. (2018) have shown bacteria may change their genetic code, resulting in resistant genes that provide a selection pressure. These antibiotic-resistant genes (ARGs) can be passed on to the next generation of microbes, facilitated by horizontal gene transfer (HGT) (Jia *et al.*, 2018; Zhou *et al.*, 2018). According to Sundsfjord *et al.* (2004), the genetic basis of bacterial resistance stems from newly obtained DNA through HGT or cellular gene mutations as a result of acquired genes that alter antimicrobial target sites or gene expression. Figure 2.4 illustrates how the various resistance mechanisms can be carried out.

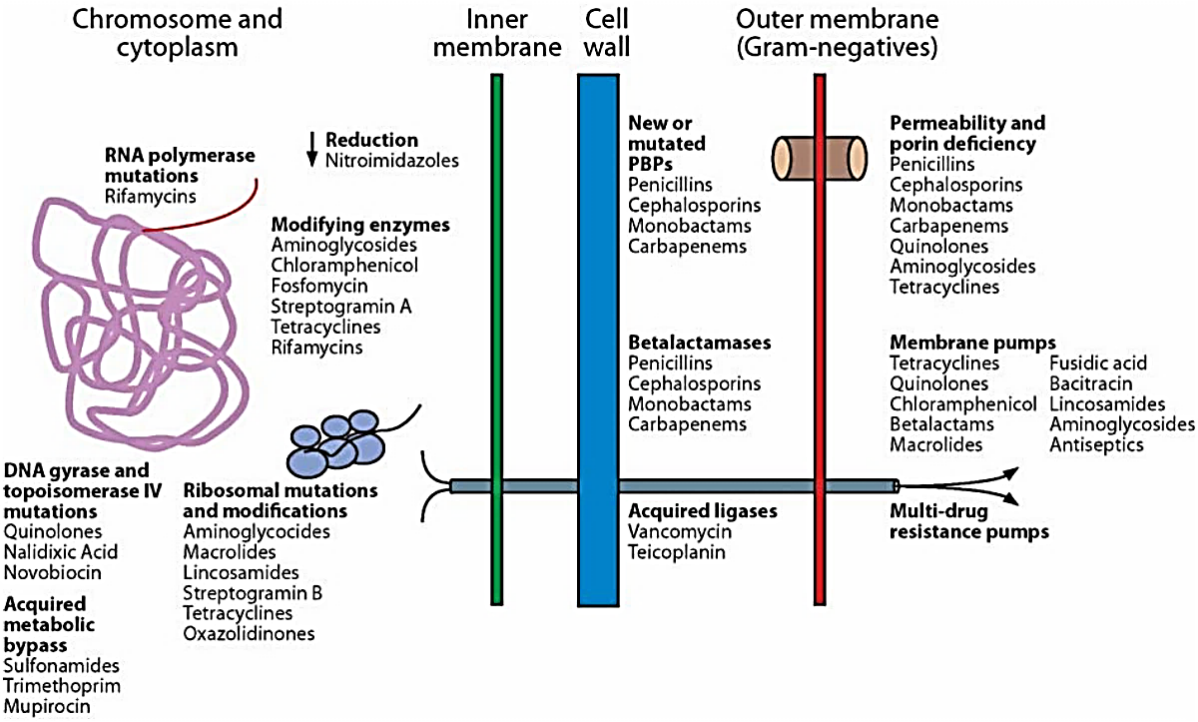

Figure 2.4: An illustration of how antibiotics can obtain resistance genes through various resistance mechanisms (Sundsfjord *et al.*, 2004).

Studies by Zhou *et al.* (2018) and Ben *et al.* (2019) illustrate how environmental compartments that have increased anthropogenic antibiotic pressures are often the most significant source of ARG contamination and give rise to concern for human and animal health. Some antibiotics often used in hospitals and for livestock, according to Jia *et al.* (2018), are sulfamethazine (SMZ) and sulfadiazine (SDZ); Tetracyclines: chlortetracycline (CTC), oxytetracycline (OTC), tetracycline (TC); Quinolones: ciprofloxacin (CIP), norfloxacin (NOR); β-lactams: cefotaxime (CTX), cefazolin (CFZ), penicillin G (PEN G); and Macrolides: erythromycin (ERY), roxithromycin (ROX); chloramphenicol (CHP) and trimethoprim (TMP).

2.10.1 β-Lactams

β-lactams are one of the major classes of antibiotics used in anthropogenic, veterinary and agricultural sectors. Henton *et al.* (2011) state that in South Africa from 2002 – 2004, β-lactam antibiotics constituted up to 11% of all antibiotics sold and were among the most frequently used antibiotics as growth promoters in poultry and pigs. In Europe, β-lactam antibiotics are most commonly used in the veterinary sector. Their use increased to include countries in the far east (Elander, 2003). A study by Graham *et al.* (2016) indicates that soil samples collected from 1923 – 2010 contained a high abundance of four β-lactam ARGs (*bla*$_{TEM}$, *bla*$_{SHV}$, *bla*$_{OXA}$ and *bla*$_{CTX-M}$). Gillings *et al.* (2015) listed the class 1 integron genes (*intI1*) as a proxy for anthropogenic pollution.

2.10.1.1 β-Lactamases

One of the primary mechanisms for the hydrolysis of β-lactam antibiotics is the β-lactamase enzymes. β-lactamases all have an underlying catalytic activity (Guenther *et al.* 2011), which is the hydrolysis of the β-lactam ring. Each β-lactamase inhibitor of these mechanisms, results in the inaccessibility and modification of target enzymes or the deactivation of the antibiotics (Zhang *et al.*, 2009).

AmpC β-lactamases are bacterial enzymes that hydrolyse 3rd generation cephalosporinases and are encoded on chromosomes of many *Enterobacteriaceae* species (Ye *et al.*, 2017). AmpC β-lactamases are inducible and high expression levels cause them to mutate. The overexpression in clinical Gram-negative isolates, gives resistance to therapeutic drugs in one of two ways: deregulation of the AmpC chromosomal gene or through the acquisition of transferable genetic material like plasmids and transposons (Girlich *et al.*, 2000; Perez-Perez & Hanson, 2002).

AmpC-producing isolates are not only prominent in clinical settings but also in areas with environmental water and agricultural vegetation. They are also prevalent in recreational water and wastewater treatment plants, including irrigation water sources and vegetation (Manzetti & Ghisi, 2014; Njage & Buys, 2015; Schwartz *et al.*, 2003) giving rise to a health concern. Plasmid-mediated AmpC β-lactamases include*: FOX-, MOX-, CIT-,* and *ACC*-type and the *CMY*-2 of *CIT*-type enzymes, which have the broadest geographical spread and are principal contributors to β-lactam resistance (Perez-Perez & Hanson, 2002).

Pei *et al.* (2006) state that antibiotic resistance gene transfer could occur through the consumption of animal products or interactions with surface water or vegetables contaminated with faecal microbiota (*E. coli*). The prevalence of antibiotic resistance genes and similar gene types over various environmental settings can be studied. This may help to illuminate the relationships between riverine systems and environmental bacteria and antibiotic resistance genes transfer to

humans. Muraleedharan *et al.* (2019) explained that the β-lactamases producing bacterial isolates in the environment are problematic, especially from urban settings receiving antibiotic-resistant genes from stormwater, surface runoff and wastewater effluent.

Both genotypic and phenotypic methods are viable options to determine antibiotic resistance. However, there are some advantages to the genotypic methods. These include the identification of specific genes or integrons, which are detectable through PCR-based methods with the appropriate primers (Sundsfjord *et al.*, 2004). A major disadvantage of the molecular method, as opposed to the disk diffusion method, is that there are only a limited number of known genes to screen for, resulting in unknown resistance genes going undetected (Sundsfjord *et al.*, 2004).

2.10.2 Integrase gene

Integrase genes are versatile genetic elements that allow for the gaining and expression of exogenous genes. These genes are featured in bacterial genomes, residing in the chromosomes (Koczura *et al.*, 2016). These genes' genetic mechanisms allow bacteria to evolve rapidly through capturing and expressing different genes. Studies done on the Integrase gene indicated the evolution of the integrase genes as they transition from clinical to environmental settings. This also included the correlation between class 1 integrase genes (*intI*1), antibiotics and genetic elements in association with heavy metal pollutants, in waste treatment plants and surface water (Di Cesare *et al.*, 2016; Gillings, 2014).

Integrase has recombinant features (*intI, attC, attI*) that allow it to incorporate a variety of resistance genes and express them (Figure 2.5). Moreover, these features can be transferred by lateral gene transfer into non-pathogenic bacteria (Vaz-Moreira *et al.*, 2014). These antibiotic resistance genes can be clustered in the same gene cassettes with other elements, resulting in the microorganisms having a distinct ecological advantage (Japoni *et al.*, 2008). The arrangements of antibiotic resistance genes that are simultaneously transferred co-select other resistant genes composed in the genome (Martinez, 2009)

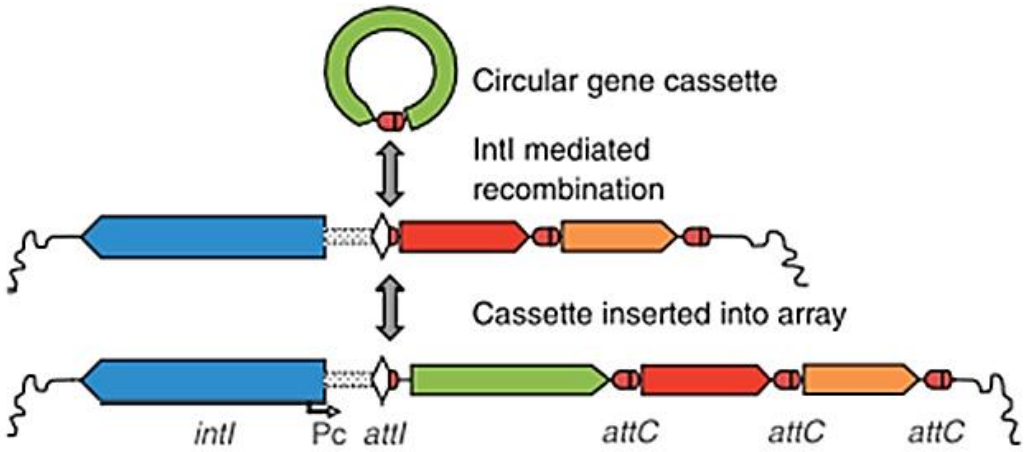

Figure 2.5: Schematic diagram of how integrase incorporates genes cassettes into its genome. Integron-integrase (*intI*) that catalyses recombination between the site of circular gene cassettes (*attC*) and the attendant integron recombination site (*attI*).

Integrase confers resistance on antibiotics, heavy metals and disinfectants and are said to exhibit a rapid response to environmental pressure (Japoni *et al.*, 2008). Integrase abundance can be observed in the environment through commensal microbiota in clinical settings, mining effluents, agricultural settings and water systems (Gillings *et al.*, 2015; Labbate *et al.*, 2008). This abundance makes it possible for the integrase gene to adapt to environmental pressures by modifying themselves and be incorporated into mobile genetic elements (Czekalski *et al.*, 2015).

Under stress-enhanced environment induced by pollutants (antibiotic residues, faecal matter, heavy metals, wastewater and agricultural runoff) the potential for co-selection of resistant genes is highly induced (Di Cesare *et al.*, 2016). The drive for its co-selection is activated, due to the physical location of integrase on plasmids and transposons which carry antibiotic resistance genes, as thus there is a strong correlation between antibiotic resistance genes and integrase (*intI1*) genes in reclaimed water, wastewater effluent and animal farming manure (Gillings, 2014).

2.10.3 Phenotypical methods

2.10.3.1 The Kirby-Bauer disk diffusion method

The Kirby-Bauer disk diffusion method is a standardised disk diffusion method describes by Bauer *et al.* (1966) which is a reliable means of determining which micro-organisms are resistant to which antibiotics. To select a broad spectrum of antibiotics, the European Committee on Antimicrobial Susceptibility Testing (EUCAST) has a diverse database of all the different micro-organisms and their related antibiotic susceptibility/resistance results (EUCAST, 2017).

The Kirby-Bauer disk diffusion method can be applied generally on Mueller-Hinton agar, followed by a surface inoculation (a spread plate). Commercially available antibiotic-impregnated disks are aseptically placed on the inoculated agar and incubated under prescribed conditions (Bauer *et al.*, 1966). The diameter of an organism's inhibition zone indicates the organism's resistance or susceptibility to an antibiotic (Biemer, 1973; EUCAST, 2017).

2.10.4 Molecular methods

The diversity and prevalence of resistance genes are quite extensive in the aquatic environment. It is, therefore, more crucial to develop and apply molecular techniques to investigate these occurrences. The transport and fate of antibiotic resistance genes can be monitored with specific and multiplex PCR, real-time PCR, DNA microarrays (Japoni *et al.*, 2008; Ye *et al.*, 2017).

2.10.4.1 The prevalence of AmpC β-lactamase genes

A commonly used technique to detect the occurrence of AmpC β-lactamase genes is with 16S rRNA gene sequencing (Zhou *et al.*, 2018). This can be done with pure samples or mixed environmental samples. Environmental DNA that has a low concentration can be amplified by PCR-based methods (Japoni *et al.*, 2008). To ensure time and cost efficiency, multiplex PCR can be used to simultaneously determine multiple environmental ARGs. This can be done with different primer pairs to amplify the DNA fragments of different genes at the same time. One drawback of this method is that some DNA amplification can be inhibited and the primer dimers may disrupt the expected results (Perez-Perez & Hanson, 2002). Therefore, to ensure accurate results, conventional PCR can be pursued.

2.10.4.2 Next-Generation Sequencing

Next-Generation Sequencing (NGS) is a sequencing platform that enables a cost-effective means of sequencing multiple samples in a single sampling run (Derakhshani *et al.*, 2016; Dumur, 2015). When NGS is compared with Sanger sequencing, NGS is based on the sequencing of all the nucleic acid molecules in a sample (Dumur, 2015). This also allows for multiplex sequencing of millions of sequence reactions with the "barcoding" feature. NGS generally serves as a means to determine the composition of a bacterial community and diversity by analysing the 16S ribosomal RNA gene (Tawfik *et al.*, 2018). The Illumina MiSeq sequencing platform is often used to sequence the V3 – V4 and V4 hypervariable regions of the 16S rRNA gene in an environmental DNA sample. The sequence reactions are coded with barcodes during library preparation (Derakhshani *et al.*, 2016; Dumur, 2015). Library construction consists of modified forward and reverse primers (Herlemann *et al.*, 2011; Sinclair *et al.*, 2015). Sinclair *et al.* (2015) found that the 16S rRNA gene region is optimal for cross-examining bacterial communities.

2.11 LC/MS analysis

The principle of gas chromatography or liquid chromatography (LC) with mass spectrometry (MS) is one of the most useful means of quantifying dynamic concentrations of chemical constituents in environmental water samples. This analytical method has been extensively used in the study of pharmaceuticals in the environment, where approximately 3000 different active substances are used in both human and veterinary medicine (Hernández *et al.*, 2007).

An LC/MS system typically consists of an autosampler, an LC system, an ionisation source (the interface combining the LC to the MS) and an MS (Korfmacher, 2005). The analysis consists of two main stages (Berg *et al.*, 2013). First, chromatographic separation of compounds (the liquid phase) takes place through reversed-phase LC. This separation is based on hydropathy using either a water–acetonitrile, or a water-methanol gradient (Covington *et al.*, 2017). Hydrophobic interaction chromatography (HILIC) is preferred when working with antibiotics over reversed-phase LC because the retention time of polar antibiotic compounds and their metabolites is longer. During reversed-phase LC antibiotic compounds elutes first and non-polar antibiotic compounds and their metabolites are retained for longer (Kamleh *et al.*, 2008; Scorciapino *et al.*, 2017). LC can be used to identify compounds provisionally based on their respective retention times (Dass, 2008) after this follows MS. This analytical technique measures the mass-to-charge ratio (m/z) of ions. Antibiotic compounds are ionised and separated based on their mass-to-charge ratio by accelerating them in a flight tube, and can be identified through the intensity of the deflected ions when compared to compounds with known masses (Gross, 2017). Therefore the combination of LC-MS generates characteristic retention times for antibiotic compounds and metabolites to aid in the identification of antibiotic compounds in samples (Berg *et al.*, 2013).

Finally, the quantified antibiotics can be compared with the predicted no-effect concentrations (PNEC). These concentrations are set to indicate the limit at which particular antibiotics can be deemed permissible to have no effect on the ecological environments that the antibiotic is found in (Tran *et al.*, 2019).

2.12 GIS

Many ecological studies are done in the field of microbiology. However, few studies can show the geospatial component of these studies, whether it is a cause and effect visualisation, or the environmental implications. GIS can be used to incorporate both the microbiological and geospatial components to create a visual representation of the study and to see the “big picture”. In this case, GIS will be used to illustrate the change in water quality over time and to show any contamination events that have occurred. With that in mind, this opens a new window for predictive contamination visualisation in the field of environmental microbiology.

GIS is a vast and dynamic subject. Grueau (2018) and Longley *et al.* (2004) describe GIS as a special class of information systems. To grasp the concept of GIS in its entirety, several vital definitions and aspects need to be understood. According to Longley *et al.* (2004), GIS is a computer-based information system to manage the input, analysis and output of geographic data and information. GIS software has both paid and free options. The freeware software (qGIS) is available at (https://qgis.org/en/site/), whereas ArcGIS (10.5.1) developed by ESRI (Environmental Systems Research Institute) is commercially available at (www.esri.com).

GIS is a diverse set of tools to aid in the study of geographic entities or locations in regard to the lithosphere on different scales, such as a temporal or a spatial scale (Goodchild, 2015). However, GIS is not limited to geographic fields such as the lithosphere. Fields such as hydrology, biology, and engineering, to name a few, can also utilise GIS for their respective research fields. Wrublack *et al.* (2018) stated that GIS is a useful means to provide information such as land use and occupancy. According to Raju (2004), GIS can be used i) to maximise planning efficiency and decision making, ii) to minimise redundant data, iii) to integrate information from many sources, and iv) to apply complex analysis/queries involving geographically referenced data to generate new information. Raju (2004) adds that GIS can answer general questions such as those pertaining to a location (What is found at a specific location?); conditions (Identify where certain conditions exist); trends (Historical changes); patterns (What are the spatial patterns that occur?) and modelling (What if?).

GIS in its entirety is a collective of processes working together. This includes, but is not limited to the identifying of problems, manage and respond to events, perform forecasting, set priorities, understand trends and monitor change. The latter two are crucial aspects of this study. This will allow the monitoring and visualisation of the data to understand patterns caused by possible pollution sources and possibly understand how and why these pollutants are in the environment.

2.12.1 Basic GIS concepts

2.12.1.1 Map features

2.12.1.1.1 Raster

A raster data model is defined as interconnected rows and columns (Figure 2.6) of equally sized pixels form a planar surface. (Campbell & Shin, 2017; Ladra *et al.,* 2017). Campbell and Shin (2017) also state that these pixels serve as building blocks to create points, lines, areas, surfaces and networks.

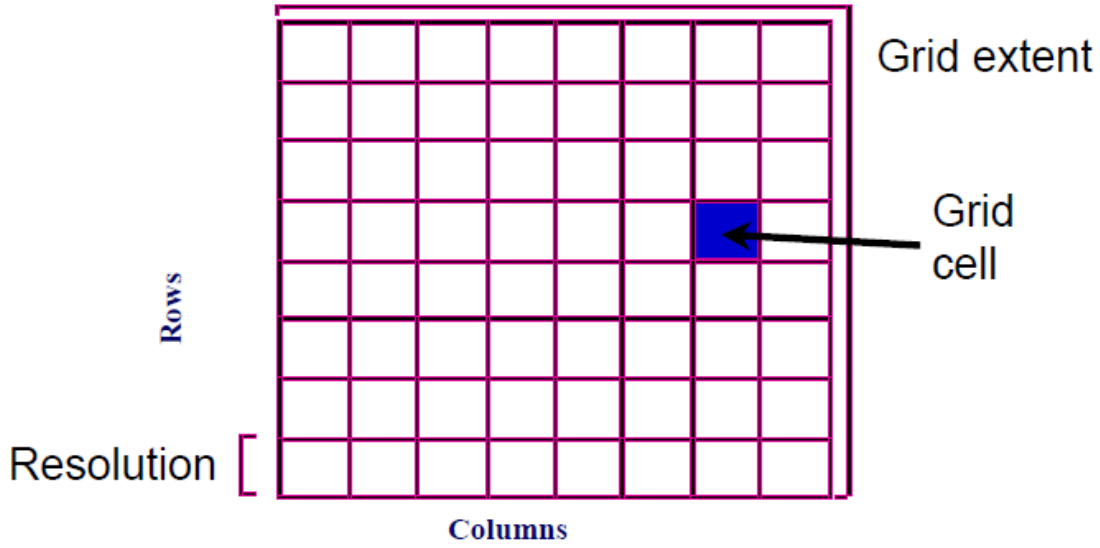

Figure 2.6: Raster grid showing the columns and rows system to generate a cell grid in the form of pixel resolutions (Campbell & Shin, 2017)

With each cell, there must be a cell reference or value (Shirzadi *et al.*, 2019) as seen in Figure 2.6. The use for Raster data format is appropriate for data capturing for example document scanning, image processing or remote sensing (Shirzadi *et al.*, 2019).

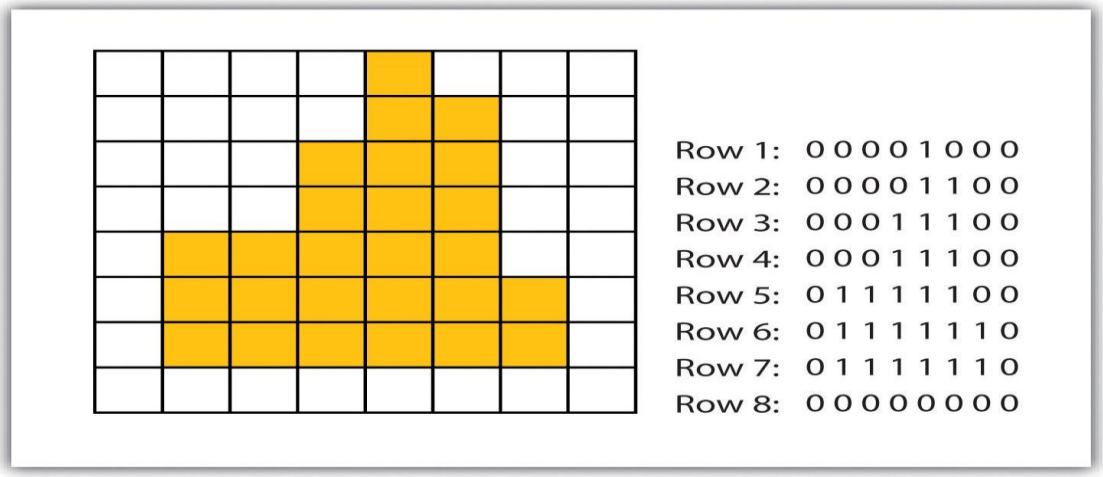

Figure 2.7: Raster data input with a cell value creating a shape in the cell grid (Campbell & Shin, 2017).

With Raster data formats, (Campbell & Shin, 2017; Shirzadi *et al.*, 2019) state that only a single data value can be used per individual cell (Figure 2.7). Furthermore, a pixel yields only a single value because the Raster model averages all values within the specific pixel and concludes that the bigger the area of the pixel, the less accurate the data value. An example given by Campbell and Shin, (2017) shows that the covered area by a pixel determines the spatial resolution where the pixel represents 10m by 10m (100 square metres) the real world would have a spatial resolution of only 10m. When a heavily pixelated Raster data model is used, then there may be information loss because of the low resolutions.

2.12.1.1.2 Vector

A typical map relies on three geometric objects and they are vector types: the point, the line and the polygon (Campbell & Shin, 2017). A point as the x and y coordinates (longitude and latitude); a line is the connecting of two or more points without crossing of closing at the initial point. A polygon follows the same principle as a line, except that it is an enclosed multi-sided shape (Tian *et al.*, 2015). Figure 2.8 shows how these geometric objects are represented in a map. An important aspect about Vector data models is that they utilize the spatial information and the attribute information and are linked with a special identification number that is unique to each feature in a map to (Campbell & Shin, 2017).

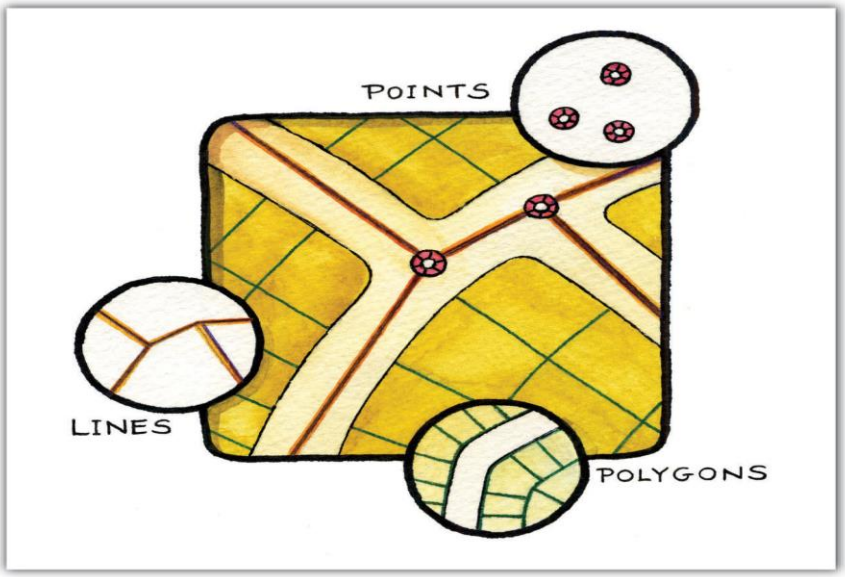

Figure 2.8: The tree basic map features used to create a vector map (Campbell & Shin, 2017)

However, all these points and lines can overwhelm the map user and so these geometric objects can be uniquely characterised for example different size points can be in different colours and certain lines can be “dash-lined” etc.

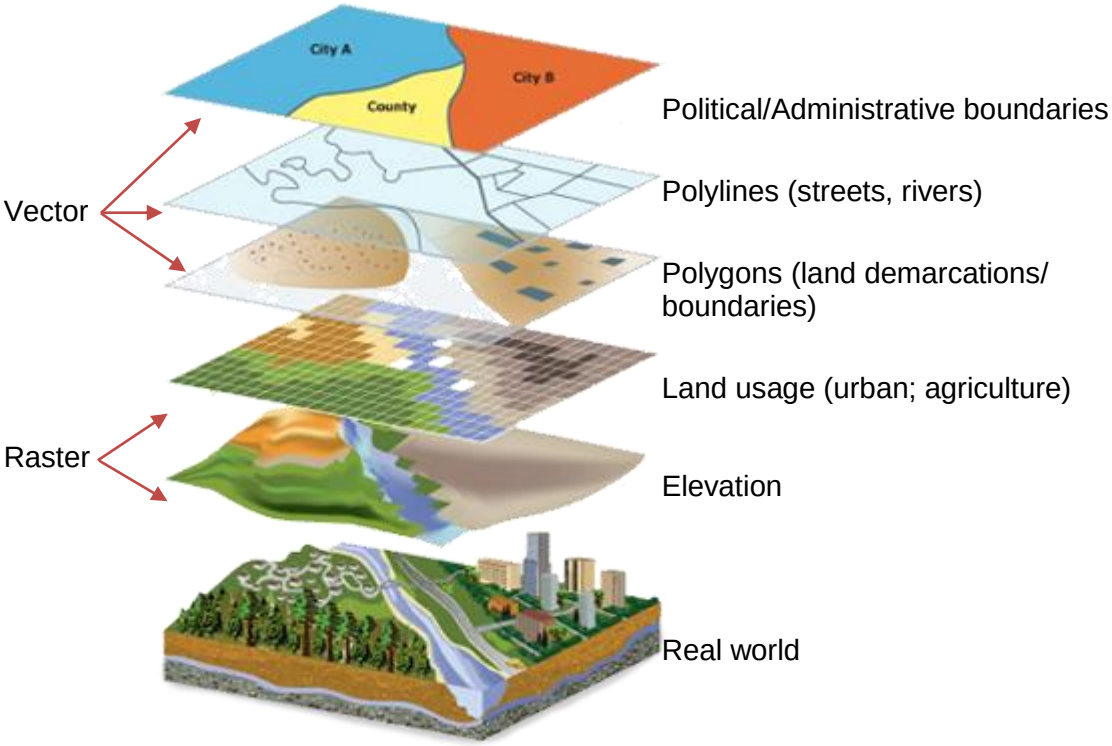

https://www.esri.com/arcgis-blog/wp-content/uploads/2018/02/05-fig-5-4-v2.png

Figure 2.9: Raster and vector layers used to create various representations of the “Real World” (Campbell & Shin, 2017)

Through the combination of the combination of raster and vector data layers, a general o specific map type can be created to digitally visualise the real world as illustrated in Figure 2.9

2.12.2 Geospatial analysis of water chemistry in a river system

Geospatial analysis, maps and pollution indices to show potential health hazards can be derived from ArcGIS-10.5 software developed by ESRI (Shil & Singh, 2019). GIS is an important tool that can be used to convert and store spatial information and distributions in a digital mapping format. In fact, this demonstrates the importance of GIS as a tool to use for spatial representation and analysis of the desired study area. Bu *et al.* (2014) studied the effects of the agricultural and industrial activities has on the Taizi River over the last 10 years. The authors also stated that there was severe pollution of the river and its major tributaries, particularly areas where domestic and industrial pollution was prominent. Lastly, the authors pointed out that these land use activities may lead to nonpoint source pollution, especially during the rainy season.

To develop these spatial distributions of nutrients, pollutants and metals in water systems, data from several sampling points needed to be obtained (Wijesiri *et al.*, 2019). One application of this is to use the data factors of the river water with given latitude and longitude coordinates. With these data, spatial (raster) maps can be created to visualise any type of variation in the nutrients and or metals. This approach was applied by Wijesiri *et al.* (2019) by using the data to create a raster map to visualise the spatial correlation from distance and direction of associated sampling points. Some studies on water chemistry in river systems make use of thematic maps to visualise the distribution of pollutant distribution. Bashir *et al.* (2020) created a thematic map of the river system through an interpolation technique of inverse distance weighting (IDW) to create a water quality index. Through the combination of vector (point, line and polygon) and raster (thematic) maps, it is possible to create a geospatial analysis of water chemistry.

2.12.3 Inverse Distance Weight Interpolation

The impact of water chemistry and the effect it has on the environment can be shown with the aid of geospatial applications like GIS. Madhloom *et al.* (2017) reported that one of the advantages of using GIS to observe water quality is that GIS provides spatial and temporal characteristics when monitoring these parameters. To accommodate the unknown location and distance values between the known data points, the Inverse Distance Weight (IDW) technique can be applied. The reasons for using the IDW interpolation technique is that it ensures that the data estimation, especially pertaining to rivers, is as accurate as possible.

Borges *et al.* (2018) mathematically explained the IDW method. The concept behind the IDW method accounts for the spatial interpolation procedures for the given data. The method also

calculates the cell values, utilising a linearly-weighted combination, when the data has a continuous set of sample points (Lu & Wong, 2008). The IDW formula is mathematically expressed (Equation 2.2), and used to estimate the unknown variable $\boldsymbol{Z^{(S_0)}}$ from the monitoring stations. The $\boldsymbol{n}$ variable is used for the number of stations when looking at the observed values $\boldsymbol{Z(Si)}$ (Lu & Wong, 2008; Madhloom *et al.*, 2017).

$$Z^{(S_0)} = \sum_{i=1}^{n} W_i Z(S_i) \tag{2.2}$$

The weight (Wi) is expressed as follows:

$$W_i = \frac{doi}{\sum_{\iota}^{n} doı^{-\alpha}} \tag{2.3}$$

With:

$$\sum_{i}^{n} Wi = 1 \tag{2.4}$$

Every data measurement is multiplied (Equation 2.3) by the inverse of the distance $doi \geq 0$**.** The distance $\boldsymbol{d}$ is multiplied with the end station $\boldsymbol{o}$ and with the initial station i with $\boldsymbol{\alpha}$ exponent. Then each product is divided by the sum of the term $\boldsymbol{1/doi - \alpha}$ over all the stations $\boldsymbol{i}$ so that the sum of all Wi's for a non-sampled station will be unity (Equation 2.4). The power $\boldsymbol{\alpha}$ of the distance must be chosen appropriately depending on the interpolated variable.

2.13 Land use and microbial contamination

Numerous studies have indicated that land use/land cover has a significant impact on faecal contamination in water (Liang *et al.*, 2013; Long & Plummer, 2004; Vereen *et al.*, 2013; Viau *et al.*, 2011; Wu *et al.*, 2016). Land use and cover changes can be documented and interpreted using remote-sensing data and aerial photographs. An important driver of any water contamination is hydrological runoff (Esselman *et al.*, 2018).

Land use maps are generally used to substantiate sources of microbial contamination originating from contributors of faecal matter to water sources. For example, Wu *et al.* (2016) mentioned that land use components were associated with *Methanobrevibacter smithii* which is an indicator of human-source contamination of septic tanks during wet weather events. There was also a positive correlation between human-specific *Bacteroidetes*, and sampling sites located downstream of wastewater treatment plants during dry seasons (Wu *et al.*, 2016).

Microbial contamination can be a powerful means of portraying the fate and interactions of quantifying faecal indicator organisms (FIO) (Oliver *et al.*, 2016). Visually representing microbial contamination may also further the understanding of the population dynamics of *E. coli* in different farm practices, but visualising the fate of faecal indicator organisms in a geospatial context poses many challenges (Coffey *et al.*, 2007). Oliver *et al.* (2016) explain these challenges as a result of an inadequate understanding of FIO behaviour in the environment when compared with agricultural pollutants such as phosphorus (P) and nitrogen (N).

2.14 Summary of the literature review

South Africa is a water-scarce country, and this precious resource needs to be protected to ensure that it can be used by future generations. The literature review listed the aspects of water quality in a broad sense for this study. Water quality data are usually represented as a separate database. The literature review listed the use of GIS to represent these databases geospatially in a South African context, with a specific focus on the Loopspruit River in the North West Province. Within this particular study area, the possible influences and uses of the Loopspruit River were explained and how that potential contaminant can travel in the Loopspruit River.

The water quality of the Loopspruit River includes studying physico-chemical and microbiological parameters. Furthermore, each of the parameters were presented and the need to evaluate them. The section that follows lists the reasoning for the possible methods that were considered. This included characterising of microbial isolates followed by molecular identification. Additional water quality testing was performed to determine baseline antibiotic resistance profiles of the Loopspruit

River and to quantify the antibiotic compound concentrations within the Loopspruit River. The bacterial diversity also served as an indication of the basic microbial profiles in the Loopspruit River.

In the literature study, possible visualising tools to predict and visualise water quality on a geospatial level were reviewed. The geospatial visualisation enables one to represent the water quality on a bigger scale than in tables and charts. By analysing the physico-chemical and microbiological parameters of water quality on a geospatial level, the overall water quality of the Loopspruit River can give a holistic perspective for better water management strategies so ensure that water quality is sustainable to support future generations.

CHAPTER 3: MATERIALS AND METHODS

The methodology consists of physical, chemical and microbiological analysis of the Loopspruit River with the aid of a geospatial analysis of the anthropogenic activities in the surrounding areas.

3.1 Study area

The Loopspruit River is considered a secondary river system. Sampling locations are shown in Figure 3.1 stretching from notable sites, such as the town of Fochville, to Klipdrift Dam, and finally to Potchefstroom. Aerial photographs were used to aid in the selection of the sampling locations. Samples were taken near a Wastewater Treatment Plant (WWTP) and near mine tailings (Table 3.1).

Table 3.1: Sample site location with the site description

Sample Site		Name	Latitude*	Longitude*	Characteristic
1	MU01	Mine tailings (before)	-26,438	27,5	Upstream of mining activities.
2	MD02	Mine tailings (after)	-26,479	27,538	Downstream of mining activities.
3	KW03	WWTP	-26,499	27,46	Wastewater treatment plant. Informal settlement. Urban activities
4	TS04	Taaibosch Spruit	-26,522	27,377	Agriculture (maize, cattle, pigs)
5	KA05	Kaalplaats turnoff	-26,558	27,344	Agriculture (maize, cattle)
6	KD06	Klipdrift Dam	-26,62	27,298	Dam outflow. Agriculture (maize, sunflower)
7	VA07	Vereeniging turnoff	-26,665	27,197	Agriculture (maize, sunflower, chicken)
8	GP08	Potchefstroom (Grimbeek Park)	-26,72	27,137	Urban and industrial activities

*coordinates in decimal degrees

3.2 Geographic information systems

This study utilised GIS data to analyse the sub-catchment area of the Loopspruit River in the North West Province of South Africa to create a map of the agricultural, mining and other possible anthropogenic factors relevant to this study. The data were used to explain the trends in the historical physico-chemical and microbiological observations.

3.2.1 Geospatial analysis

The geospatial analysis was carried out as a desktop analysis by using the data from a digital database from the North-West University (NWU). The analysis was based on the data obtained from the NWU database containing data of the NASA: ASTR 90m Digital Elevation Dataset; DEA: 2013 – 2014 SA National Land Cover Dataset; DWAF: Hydrology – Dams and SANBI: NFEPA River Network. The land use map was obtained from the WRC Report No K5/2347//3 (Bezuidenhout *et al.*, 2017)

3.2.1.1 Map creation

With the databases mentioned in Section 3.2.1, these were used to create a map of the sampling sites and the geological map.

The sampling map was created in ArcMAP. Firstly, three dataframes were created to create the two smaller inset maps and the one primary map of the sampling sites. The two inset maps included a map of the entire South Africa with the highlighted area of interest, and a “zoomed in” map of the North West and Gauteng Provinces. These were done by importing the vector data layer to show the polygonal border demarcation of the different provinces within South Africa. The same was done for the primary map. Layered above that, in the primary map, is the imported sample points and monitoring stations as an Excel (.xls) file. These points were imported using the “display as X Y coordinates” function. The DWAF: Hydrology – Dams databases were used to search for the vector data layers for rivers. The data were searched to create a visual vector line to represent the Loopspruit River. The datum of the map is WGS 1984. The vector lines and points were ladled according to their names. Sample sites were labelled with their names, the monitoring sites according to their DWA names.

The geological map has only one primary data frame that shows the geology across the Loopspruit River area. The bottom layer of the map is an imported polygonal vector layer containing the different geological composition data. However, when this layer is imported ArcMAP designated this layer to a monochromatic colour. Therefore, the layer data were automatically sorted by the ArcMAP programme to allocate every geological unit to its own colour.

This resulted in a multicoloured geological map to make it easier to distinguish between the various geologies. Moreover, there were three additional layers over the geological layer to show the Loopspruit River, sample points and the provincial boundaries.

3.2.1.2 Inverse Distance Weight (IDW) interpolation

A Spatial Analyst Tool in ArcGIS Desktop 10.5 was used to do an Inverse Distance Weighted (IDW) interpolation. The time-series data (concerning each physico-chemical parameter) of each monitoring stations were condensed, stacked in other words, to a single weighted value and geographically placed to where the monitoring station is situated. It is difficult to visualise every time-based data entry on a geospatial scale. It is for this reason that the IDW interpolation was chosen.

The IDW interpolation assigns values to unknown points between the data points which were calculated with the weighted average of the values available at the known points. This interpolation analysis was done within the ArcGIS Desktop 10.5 processes and resulted in a raster layer format of the interpolation. Then, a polygon was created in the shape of the Loopspruit River and saved as a layer file. The resulting IDW interpolation layer was then clipped in the shape of the Loopspruit River polygon. Finally, the clipped IDW interpolation layer was overlaid on top of a base map provided by the online ESRI database map import option.

3.2.2 Visually representing microbial point source pollutions

The water samples that were filtered and placed on the selected bacterial media were counted and recorded. The sampling sites were then allocated to the dominant land use. MU01, MD02 and GP08 were urban; TS04, KA05, and VA07 were agriculture; KW03 was WWTP and KD06 was Klipdrift Dam. The sample sites' recorded microbial counts with their respective land uses were used to calculate the average of the *E. coli* and *Enterococci* contributions by the point source pollution land uses. These averages were then visualised in GraphPad Prism (version 8.0.0 for Windows, GraphPad Software, San Diego, California USA, www.graphpad.com). *Clostridium* spp. were not added to the faecal contamination visual representation the reason being that the colony counts were too minimal to show up as a visual representation and were therefore omitted.

3.3 Sampling

Samples were taken in triplicate for the duration of the study (2018 – 2019). In the first year, sampling occurred during the wet season, April-May 2018, and then again in the dry season, July 2018. In the second year of the study (2019), sampling took place in the wet season of April – May, 2019 and the dry season of June – July, 2019.

During the sampling process, one-litre Schott-Duran bottles were used. Where access to surface water was difficult a length of rope was tied around the neck of the Schott-Duran bottle. The bottle could be manoeuvred to some extent to collect the water sample in some hard-to-reach places. Certain analyses were done at the sampling location, as will be discussed below in Section 3.4. The samples were immediately stored on ice in cooler boxes and transferred to the North-West University (NWU) microbiology laboratories. All the remaining analyses were conducted within eight hours of sample collection. The water samples were filtered, and the filters were stored at -85°C until needed for eDNA extraction.

3.4 Physico-chemical and microbiological parameters

3.4.1 Physico-chemical parameters

During sampling, a calibrated multi-meter probe (Oakton PCStestr™ 35 Thermo Fisher Scientific, US) was used to determine specific physical parameters such as the temperature (°C), electric conductivity (mS/m), pH (dimensionless) and total dissolved solids (mg/L). After each measurement, the probe was rinsed with distilled water.

The chemical constituents of the sample, such as nitrites (NO_2): 8153, nitrates (NO_3): 8039, sulphides (SO_3): 8131, sulphates (SO_4): 8051, phosphate (PO_4): 8048 and the chemical oxygen demand (COD): 8000, were determined at the NWU laboratories, using a Hach instrument (HACH DR 2800)™ (HACH, US) and reagents.

3.4.2 Microbiological parameters

3.4.2.1 Enumeration of indicator bacteria

Faecal streptococci, *E. coli,* total coliform and faecal coliforms were enumerated via the membrane filtration method. Triplicate samples (100 mL) were filtered through 0.45 µm pore size membrane filters with a diameter of 47 mm [(PALL Life Sciences, Mexico) (CAT No: GN-6 Metricel Membrane 66191)]. These filters were aseptically placed on selective agar media such as m-FC

agar (Merck, Germany), MLG agar (Oxoid, UK), and KF-Streptococcus agar with an added supplement of 1 mL of 2,3,5-Triphenyltetrazolium chloride (TTC) per 100 mL of media (Sigma and Aldrich, Germany). TTC was added to KF-Streptococcus agar media at a temperature of 60°C.

The filters placed on the m-FC agar plates were incubated at 44.5°C for 18 – 24 hours. The filters on the MLG agar plates were incubated at 37°C for 18 – 24 hours, and the KF-Streptococcus agar media were incubated at 37°C for 48 hours. After incubation, blue and yellow colony growth on m-FC agar plates was counted. Yellow colonies represented total coliforms and blue colonies faecal coliforms. The green colonies on MLG agar plates (*E. coli*) were counted, and light pink or flat dark red colonies on the KF-Streptococcus agar were presumptively represented as enterococci. Colony numbers were recorded, and colony-forming units (CFU) per 100 mL calculated.

3.4.2.2 Incubation and isolation of *Clostridium*

Clostridium is an anaerobic micro-organism and had to be cultured in capped test tubes (16 mm x 125 mm; Pyrex) filled with 7 mL of double-strength *Clostridium perfringens* agar base. After autoclaving, the test tubes were cooled to approximately 50°C, and 1 mL of water sample and 32 µL of TSC supplement with D-cycloserine (Oxoid; UK) were mixed with the agar in the test tube. An autoclaved glass inserter tube with a diameter of 8 mm was inserted into the test tube with the liquid content and sealed with the screw-cap to ensure anaerobic conditions. This was done in triplicate for each water sample taken, a total of 24 test tubes for each sample period. The sealed test tubes were incubated at 44°C for six hours (longer incubation will result in overgrowth). After incubation, black colonies were counted and documented as CFU/mL. Numbers exceeding 300 colonies were recorded as too numerous to count (TNTC) and given a value of 300 for statistical reasons. (White *et al.*, 2010).

To isolate *Clostridium* spp. the contents of the Fung double tubes were emptied into a sterile petri dish, and black colonial growth was pierced with a sterile wooden pick. The pierced colonies served as the culture to prepare streak plates of the culture, on TSC agar plates. To ensure that the streak plates could grow in anaerobic conditions, the plates were placed in an AnaeroJar (AG0025; Oxoid), with an AnaeroGen sachet (AN0025; Thermo Scientific) and an anaerobic indicator (BR0055B; Oxoid). The AnaeroJar and the plates were incubated for 24 hours at 44°C. These streak plates were sub-cultured three times on Reinforced Clostridia agar to ensure that the bacterial cultures were pure enough for further analysis.

3.4.2.3 Enumerating heterotrophic plate count bacteria

To enumerate the Heterotrophic Plate Count (HPC) bacteria, a dilution series (to 10^{-10}) was made of each of the water samples. Each of the dilutions was aseptically spread onto R2A agar plates (Becton, Dickinson & Company, France) and incubated at room temperature (approximately 23°C) for seven days. After incubation, the total colony growth of each dilution was counted and documented. Colony numbers were converted to CFU/mL. For further antibiotic and molecular studies, various morphologically different colonies, be they different in colour, shape or form, were aseptically streaked onto R2A agar plates. To ensure purity, the selected bacterial cultures were successively streaked (at least three times) on R2A agar plates.

3.4.2.4 Primary characterisation and biochemical screening of faecal enterococci, *Clostridium* sp. and HPC bacteria

3.4.2.4.1 Gram staining

The first step in any microbial characterisation is to distinguish between Gram-positive (G+) and Gram-negative (G-) bacteria and to ensure the purity of the enterococci isolates. A Gram stain was performed by preparing a bacterial smear on a glass slide and heat-fixing it before staining it with crystal violet for one minute. The crystal violet was rinsed off with distilled water. Secondly, Gram iodine was dropped onto the smear and left for one minute before rinsing it off with distilled water. The smear was de-stained with ethanol (96%) for 10 seconds and again rinsed with distilled water. Finally, the counterstain safranin was applied to the smear for one minute and rinsed off with distilled water once more. Schleifer and Kilpper-Balz (1984) described faecal streptococci as Gram-positive, elongated, ovoid-shaped cells in pairs or short chains. The presumptive result for faecal enterococci is deep purple-stained pair and short-chain cocci.

The same procedure for Gram staining was followed for the characterisation of HPC bacteria and *Clostridium* spp. However, *Clostridium* was also tested for endospore formation by using the Schaeffer and Fulton's method for endospore staining. *Clostridium* is a rod-shaped, Gram-positive endospore producing bacteria (Willey *et al.*, 2011a).

3.4.2.4.2 Catalase activity

Obligate aerobes and facultative anaerobes, such as enterococci, can produce enzymes such as catalase and peroxidase (Rolfe *et al.*, 1978). These enzymes enable chemical reactions like hydrolyse, where hydrogen peroxide (H_2O_2) is converted into water and free oxygen as end products. To test for catalase activity in *Enterococci*, a cleaned microscope slide was used.

Bacterial isolates that produced gas after exposure to 3% H_2O_2 were catalase positive. It is known that faecal streptococci (*Enterococci)* are catalase-negative.

3.4.2.4.3 Triple sugar iron test

The Triple Sugar Iron (TSI) agar (Merck, Germany) test was used to confirm the presence of *E. coli.* Purified presumptive *E. coli* isolates were inoculated with a stab and streak (continuous S-shaped streak) technique, in a TSI agar slant, using an inoculation needle. Slants were incubated at 37°C for 18 – 24 hours. A colour change in the agar slant from red to yellow was documented as well as gas production inside the test tube. When a black precipitate was present, this was indicative of Hydrogen sulphide (H_2S) production.

3.4.3 Antimicrobial susceptibility testing

Antimicrobial susceptibility testing was done by using the Kirby-Bauer disk diffusion technique. Overnight bacterial cultures from the HPC plates were used to inoculate Mueller Hinton broth (Merck, Germany). Standard discs were used to detect and measure the induced inhibition of specified antibiotic concentrations placed on Mueller–Hinton agar. The antibiotic disks used included ampicillin (10 µg), amoxicillin (10 µg), streptomycin (300 µg), oxy-tetracycline (30 µg), vancomycin (30 µg), penicillin G (10 µg), neomycin (30 µg), ciprofloxacin (5 µg), trimethoprim (2.5 µg), chloramphenicol (30 µg), sulfamethoxazole (25 µg) and colistin (10 µg). All antibiotics were obtained from Mast Diagnostics (UK). The plates were incubated for five days at room temperature (24 – 28°C). After incubation, the inhibition zone diameter was measured in millimetres (mm). The inhibition zones were interpreted as susceptible (S), intermediate (I) or resistant (R) when compared with EUCAST (2017).

All the bacteria that showed resistance or susceptibility were recorded. The resistant bacteria were set apart from the rest so that molecular tests could be performed on them to identify the resistant genes (Section 3.4.6).

3.4.3.1 Determining multiple antibiotic resistance

A Multiple Antibiotic Resistance (MAR) index serves as a means to indicate the resistance a microorganism has to a panel of antibiotics (Krumperman, 1983). This index calculated with Equation 3.5 generates a numerical value that indicates the state and resistance of an individual organism or environmental water sample.

$$MAR\ index = \frac{a}{(b \times c)} \quad (3.5)$$

Where:

a = total amount of bacterial isolates resistant to antibiotics; b = number of antibiotics tested for; c = number of isolates in the HPC sample (morphologically distinct isolates from the eight sample sites).

Isolates were classified as susceptible (S), resistant (R) or intermediate resistant (I). Furthermore, (I) and (R) isolates were used in the calculation as being resistant to antibiotics.

3.4.4 Quantification of antibiotic concentrations

3.4.4.1 Extraction of antibiotics from environmental water samples

The collected 1 L water samples were spiked with a mix of internal standards (IS) and left at room temperature. The IS mix consisted of deuterated compounds (-d3; -d5; and -d8) used to differentiate the from the compounds used in the lab and the compounds that occur in the environment. Trimethoprim-d3, ampicillin-d5 and ciprofloxacin-d8 were used to represent various antibiotics. Trimethoprim-d3 were used for trimethoprim, erythromycin and tetracycline; ampicillin-d5 were used for ampicillin and ciprofloxacin-d8 for ciprofloxacin. An automated solid-phase extraction system (SPE-DEX 4790; Horizon) was used. The specialised extraction disk holders were assembled as follows: first, the methanol cleaned metallic mesh, Oasis HLB-L cartridge disks topped with a one-micron pre-filter were placed on the disk holder. Then a collection vial was attached below the collection extraction disk holder. The water sample bottles used a specialised cap covered with foil and sealed. This was then fastened to the SPE-DEX for filtration and extraction to start.

The methods laid out by Ferrer and Thurman (2012) were followed. After initiating the solid-phase extraction on the preloaded computer programme, the disks were conditioned twice with methanol and left to soak for 30 seconds and to air dry for 15 seconds between each step. A final conditioning step allowed for the twofold conditioning, for 10 seconds with nanopure water and two-second air dry between steps. The water samples passed through the SPE system and left for a 15-minute air dry. The antibiotics were eluted in three methanol cycles, consisting of soaking the disk with methanol for 3 minutes and air-drying for 20 seconds. The final methanol eluation consisted of a one-minute soak and a one-minute air dry. The eluates were evaporated to near dryness with nitrogen gas at 35°C and reconstituted with 1 mL acetonitrile: water (50:50 ACN: H_2O). The samples were concentrated 1000 times.

3.4.4.2 LC/Q-TOF/MS targeted analysis

The extracts were analysed by ultra-high-pressure liquid chromatography (UHPLC, Agilent 1290 series) coupled to a quadrupole time of flight mass spectrometer (Q-TOF/MS, Agilent G6540A). The target list of antibiotic compounds included: Ampicillin, Ciprofloxacin, Erythromycin, Tetracycline and Trimethoprim. Each of these compounds was identified using retention time and m/z values (Table 3.3). Samples were run in positive ionisation mode using the LC and QTOF parameters listed in Table 3.2. The scanning parameters of the QTOF were set at 50 to 950 m/z and with an extended dynamic range of 2 GHz. This was analysed via MassHunter Data Acquisition (version B.05.00) and MassHunter Quantitative Analysis (version B.05.01) software. Mass axis calibration of QTOF was performed daily for reliable results with tuning mixes (G1969 – 85000, Agilent). A reference solution with masses of 121.050873 [M+H] and 922.009798 [M+H] was continuously infused as an accurate mass reference.

Table 3.2: LC and Q-TOF parameters

Parameters	**Positive ionisation**	
Injection volume	1 µL	
Column	Poroshell 120 Bonus-RP column (Agilent, 2.1 x 100 mm, 2.7 µm)	
Column temperature	25 ˚C	
Flow rate	0.2–0.6 mL/min	
Mobile phase A	Water + 0.1% formic acid	
Mobile phase B	ACN + 0.1% formic acid	
Gradient (min)	**A (%)**	**B (%)**
0	95	5
2.0	95	5
2.05	85	15
5.55	85	15
5.60	80	20
11.1	80	20
11.15	75	25
13.15	75	25
13.20	65	35
17.20	65	35
17.25	0	100
20.0	0	100
20.05	95	5
Total run-time	20.05 min	
Drying gas temperature	275 °C	
Drying gas flow	10 L/min	
Nebuliser pressure	45 psi	
Sheath gas temperature	400 °C	
Sheath gas flow	10 L /min	
VCap	3000 V	
Nozzle voltage	0 V	
Fragmentor	130 V	
Skimmer	48 V	
OCT RF Vpp	750 V	

Table 3.3: Retention times and m/z values of the target antibiotics and the internal standards analysed.

	Compounds	Retention time (min)	m/z
Antibiotics	Ampicillin	3.4	350.1216
	Ciprofloxacin	3.4	332.1446
	Erythromycin	9.0	734.4701
	Tetracycline	3.15	445.1649
	Trimethoprim	3.2	291.1473
IS	Ampicillin-d5	3.4	355.1185
	Ciprofloxacin-d8	3.4	340.1394
	Trimethoprim-d3	3.2	294.1473

IS=Internal Standard

3.4.4.3 Limit of detection (LOD)/Limit of quantification (LOQ)

A calibration curve using standards in methanol was used for quantification, and the linear range for each compound is listed in Table 4.7 in Section 4.3.2. A calibration curve was used to calculate the LOD and LOQ for the method. By using of the y=mx+c, LOD is calculated with Equation 3.6 and LOQ with Equation 3.7; where $\boldsymbol{Sa}$ is the standard deviation of the intercept (abundance) and $\boldsymbol{b}$ is the slope of the calibration curve (Schoeman *et al.*, 2015). Linearity is assessed using the R-square of the calibration curve (Equation 3.8). All the compounds had an R^2 of 0.9 or better for all the analyses, indicating excellent linearity.

$$LOD = 3 \times \frac{Sa}{b} \tag{3.6}$$

$$LOQ = 10 \times \frac{Sa}{b} \tag{3.7}$$

3.4.4.4 Data analysis

The concentration of antibiotics was determined by using Equation 3.8:

$$X_{antibiotic} = \frac{\left(\frac{native}{stable\ isotope}\right) - c}{m} \times ISO_{conc} \quad (3.8)$$

where:

$X_{antibiotics}$ = calculated analysed concentration.

Native = native abundance.

Stable isotope = stable isotope abundance.

c = calibration curve y-intercept.

m = slope of calibration curve.

ISO concentration = internal standard concentration.

The risk that the antibiotics might contribute to the process was calculated with the risk selection index as explained by Tran *et al.* (2019) and is expressed as follows in Equation 3.9.

$$RQ_{AMR} = \frac{MEC_{AMR}}{PNEC_{AMR}} \quad (3.9)$$

Where:

RQ_{AMR}: Risk Quotient of the antibiotic.

MEC_{AMR}: Measured Environmental Concentration of the antibiotic.

$PNEC_{AMR}$: Predicted No Effect Concentration of the antibiotic.

3.4.5 DNA isolation, amplification and identification

This section describes the DNA isolation, amplification and identification of the faecal enterococci, *Clostridium* spp., *E. coli* and HPC isolates. It includes the determination of bacterial resistant genes.

3.4.5.1 DNA isolation

DNA isolation from presumptive *E. coli,* enterococci and HPC isolates was carried out using a Chemagic DNA bacteria kit (PerkinElmer, Germany). The isolation protocol provided by the manufacturer was used as a guide to obtaining genomic DNA. After the DNA had been isolated, the quality (A_{260nm}: A_{280nm}) and concentrations were determined by using a NanoDropTM 1000 Spectrophotometer (Thermo Fischer Scientific, US).

The DNA extraction for the *Clostridium* sp. isolates was done as follows: a single colony from the *Clostridium* spp. streak plates was inoculated into nutrient broth and incubated at 44°C for 24 hours. Then 20 µL of the inoculated broth was transferred to a 1.5 mL microfuge tube and centrifuged (4000 rpm; for 15 seconds) to collect bacterial cells at the bottom of the tube. The supernatant was removed, and the pellet resuspended in 20 µL MilliQ. The tubes were placed in a microwave for two minutes at full power (700 W) and centrifuged again (12800 rpm; for two minutes) to allow the cell debris to accumulate at the bottom of the tube. Finally, 2 µL of the supernatant containing DNA was used for subsequent PCR reactions.

3.4.5.2 DNA amplification

eDNA and DNA extracted in Section 3.4.5.1, as amplified by PCR. The PCR mixture included 8.5 µL RNase/DNase free water H_2O (Fermentas Life Sciences, US); 12.5 µL 2x PCR Master Mix (0.05 U/µL Taq DNA Polymerase in reaction buffer, 0.4 mM of each dNTP, 4 mM $MgCl_2$) (Fermentas Life Sciences, US); 1 µL of each primer 27F5'-AGAGTTTGATCMTGGCTCAG-3' and 1492R 5'-CGGTTACCTTGTTACGACTT-3' (Jordaan & Bezuidenhout, 2016) for the presumptive *E. coli* and HPC isolates. The primer pair used for the enterococci isolates was 1 µL 341F 5'-CCTACGGGAGGCAGCAG-3' and 907R 5'-CCGTCAATTCCTTTGAGTTT-3' (Muyzer *et al.*, 1993), respectively. Finally, with the addition of 2 µL template DNA, the final volume of the PCR mix was 25 µL. The PCR was done with the ICycler Thermocycler (Bio-Rad, US), with an initial denaturation at 95°C for 300 seconds followed by 35 cycles of denaturation, annealing and extension for 30 seconds at 95°C, 30 seconds at 52°C and 60 seconds at 72°C, respectively. The final extension was done at 72°C for 180 seconds.

3.4.5.3 Agarose gel electrophoresis

The integrity of the extracted DNA and PCR products was determined by agarose gel electrophoresis. Three µL of PCR product were mixed with 2 µL of Orange Loading Dye (Thermo Scientific; US) containing GelRed (Biotium, US). The PCR mix was loaded on a 1.5% (w/v) agarose gel. A one µL of the 100 bp molecular weight marker (O'GeneRuler, Fermentas Life Sciences, US) was used as a size marker. Electrophoresis was done at 80 V for 45 – 50 minutes in 1 x TAE buffer. Gene Bio Imaging System (Syngene, Synoptic, UK). GeneSnap software (version 6.00.22) was used to adjusted images to show band contras.

3.4.5.4 Sequencing and identification

3.4.5.4.1 First clean-up for sequencing

All residual primers and primer dimers were removed from the PCR products with the AMPure XP beads. The beads were vortexed for 30 seconds to ensure that they were evenly dispersed. Then 20 µL AMPure XP beads were transferred to the PCR tubes containing PCR products and mixed thoroughly by pipetting up and down followed by incubation at room temperature for 5 minutes. The PCR tubes were placed on a magnetic stand, and all the supernatant was removed and discarded. The beads were washed by adding 200 µL 80% ethanol and incubating for 30 seconds. The supernatant was again removed. The beads were allowed to air dry for 10 minutes on the magnetic stand. The PCR tubes were removed from the magnetic stand and 52.5 µL of 10 mM Tris (pH 8.5) added and mixed by pipetting up and down. The PCR tubes were incubated for two minutes at room temperature and placed back on the magnetic stand. Finally, 50 µL of the supernatant was collected and placed in a clean sterile PCR tube.

3.4.5.4.2 Second clean-up

The final purifying process was done using a ZR (Zymo Research) Sequencing Clean-up Kit (The Epigenetics Company, US) as per the manufacturers instructions. A Cycle Sequencing BigDye Terminator Kit (Zymo Research, US) was used to perform PCR sequencing. The reaction mixture consisted of 4 µL 1:10 dilution Ready Reaction Premix (2.5x), 2 µL BigDye Sequencing Buffer (5x), 3.2 pmol 27F/1492R primers (Inqaba Biotech, SA), 1 µL template DNA (10 ng) and 12 µL of nuclease-free water (Fermentas Life Sciences, US) to make up a final volume of 20 µL. Cycling conditions for the thermocycler (Bio-Rad, US) were 96°C for the 1-minute initial denaturation, followed by 25 cycles of 96°C for 10 seconds, 50°C for 5 seconds and 60°C for 4 minutes. A Zymo Research DNA-Sequencing Clean-up kit™ (Zymo Research, US) was used to purify the sequencing PCR products following the manufacturer's protocol. Amplicons were sequenced in-house, using an ABI 3130 Genetic Analyser (Applied Biosystems, UK). Chromatograms were

obtained and viewed in Geospiza Finch TV software (version 1.4; http://www.geospiza.com/ftvdlinfo.html). The DNA sequence information was compared with the GenBank database using the Basic Local Alignment Search Tool (BLAST) (http://www.ncbi.nlm.nih.gov/BLAST) and with the EzTaxon database (http://www.ezbiocloud.net) to determine the identity of the amplified sequences.

3.4.5.5 Illumina MiSeq sequencing

Microbial genomic DNA was obtained from membrane filters and normalised to a concentration of ≤ 10 ng/µL. The sequence library preparation guide was followed as per the manufacturer's instructions (Illumina Inc.). Microbial diversity was determined using the 16S rRNA gene (V3–V4) region (≈460 bp) analysis with locus-specific primers 341F (5´-CCTACGGGNGGCWGCAG-3´) and 805R (5´- GACTACHVGGGTATCTAATCC-3´) (Herlemann *et al.*, 2011). Illumina forward and reverse overhang adapters (Illumina Inc., CA, USA) were attached to the 5´-end of forward and reverse primers respectively. The Illumina MiSeq sequencing run, de-multiplexing and secondary analyses of the reads were done with the MiSeq reporter software (Illumina Inc., California, USA).

The QIIME2 pipeline was used to improve the quality of the Next Generation Sequencing (NGS) data by eliminating the effect of random sequencing errors, deleting unreliable data from the libraries (q-value < 25) and removing reads shorter than 200 bp to classify the sequences to operational taxonomic units (OTUs) with 97% similarity. Taxonomic information of sequences by the Ribosomal Database Project (RDP) classifier for the 16S rRNA gene was assigned at a confidence cut-off of 0.5.

The output tables obtained from QIIME2 were cleaned through the R programming language to create the final OTU table to use for further analysis. From the table, a metadata and OTU file were created to generate results in a web-based tool MicrobiomeAnalyst (Dhariwal *et al.*, 2017). Here the alpha diversity was produced with the Chao1, and Shannon diversity indices and beta diversities were created with the Bray–Curtis dissimilarity distance distribution. The OTU data were also used for the metagenome analysis using PICRUSt (pronounced "pie crust") (Langille *et al.*, 2013).

3.4.6 Bacterial resistance genes

PCR amplification of the *intI1* and plasmid-mediated *AmpC* β-lactamase genes was done using the primers listed in Table 3.4. Every reaction tube contained 1 x PCR MasterMix (Thermo Scientific, USA), 0.4 µM of forward and reverse primers, 2 µL (~1.2 to 28.8 ng) of the different samples' template DNA, and nuclease-free water to a final reaction volume of 25 µL in each tube. The *intI1* PCR cycling conditions for the initial denaturation were set at 95°C for 300 seconds

followed by 30 cycles of denaturation at 94°C for 30 seconds, annealing at 64°C for 30 seconds and an extension at 72°C for 60 seconds. The final extension was at 72ºC for 300 seconds (Perez-Perez & Hanson, 2002). Plasmid-mediated *AmpC* β-lactamase amplification cycling conditions were an initial denaturation at 94°C for 180 seconds, followed by 35 cycles of denaturation at 94°C for 30 seconds, and annealing at 64°C for 30 seconds for the *ACC, CIT*, and *FOX* primers. Extension was at 72°C for 60 seconds. The final extension was at 72ºC for 420 seconds. The annealing temperature for *MOX* was 59ºC for 30 seconds.

Table 3.4: A tabulated list of the *AmpC* β-lactamase target gene primer sequences.

Target gene	**Primer**	**Primer Sequence (5'-3')**	**Product size (bp)**	**Reference**
intI1	*intI1*-F	CCTCCCGCACGATGATC	280	Ma *et al.*, 2019; Rajaei *et al.*, 2011
	intI1-R	TCCACGCATCGTCAGGC		
ACC	ACCMF	AACAGCCTCAGCAGCCGGTTA	346	Perez-Perez & Hanson, 2002; Zhang *et al.*, 2009
	ACCMR	TTCGCCGCAATCATCCCTAGC		
FOX-1 to *FOX-5b*	FOXMF	AACATGGGGTATCAGGGAGATG	190	Perez-Perez & Hanson, 2002; Zhang *et al.*, 2009
	FOXMR	CAAAGCGCGTAACCGGATTGG		
LAT-1 to *LAT-4, CMY-2* to *CMY-7, BIL-1*	CITMF	TGGCCAGAACTGACAGGCAAA	462	Perez-Perez & Hanson, 2002; Zhang *et al.*, 2009
	CITMR	TTTCTCCTGAACGTGGCTGGC		
MOX-1, MOX-2, CMY-1, CMY-8	MOXMF	GCTGCTCAAGGAGCACAGGAT	520	Perez-Perez & Hanson, 2002; Zhang *et al.*, 2009
	MOXMR	CACATTGACATAGGTGTGGTGC		

3.5 Statistical analysis

Data collection comprised field sampling and laboratory experiments and procedures. The data collected from the physico-chemical and microbiological tests were manipulated and processed in Microsoft Excel to calculate averages, means, and standard deviations.

R was used for all statistical analyses (R Core Team, 2013). Analysis of variance (ANOVA) was used to analyse the randomized complete block design, using each independent experiment as a block. Residuals were used to test for normality and equality of variances and log-transformed data where appropriate. Tukey's HSD (honest significant difference) test was used to determine which treatments were significantly different from each other.

Statistically significant differences in the physico-chemical generated data were analysed. Each set of historical, seasonal and sample location data was tested using contrasts performed with the glht function in the multcomp package (Kurenbach *et al.*, 2018) with a two-sided alternative and sequential Bonferroni procedure. These contrasts were fitted to an ANOVA model treating each combination of sampling seasons and sampling locations category.

Statistical analysis for the LC/MS data underwent descriptive statistics such as mean, standard deviation and correlation of variance per site and sampling event. Also, an ANOVA for normally distributed data or Kruskal Wallis for non-normally distributed to determine any differences in the average levels between sites/seasons.

Analysis of molecular variance (AMOVA) was applied in R with the extension of vegan library's bioenv() function that was used to find the best set of environmental variables with maximum (rank) correlation. Community correlation dissimilarities were plotted as vectors along with the best subset of taxas on the NMDS plot. This was done to test whether the spatial separation of the sampling locations visualized in the NMDS plots was statistically significant. Tukey's HSD was used as a post hoc test to determine which of the upstream vs. downstream groups and/or sites had a difference in variance. Only statistically significant variables ($p<0.05$) were selected for further analysis. Data were respectively $\log_{10}$-normalized, and z-score standardized before analysis.

Statistical analyses on community data were performed using rarefied and normalized data. The vegan package was used to calculate the range of diversity indices. Richness (i.e. observed OTUs) was determined with the Shannon index and Chao1 index as measures of alpha- diversity. Beta-diversity analyses involved clustering of samples using the Bray-Curtis distance metric. The resulting distance matrices were visualized using ggplot2 package creating a non-metric multidimensional scaling (NMDS).

Predicted metagenome analysis and microbial metabolic pathways were estimated based on the 16S rRNA gene data using PICRUSt v1.1.0. OTU abundances were mapped against the Greengenes (v13.8) database that achieved a 97% identity level. The rarefied OTU table was used to normalize the 16S rRNA gene copy number and was predicted from the normalized data. Predicted metagenomes were then inferred to KEGG Pathways and gene counts were normalized to relative abundance using predicted functional trait settings. PERMANOVA was used to test whether upstream and downstream bacterial communities harbour significantly different metagenomes.

CHAPTER 4: RESULTS

Surface water samples from the Loopspruit River were collected at publicly accessible locations in the North West and Gauteng Provinces of South Africa. There were eight sample sites, namely MU01, MD02, KW03, TS04, KA05, KD06, VA07 and GP08. All eight samples were collected using a “fishing” technique to account for the more difficult sample sites (see Figure 4.1).

The data are represented as follows: First, the physico-chemical data obtained during sampling during the wet and dry seasons were analysed. Secondly, the visual representation created for the physico-chemical parameters of the historical data was checked, and this was followed by microbiological data, including an overview of the microbial water quality levels, a visual representation to indicate how this contributes to faecal contamination. After that, the results obtained from testing the antibacterial resistances and their concentrations in the environment are presented. Then followed the results of DNA identifications of the isolates, the detection and quantification of resistant genes, and the determined bacterial communities. Finally, the physico-chemical and microbiological data were brought together via predicted metagenomic analysis. In this chapter, it is to be assumed that there were no significant differences in the data, meaning that there were no statistical differences ($p > 0.05$) unless otherwise indicated.

4.1 Sampling sites

Sampling sites were identified with the aid of GIS ArcMap 10.4, and aerial photographs resulting in Figure 4.1. The sample sites were chosen along the Loopspruit River with the related anthropogenic activities in mind. This includes feedlot locations, mining and agricultural activities, as well as wastewater treatment plants, which were observed via aerial photographs. The chosen sampling locations were close to public roads to ensure that there would be no trespassing on private property. Water samples were taken from the Loopspruit River in sterile one-litre glass Schott Duran bottles.

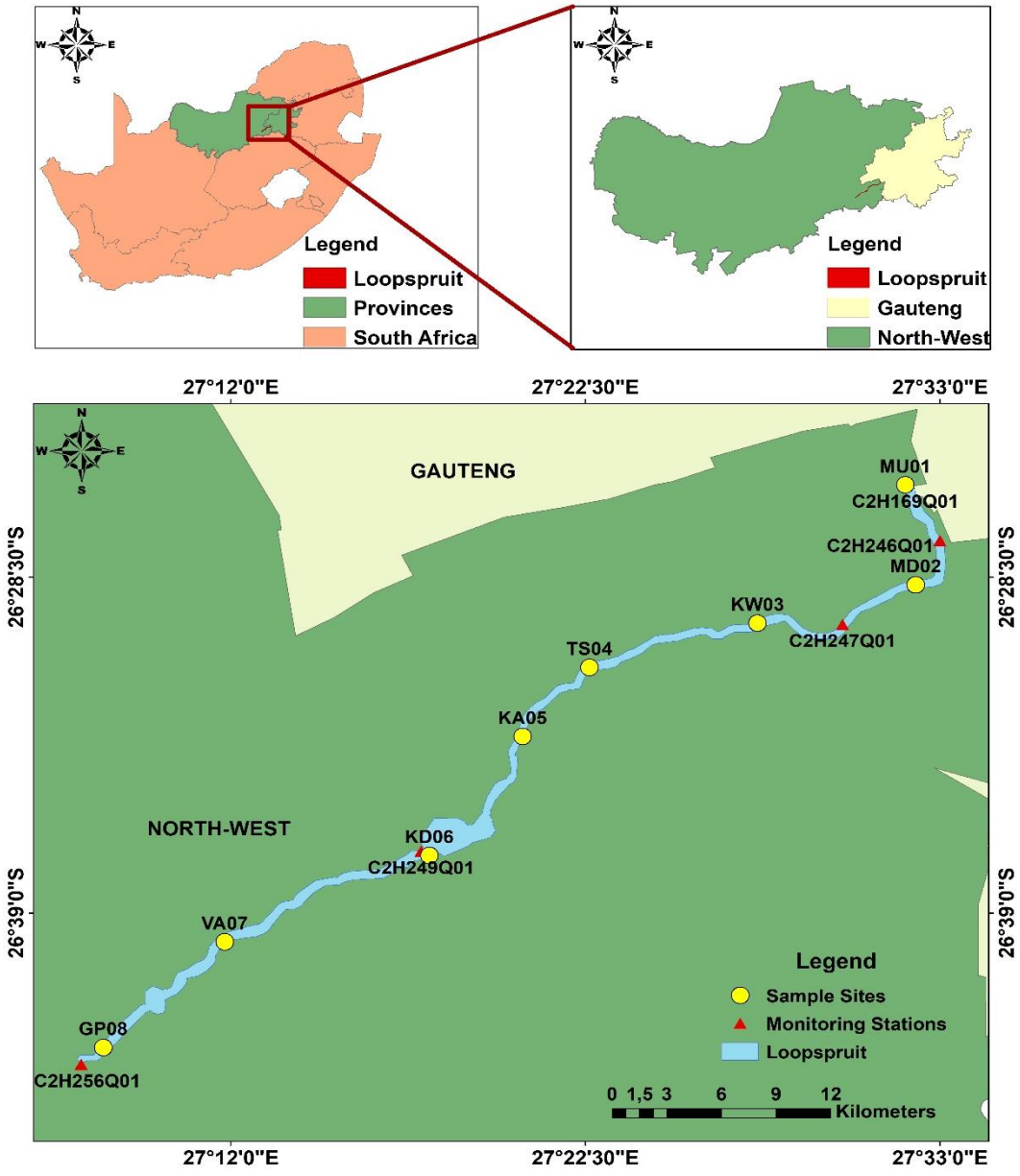

Figure 4.1: Sampling site map with the selected sampling sites accompanied with monitoring stations.

4.1.1 Site description

The major land covers (Figure 4.2) in this sub-catchment are natural (~65%), agricultural (~30%), urban (~3%) and wetlands (~1%). The urban land cover of approximately 3%, is in close proximity to the river, and therefore urban runoff may cause non-point pollution problems. The WWTP in the sub-catchment may cause some point source pollution, especially if the relevant infrastructure is outdated and/or inadequate and/or operated by unqualified operators.

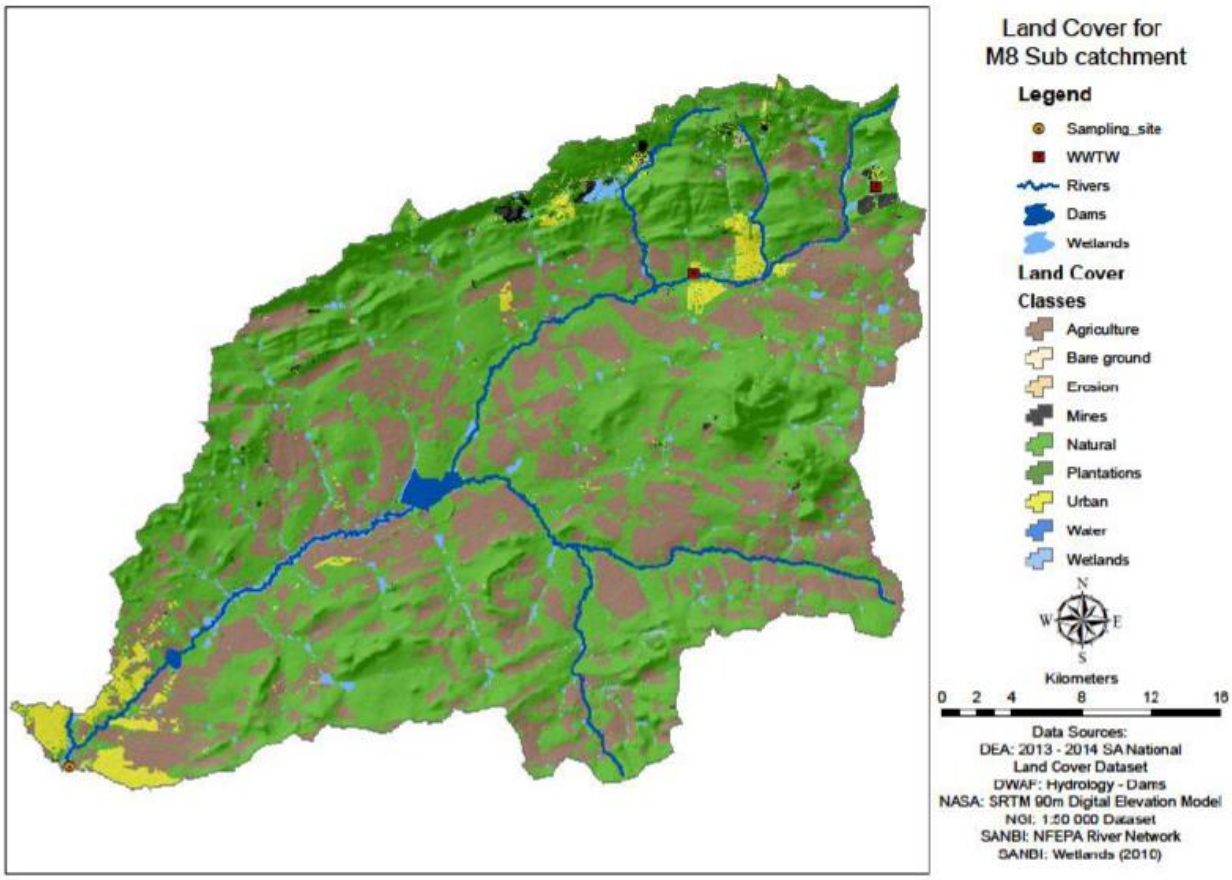

Figure 4.2: Site description of the land cover of the Loopspruit sub-catchment (Bezuidenhout *et al.*, 2017). The authors of the report refer to the Loopspruit sub-catchment as the M8 sub-catchment.

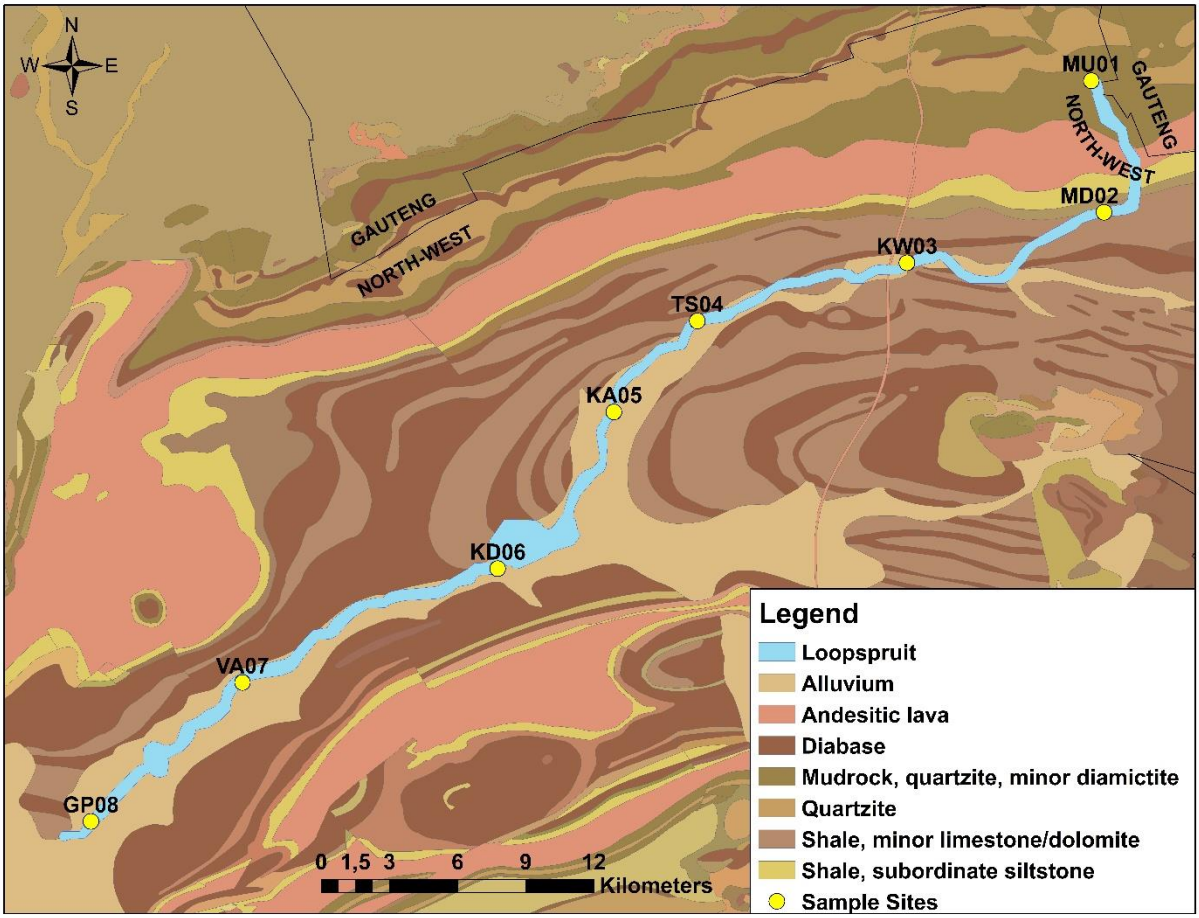

Figure 4.3: The geological profile setting of the Loopspruit sub-catchment.

Figure 4.3 shows the Loopspruit River sub-catchment geology. This catchment encompasses the Pretoria Group rock and stretches towards the south. On top of the Pretoria Group, which is part of the greater Transvaal Supergroup, lies the younger Karoo-age shales (with minor limestones and or dolomites), and sandstone, coal seams of the Ecca Group and tillite of the Dwyka Formations are located in the dolomitic depressions (Malan, 2012).

4.1.2 Time series of the historic data water chemistry of the Loopspruit River

The historic physico-chemical data used for the visualisations were obtained from the Open Downloads link from the Centre for Water Science and Management in the NWU, Potchefstroom, South Africa (https://www.waterscience.co.za/waterchemistry/data.html).

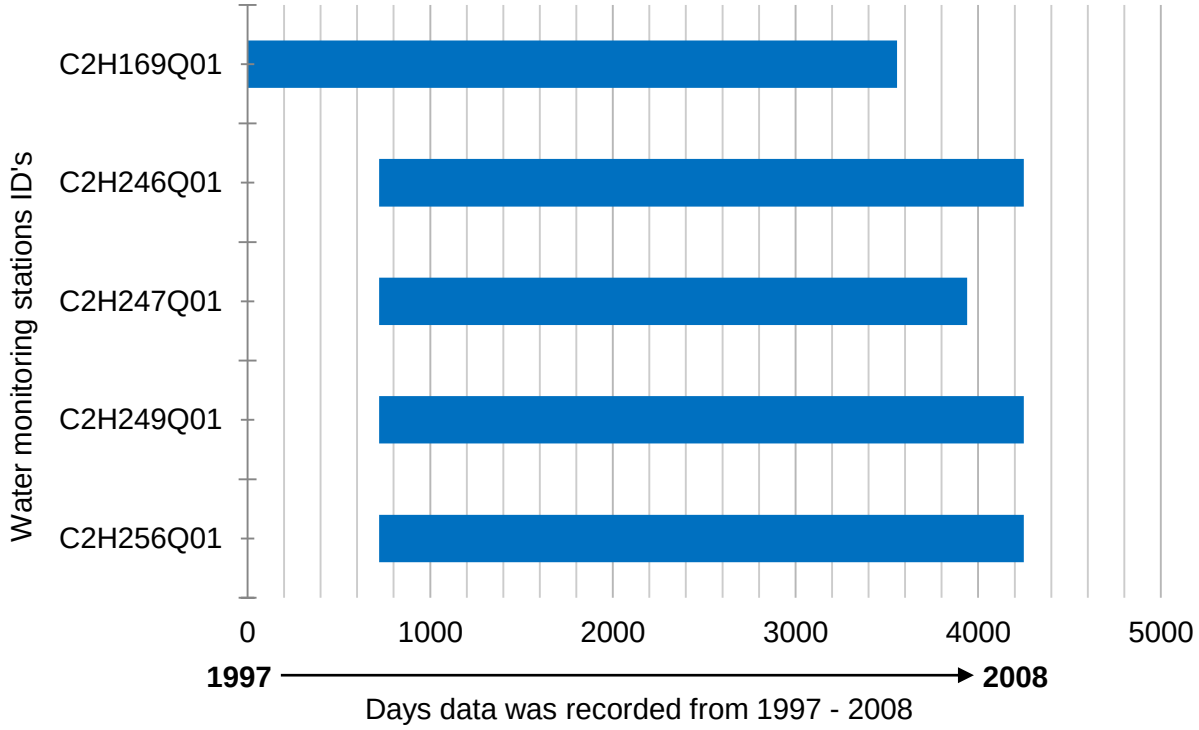

Figure 4.4: Consecutive days the water chemistry was monitored by the water monitoring stations.

Figure 4.4 shows a time series graph on how long the monitoring stations recorded water chemistry data. Furthermore, the data were sorted, filtered and managed in Excel (Microsoft Office 365 ProPlus). The criteria selected to be sorted and filtered were based on the monitoring station IDs and where they may be located to ensure that only these monitoring stations generated the relevant water quality data. These monitoring stations showed the major ion chemical composition of the pH, TDS, Na, Mg, Ca, NO_2, NO_3, SO_4, and PO_4. The software used to create the water chemistry visual representations was the Environmental Systems Research Institute, ArcGIS Desktop 10.5. The Excel file was exported into ArcGIS. The desired chemical constituents and their monitoring station coordinates (in decimal degrees) were projected with the WGS 1984 Geographical Coordinate System to indicate where the monitoring stations are located.

4.2 Physico-chemical analysis

4.2.1 Visual representations of physico-chemical contaminations

The following Figures (Figures 4.5 to 4.7) are geospatial visual representation representing water quality parameters from collected historical data. The areas of note are urban and agricultural activities, a wastewater treatment plant, mining activities and informal settlements (Table 3.1 in Section 3.1). The impact that each of these land uses may have on water quality will be considered below. The Loopspruit River had a low Mg concentration of 12.60 mg/L supplementary material (Appendix B as Figures B.1 to B.6) and will not be discussed here. The selected visual representations include a pH visual representation, the reason being that the majority of water quality constituents are dependent on the pH of the water. The Magnesium (Mg) visual representation was selected as an exception to the other visual representations that roughly looked similar. Finally, the Sum Total visual representation was chosen to show the questionable areas based on all the point source contamination visual representations. The Loopspruit River polygon was not made to actual scale, to better visualise the colour ramp.

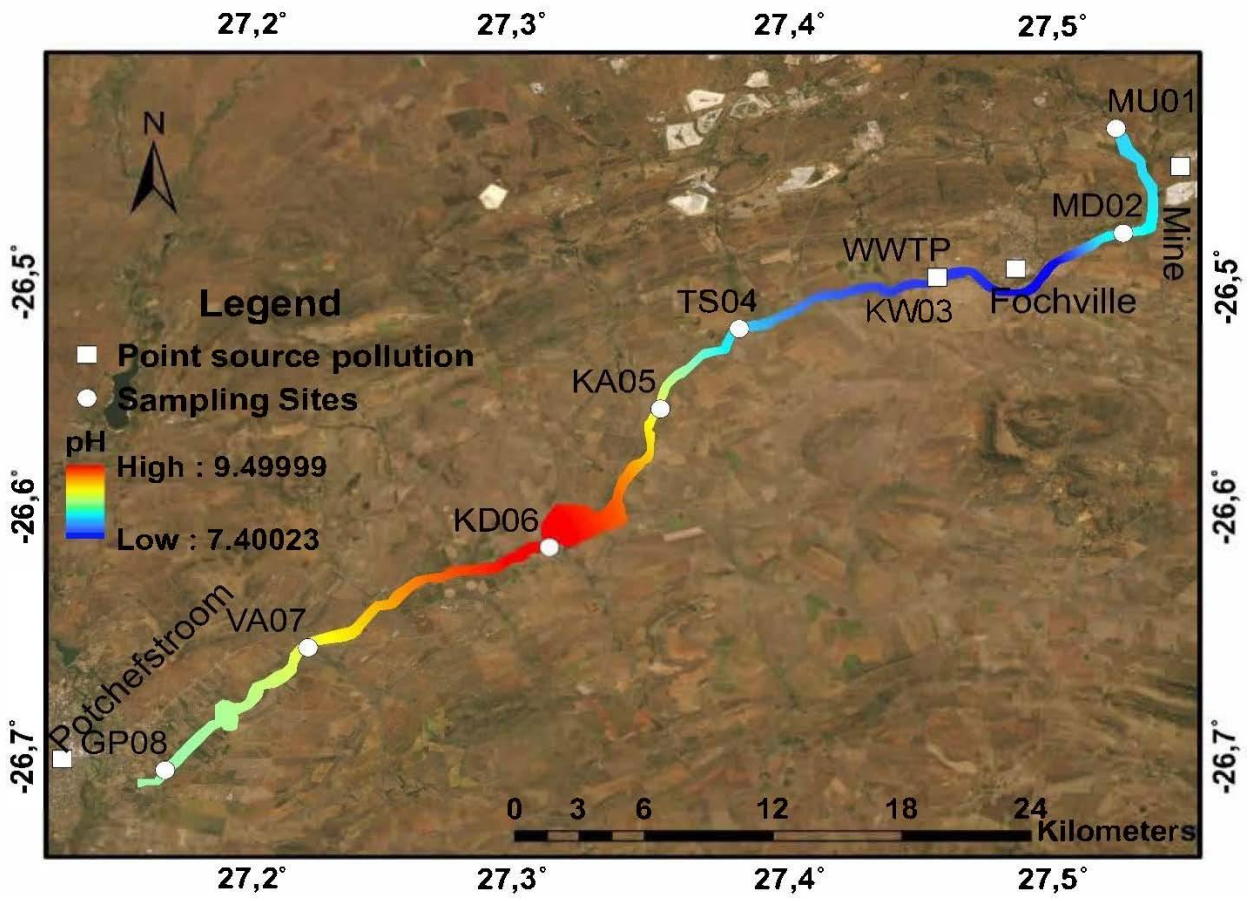

Figure 4.5: A geospatial visual representation of the Loopspruit River with pH.

The visual representation of pH shows a range of 7.40 – 9.49 (Figure 4.5). Attention is immediately drawn to the red in the centre, where the pH was 9.49. This is where the surface water flows into Klipdrift Dam, and when the dam is at capacity, the water continues to flow downstream at the dam outlet. Here the pH was above the maximum RWQO pH of 8.5. The pH was moderately low at the sites near urban and mining activities towards the top-right of Figure 4.5. As the water flows into Klipdrift Dam, the pH increased, and then it decreased downstream, passing the military base, agricultural activities and urban activities, before the Loopspruit River flows into the Mooi River.

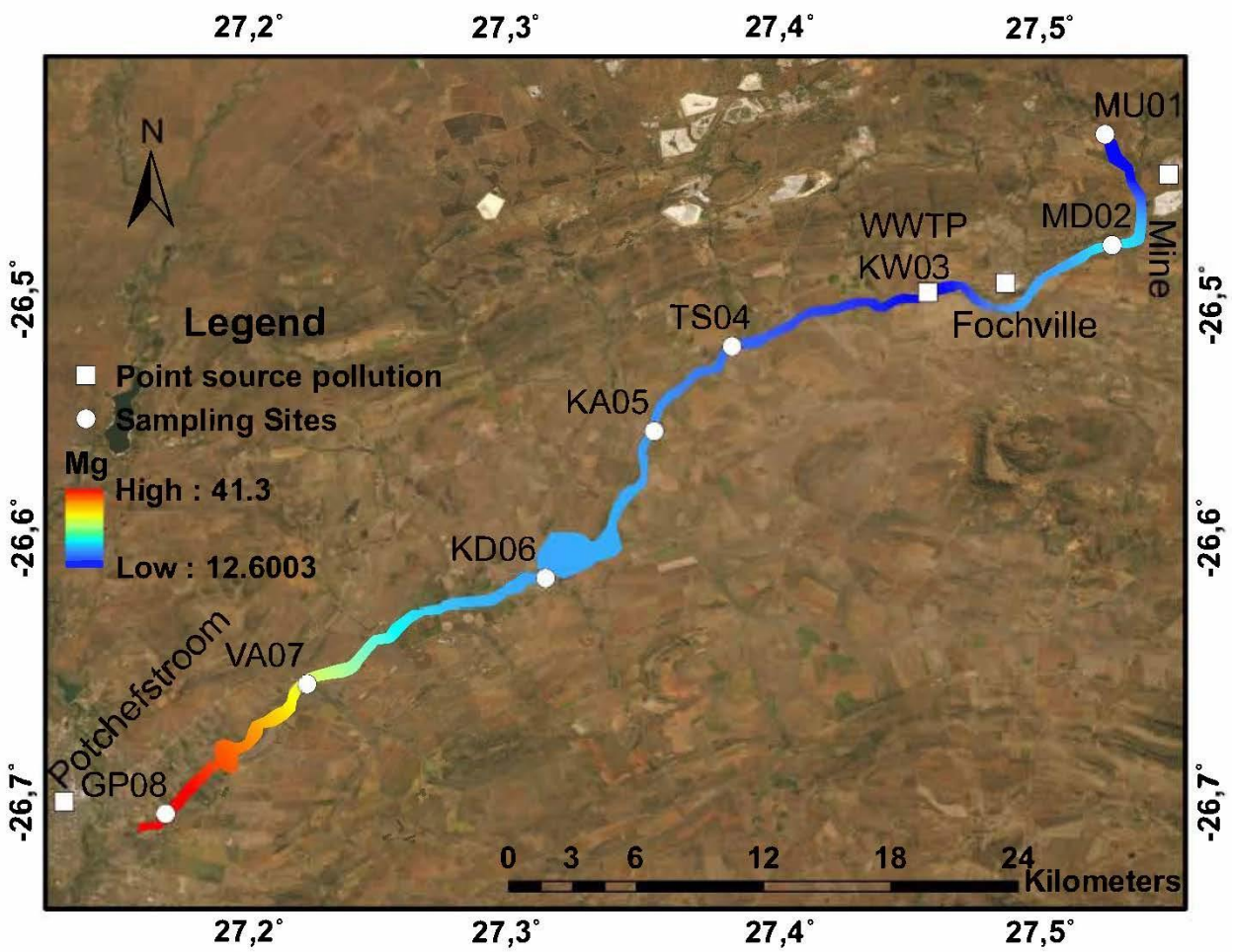

Figure 4.6: A geospatial visual representation of the Loopspruit River with the magnesium (Mg).

The Loopspruit River had a low Mg concentration of 12.60 mg/L (Figure 4.6). At sample site MD02 and flowing downward towards the Mooi River, the Mg increased to a high of 41.30 mg/L where there is an increase in urban activities. Magnesium is typically not referred to when considering RWQO, but DWAF (1996a) sets the upper limits for “safe” at 30 mg/L Mg. It was evident that these levels exceeded these requirements of the urban areas in the lower end of the Loopspruit River.

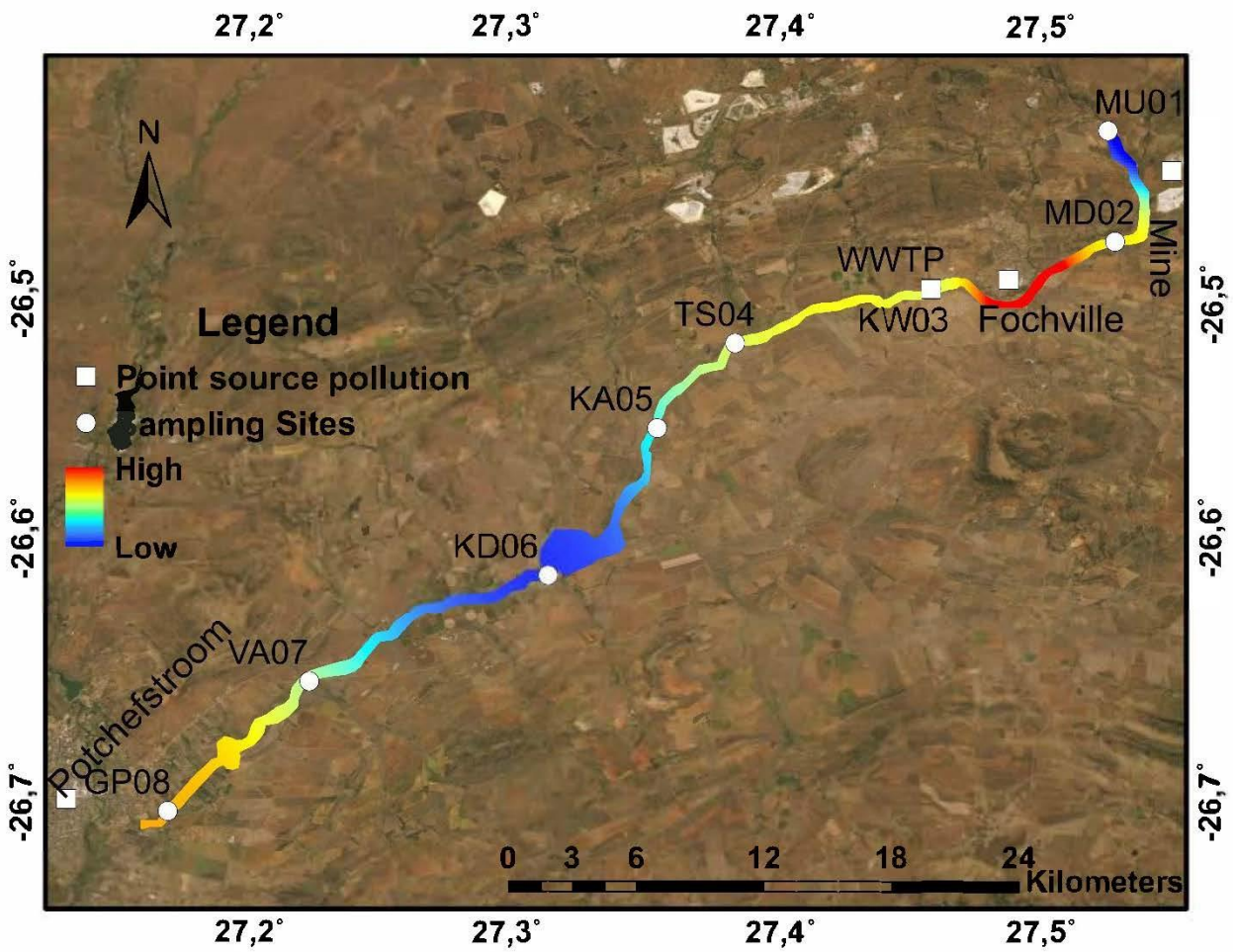

Figure 4.7: A summative physico-chemical visual representation showing the contamination of locations prone to contamination.

All the physico-chemical visual representations created show the problematic areas with regard to their respective parameters. In Figure 4.7, there may be a possibility that the questionable areas contributing to pollution are mainly urban areas. These river waters' physico-chemical parameters near the urban centres span the length where the river is yellow to red in the visual representation, which indicates a high contribution to pollution from the urban areas. These are considered to be "hot" zones. The area MD02 and KW03 contributed to most of the pollution in the Loopspruit River. Here the dominant land uses are a WWTP, informal settlements and urban land use. Moreover, at sample site KD06, pollution is indicated as low, having the blue colour index. This is where the lowest amount of pollution takes place. This result may be attributed to a lack of urban activities and a prevalence of agricultural activities.

4.2.2 Physico-chemical parameters measurements

Data in Tables 4.1 and 4.2 show the water quality parameters observed during the 2018 – 2019 sampling sessions of the two wet and two dry seasons. All the parameters in Table 4.1 were within the resource water quality objective (RWQO) except for the TDS and COD, which exceeded the RWQO at every site. TDS ranged from 588.00 – 806.33 mg/L (TDS RWQO is <450 mg/L), and the COD ranged from 99.00 – 131.67 mg/L (COD RWQO is <100 mg/L). Temperature ranged from 10.17 – 14.47°C during the cold dry season. One parameter of note was the PO_4 at sites KW03 and KA05 that exceeded the RWQO at 1.11 mg/L and 1.25 mg/L, respectively. MU01 adhered to six of the eight parameters (temperature excluded) with 75% adherence. All the other sites adhered to only four of the eight, with 50% adherence.

Table 4.1 also shows the data captured during the wet season. During this season, the pH, NO_3, SO_4 and COD were all below the RWQO. TDS was still above the RWQO even after seasonal changes ranging from 540.33 – 783.50 mg/L. The PO_4 was excessively high at sites KW03, TS04 and KA05 with concentrations of 4.00 mg/L, 2.91 mg/L and 2.68 mg/L respectively. NO_2 exceeded the RWQO from sites KW03 to GP08 ranging from 6.00 – 11.00 mg/L. During the wet season, sites MU01, MD02 and VA07 adhered to six of the eight parameters (temperature excluded) with 75% adherence. Site GP08 complied with the RWQO with five of the eight parameters (temperature excluded) showing 63% compliance, and site KW03, TS04, KA05 and KD06 complied with only half of the sites.

During the 2018 dry and wet seasons, the water quality at all sampling sites was closer to the RWQO than during the wet season. All the parameters tested during the dry season were at a compliance rate of 47% relative to RWQO, compared to 61% for the wet season. During the 2018 sampling year, the Loopspruit River had a compliance of 61%.

Table 4.1: Physico-chemical results during the dry season (May 2018) and wet season (September 2018)

	pH	T (°C)	TDS (mg/L)	PO_4 (mg/L)	NO_2 (mg/L)	NO_3 (mg/L)	SO_4 (mg/L)	COD (mg/L)
RWQO	**6.5–8.5**	**N/A**	**<450**	**<0.4**	**<6**	**<6**	**<200**	**<100**
Dry season sample sites								
MU01	7.40 ±0.11	13.43 ±0.15	612.67 ±3.79	0.23 ±0.07	4.33 ±1.53	1.93 ±0.65	112.00 ±6.24	99.00 ±19.92
MD02	8.32 ±0.04	10.17 ±0.21	806.33 ±4.73	0.79 ±0.07	4.67 ±1.53	2.07 ±1.00	112.00 ±9.85	111.00 ±19.97
KW03	8.01 ±0.04	11.00 ±0.35	745.33 ±4.04	1.11 ±0.04	4.33 ±1.53	3.27 ±1.04	110.00 ±2.00	131.67 ±2.08
TS04	8.25 ±0.07	11.00 ±0.35	729.33 ±6.03	0.57 ±0.19	5.33 ±1.53	3.30 ±1.51	111.33 ±4.62	123.67 ±7.77
KA05	8.30 ±0.15	11.40 ±0.20	748.00 ±4.58	1.25 ±0.03	5.67 ±1.53	3.87 ±2.19	109.33 ±9.50	117.67 ±17.93
KD06	8.25 ±0.14	14.40 ±0.00	588.00 ±5.00	0.36 ±0.08	4.33 ±1.15	2.20 ±0.53	110.00 ±2.00	131.67 ±8.08
VA07	7.88 ±0.08	12.03 ±0.35	672.67 ±1.53	0.68 ±0.16	5.33 ±1.15	1.63 ±0.25	111.33 ±5.51	116.00 ±6.56
GP08	8.37 ±0.07	14.47 ±0.74	676.33 ±1.53	0.92 ±0.87	6.00 ±1.73	1.03 ±0.38	68.00 ±2.65	131.67 ±5.86
Wet season sample sites								
MU01	7.92 ±0.30	14.67 ±0.15	540.33 ±1.53	0.22 ±0.18	4.00 ±0.58	3.23 ±2.42	44.67 ±2.65	49.00 ±2.52
MD02	8.36 ±0.07	12.95 ±0.06	783.50 ±3.06	0.31 ±1.00	5.00 ±1.00	3.53 ±0.20	46.33 ±1.00	29.00 ±1.53
KW03	8.04 ±0.01	14.47 ±0.06	686.67 ±1.73	4.00 ±0.46	7.00 ±3.61	5.00 ±0.20	44.67 ±3.22	59.00 ±1.53
TS04	7.52 ±0.03	15.93 ±0.12	714.33 ±1.53	2.91 ±0.42	8.67 ±1.53	5.83 ±0.12	40.00 ±5.03	51.67 ±2.08
KA05	7.96 ±0.03	16.00 ±0.15	706.67 ±0.58	2.68 ±0.73	11.00 ±3.00	6.63 ±0.67	51.67 ±1.53	61.67 ±6.11
KD06	8.84 ±0.04	17.90 ±0.06	643.67 ±1.15	0.44 ±2.49	7.00 ±2.31	3.07 ±0.29	52.67 ±2.08	92.67 ±1.15
VA07	7.98 ±0.07	15.40 ±0.06	781.67 ±0.58	0.64 ±0.69	6.00 ±2.52	2.80 ±2.57	147.00 ±3.06	70.33 ±37.04
GP08	8.27 ±0.03	16.63 ±0.00	754.67 ±1.53	0.26 ±0.27	6.67 ±2.00	2.63 ±0.30	45.00 ±2.52	45.33 ±4.93

(DWAF, 1996; SA WQ Guidelines (2nd edition) Vol 1–7). RWQO = Resource Water Quality Objectives; TDS = Total Dissolved Solids; PO_4 = Phosphate; NO_2 = Nitrite; NO_3 = Nitrate; SO_4 = Sulphate; COD = Chemical Oxygen Demand

Table 4.2: Physico-chemical results during the wet season (February 2019) and the dry season (July 2019).

	pH	T (°C)	TDS (mg/L)	PO_4 (mg/L)	NO_2 (mg/L)	NO_3 (mg/L)	SO_4 (mg/L)	COD (mg/L)
RWQO	**6.5–8.5**	**N/A**	**<450**	**<0.4**	**<6**	**<6**	**<200**	**<100**
				Wet season sample sites				
MU01	7.47 ±0.3	19.33 ±0.15	808.33 ±1.53	5.25 ±0.18	34.33 ±0.58	25.97 ±2.42	83.00 ±2.65	14.33 ±2.52
MD02	7.59 ±0.07	19.43 ±0.06	723.33 ±3.06	3.89 ±1.00	6.00 ±1.00	1.90 ±0.20	70.00 ±1.00	18.67 ±1.53
KW03	7.25 ±0.01	20.27 ±0.06	488.00 ±1.73	3.14 ±0.46	14.00 ±3.61	5.80 ±0.20	94.33 ±3.21	114.67 ±1.53
TS04	7.22 ±0.03	21.43 ±0.12	413.67 ±1.53	2.68 ±0.42	17.33 ±1.53	8.03 ±0.12	65.67 ±5.03	71.67 ±2.08
KA05	7.33 ±0.03	21.93 ±0.15	363.33 ±0.58	3.48 ±0.73	39.00 ±3.00	11.67 ±0.67	62.67 ±1.53	23.67 ±6.11
KD06	9.06 ±0.04	25.53 ±0.06	582.67 ±1.15	2.41 ±2.49	24.67 ±2.31	4.43 ±0.29	56.67 ±2.08	46.33 ±1.15
VA07	7.72 ±0.07	24.07 ±0.06	709.33 ±0.58	2.91 ±0.69	7.33 ±2.52	6.17 ±2.57	71.67 ±3.06	70.00 ±37.04
GP08	7.2 ±0.03	20.03 ±0.00	770.67 ±1.53	3.34 ±0.27	8.00 ±2.00	2.60 ±0.30	89.33 ±2.52	17.67 ±4.93
				Dry season sample sites				
MU01	7.9 ±0.44	11.20±0.46	700.27 ±6.40	3.70 ±1.84	7.30 ±1.53	2.90 ±0.38	118.30 ±2.08	6.70 ±1.53
MD02	8.00 ±0.22	8.40 ±0.15	752.00 ±1.00	2.40 ±0.55	6.00 ±1.00	3.70 ±0.15	112.70 ±2.08	11.00 ±3.61
KW03	7.92 ±0.05	10.93 ±0.15	712.67 ±0.58	3.75 ±0.63	5.33 ±0.58	5.77 ±0.32	94.67 ±3.06	13.67 ±3.51
TS04	7.81 ±0.03	10.90 ±0.10	679.67 ±3.79	3.01 ±0.56	6.67 ±1.16	2.33 ±0.31	79.33 ±1.53	21.00 ±2.00
KA05	7.76 ±0.03	11.23 ±0.15	654.33 ±2.08	2.74 ±0.14	6.00 ±1.73	1.93 ±0.21	83.00 ±3.00	16.67 ±8.96
KD06	9.40 ±0.04	12.40 ±0.00	544.00 ±6.25	1.22 ±0.15	6.00 ±2.00	2.10 ±0.27	74.33 ±2.52	29.67 ±1.16
VA07	8.11 ±0.04	10.00 ±0.10	702.33 ±0.58	0.40 ±0.22	5.33 ±1.53	1.53 ±0.15	80.33 ±2.08	27.33 ±4.73
GP08	8.20 ±0.04	11.80 ±0.06	692.00 ±2.00	3.10 ±0.19	6.00 ±1.73	1.60 ±0.06	74.70 ±2.52	36.30 ±2.08

(DWAF, 1996; SA WQ Guidelines (2nd edition) Vol 1–7). RWQO = Resource Water Quality Objectives; TDS = Total Dissolved Solids; PO_4 = Phosphate; NO_2 = Nitrite; NO_3 = Nitrate; SO_4 = Sulphate; COD = Chemical Oxygen Demand

In Table 4.2, the data show the water quality parameter concentrations during the wet and dry seasons of the 2019 sampling year. PO_4 exceeded the RWQO set at 0.4 mg/L with values ranging from 2.41 mg/L to 5.25 mg/L (Table 4.2). TDS also fell outside the RWQO at all the sites with the of sites TS04 and KA05 with values of 413.67 mg/L and 363.33 mg/L. NO_2 also exceeded the RWQO, ranging from a minimum of 6.00 mg/L to a maximum of 39.00 mg/L, which are three to six times the RWQO of 6.0 mg/L. NO_3 exceeded the RWQO at five of the eight sites, where MU01 and KA05 had the highest concentrations of 25.97 mg/L and 11.67 mg/L, respectively. The remaining parameters were all within the RWQO. Table 4.2 also shows the dry season during 2019, where the TDS exceeds the RWQO with sample values ranging from 544.00 – 752.00 mg/L. PO_4 levels were also above the limits set by the RWQO, ranging from 0.4 – 3.75 mg/L. NO_3 levels increased or decreased slightly at the maximum limit, which was set at 6.0 mg/L, with values ranging from 5.33 – 7.30 mg/L.

Overall the sample sites along the Loopspruit River showed compliance during the wet season with sites MU01, KD06 and VA07 with a compliance of 38%, sites KW03 and GP08 had a compliance of 50%, and MD02, TS04 and KA05 all a compliance of 63%. Overall compliance of the Loopspruit River was 59% during the dry season site KD06 at 50% compliance, MU01, MD02, KW03, TS04, KA05 and GP08 63% and VA07 at 75%. During the 2019 sampling year, the Loopspruit River had a compliance of 54.5%

4.3 Microbiological analysis

4.3.1 Microbiological water quality

Microbial data for the Loopspruit River are presented in Table 4.3 and Table 4.4. During the bacterial colony count analysis, the bacterial membranes that had >350 colonies were considered too numerous to count and were therefore given a value of 350 CFU/100 mL. In Table 4.3, the total coliforms, faecal coliforms and *Enterococci* (faecal *streptococci*) were below the RWQO.

Table 4.3 also shows the total coliforms ranging from a minimum of 22 CFU/100 mL to a maximum of 91 CFU/100 mL. Sites MU01 and KD06 had the highest counts of total coliforms with a minimum of 64 CFU/100 mL and 86 CFU/100 mL, respectively. Also, there were some significant differences between sites MD02 to KW03, KD06 to VA07 and also between VA07 to GP08, where p values were <0.03; <0.04 and <0.04 for the respective paired sites. The faecal coliforms ranged from a minimum of 0 CFU/100 mL to a maximum of 36 CFU/100 mL

through the sample sites. The biggest contributors to faecal coliforms were sites KW03, KD06 and GP08 with an average faecal coliform count of 18.33 CFU/100 mL for KW03 and 13.00 CFU/100 mL for both KD06 and GP08. There was also a significant difference at sites TS04 and KA05 for faecal coliforms ($p<0.03$). The *Enterococci* levels ranged from a minimum of 0.00 CFU/100 mL to a maximum of 74.00 CFU/100 mL during the warm and wet seasons. The HPC CFU/mL ranged from 0.00×10^0 – 3.50×10^5 CFU/mL. The average HPC ranged from 1.95×10^5 CFU/mL – 2.54×10^5 CFU/mL with only MU01 2.08×10^2 CFU/mL with average values below the RWQO of 1×10^3 CFU/mL. *Clostridium* counts remained low, apart from sites KW03, TS04 and KA05, where there were average counts of 8.00, 2.00 and 3.00, respectively. Only the HPC and *Clostridium* counts are expressed as CFU/mL.

In Table 4.4, none of the microbiological parameters met the requirements set by the (RWQO) during the cold dry seasons. The total coliforms ranged from an average of 25.67 – 350.00 CFU/100 mL, while the average faecal coliforms ranged from 10.83 – 350.00 CFU/100 mL. Enterococci had an average range of 50.00 – 350.00 CFU/100 mL. The average range of the HPC was 1.28×10^4 – 1.87×10^5 CFU/mL, *Clostridium* counts had an average range of 0.50 – 33.67 CFU/mL.

The most significant contributor to microbiological pollution during both the wet and the dry seasons is the WWTP near KW03. As expected, microbiological pollution was highest during the dry season.

Table 4.3: The microbiological results at the sample sites of the Loopspruit River, during the two dry seasons.

		Total coliforms (CFU/100 mL)	Faecal coliforms (CFU/100 mL)	*Enterococci* (CFU/100 mL)	HPC (CFU/mL)	*Clostridium*
Sample site	**RWQO**	**<100**	**<100**	**<100**	**<1000**	**NA**
MU01	**Min**	60.00	0.00	2.00	6.00×10^3	0.00
	Max	67.00	40.00	31.00	3.50×10^5	0.00
	Avg	64.00	20.83	15.50	2.08×10^2	0.00
	SD	3.61	17.39	13.84	1.63×10^5	0.00
MD02	**Min**	29.00	0.00	4.00	0.00×10^0	0.00
	Max	34.00	28.00	20.00	3.50×10^5	1.00
	Avg	31.33	9.83	12.67	1.95×10^5	0.33
	SD	2.52	12.21	6.62	1.68×10^5	0.58
KW03	**Min**	25.00	0.00	0.00	6.00×10^3	6.00
	Max	28.00	36.00	10.00	3.50×10^5	10.00
	Avg	26.67	18.33	2.67	2.54×10^5	8.00
	SD	1.53	17.00	4.08	1.46×10^5	2.00
TS04	**Min**	17.00	3.00	1.00	1.30×10^4	0.00
	Max	24.00	13.00	23.00	3.50×10^5	4.00
	Avg	20.67	8.83	10.67	2.10×10^5	2.00
	SD	3.51	4.02	9.77	1.61×10^5	2.00
KA05	**Min**	1.00	0.00	1.00	0.00×10^0	2.00
	Max	28.00	10.00	18.00	3.50×10^5	4.00
	Avg	14.33	6.00	9.33	2.38×10^5	3.00
	SD	13.50	3.52	7.76	1.62×10^5	1.00
KD06	**Min**	72.00	10.00	0.00	4.00×10^3	0.00
	Max	91.00	19.00	7.00	3.50×10^5	0.00
	Avg	83.00	13.00	3.00	2.33×10^5	0.00
	SD	9.85	5.20	3.35	1.64×10^5	0.00
VA07	**Min**	23.00	1.00	0.00	4.00×10^3	0.00
	Max	31.00	14.00	10.00	3.50×10^5	1.00
	Avg	26.67	3.83	2.50	2.41×10^5	0.33
	SD	4.04	5.08	3.99	1.56×10^5	0.58
GP08	**Min**	35.00	2.00	3.00	0.00×10^0	0.00
	Max	47.00	29.00	74.00	3.50×10^5	1.00
	Avg	41.67	13.00	22.67	2.34×10^5	0.67
	SD	6.11	9.32	27.28	1.62×10^5	0.58

SD = Standard deviation; Avg = Average; HPC = Heterotrophic plate count bacteria; CFU = colony forming units

Table 4.4: The microbiological results at the sample sites of the Loopspruit River, during the two wet seasons.

		Total coliforms (CFU/100 mL)	Faecal coliforms (CFU/100 mL)	*Enterococci* (CFU/100 mL)	HPC (CFU/mL)	*Clostridium*
Sample site	**RWQO**	**<100**	**<100**	**<100**	**<1000**	**NA**
MU01	**Min**	66.00	16.00	8.00	0.00×10^{0}	0.00
	Max	69.00	350.00	99.00	7.70×10^{4}	2.00
	Avg	67.33	149.00	50.00	1.28×10^{4}	0.50
	SD	1.53	148.59	45.61	2.68×10^{4}	0.84
MD02	**Min**	79.00	162.00	24.00	0.00×10^{0}	0.00
	Max	86.00	350.00	350.00	3.50×10^{5}	11.00
	Avg	82.00	264.67	137.50	1.80×10^{5}	2.50
	SD	3.61	94.81	132.85	1.82×10^{5}	4.23
KW03	**Min**	350.00	350.00	350.00	0.00×10^{0}	17.00
	Max	350.00	350.00	350.00	3.50×10^{5}	59.00
	Avg	350.00	350.00	350.00	1.84×10^{5}	33.67
	SD	0.00	0.00	0.00	1.79×10^{5}	15.92
TS04	**Min**	99.00	22.00	42.00	0.00×10^{0}	1.00
	Max	123.00	350.00	111.00	3.50×10^{5}	39.00
	Avg	111.00	124.50	75.17	1.77×10^{5}	16.67
	SD	12.00	120.77	32.64	1.85×10^{5}	17.49
KA05	**Min**	81.00	173.00	28.00	0.00×10^{0}	0.00
	Max	87.00	350.00	281.00	3.50×10^{5}	26.00
	Avg	84.67	265.83	157.83	1.78×10^{5}	11.33
	SD	3.21	92.40	129.30	1.84×10^{5}	11.20
KD06	**Min**	22.00	0.00	44.00	2.00×10^{3}	0.00
	Max	28.00	23.00	132.00	3.50×10^{5}	30.00
	Avg	25.67	10.83	84.33	1.87×10^{5}	13.00
	SD	3.21	11.89	41.43	1.75×10^{5}	13.89
VA07	**Min**	29.00	65.00	8.00	0.00×10^{0}	0.00
	Max	38.00	350.00	121.00	3.50×10^{5}	3.00
	Avg	33.50	212.00	62.33	1.65×10^{5}	1.00
	SD	6.36	151.25	56.49	1.68×10^{5}	1.26
GP08	**Min**	201.00	4.00	63.00	2.00×10^{3}	0.00
	Max	211.00	231.00	96.00	3.50×10^{5}	11.00
	Avg	206.00	107.33	82.00	1.72×10^{5}	4.50
	SD	7.07	114.09	11.54	1.62×10^{5}	4.32

SD = Standard deviation; Avg = Average; HPC = Heterotrophic plate count bacteria; CFU = colony forming units

4.3.2 Characterisations of microbial isolates

There was a total of 46 presumptive *Enterococci* isolates (Table 4.5) where all 46 isolates were Gram-positive. Twenty-four (52%) of these isolates tested positive for catalase activity. Since *Enterococci* are known to be Gram-positive and catalase-negative the 22 catalase-negative ones were selected for 16S sequencing.

The 49 *Clostridia* isolates in Table 4.5 that were grown on selective media, Reinforced Clostridia Agar (RCA), were endospore- stained and Gram stained. Of the 49 isolates, 36 (73%) isolates were endospore-forming. Only 31 (63%) were Gram-positive and were selected for 16S sequencing. The isolates that did not meet the staining criteria were discarded.

All the *E. coli* isolates (Table 4.5) were picked from MLG and MFC agar plates and purified. A total of 80 isolates were Gram-stained, and all were Gram-negative. These isolates were inoculated in a TSI agar reaction test tube where the top slant and bottom butt were monitored for colour changes. The test tube was also checked for gas production and black colouring of the agar, which indicates the production of hydrogen sulphide. *E. coli* is known to produce a yellow slant and a yellow butt, is positive for gas production and does not produces H_2S. Of the 80 isolates, 47 (58.75%) complied with the criteria for *E. coli* during the TSI test.

Table 4.5: The primary characterisation of isolated presumptive *Enterococci, Clostridium* and *E. coli*.

	***Enterococci* characterisation**			
	No. of isolates	**Gram reaction Positive**	**Catalase Negative**	**16S Sequencing**
MU01	5	5	4	4
MD02	5	5	5	5
KW03	1	1	1	1
TS04	4	4	4	4
KA05	5	5	5	5
KA06	12	12	0	0
VA07	3	3	3	3
GP08	11	11	0	0
Total	46			22

	***Clostridium* characterisation**			
	No. of isolates	**Gram reaction Positive**	**Endospore stain Positive**	**16S Sequencing**
MU01	7	5	6	5
MD02	8	4	4	4
KW03	8	6	6	6
TS04	2	2	2	2
KA05	4	3	4	3
KA06	9	3	3	3
VA07	5	5	5	5
GP08	6	3	6	3
Total	49			31

	***E. coli* characterisation**			
	No. of isolates	**Gram reaction Negative**	**TSI**	**16S Sequencing**
MU01	9	9	5	5
MD02	10	10	2	2
KW03	11	11	10	10
TS04	6	6	6	6
KA05	12	12	4	4
KA06	10	10	3	3
VA07	11	11	8	8
GP08	11	11	9	9
Total	80			*47 (32)

*Of the 47 isolates, 15 did not amplify with PCR, which resulted in 32 isolates being usable for 16S sequencing.

4.3.3 Land use representation of faecal contamination

During the wet and dry seasons, the distributions and concentrations of the faecal bacteria may differ. The contributions of faecal contamination through the mechanics of surface runoff were showcased during wet and dry seasons and are represented in Figure 4.8. *E. coli* contribution from the WWTP (KW03) during the wet season is shown as 55%, and during the dry season as 44%. Enterococci contributions from the WWTP (KW03) during the wet season are 44% and it decreased to 8% in the dry season. *E. coli* contributions that Klipdrift Dam (KD06) makes are low compared to enterococci. Agricultural (TS04, KA05 and VA07) and urban (MU01, MD02 and GP08) contributions to both *E. coli* and enterococci during the wet season remain constant with no statistical significance ($p>0.05$). During the dry season, the *E. coli* and enterococci increase as a result of urban activities. Impacts in terms of *E. coli* from the dam and agriculture are fairly low when compared to their contribution to enterococcal levels.

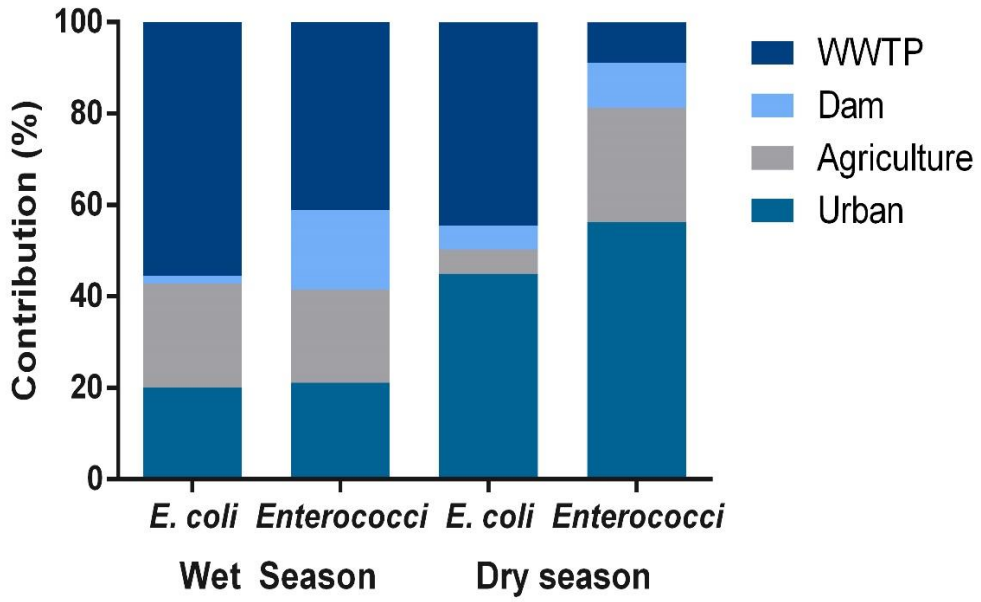

Figure 4.8: A faecal contamination visual representation showing the faecal contributions from various land uses during the wet and dry seasons.

4.4 Antibiotic susceptibility and concentrations

Microorganisms were screened for their susceptibility to ampicillin (10 µg), amoxicillin (10 µg), streptomycin (300 µg), oxy-tetracycline (30 µg), vancomycin (30 µg), penicillin G (10 µg), neomycin (30 µg), ciprofloxacin (5 µg), trimethoprim (2.5 µg), chloramphenicol (30 µg), sulfamethoxazole (25 µg) and colistin (10 µg). The concentration of tetracycline, trimethoprim, ampicillin, ciprofloxacin and erythromycin in water samples were determined.

4.4.1 Multiple antibiotic resistances

The Multiple Antibiotic Resistance (MAR) index serves as an indication of the number of antibiotic-resistant bacteria at the different sampling sites, as indicated in Table 4.6. Values above 0.2 indicate contamination of antibiotics within the environment they are used. It is evident that during the dry season, the MAR index was higher at all the sample sites compared to the wet season. The MAR index during the dry season ranges from 0.38 to 0.75. At site KA05 it reached 0.75. This is the highest value in both wet and dry seasons. The land-use activities at site KA05 are mainly agricultural. A possible trend during the dry season is that the MAR remains relatively stable with little deviation from a MAR of ~0.60 and 0.37 at VA07.

On the other hand, during the wet season, the MAR index values were almost half of those in the dry season (Table 4.6) and ranges from 0.06 to 0.37. At site MU01 the MAR index is at 0.37 during the wet season. The land use at that site can be characterised as mining. There is a visible trend of a decrease in the MAR index from sites MU01 to TS04, followed by an increase at site KA05. Moreover, sites KA06 and GP08 in the wet season are the only sites below the risk level of 0.2.

The 0.06 (KD06) and 0.07 (GP08) values are well below the 0.2 risk value. This means that these values are considered to be artefact. The observance of the MAR index at these sites are not naturally present but occurs as a result of the preparative or investigative procedures.

Table 4.6: A tabulated comparison between the Multiple Antibiotic Resistances (MAR) during the wet and dry seasons based on the HPC isolates.

Sample sites	**MAR (Dry)**	**MAR (Wet)**
Risk	**<0.2**	**<0.2**
MU01	0.61	0.37
MD02	0.61	0.28
KW03	0.47	0.24
TS04	0.60	0.21
KA05	0.75	0.30
KD06	0.55	0.06
VA07	0.38	0.31
GP08	0.58	0.07

Figure 4.9 further explains how the antibiotic resistance of bacterial isolates can be attributed to the contributions to the MAR index. All the antibiotic segments are plotted on the Coxcomb diagram. However, only the antibiotics that contributed to the MAR index are shown, resulting in some segments being overlaid. The bacterial resistance table can be seen in Appendix C, Tables C.1 and C.2. During the cold dry season (Figure 4.9), antibiotics to which most bacterial isolates were resistant to were ciprofloxacin, neomycin, sulphamethoxazole, amoxicillin, ampicillin, colistin and trimethoprim. At five of the sites, isolates were resistant to neomycin and sulphamethoxazole. However, isolates had resistance to ampicillin at all the sample sites, but also made the same contribution segments as some of the other antibiotics, and as a result, did not clearly show its contributing segment. Ampicillin can be seen at MD02, KA05, KD06 and VA07.

The number of isolates that had resistance to antibiotics in Figure 4.9 correlates with their respective MAR index. Sites MU01 (mining activities), MD02 (urban activities) and KA05 (agricultural activates) had a high MAR index value of 0.61 for both MU01and MD02 and 0.75 for KA05. Land uses around these sites include gold mining activities, maize, cattle and chicken agriculture activities. In other words, a greater number of isolates from the sites were resistant to a larger number of antibiotics. With this in mind, colistin showed some cause for concern. In Figure 4.9, bacterial isolates at KA05 were resistant to colistin. The latter antibiotic, which is considered one of the last resort antibiotics in cases where all other antibiotics are ineffective.

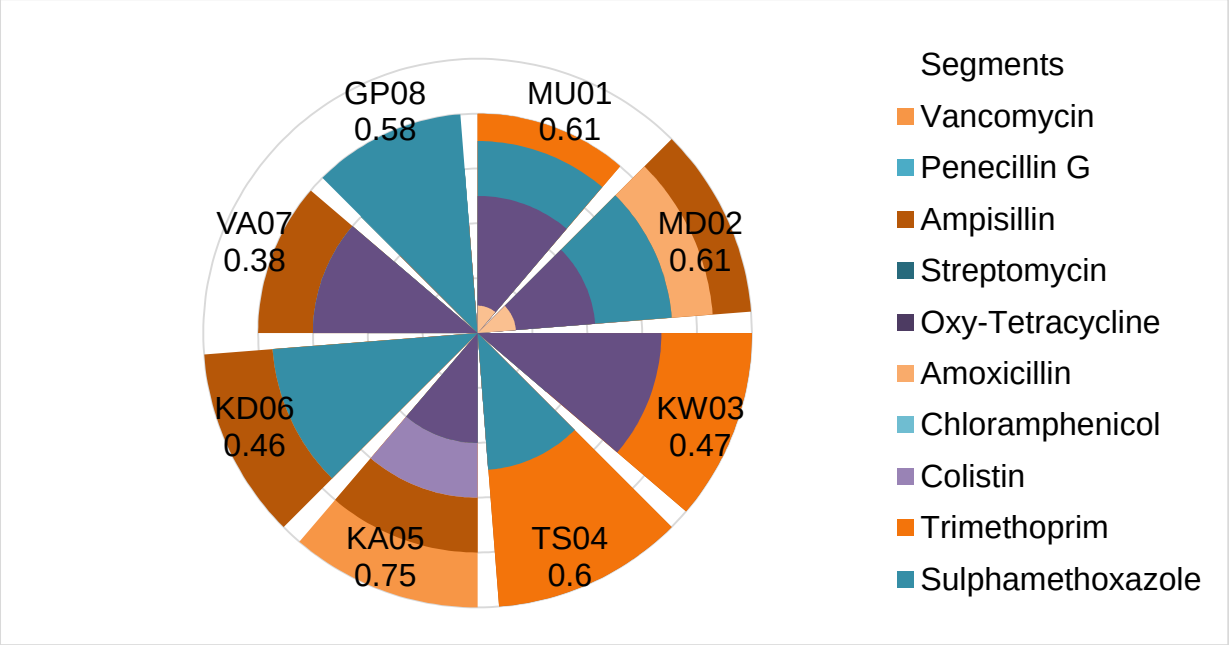

Figure 4.9: A Coxcomb diagram showing how many resistant bacterial isolates contributed to the MAR index at each sample site during the dry season

4.4.2 LC/MS

The analytical method was validated with acceptable linearity (Table 4.7). The limit of detection (LOD) and limit of quantification (LOQ) for all compounds were calculated (Table 4.7).

Table 4.7: Linearity, LOD and LOQ of each antibiotic analysed using this method

	Linear range (ng/mL)	**Linearity**	**LOD**	**LOQ**
			ng/mL	**ng/mL**
Ampicillin	0; 70.8; 150.6; 310.2; 2 500; 5 000; 10 000	0.9977	2.6	8.5
Ciprofloxacin	0; 39; 78; 156; 312; 625; 1 250	0.9985	0.262	0.874
Erythromycin	0; 2.5; 4.8; 9.7; 19.5; 39; 78	0.9994	0.3	1.0
Trimethoprim	0; 9.7; 19.5; 39.; 78.1; 156; 312	0.9992	0.021	0.071
Tetracycline	0; 9.7; 19.5; 39.; 78.1; 156; 312	0.9997	0.035	0.1182

The linear regression (Table 4.7) had a linearity of all the compounds randing 0.9977 – 0.9997. this means that all the compounds had a linearity better than 0.9 for all the analyses, indicating excellent linearity.

Table 4.8 shows the measured environmental concentrations (MEC) of five antibiotics, namely tetracycline, trimethoprim, ampicillin, ciprofloxacin and erythromycin. The levels of these antibiotic compounds were compared to a predicted no-effect concentrations (PNEC). The lowest PNEC reported by Bengtsson-Palme and Larsson (2016); Tran *et al.* (2019); and was used for the purposes of the comparison. PNEC is a level at which the compound does not affect the environment and ecological settings. Only tetracycline MEC values were fewer than the PNEC all at sample sites (Table 4.8). Trimethoprim's PNEC is set at 500 ng/L where sites KW03, TS04 and KA05 MEC are above this value and concentrations were 1247.07 ng/L, 6460.62 ng/L and 3751.35 ng/L, respectively. The MEC values for erythromycin were above the PNEC (40 ng/L) at only two sites, namely KW03 and TS04 where the measured values were 57.51 ng/L and 87.96 ng/L, respectively (Table 4.8). Erythromycin at all the other sites was below the detection limit (<LOD).

The ampicillin MEC is very high, compared with the other antibiotic MECs. Here MEC values range from 2546.81–146679 ng/L. Site VA07 has the lowest ampicillin concentration (2546.81 ng/L), whereas KA05 has the highest (146679 ng/L). The highest MEC is 1956 times the concentration of the PNEC in the environment.

When the levels of the selected antibiotics at the various sites are considered it evident that VA07 contributes the least to the antibiotic pollution, followed by KA06, GP08, MU01 and MD02. The most significant contributors to the high antibiotic levels are KW03, TS04 and KA05. The site with the lowest antibiotic contribution to the Loopspruit aquatic ecosystem is characterised by urban land use activities whereas the high MEC sites are predominantly located in agricultural areas.

The ecological risk of antibiotics in aquatic environments can be explained through the risk selection (RQ) index. When RQ ≤1.0, there is low risk and if RQ ≥1.0 then there is a possible risk to the aquatic ecosystem (Tran *et al.*, 2019). Tetracycline shows no risk with RQ index values of 0.24. On the other hand, trimethoprim, ampicillin, ciprofloxacin and erythromycin all show a possible risk. Ciprofloxacin and erythromycin are only slightly above the RQ index with 1.26 and 1.82, respectively, but ampicillin has an RQ value of 637.95, which far exceeds the no-risk limit.

Table 4.8: Measured environmental antibiotic concentrations at the various sample locations of the Loopspruit River.

	Tetracycline		**Trimethoprim**		**Ampicillin**		**Ciprofloxacin**		**Erythromycin**	
PNEC	**300 (ng/L)**		**500 (ng/L)**		**75 (ng/L)**		**20 (ng/L)**		**40 (ng/L)**	
	Mean (ng/L)	**%RSD**	**Mean (ng/L)**	**%RSD**	**Mean (ng/L)**	**%RSD**	**Mean (ng/L)**	**%RSD**	**Mean (ng/L)**	**%RSD**
MU01	18.59 ±0.00	17.17	36.83 ±0.00	4.04	42444.64 ±22.05	51.94	24.16 ±0	3.38	< LOD	
MD02	7.79 ±0.00	10.06	150.79 ±0.01	5.54	42618.51 ±9.89	23.22	23.66 ±0	1.69	< LOD	
KW03	43.51 ±0.01	14.06	1247.07 ±0.05	3.84	57159.71 ±1.98	33.38	26.42 ±0	8.61	57.51 ±0.01	14.48
TS04	90.38 ±0.01	14.70	6460.62 ±0.26	3.95	57159.71 ±1.98	3.47	26.68 ±0	15.5	87.96 ±0.01	7.77
KA05	221.44 ±0.04	20.09	3751.35 ±0.64	16.96	146679.04 ±47.22	32.2	25.54 ±0	4.11	< LOD	
KA06	31.42 ±0.00	6.23	179.27 ±0.04	22.35	12635.53 ±2.67	21.14	25.29 ±0	2.76	< LOD	
VA07	88.61 ±0.01	19.30	105.66 ±0.01	5.63	2546.81 ±0.45	17.82	25.29 ±0	5.44	< LOD	
GP08	63.43 ±0.01	10.73	76.94 ±0.01	15.53	21526.71 ±0.06	0.30	23.91 ±0	3.79	< LOD	
RQ	0.24		3.00		637.95		1.26		1.82	

%RSD = Relative Standard Deviation; LOD = Limit Of Detection; RQ = Risk Quotient; PNEC = Predicted No-Effect Concentrations (Bengtsson-Palme & Larsson, 2016; Tran *et al.*, 2019)

4.5 Bacterial identification by16S rRNA gene sequencing

The bacterial isolates identified using 16S rRNA gene sequencing (Figure 4.10 and Figure 4.11) are represented as a neighbour-joining phylogenetic tree. Reference 16S rRNA sequences and their related accession numbers were exported from the NCIB GenBank database. The supporting bootstrap values are shown at the tree's branch nodes. The number in block-brackets indicates the number of isolates identified as the same organism.

The presumptive *E. coli* and *Enterococci* isolates, together with *Clostridium* species, are resented in Figure 4.10. These were grouped together because they are all bacteria from faecal origin. The tree is divided into two main clusters, A and B. Cluster A is further divided into three sub-clusters, A1, A2 and A3, and cluster B has two sub-clusters B1, B2 and B3. Sub-cluster A1 consists predominantly of *Clostridium perfringens* with *C. baratii* and *C. nitritogenes.* Sub-cluster A2 consists of *Enterococcus* species such as *E avium, E. dispar, E. canintestini, E. facium, E. pallens, E. florum* and *E. gilvus,* with *E. facium* the most abundant. Sub-cluster A3, is another branch of the Clostridia species, which includes *C. bifermentans* and *C. sordellii.*

Clustering in cluster A were only the Gram-positive bacteria. Sub-clusters A1 and A2 have a common ancestor with sub-cluster A3. *Clostridium perfringens* in sub-cluster A1 is closely related to C. *baratii* (strain 35Y8B) with a confidence bootstrap value of 100%. The branch length of sub-cluster A1 and A3 shows a 100% bootstrap correlation. In sub-cluster A3, the Clostridia spp. *C. bifermentans* (strain SH-C14) and *C. sordellii* (strain BG-C135) is supported with a bootstrap confidence value of 99%. In sub-cluster A2, *Enterococcus. dispar* and *E. canintestini* support phylogenetic similarity with a bootstrap of 92%. The *Enterococcus avium, E. facium, E. pallens, E. florum* and *E. gilvus* show a relatedness with a bootstrap ranging from 24% to 92%.

Cluster B has three sub-clusters, B1, B2 and B3. B1 contains only *Shewanella xiamenensis.* Sub-cluster B2 is represented by *Aeromonas hydrophila.* Finally, sub-cluster B3 consists mostly of *E. coli* species. However, other bacteria were also present, such as *Serratia marcescens, Klebsiella aerogenes, Enterobacter cloacae, Enterobacter asburiae, Citrobacter freundii* and *Enterobacter cloacae*. *E coli* (DPRA1) was the dominant strain, with a moderate confidence correlation of 54% with *Serratia marcescens, Klebsiella aerogenes, Enterobacter cloacae, Enterobacter asburiae, Citrobacter freundii* and *Enterobacter cloacae*.

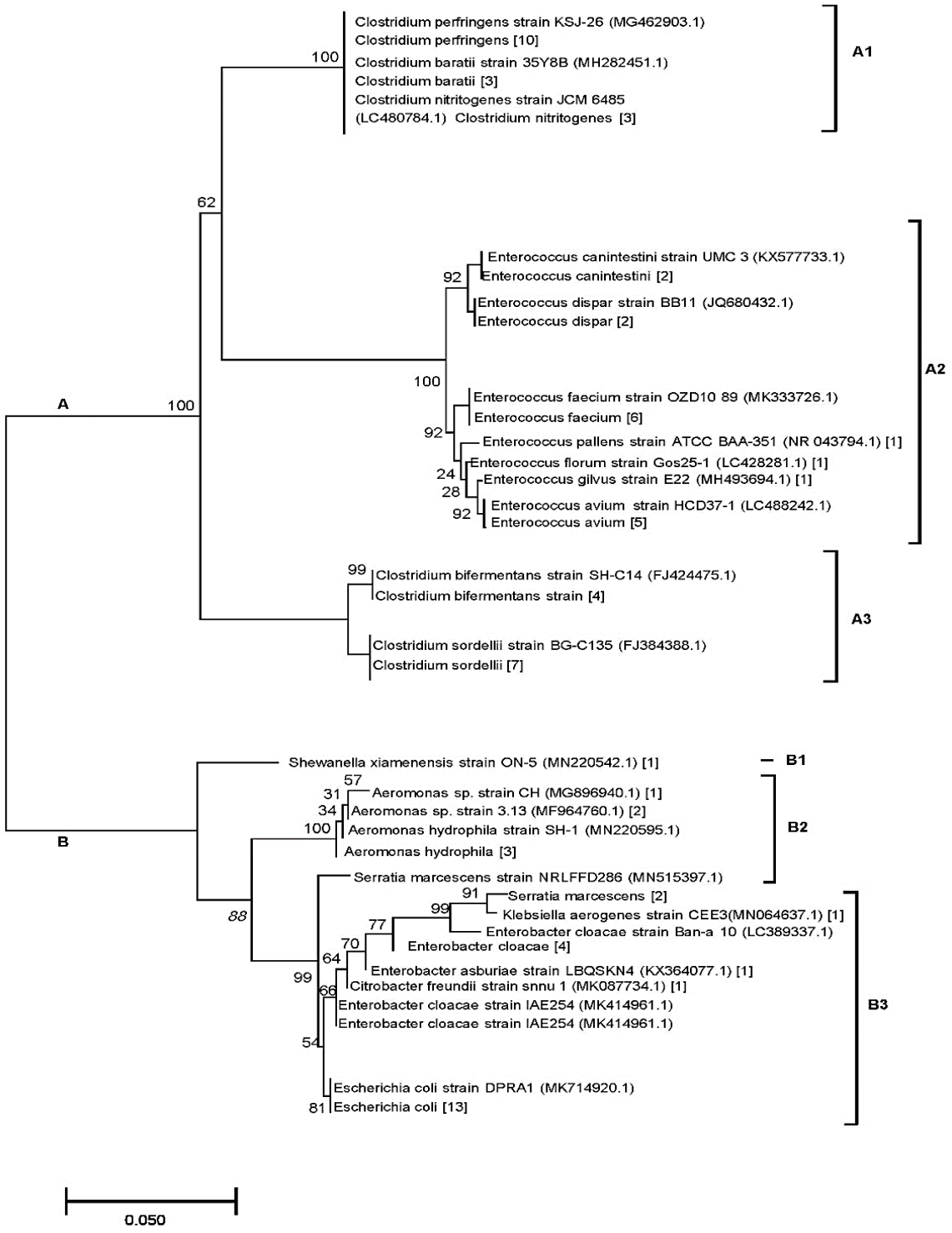

Figure 4.10: A neighbour-joining tree presenting the phylogenetic relationships of presumptive faecal associated bacteria. These include 29 *E. coli*, 17 *Enterococci* and 27 *Clostridia*. The evolutionary distances were computed using the Kimura 2-parameter method, clustered together with 10000 bootstraps and the variation rate was modelled with a gamma distribution in MEGA X. Percentages are indicated at the branching points of the dendrogram.

The phylogenetic tree presenting the phylogenetic relationships of HPC bacteria is divided into two clusters, A and B, and further subdivided into six sub-clusters, namely A1, A2, A3, B1, B2, B3 and B4 (Figure 4.11). The A and B clustering might be according to the strain. Sub-cluster A1 consists of *Flavobacterium* sp. with some *F. gyeonganense* (strain HME7524), *F. hibisci* (strain THG-HG1), *F. johnsoniae* (strain A3), *F. limicola* (strain SQ97) and *F. rivuli* (strain WB3.3-2). Sub-cluster A2 has *Sphingobacterium* sp. (strain Jaber 3) and *Chryseobacterium indoltheticum* (strain IMCC34920). Sub-cluster A3 consists solely of *Arcicella rigui* (strain HMF3820). The *Flavobacterium* sub-cluster has a high sequence similarity (98%) supported bootstrap value. Sub-cluster A1 has a moderate confidence supported bootstrap value of 61% with A2. Sub-clusters A3 and B1 both represent an individual branch in their respective clusters.

Sub-cluster B2 consists of *Beta proteobacteria* (strain HJX14), *Janthinobacterium lividum* (strain TPD7014) (Figure 4.11). The sub-cluster represented by B3 consists of *Rheinheimera* sp. and, *Aeromonas* sp. A *Pseudomonas* cluster represented by sub-cluster B4 consists of *P. fluorescens* (strain G21), *P. putida* (strain RCA28), *P. cichorii* (strain 150-HR4) and *P. fluorescence* (strain DS3).

The *Flavobacterium rivuli* (strain WB3.3-2) has a 100% similarity supported bootstrap, with the other *Flavobacterium* isolates in sub-cluster A1. Although sub-cluster A2 does not have the same isolates as A1, it does have a common ancestor with a bootstrap value of 61. Furthermore, sub-cluster A3 *Arcicella rigui* (strain HMF3820) might be an outlier in cluster A, but it does share a common ancestor with sub-clusters A1 and A2 with a 100% supported bootstrap value.

Sub-clusters B2 and B4 both have a distantly related branch length toward each other. On the other hand, sub-cluster B3 has a varying branch length between *Rheinheimera* sp. and the *Aeromonas* species. Sub-cluster B4 grouped the *Pseudomonas* species with a varying bootstrap confidence value of 47% to 97%. Furthermore, sub-clusters B3 and B4 share a common ancestor with a confidence bootstrap value of 98%.

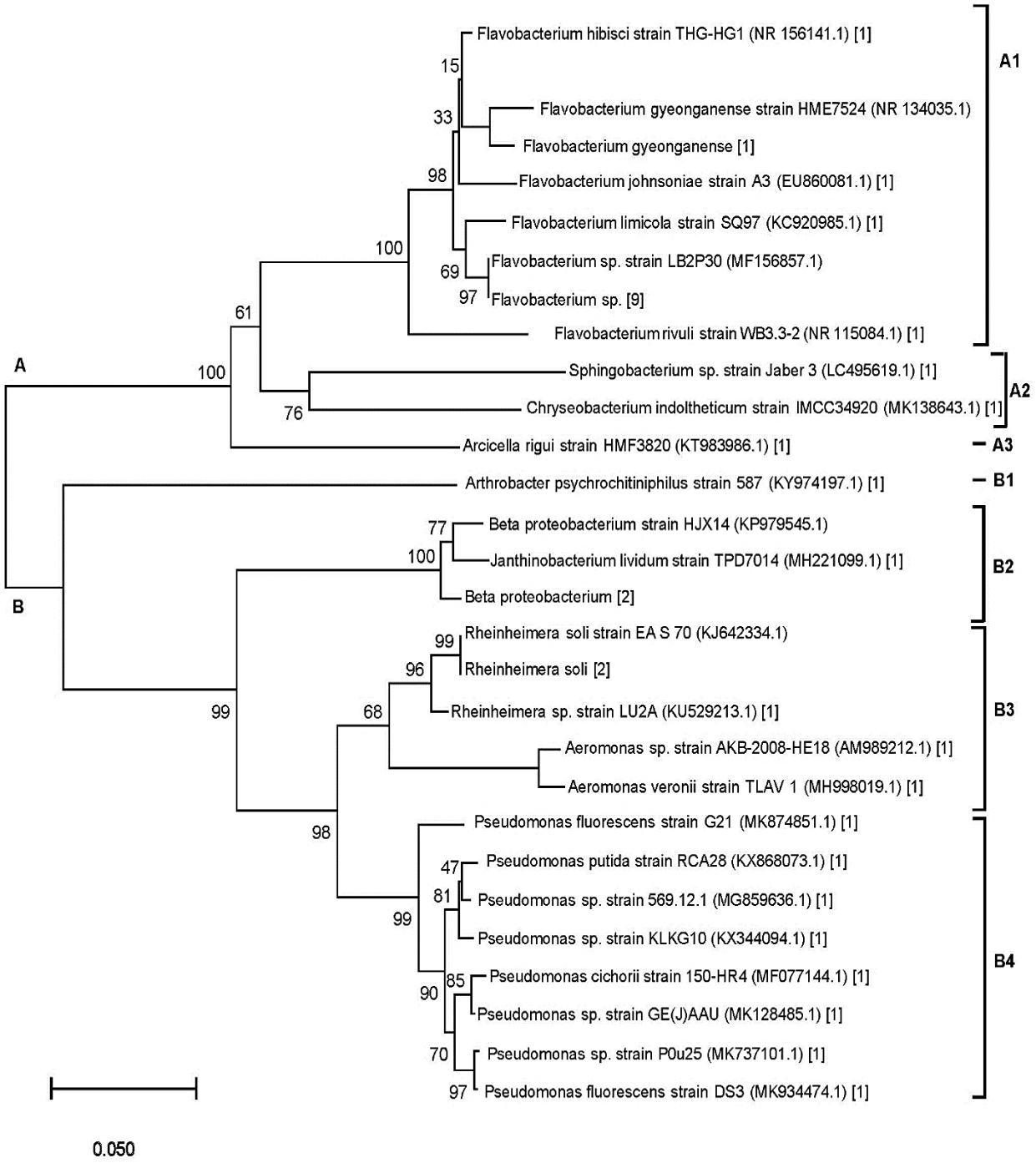

Figure 4.11: A neighbour-joining tree presenting the phylogenetic relationships of HPC bacteria. These include 39 isolates. The evolutionary distances were computed using the Kimura 2-parameter method, clustered together with 10000 bootstraps and the variation rate was modelled with a gamma distribution in MEGA X. Percentages are indicated at the branching points of the dendrogram.

4.6 β-Lactamase resistant genes

The β-Lactamase resistant genes were detected using eDNA obtained samples collected at the different sample sites. Figure 4.12 represents only an image of an agarose gel of one of a β-Lactamase resistance gene, *FOX* (Figure 4.12A) and *intI1* (Figure 4.12B) genes. The approximate size of the *FOX* target gene is 190 bp, and the *intI1* target gene size is 280 bp. All the eDNA samples were used for the gene detections and sequenced duplicates. Figure 4.12 shows the duplicate resistant genes for Sample site MU01.

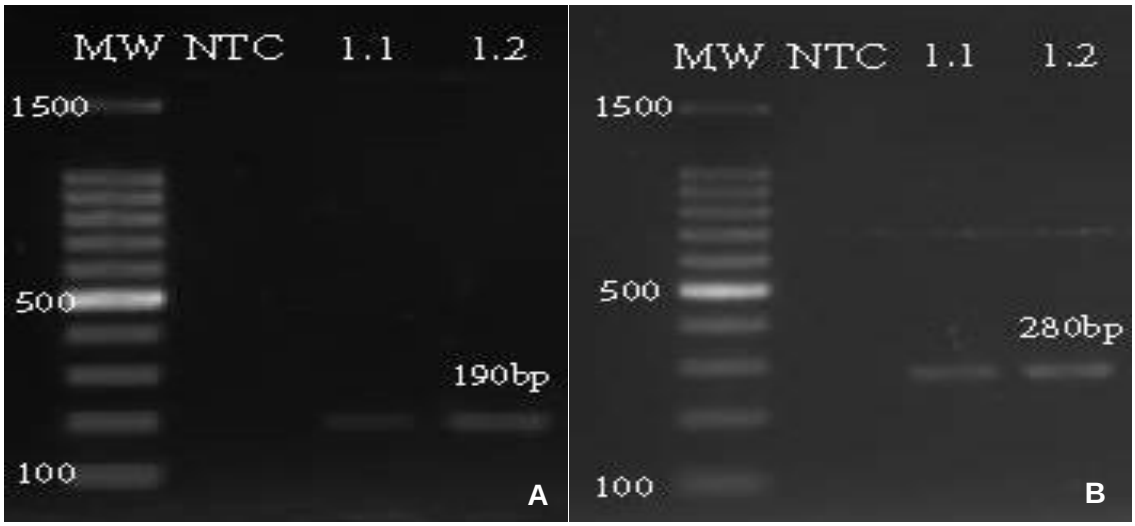

Figure 4.12: Agarose gel electrophoresis (1.8% (w/v agarose gel) image for the detection of the *FOX* (A) and *intI1* genes (B), respectively. MW = 100 bp molecular marker (O'GeneRuler, Thermo Scientific, US). NTC represents non-template control. The amplicons were mixed with GelRed for visualisations.

In Figure 4.13, the *intI1* gene was detected in the eDNA of all the sample sites except at VA07, while the *FOX* gene (Figure 4.13) was detected at all the sites except at TS04. The *MOX* gene was present only at sample site KA05. *ACC* and *CIT* were not detected at any of the sites. The detection of these genes in the eDNA from the various sites shows an association with the MAR Table 4.6 and Figure 4.9 in Section 4.4.1.

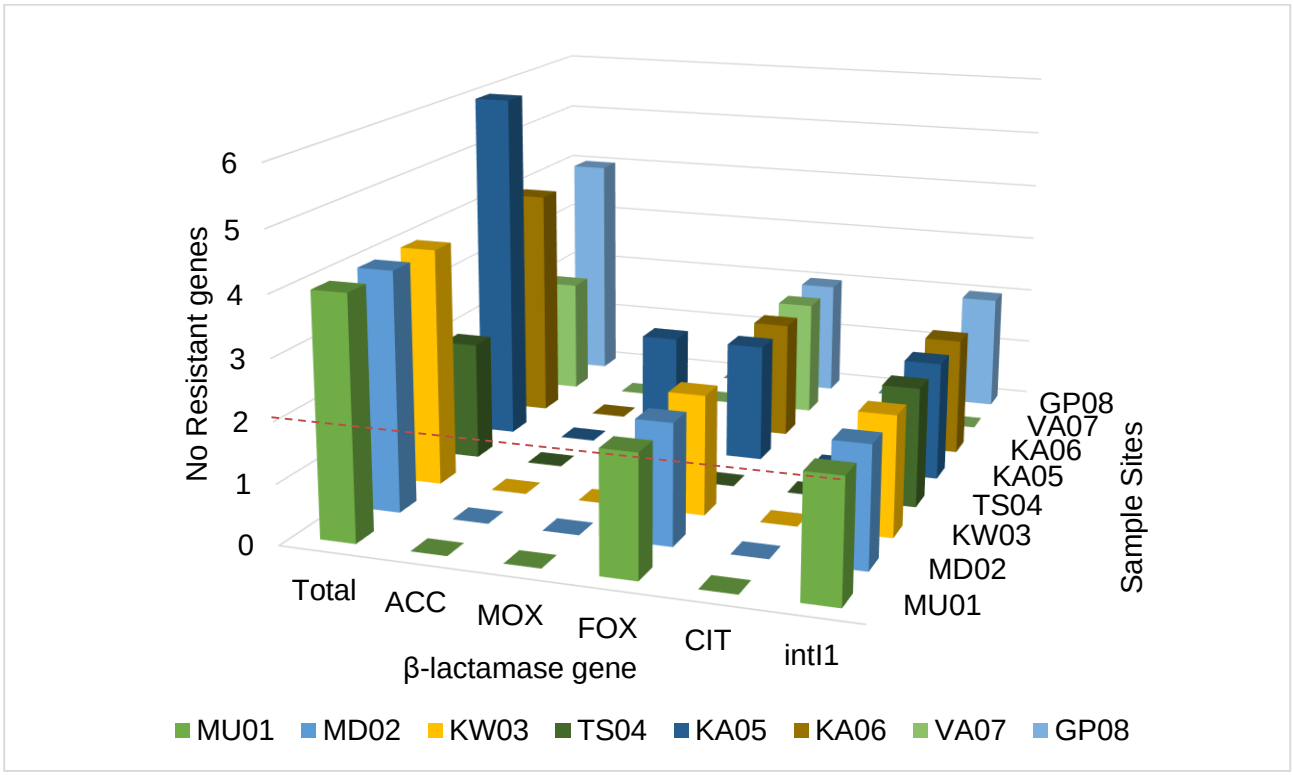

Figure 4.13: A 3D column chart illustrating the eight sample sites with six variants of AmpC β-lactamase resistant genes with the integrase (*intI1*) gene.

4.7 Bacterial diversity

Bacterial taxonomy can be a difficult concept to illustrate, as the data are hierarchical. Most of the data can be represented only on a linear scale, where only one level of the bacterial taxonomy can be shown. With a heat tree representation, more than one level can be represented. In Figure 4.14 the Loopspruit River taxa are represented in three taxonomic levels: kingdom, phylum and order which were obtained from the operational taxonomic unit (OTU) table for the dry season of 2019. The colours indicate the percentage of observed taxonomic units (OTU), the node size represents the number of OTUs that were assigned to each taxon, and the branch length indicates the number of OTU reads.

Figure 4.14 shows that all OTUs belong to the bacteria kingdom and are represented as the most prominent node. Extending from the bacteria kingdom, three branches and nodes (darker green) have high OTUs, counts that include *Proteobacteria, Bacteroidetes* and *Firmicutes* represented on a phylum level. Branches and nodes can extend and split further from the phylum level to create sub-branches. For example, representing the bacteria class such as the *Firmicutes*, which branches to the Order *Clostridia*.

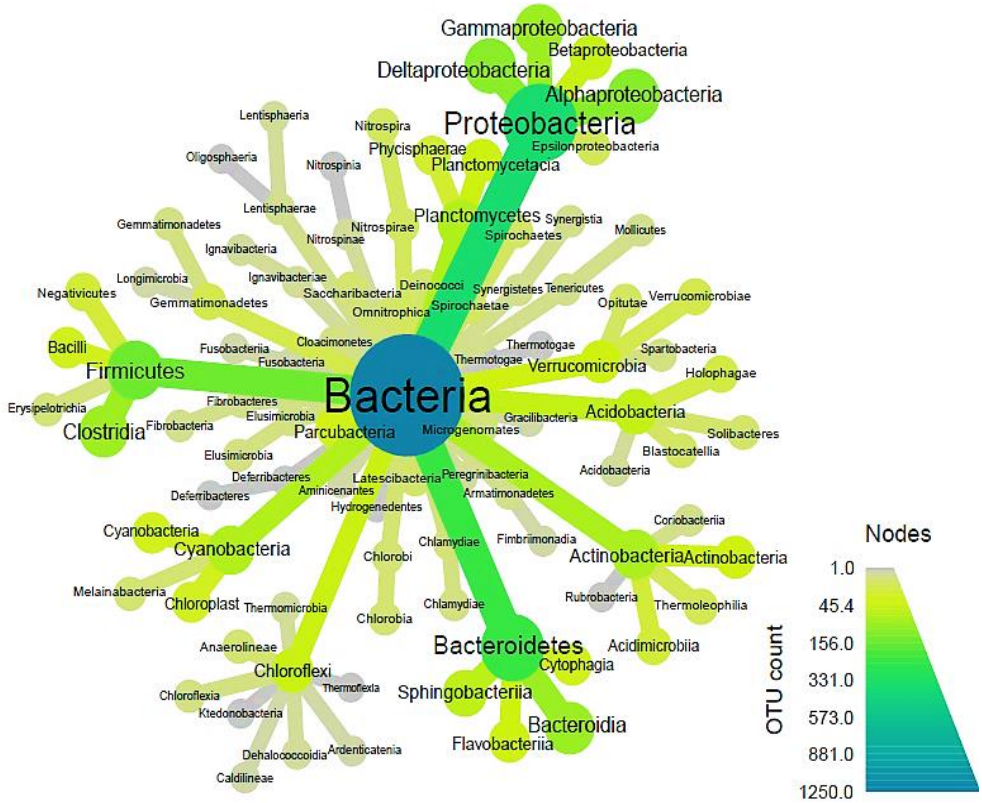

Figure 4.14: A heat-tree summary using the taxa from the Loopspruit River as OTU counts. The heat-tree shows the taxa from the bacterial kingdom, phylum and order. The heat-tree was generated in RStudio programming language with the Metacoder package.

4.7.1 Alpha-diversity

The boxplots in Figure 4.15 represent the alpha-diversity indices which reflect the consistency and abundance at each site. The Chao1 boxplots reflect the abundance of the bacterial OTUs, whereas the Shannon boxplots reflect the diversities in the samples. As the Chao1 index increases, the expected species richness also increases, and a high Shannon index results in a higher diversity. The boxplots are representative of the interquartile range (IQR) between the first quartile (25th percentile) and the third (75th percentile). The line in the middle of the box represents the median, and the whiskers serve to show the lowest and highest.

In Figure 4.15A the Chao1 index reveals that site MD02 has the highest bacterial OTU abundance, followed by KW03 and MU01. Sites KA05, KD06 and GP08 had a similar OTU abundance ranging from an estimated ~160 – 255. Site VA07 had the smallest OTU abundance. Figure 4.15B shows that the species diversity at site MD02 had a mean of ~3.68, where the whiskers range from a minimum of ~3.26 to a maximum of ~4.4. Site MD02, therefore, has the highest bacterial diversity. Site MU01 had the second-highest bacterial diversity, ranging from ~2.86 to ~4.24 with a median of 3.6. Sites KW03 and GP08 both had a small bacterial diversity range, whereas site VA07 had the lowest bacterial diversity which was significantly different ($p<0.05$) from all the other sites except MU01 and MD02. VA07, therefore, has the lowest diversity according to the Shannon index. In both Figure 4.15A and 4.15B, the abundance and diversity were high at sites MU01 and MD02 in the Loopspruit River, with mining activities and urban activities being dominant.

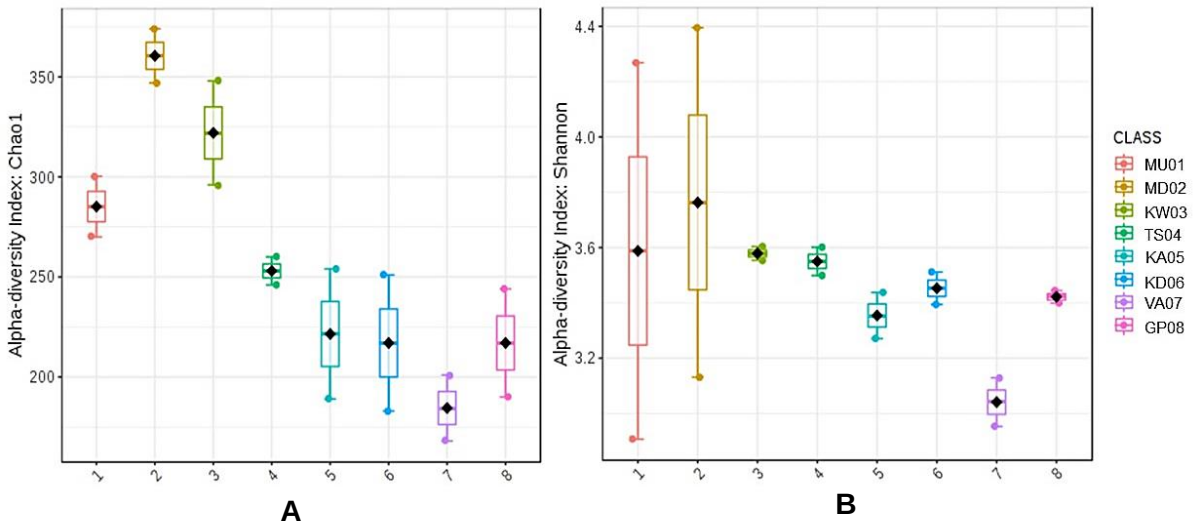

Figure 4.15: The alpha-diversities presented as a boxplot. The data were normalised, and a T-test/ANOVA statistical method was applied. The data were plotted with the Chao1 (A) ($p< 0.05$) and Shannon (B) diversity indices ($p<0.05$).

4.7.2 Beta-diversity

Beta-diversity of the sample sites along the Loopspruit River shows the difference between the various microbial compositions at these sites. The diversity in each of the bacterial communities has its own taxonomic abundance profiles. With this in mind, the sample site environments should plot together if their taxonomic abundance profiles are similar. In Figure 4.16, the site diversities plot together based on their similarity. The Bray–Curtis dissimilarity distance distribution uses the abundance or read count and determine differences in bacterial abundances. This is then plotted against values that range from 0 – 1, where 0 indicates that the sample sites have the same species and abundance. On the other hand, 1 indicates that the sample sites have entirely different species and abundances.

Geographically close sites formed associations as illustrated in Figure 4.16. Sites TS04 and KA05 are grouped with a range of ~0.15 to ~0.28. Both sites MU01 and KW03 display similarities close to zero (0) on both the y-axis and the x-axis. Sites VA07 and GP08 are also similar in terms of bacterial abundance. Sites KD06 and MD02 are on the outermost ranges, where KD02 has a distance distribution of -4.5 on the x-axis, and KD06 lies on a distance distribution value of >0.3.

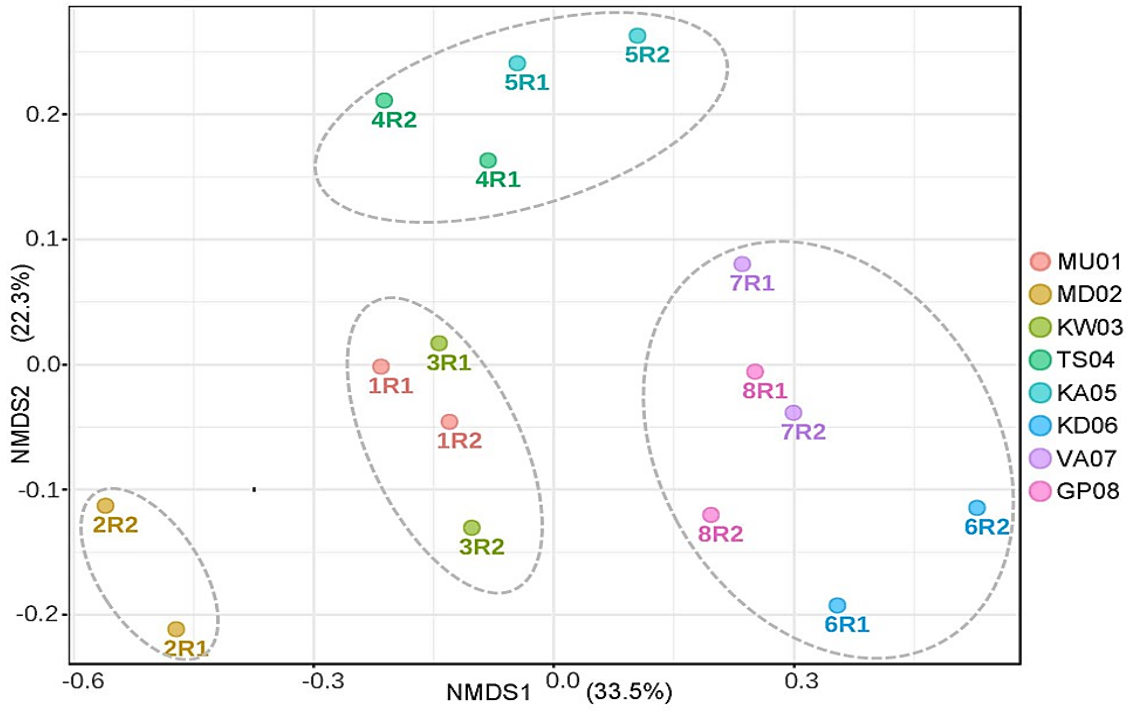

Figure 4.16: The NMDS diagram shows the β-diversity among the sample sites on a phylum taxonomic level. The statistical method used here was analysed for group similarities (ANOSIM p≤0.001) and applied a Bray–Curtis dissimilarity distance distribution with the sample sites with a correlation of R=0.75.

4.7.3 Bacterial community structure

In Figure 4.17, the bacterial communities are represented on a stacked bar-chart and accompanied by a Bray-Curtis dissimilarity dendrogram on phylum taxonomic level. Here the *Proteobacteria* was detected as the most common phylum, ranging from 30 – 60%. This was followed by *Bacteroidetes* with a frequency of 13 – 30%. Total contribution by *Cyanobacteria, Actinobacteria* and *Verrucomicrobia* all showed broad variation among samples. Some phyla contributing to the overall diversity include the unassigned isolates, *Percubacteria* and *Firmicutes.* At sites MU01 and KW03, the *Cyanobacteria* is the second most dominant bacterium, ranging from 5 – 45% of the total taxonomic contribution. At the sample sites in the lower reaches of the Loopspruit River, KD06, VA07 and GP08, the *Actinobacteria* contributed a significant portion of the total taxonomy, ranging from 5 – 25%.

Sites KD06 and VA07 have a bacterial community closely related to that at site GP08. Sites TS04 and KA05 have almost the same bacterial distribution and abundance. TS04 and KA05 are substantiated by the existence of a dissimilarity distance of 0.07. MU01 and KW03 are also closely related in terms of bacterial contributions, having a dissimilarity distance distribution of 0.3. The total taxonomic contribution at site MD02 differs significantly from that at all the other sample sites. It has a very different bacterial contribution at varying ranges. These bacteria include *Saccharibacteria, Acidobacteria, Omnirophica, Chloroflexi* and *Planctomycetes*.

The majority of the genera in Figure 4.18 were made up of *Flavobacterium* making up to 30% of the bacterial community at all sites. Some sites showed even higher *Flavobacterium* levels ranging up to 70 % at TS04 and KA05. Following Flavobacteria is *Hydrogenophaga* with the second most abundant bacterium in the Loopspruit River's bacterial community structures. *Hydrogenophaga* was previously classified under *Pseudomonas* and then, *Acidovorax, Pseudomonas, Verrucomicrobia* and *Massilia* respectively followed in broad variation among sample abundance.

Figure 4.18 shows the represented bacterial communities on genera level. Only the top 20% genera were used to generate the Bray-Curtis dissimilarity dendrogram. The R script that was used has been modified a bit to also incorporate the isolated genera *E. coli, Enterococcus* spp and *Clostridium* spp. The results showed in Figure 4.18 *Clostridium* spp ranged from ~8% to 50% throughout all the sites. GP08 showed the highest clostridium levels followed by KD06, VA07 and then MU01. However, *E. coli* and *Enterococcus* were not notably detected in the Bray-Curtis dissimilarity dendrogram.

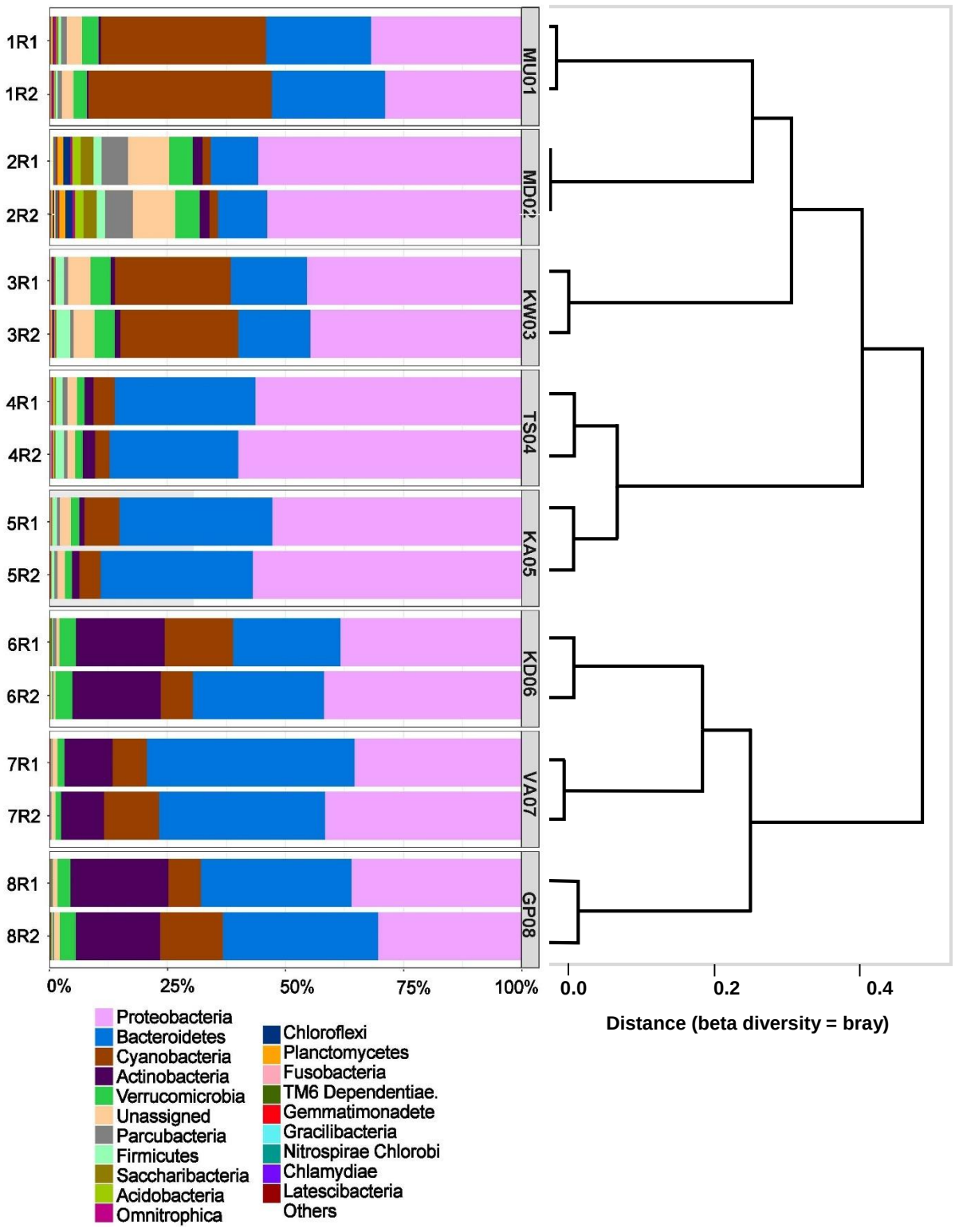

Figure 4.17: Bray-Curtis dissimilarity dendrogram indicating how related the bacterial communities are with regards to the phyla throughout the eight sample sites. The relative abundances are expressed as proportional percentages of the overall community.

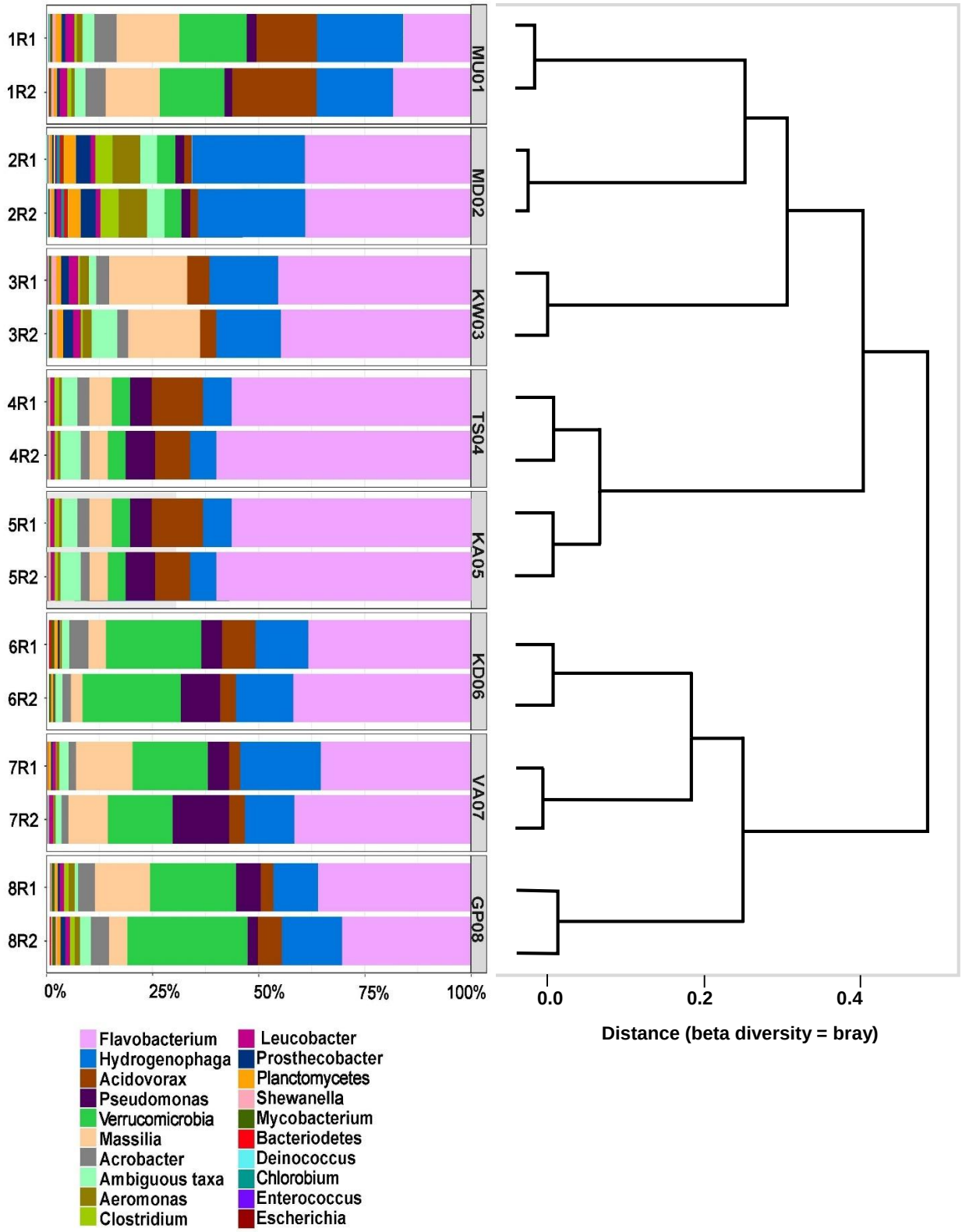

Figure 4.18: Bray-Curtis dissimilarity dendrogram indicating how related the bacterial communities are with regards to the genera throughout the eight sample sites. The relative abundances are expressed as proportional percentages of the overall community.

Non-metric multidimensional scaling (NMDS) was used to show where the data are collapsed in multiple dimensions of the sample sites, bacterial taxa and physico-chemical data. The NMDS scaling ensures that the data can be interpreted simultaneously and makes the analysis of the data flexible. In Figure 4.19, the majority of the sample sites (indicated by the coloured dots) seem to cluster around the zero (0) point, except for sample sites MD02 and KD06. This can also be seen in Section 4.7.2 of Figure 4.16. The *Bacteroidetes* favour the increased temperatures, which can be verified in Figure 4.19 at sites TS04 – GP08. The *Verrucomicrobia* and *Proteobacteria* favour low COD, while *Omnitrophica* and *Chlorobi* both are impacted by higher electrical conductivity. *Fusobacteria*, *Lentisphaerae* and *Gracilibacteria* are negatively impacted by the physico-chemical parameters temperatures, COD and EC. These bacteria may also be abundant at sites TS04 and KA05, where these physico-chemical parameters have less influence on the bacteria.

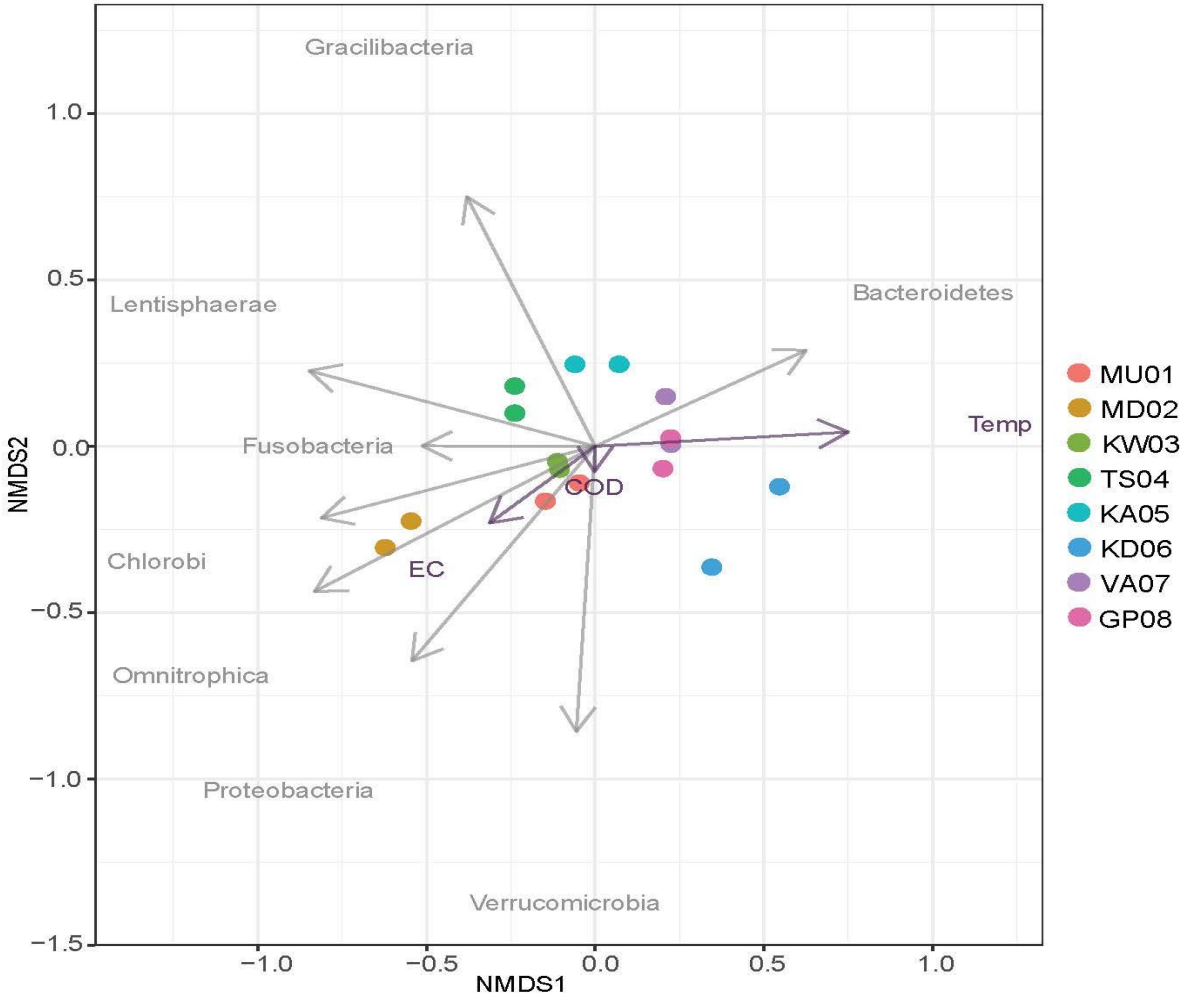

Figure 4.19: A CCA plot showing the analysis of variance by using distance matrices indicating the best set of significant environmental variables (p-value 0.048), to describe the community structure.

4.8 Predicted metagenome analysis

4.8.1 Physico-chemical and microbiological correlations

In Figure 4.20, the correlation between the physico-chemical and microbiological parameters is illustrated. The temperature has negative correlations with *Patescibacteria, Nanoarchaeaeota* and *Firmicutes*. The negative correlation is strongest towards *Patescibacteria*. SO_4 shows a weak correlation with only *Fusobacteria*. pH has a negative correlation toward *Bacteroidetes*, while COD has the strongest negative correlation toward *Nanoarchaeaeota*. The most significant node is *Patescibacteria.*

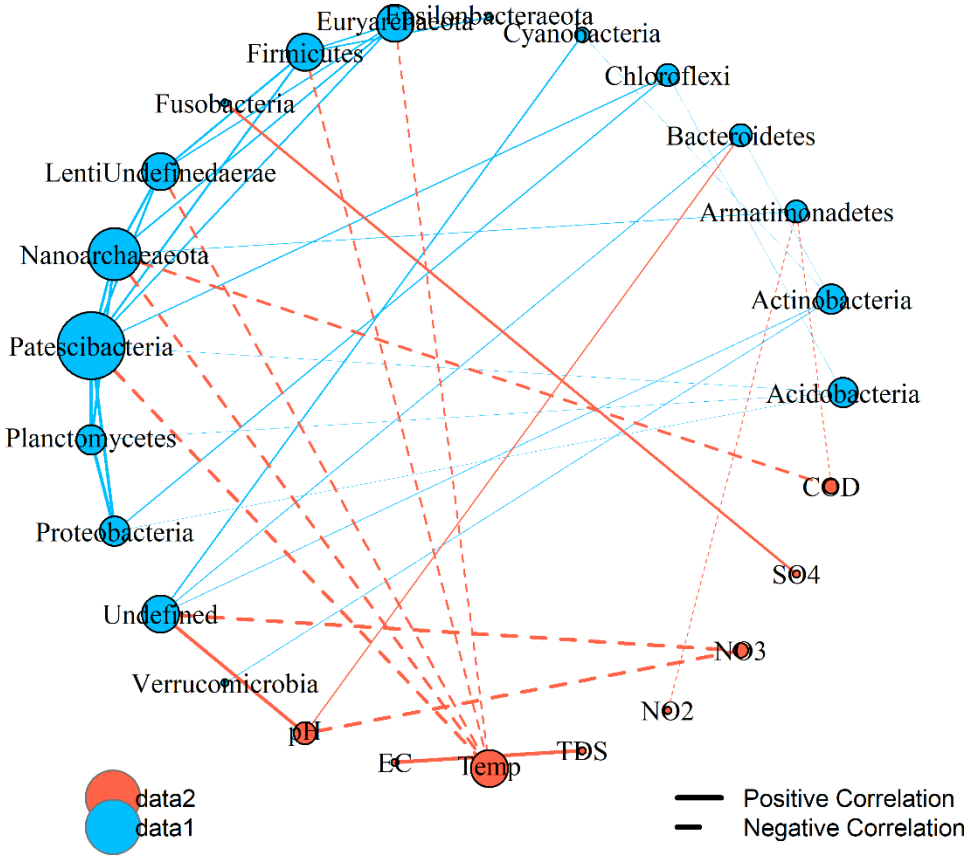

Figure 4.20: A physico-chemical and microbiological network analysis using the OTUs relative abundance at the phylum level. The nodes represent the bacterial abundance and the bacterial physico-chemical dependency. The correlation line thickness represents the magnitude of the relationship strength. Data1 describes the physico-chemical parameters and Data2 the microbiological parameters. The network analysis and visualization with the R package igraph

4.8.2 Microbial metabolism pathways (agrochemicals)

In Figure 4.21, site 3 (KW03) and site 8 (GP08) show the metabolic pathways when all the bacteria at the respective sites are considered. The reason for choosing only these two sites for analysis was based on the GIS analysis of historical physico-chemical data. These indicated consistently elevated levels of some of the parameters (indicated by the yellow-orange-red colour ramp visible in Figure 4.7). During the present study, these two sites also had the highest levels of physico-chemical parameters. In Figure 4.21A, the taxonomic mapping shows 24.6% of the total output was predicted to use the ammonia oxidizer metabolic pathway, followed by dehalogenation (20.2%). The sulphate reducing capacity was predicted to be present among 15.7% of the OTUs, whereas sulphide oxidiser capacity was predicted among 11.6% of the OTUs. Nitrite reducer capacity was predicted among 14.7% of OTUs.

Figure 4.21B shows the predicted metabolic pathways at site 8 (GP08). Here the predicted pathways show that dehalogenation contributes 32.7% of the abundance followed by the ammonia oxidisers (30.8%). The nitrite reducing pathways were higher in this case (26.9%), and so were metabolic pathways for nitrogen fixation (4.9%) when compared to site 3 (KW03). Also, the sulphate reducers and sulphide oxidiser pathways were higher (25.8% and 22.4%, respectively).

At both sites, unknown predicted metabolic pathways were higher than 50%, meaning that more than half of the metabolic pathways were ascribed to identified OTUs. This is an aspect that requires further investigation as the OTUs may provide further insights into the actual metabolic capabilities of the Loopspruit River.

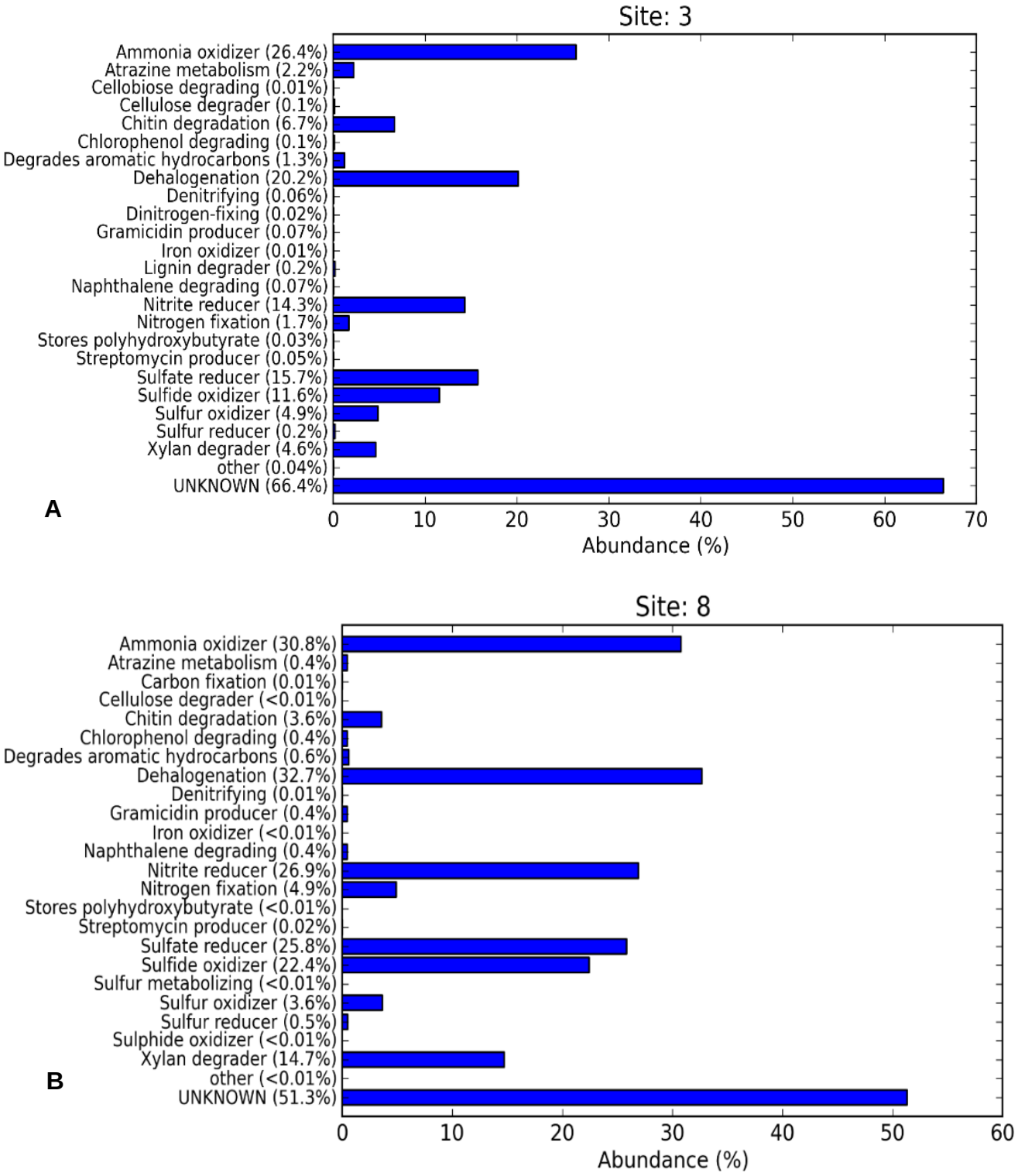

Figure 4.21: The taxonomic to phenotype mapping of OTUs at site KW03 (A) and GP08 (B) that shows predicted metabolic activities.

4.9 Chapter 4 Summary

The physico-chemical data for 2018 and 2019 are not a cause for concern ($p>0.05$), with exceptions for TDS, nitrite and phosphate levels that exceeded the RWQO for both 2018 and 2019. There were massive increases in nitrites during 2019 when compared to 2018. An excessive amount of phosphates was also detected in 2019 in both the wet and dry seasons, exceeding the RWQO. The physico-chemical visual representations showed that there are two main sites that possibly contribute to the physico-chemical contamination in the Loopspruit River. These sites are KW03 and upstream WWTP and GP08 which is associated with urban activities.

The microbiological analysis of the water quality showed definitive faecal contamination which included faecal contamination from agricultural and urban settings. These faecal contaminants included bacteria such as *E. coli, Enterococci* and *Clostridium.* The total coliforms and faecal coliforms did not fall within the RWQO. There was an overall abundance of HPC bacteria in the Loopspruit River, including significant microbial contamination in the Loopspruit River. Some of the identified HPC bacteria included opportunistic pathogens such as *Aeromonas, Pseudomonas* and *Flavobacterium*. A faecal contamination visual representation was created to predict possible contamination sources. It was clear that urban and WWTP were the greatest contributors to faecal pollution.

The MAR index revealed higher values during the dry season compared to the wet season with no significant differences ($p>0.05$). Here the results also indicated that the agricultural and urban activities were the most significant ($p<0.05$) contributors to high MAR index values. These results were confirmed by detecting the antibiotic concentrations in the Loopspruit River. The risk selection index showed that all but tetracycline showed some risk to the ecological environment. Ampicillin showed a risk of 637.95 where it should ideally be <1.

The alpha-diversity showed that site MD02 has the highest abundance and species richness. Beta-diversity showed that site MD02 did not group close to the other sites. The community structure showed an abundance of *Proteobacteria* followed by *Bacteroidetes*, *Cyanobacteria, Actinobacteria* and *Verrucomicrobia.*

Finally, the predicted metagenome analysis revealed correlations between physico-chemical and microbiological parameters. SO_4 only had a correlation with *Fusobacteria.* The predicted metabolic pathways showed that 24.6% used the ammonia oxidizer metabolic pathway, followed by dehalogenation with 20.2%. The sulphate reducing bacteria, sulphide oxidisers, nitrite reducers and nitrogen fixation bacteria were also prominent.

CHAPTER 5: DISCUSSION

In recent years, there has been an increase in changes in land-use practices as urbanisation increased, resulting in deteriorating water quality of surface water sources (Ngoye & Machiwa, 2004). Pullanikkatil *et al.* (2015) stated that water quality and land uses are closely associated.

Eight sample sites (MU01, MD02, KW03, TS04, KA05, KD06, VA07 and GP08) along the Loopspruit River were selected for analysis. The sample sites were selected based on their surrounding land use activities such as agriculture, mining and urbanization. Sampling was done in 2018 within a wet and dry season and the same for 2019. The physico-chemical parameters were measured, and the microbiological results were analysed in the laboratory. These parameters are discussed with respect to the measured levels, taking into account some historical available data. Various land uses in the vicinity of the different sample sites were also considered. The discussion in the following sections deals with physico-chemical effects which will be addressed first, followed by the microbiological analysis, the antibiotic susceptibility, isolate identification, bacterial diversity and finally predicted microbiome analysis.

5.1 Geospatial analysis visual representations

Geospatial data can be used to connect the roles between data acquisition, data modelling, data visualization, and data analysis (Breunig *et al.*, 2020). In this study, the combination of raster and vector data formats was used to visualise certain physico-chemical and microbiological characteristics of the Loopspruit River. A fruitful option is to join different informational indices to improve the subsequent data layer. Such an information combination approach can, for instance, depend on cutting edge GIS activities to join distinctive spatial arrangements (i.e., raster-, vector- and table layers). For instance, GIS data can be joined with remotely detected data as intermediaries for boundaries. This methodology can be utilized to determine exceptionally itemized land use and building use formation by associating temporal, spatial and spectral information patterns to particular human activities, often with the help of deep learning algorithms (Masson *et al.*, 2020). It is significant, nonetheless, to have good data about the nature of every datum set, as they may contain similar data with various characteristics or spatial goals.

Water resources are inconsistently spread both spatially and temporally. Throughout the years, expanding populations, urbanization, and augmentation in agriculture and residential water usage

have complemented the conditions. Water contamination, not just influences water quality, it also threatens human wellbeing, has financial implications, and impacts on social success. Water quality results from a geospatial analysis can give the necessity of making the public, local administrator and the government to be aware of poor water quality (Panwar *et al.*, 2015).

The use of geospatial analysis applications has the potential to revolutionize water monitoring and management in the future. Quickly extending GIS innovation will assume a focal job in taking care of the voluminous spatial-temporal information and their successful understanding, investigation, and introduction to environmental management and decision making. Finally, the use of geospatial studies can be utilized as a successful means to anticipating and observing water quality, in this manner diminishing the efforts, and the material expenses (Madhloom *et al*., 2017).

5.1.1 Application of the IDW interpolation

In Section 2.12.2, the geospatial analysis of water chemistry was explained. The combination of the raster and vector data helped to further strengthen the data layer in ArcMAP. The raster data layer visually showed the Loopspruit River as a thematic map. This raster data layer was generated by the IDW interpolation technique in ArcMAP. Each cell had a different calculated weighted value assigned to it where the higher values were given a red (hot) colour and the lower values were given a blue (cooler) colour. However, the grid heavy visuals were not desired to represent a river, so the raster data layer was "stretched" to give it the desired "flow" aesthetic. On the other hand, the vector data layer was used to give some reference and context to the map. The vector data points used, indicated the sample sites and the noteworthy areas.

To reiterate, the concept of the IDW interpolation technique is fundamentally based on Waldo Tobler's first law of geography "*everything is related to everything else, but near things are more related than distant things*" (Ogbozige *et al.*, 2018). The IDW method is based on Tobler's law (Sówka *et al.*, 2020). The IDW interpolation technique was used fruitfully in various studies (Cannarozzo *et al.*, 2006; Chen *et al.*, 2017; Gemmer *et al.*, 2011; Lu & Wong, 2008)

The study done by Cannarozzo *et al.* (2006) applied the IDW method to create a raster thematic map on the rainfall trends in Sicily with historic data from 1921 – 2000. Chen *et al.* (2017) compared spatial interpolation schemes for rainfall data with the application in hydrological modelling. The authors noted that hourly rainfall data showed the best IDW results for their study. Moreover, Gemmer *et al.* (2011) studied the trends in precipitation extremes in the Zhujiang River Basin, South China. They used the IDW and Kriging methods and found few discrepancies.

Finally, the study by Lu and Wong (2008), applied the IDW method because it does not use computationally intensive procedures.

The implementation of the IDW interpolation technique proved to be successful in the current study. Through generating the geospatial representations of the physico-chemical parameters with the historic data it is clear that this interpolation technique is a viable and trustworthy application. With that having been said, this application in this study shows which areas have higher levels of the related physico-chemical parameter such as the pH and the Mg. This can help with environmental decision-making and management.

5.1.2 Physio-chemical visual representations

The geospatial visual representations represented by Figures 4.5 to 4.7, Section 4.2.1, indicate "hot" zones where the physico-chemical parameters are high, and thereby predict possible pollution sources in the area. The geospatially represented pH was high at Klipdrift Dam (KD06) with a value of 9.49, and the visual representation of Mg was high at site GP08 (41.30 mg/L), which is an urban area. Both of these visual representations showed "hot" zones where their respective parameters were above the RWQO. These two visual representations were chosen because pH is used as the basis of any water quality test to determine possible pollutions. The Mg visual representation was chosen as a representation of an outlier. Also, a summative visual representation was created to represent all of the physico-chemical visual representations that were created listed in (Appendix B). The summative visual representation showed that site KW03 and GP08 had the "hottest" zones based on all the other physico-chemical visual representations.

A study done by Yang *et al.*, (2019) revealed that in a river polluted with Mg, the pH levels were lower. Also, when the pH levels were elevated there was a decreased level of Mg. This was the case in this study as represented in Figures 4.1 and 4.2 where the pH was higher at site KD06 and low at site GP08. Mg was high at GP08 and low at KD06. In this way, particular examples of bacterial community structure and circulation may result from both the determination of ecological pressure and specific adaptation strategies of microbial species (Yang *et al.*, 2019). From a physico-chemical perspective, Gelli *et al.*, (2018) noted that particles dissolve more rapidly in lower pH levels than at higher pH levels. The Mg ions are soluble at low pH levels and do not reform (recrystallise), hence the increased Mg labels at the lower pH areas.

With the elevated Mg levels at the urban area GP08 near Potchefstroom, these elevated Mg levels also pose health threats to the surrounding environment. When exposed or ingesting high amounts of Mg, these can lead to hypermagnesemia (Jahnen-Dechent & Ketteler, 2012) which can lead to renal failure. DWAF (1996a) set the upper limits for "safe" at 30 mg/L Mg and excess

Mg can lead to diarrhoea. The health-related effects of pH levels are further discussed in Section 5.2.1.

A study by Shil and Singh, (2019) investigated the health risk assessment and spatial visualisation of dissolved heavy metals and metalloids within a tropical river basin system. The river system is located in the Mahaldiram Hill of Siwalik Hi- Malayan ranges in the Darjeeling District of West Bengal, India. This investigation revealed that in a pre-monsoon season the pH was more alkaline, which was the case in this study. The authors further explained that the bioavailability, solubility and mobility of nutrients and metal(loid)s are greatly influenced by the pH of the water.

Research study by Wijesiri *et al.* (2019) investigated the geospatial distribution and interaction of nutrients and metals between water and sediment phases in a river system. The study area is situated in the Shenzhen River, which is located in Shenzhen, South China. This study was carried out by using innovative statistical and geospatial analyses. Metals detected in the water can be a result of urban stormwater runoff (Isiyaka *et al.*, 2019; Wijesiri *et al.*, 2019). This effect correlated with the findings in this study where the Mg was higher at the urban settings at site GP08. Parallel to Wijesiri *et al.* (2019), the possible reason for the elevated Mg levels in this study can be due to stormwater runoff.

Madhloom *et al.* (2017) investigated the spatial distribution of some contamination within the lower reaches of the Diyala River. The authors visually represented the geospatial analysis of heavy metals: copper (Cu), chromium (Cr), manganese (Mn), and iron (Fe) together with total suspended solids (T.S.S) and total dissolved solids (T.D.S.). Moreover, the authors concluded that pollution was visibly shown downstream of the WWTP. This effect was also seen in the current study. Finally, this is an excellent example of how the simulated results obtained by the GIS through geospatial analysis, can be used for extracting water quality maps.

Considering the discussion on geospatial visual representations above, it is therefore clear that more studies from a geospatial perspective are needed. Geospatial studies are important resources that aids in sustainable green socio-economic development and natural assurance on the planet, particularly in dry and semi-parched districts of the globe (Gidey, 2018). Geospatial analysis can even be applied to the microbiological data, such as determining the link to the landscape patterns and microbial contamination (Wu, 2019).

5.1.3 Microbiological visual representations

One example of microbiological geospatial analysis is the study of Elliott *et al.* (2016). Here the authors investigated the spatially distributed mean annual loads of total nitrogen, total phosphorus, sediments and *E. coli*, and concentration of nutrients throughout New Zealand. Elliott

et al. (2016) did a geospatial analysis of the entire country of New Zealand in GIS. The authors also noted that the annual *E. coli* loads were higher in the summer (wet seasons).

A study was done by Xue *et al.* (2018) in China that focused on the tempo-spatial controls of total coliform and *E. coli* contamination in a subtropical hilly agricultural catchment. The study included samples from surface waters and groundwater reservoirs. The authors concluded that the total coliform and *E. coli* levels increased during an intense rainstorm event. Furthermore, Xue *et al.* (2018) studied the total coliform and *E. coli* levels in various land-use settings which included residential land uses, industrial waste works, intensive cattle feedlots and a pig slaughterhouse.

It is quite difficult to visually represent total coliform and *E. coli* levels on a geospatial level, because of limited data in South Africa, however, this is not impossible with the aid of sufficient continuous time-series data of, for example, *E. coli*. In the context of this study, there were not enough microbiological data to attempt a geospatial representation of the Loopspruit River. The microbiological data obtained in this study was deemed insufficient and will not be able to give a holistic geospatial perspective on the Loopspruit River.

5.1.4 Additional geospatial analysis applications

Other possible studies on microbiological water quality include, but are not limited to, groundwater, oceanic, and antibiotic studies. Examples of a groundwater geospatial study include Gidey (2018). Here the study investigated the overall groundwater water quality for irrigation use. Gidey (2018) concluded that GIS and irrigation water quality indices provide better methods for irrigation water resources management to improve food security and longer sustainability This will ultimately avoid the probability of increasing environmental problems for the future generation. Furthermore, Islam *et al.* (2020) applied analysed groundwater at the southern coastal region of Bangladesh. The study used spatial autocorrelation index and fuzzy GIS analysis to delineate the suitability of groundwater at coastal regions for drinking water.

Alvarez-Romero *et al.* (2013) did a study on the approach to show how ecosystems are affected by land-based pollutants. The study was done at Coral Sea, off the coast of Queensland in north-east Australia, and a World Heritage Site since 1981 (Alvarez-Romero *et al.*, 2013). Results showed geospatial analysis was an effective means to map plumes and qualitatively assess exposure to land-based pollutants on the coast. The authors concluded that plume spatial-temporal dynamics offers a method to monitor exposure of coastal-marine ecosystems to plumes and explore their ecological influences.

Alternatively, the water quality influenced by antibiotics can also be geospatially analysed and visualised. Legenza *et al.* (2019) used spatial interpolation methods on *E. coli* susceptibilities to

create geographic antimicrobial resistance visualisations in the state of Wisconsin in the United States of America. The study included *E. coli* susceptibilities to amoxicillin-clavulanate, ampicillin, ampicillin-sulbactam, ciprofloxacin, levofloxacin, nitrofurantoin, and trimethoprim-sulfamethoxazole (Legenza *et al.*, 2019). This is a novel idea for the clinical sector for education and a decision-making tool on the amount of antibiotics that are in the environment.

5.2 A physico-chemical analysis of the Loopspruit River

5.2.1 pH

Results indicated that the pH remained relatively constant with values during the wet and dry seasons of 2018 and 2019 ranging from 7.40 – 9.40 (Table 4.1 and Table 4.2). Various anthropogenic activities can contribute to the pH levels which Dallas & Day, (2004) lists as runoff from agricultural fields, mining activities and the infiltration of untreated wastewater. These contributing factors are all present in the Loopspruit River

The results from this study is corroborated by the findings of Jordaan *et al.* (2019) who studied the response of bacterial communities to anthropogenic contaminants in the Wonderfonteinspruit River flowing north of the Loopspruit River. The authors found that the pH ranged from 7.17 to 8.29 in the Wonderfonteinspruit River, situated, possibly as a result of dolomitic dissolution at the headwaters of the Wonderfonteinspruit River system.

The Loopspruit River sub-catchment are situated on the Pretoria Group (see Section 4.1.1), possibly giving rise to carbonates. There is a dolomitic presence at the headwaters of the Loopspruit River sub-catchment which may thus be contributing towards the pH stability in the river system. Acidic waters generated by mining activities result in the dissolution of dolomites ($CaMg(CO_3)_2$). This may contribute to the rise in macronutrients such as magnesium (Mg) and calcium (Ca) in the Mooi River catchments systems, including the Loopspruit River (van der Walt *et al.*, 2002). A study by Copatti *et al.* (2019) focussed on the protective effect of hard water on pacu juveniles (a fish species *Piaractus brachypomus*) in acidic or alkaline waters. The authors found that low carbonate levels reduce the buffering capacity of acidic water resulting in pH fluctuation. This buffering effect may take place in the Loopspruit River where the carbonates act as a buffer to raise the pH of the acidic water generated through mining activities. An alkaline pH has an effect on the microbial community and diversity as a stimulating factor (Constancias *et al.*, 2015).

5.2.2 Temperature

Temperature is one of the main driving forces that affect almost all physico-chemical equilibria and biological processes is the temperature (Delpla *et al.*, 2009). The temperature ranged from 8.40°C at site MD02 in the cold dry season (winter) of 2019 to 25.53°C during the warm wet season of 2019. TDS, phosphates, nitrites and nitrate levels increased as the temperatures increase in the warm-wet season of 2019 (Table 4.1 and 4.2). The opposite trend can be seen in 2018 when the temperature decreased in the cold-dry season, the physico-chemical parameters

also decreased. This may indicate that the physico-chemical parameters were affected by temperature ($p>0.05$).

An increase in temperature may result in an increase in the adsorption of ions and increase solution of dolomite resulting in higher concentrations of Mg and Ca (Fattahi Mehraban *et al.*, 2019; Masindi *et al.*, 2015). The Mg steadily increases and goes in dissolution whereas the Ca keeps decreasing, possibly through reaction with carbonate groups to form Ca_2CO_3. This may also explain why Ca levels were high at sites MD02 and KW03 (Figure B.3, Appendix B). Ca ions have not yet reacted with the carbonate groups as carbonate levels are likely higher after the dissolution of dolomite [$CaMg(CO_3)_2$]. The Mg ions were abundant at site GP08 (Figure 4.6) because the Mg ions were carried downstream without reacting with compounds and therefore accumulated along the Loopspruit River up to site GP08.

The levels of coliforms increased during the warm wet seasons and decrease during the cold dry season (Tables 4.3 and 4.4). Using the WASP model and analysis of the Shenandoah River watershed in West Virginia, USA, Mbuh *et al.* (2019) demonstrated that temperature affects microbial growth.

5.2.3 Total dissolved solids

The TDS levels during the wet and dry seasons of 2018–2019 ranged from 363.33 – 808.33 mg/L. The relatively high TDS levels throughout the Loopspruit River decrease slightly during the wet seasons which can be explained by a dilution effect. TDS remained above the RWQO at the urban land use areas throughout 2018 – 2019s wet and dry seasons. Kora *et al.* (2017) screened physico-chemical and bacterial parameters in the Hussain Sagar Lake, which is an urban wetland in India. Here the authors found that during their dry seasons the TDS levels ranged from 768.4 – 814.6 mg/L in August 2014 and 715.2 – 793.0 mg/L in September 2014. The authors also indicated that the TDS levels also exceeded the Indian water standards of 500 mg/L.

In a South African context, van der Walt *et al.* (2002) found that the TDS levels were elevated in dolomitic headwaters within the Mooi River catchment. This supports the findings of this study on the Loopspruit River which is situated within the Loopspruit River sub-catchment within the greater Mooi River catchment. The dissolution of dolomite resulted in elevated Ca and Mg macromolecules and TDS. This process is dependent on pH that controls the buffer capacity in the Loopspruit River. During the warm wet season, the TDS levels were slightly lower. This trend is in contrast with the study done by Mhlongo *et al.* (2018) that found the TDS was higher during warmer temperatures. Elevated TDS levels point to increased ion concentrations affecting crop production.

Changes in TDS could also be due to changes in land-use activities. Adeola Fashae *et al.* (2019) conducted a study in Osogbo, the capital of Osun state in Nigeria, to analyse the impact that land use has on surface water quality. The authors found that there were higher levels of TDS in urban settings. Most of the catchment of the Mooi River is through a rural area. However, higher TDS levels in the case of this study were due to other parameters and not necessarily urban land-use.

5.2.4 Sulphates

Sulphate levels during the dry season of 2018 were above 200 mg/L and during the wet and dry seasons of 2019 sulphate levels were below value. The sulphate levels at site MU01, MD02 and KW03 remained elevated compared to the other sample sites. This is to be expected because of the mining activities around these sample sites. During mining activities, processed debris are deposited in a mine tailings dam where excess sulphates are carried through surface runoff to the Loopspruit River. These sulphates, in small quantities, can contribute to the nutrient composition of water (WHO, 2006) which sulphate reducing bacteria like *Clostridium* spp. can use. Sulphate levels were lower at sample sites after the WWTP (KD03) likely due to a dilution effect as the Loopspruit River flows downstream.

High sulphate levels in rural farming areas were probably a result of fertiliser use through surface runoff, sewage effluent and fertilisers (Khatri & Tyagi, 2015). A study by Mhlongo *et al.* (2018) on water quality in mining regions of South Africa found that sulphate levels can serve as an indicator of salinity. The salinity can, to some extent, also be indicative of the TDS. Moreover, the findings from the Water Research Commission (WRC) report by (Bezuidenhout *et al.*, 2017) indicated that varying sulphate levels were detected in the Mooi River catchment. Another probable reason for the sulphate levels may in the result of sulphur-bearing minerals and mining activities.

Furthermore, these sulphates in combination with disinfectants and dissolved oxygen result in taste and odour problems (Kristiana *et al.*, 2010). Since the sulphate levels are below the RWQO of 200 mg/L there is no cause for concerns. There are also no adverse effects listed by the World Health Organisation that may affect humans at the levels present in the Loopspruit River (WHO, 2011).

5.2.5 COD

The COD levels in the 2018 dry season were higher than values measured in the wet season. In COD levels were higher in the wet season. During the dry season of 2018, COD levels were higher than 100 mg/L. COD levels were elevated at sample sites with urban and mining land uses. Kora *et al.* (2017) did a physico-chemical screening of an urban wetland and also found that COD levels were elevated due to untreated domestic sewage containing oxidizable organic matter. The

COD levels also coincide with the change in temperature where the COD levels are elevated during the cold dry seasons due to the increase in oxidizable organic matter and lack of dilution within the Loopspruit River. Something to consider at lower temperatures is that the microorganisms are less active, lowering the breakdown of organic material, thus resulting in an increase of COD.

Similar trends in the increased COD during the wet season, corroborate the study done by Choi *et al.* (2019). The authors characterised the BOD and COD export from paddy fields during rainfall and non-rainfall periods. During the wet season, the authors reported COD increases from rice paddy fields at higher temperatures. Şener *et al.* (2017) generated a water quality index for the Aksu River in Turkey. Here the authors found that COD and Mg had the highest effect on the water quality and concluded that it was as a result of anthropogenic factors which are the same conclusions made with the findings of the present study.

5.2.6 Nitrite and nitrate

Nitrite levels during 2018 remained relatively constant, in terms of the wet and dry seasons at site MU01 when, it increased from 4.00 mg/L to 34.33 mg/L. In 2019 at site KA05, the nitrite increased from 11.00 mg/L to 39.00 mg/L. Fadiran and Mamba (2005) conducted a study in Swaziland to analyse nitrates and nitrites from water effluents in surface waters. The authors stated that the excess nitrate and nitrite (apart from those generated from industry and urban areas) are indicative of artificial(man-made) pollution from the agricultural sectors. This can be as a result of fertiliser leachate that collected and deposited in the Loopspruit River through surface runoff.

These human health risks include biofilms harbouring opportunistic pathogens (Liu *et al.*, 2019). Fadiran and Mamba (2005) argued that raw waste from industries, WWTPs and especially agriculture delivers high levels of ammonia and nitrogenous waters. This agrees with this study, where nitrite and nitrate levels are increased in agricultural settings that may use fertilisers and at the WWTP environments. A previous study showed that nitrate contribution from commercial land use was higher compared to the residential or agriculture land use (Adeola Fashae *et al.*, 2019); however, this was not the case in this study. The highest nitrite and nitrate levels were detected at the agricultural areas of TS04 and KA05. High nitrite levels are also a cause for concern, especially for infants younger than six months of age (DWAF, 1996a), but fortunately, these detected levels in this study cause no need for concerns.

5.2.7 Phosphate

Phosphates remained relatively constant during both wet and dry seasons in 2018, except for increased levels at site KW03, with 1.11 mg/L during the dry season and 4.00 mg/L in the wet

season. In 2019, phosphates levels at KW03 ranged from 0.40 – 5.25 mg/L exceeding the RWQO of 0.40 mg/L. All physico-chemical parameters were acceptable except for phosphates and TDS levels. Both were over the RWQO, and both are indicative of faecal pollution in the Loopspruit River. These results correlate with the notion that phosphates increase with runoff from agricultural fields and sewage from urban settings (Jarvie *et al.*, 2006; Parry, 1998). In the present study, phosphate levels were also higher during the wet seasons, a differing outcome to the findings of Jarvie *et al.* (2008). The authors mentioned that the seasonal times series for these sites indicated an articulated decrease in NO_3–N concentration throughout the spring and summer months, with an increase in NO_3–N concentrations during the autumn.

A carbon, nitrogen and phosphorus ratio (C:N:P) of 100:10:1 is generally considered to be ideal for microbial growth. Chen *et al.* (2019) explained that with C:N:P addition, the microorganisms that have rich phosphorus surroundings can grow. When the microorganisms are in a poor phosphorus environment, they undergo “maintenance mode” to remove the nutrient limitation. A study by Adeyemo *et al.* (2013) on seasonal changes in the physico-chemical parameters and nutrient load in river sediments in Ibadan City, Nigeria, contributed high phosphorus levels to surface runoff from agriculture during the wet seasons. This can also be seen in the present study where the high levels of phosphorus were seen at sites TS04 and KA05 during wet and dry seasons of 2018 and 2019.

Modern agricultural practices use several fertilisers containing nitrogen and phosphorus to enhance crop growth (Walmsley, 2000). River systems with high levels of these nutrients are prone to eutrophication, which alters the structure and functioning of biotic communities (Diaz & Rosenberg, 2008). According to van Ginkel (2011), extensive eutrophication of South African dams is problematic. This is indicative of pollution from agricultural depositing these nutrients in the Loopspruit River through surface runoff. These high carbon and nitrogen levels promote cyanobacterial growth resulting in a eutrophic river system.

5.3 Microbiological water quality analysis of the Loopspruit River

Through the duration of the two wet and two dry seasons (2018 and 2019), the microbiological water quality at all the different sample sites was substandard with total and faecal coliform values exceeding the RWQO.

5.3.1 Heterotrophic plate count bacteria

Heterotrophic plate count is often used as an indicator of microbial water quality, and should not exceed 1000 CFU/mL (DWAF, 1996a). The HPC ranged on average from 2.08 x 10^2 CFU/mL to 2.54 x 10^5 CFU/mL during the dry seasons and ranged from 1.28 x 10^4 CFU/mL to 1.87 x 10^5 in the wet season. The highest HPC was observed at site KW03 during the dry season and KD06 during the wet season. None of the sample sites complied with the RWQO.

A study by Paulse *et al.* (2009) focused on comparing the microbial contamination of the Plankenburg- and Diep Rivers, Western Cape, South Africa. The authors observed high HPC levels in the Plankenburg River and concluded that it is as a result of effluent from an informal settlement, where waste was carried into the river by stormwater drainage pipes. Additional contamination sources included agricultural and urban activities along the Plankenburg River.

16S rRNA gene sequencing identified *Flavobacterium* sp*., Sphingobacterium* sp., *Chryseobacterium*, *Arcicella, Arthrobacter, Beta proteobacteria, Janthinobacterium*, *Rheinheimera* sp., *Aeromonas* sp. and *Pseudomonas* sp. *Flavobacterium* sp. was the most abundant from the isolated HPC bacteria Plankenburg River study. Jordaan *et al.* (2019) listed taxa in their study that correlate with the findings of this study such as *Flavobacteria. Flavobacteria* were mostly isolated at sites MU01 and MD02, where mining is the dominant land use activity. Here the *Flavobacteria* can metabolise the increased sulphate levels produced by the mining activities (De Figueiredo *et al.*, 2012; Jordaan *et al.*, 2019).

Some of the isolated HPC bacteria present at the sample site in this study included opportunistic pathogens such as *Aeromonas, Chryseobacterium, Flavobacterium* and *Pseudomonas* (Cui *et al.*, 2019; Pavlov *et al.*, 2004). These opportunistic pathogens pose a significant threat to infants and toddlers, the elderly and immune-compromised individuals (Cui *et al.*, 2019; Pavlov *et al.*, 2004; Payment *et al.*, 2003). Within the North West Province, most of the population are dependent on groundwater. Groundwater may not be safe for consumption because the pathogens may be in the recharge water from the surface. If the communities of the North West Province were supplied with water containing high levels of HPC bacteria, their risk of disease would increase.

It should be noted that these opportunistic pathogens proliferate when deposited onto food (Allen *et al.*, 2004). When contaminated food is ingested, there is an increased risk of gastroenteritis. Therefore, extra precaution should be taken to check food and also food preparation. Many rural communities rely on groundwater as a drinking water source. This stresses the importance of HPC analysis to determine the possible health risks to ensure food safety.

The HPC isolates were tested for antibiotic resistance. Ampicillin, amoxicillin, and trimethoprim resistances were the most prevalent amongst the organisms tested, followed by resistance to sulphamethoxazole and colistin. In a study by Knapp *et al.* (2010) the authors found that the overall antibiotic resistance and resistant genes increased over time, based on the land-use practices and anthropogenic activities. With that in mind, this serves as a possible explanation for HPC species having similar antibiotic resistance profiles in the present study.

5.3.2 Total coliforms and faecal coliforms

Typically, *E. coli* is distinguished as one of the best organisms to use for monitoring faecal coliforms by the World Health Organization (WHO). *E. coli* cannot grow in non-polluted river waters making it the ideal faecal indicator organism Baudišová (1997). The faecal coliforms during the dry season ranged from an average of 3.83 – 20.83 CFU/100 mL, not exceeding the RWQO of 0 CFU/100 mL during the wet season. During the wet season; faecal coliforms counts increased significantly as a result of surface runoff (10.83 – 350.00 CFU/100 mL). This may be a result of nutrient accumulation from various sources from the surface runoff resulting in the increased coliform growth.

Sample sites MU01 to KA05 close to urban and agricultural activities showed the highest coliform counts. As mentioned previously (Section 5.2.2), temperature has an influence on bacterial growth. Higher temperatures are favoured by most bacteria ranging from 20°C to 45°C. During a precipitation event, the runoff and increased streamflow of a river carry these total coliforms for quite some distances. A study by McGinnis *et al.* (2018) illustrated that rain surface runoff, in combination with sewer overflows, resulted in high levels of human faecal pollution. The total coliform bacteria identified in site MD02 and KW03 contributed most of the total coliforms that may originate from urban settings. From an agricultural perspective, a study by Xue *et al.* (2018) showed that there is a higher risk of microbial (coliform) contamination after a precipitation event. The authors found that the coliforms range from 4.39 – 7.11 CFU/100 mL during the wet seasons. This is in agreement with the results found in the present study where the total coliforms ranged from an average of 25.67 – 350.000 CFU/100 mL during the wet season.

The areas with high levels of coliform contamination may be as a result of cattle, pig and sheep farming in the area where sites TS04 and KA05 are located. Site TS04 and KA05 showed the highest levels of coliform contamination in agricultural settings. This would suggest that farm animals are likely the main contributors to the faecal pollution. This is supported by the findings of Abia *et al.* (2015a) that found elevated levels of faecal coliform (*E. coli*) counts observed during the wet season, especially at the tributary areas with agriculture and informal settings.

According to DWAF (1996b), the health risks to humans when exposed to total and faecal coliforms contaminated might be from irrigation water, such as gastrointestinal disease. These contaminated irrigation waters are used on fresh vegetables consumed by humans. This is problematic because it may facilitate the distribution of viral and bacterial pathogens (Heaton & Jones, 2008; Steele & Odumeru, 2004). Unfortunately, the total and faecal coliforms levels in this study showed some cause for concern for irrigation.

5.3.3 Enterococci

The highest levels of enterococci in the dry season was observed at site GP08 near Potchefstroom, an urban setting and in the wet season it was at site KW03. During the wet season, surface runoff from the KW03 may have led to the increased enterococcal levels, considering that faecal coliforms numbers indicate that there was faecal contamination at all the sites. The conclusion may be drawn that the Loopspruit River is heavily polluted with faecal material because enterococcal species mainly originate from the gastrointestinal tract of humans and animals. A study by Molale, (2016) on characterising enterococci from water sources in the North West Province, correlates with the current research that the increased enterococcal levels are a result of faecal pollution from the WWTP. Here the authors listed the spread of enterococci with virulence genes in ecological surface water sources that are utilized for different agricultural and WWTP activities.

A study by Rothenheber and Jones (2018) found a relationship to enterococci being associated with human faecal contamination. The authors found that enterococci levels are associated with mammalian faecal contamination. It is, therefore, reasonable to assume that enterococcal contaminations are from human faecal pollution (Hamiwe *et al.*, 2019). Enterococci are well adapted to live longer in aquatic environments, compared to other coliform organisms (Boehm & Sassoubre, 2014) and therefore can be a good indicator of faecal pollution.

Proper medical care is often a challenge in informal settlements, like the one KW03. With the high levels of enterococci contamination in the area, there is cause for concern. Molale, (2016) and Tatsing Foka *et al.* (2019) found that possible pathogenic enterococci such as *E. faecium* and *E. faecalis* may be detrimental to immune-compromised individuals. When exposed to high levels *E. coli* or *Enterococcus* species, there is an increased risk of contracting gastrointestinal illnesses.

5.3.4 Clostridia

It is essential to use sulphite-reducing *Clostridium* (SRC) species along with *E. coli*, total coliforms, faecal coliforms, and *Enterococci* as an indicator of faecal surface water contamination (Henry *et al.*, 2016; Pascual-Benito *et al.*, 2020). The *Clostridia* counts during the dry seasons were low

compared to the wet seasons, ranging from 0 counts to a maximum of 59 at site KW03. Some health concerns of certain pathogenic clostridia species include gastrointestinal disease.

The SRC levels during the dry and cold seasons were lower and higher levels were detected during the wet and warmer seasons. This can be explained because the SRC has an optimal growth rate of 44°C, where the temperatures ranged from an average of 13 – 25.53°C in 2018 – 2019. Most mesophilic bacteria grow rapidly at 25°C. A possible explanation for the high SRC counts is the surface runoff from mine tailings which contribute to an increase of sulphate levels in the Loopspruit River providing nutrients to SRC (Biggs *et al.*, 2013; Lucas *et al.*, 2014). The study done by Sibanda *et al.* (2013) explained that surface runoff creates a dilution effect of contaminants. The combination of the dilution effect and sulphate runoff can decrease clostridia levels.

Various studies have found an absence of SRC species in the faeces of herbivores, from agricultural activities (Mueller-Spitz *et al.*, 2010; Vierheilig *et al.*, 2013) around the Loopspruit River. The present study supports the findings of the above studies indicating that the SRC is likely the result of urban faecal pollution and not from agricultural activities

Temperature was one of the significant physico-chemical parameters limiting the levels of *Clostridium* species. This can be explained because the SRC grows optimally at 44°C. Temperature also influence dissolved oxygen (Fourie, 2017), but unfortunately, dissolved oxygen was not tested for in this study. As temperature increases during warm seasons, the gaseous solubility such as oxygen levels will decrease. Since *Clostridium* is an anaerobic organism, the reduced oxygen levels created the ideal environment for the clostridium species (Sanchez Ramos & Rodloff, 2018). The need for these ideal environments enables the *Clostridia* to grow in a broad spectrum of temperatures. The results from a previous study are in correlation with this study that during the warmer and wet seasons the clostridia levels increased. This is especially true at the point source pollution WWTP effluent and any effluent sites (Bezuidenhout *et al.*, 2017; Doyle *et al.*, 2018). During warm-rainy seasons, higher levels of *Clostridium* species were found than during the lower temperatures of the cold-dry season (Fourie, 2017).

Clostridium sp. can have serious health impacts on humans such as gastrointestinal disease (Petit *et al.*, 1999). *Clostridium perfringens* persists longer in the environment, making it difficult to prevent potential sickness caused by the *Clostridium* species.

5.3.5 Land use faecal contamination visual representation

The faecal contamination visual representation presented in Figure 4.8, indicates possible sources of contamination of the Loopspruit River. Surface runoff that carries water over land, pick

up and wash faecal material and other chemical constituents into the Loopspruit River. The results depicted in Figure 4.8 show that the WWTP contributed both *E. coli* and enterococci during the wet season and urban land use during the dry seasons. Agricultural activities contributed a moderate amount of *E. coli* and enterococci during the wet seasons and only enterococci during the dry seasons.

Hall *et al.* (2014) used multivariate statistical methods to determine the fate of faecal pollution in surface water of the Watauga River watershed in northeast Tennessee, USA. The authors found that during wet warm seasons, faecal coliform concentrations increased significantly in comparison with the dry seasons. These findings correlate with a study by Kostyla *et al.* (2015) that focused on the seasonal variation of faecal contaminations in developing countries. The differences between the wet warm and dry cold seasons are the result of climatic changes. Increased rainfall with more runoff events and higher temperature both contribute to higher faecal coliform counts during the wet season (Hall *et al.*, 2014; Kim *et al.*, 2017; Sibanda *et al.*, 2013).

5.4 Characterisation and identification of presumptive faecal bacteria and HPC isolates

Bacterial isolates were subjected to primary characterisations (Gram-staining), biochemical analysis and 16S rRNA sequencing. The biochemical tests served as a preliminary screening with selected isolates used for 16S rRNA sequencing (Figure 4.10 and 4.11).

5.4.1 Identification of presumptive *Enterococcus* isolates

The use of biochemical tests for preliminary identification is limited but it does provide useful information. From the 46 isolates tested, 22 were catalase-negative meaning that the enterococci do not produce the catalase enzyme to break down harmful substances such as hydrogen peroxide into water and oxygen. 16S rRNA sequencing was able to discern between enterococcal species groups. From these 18 were identified further as *Enterococcus* sp. including *E. avium, E. dispar, E. canintestini, E. faecium, E. pallens, E. florum and E. gilvus*. *E. faecium* was the most abundant.

E. avium was present in sample sites MU01, MD02 and KA05 and according to Tatsing Foka and Ateba, (2019) it is often associated with bird droppings. Birds nesting in trees along the Loopspruit River might be a source of *E. avium*. *E. dispar,* has previously been isolated from human waste and was present at sites MU01 and MD02 (Tatsing Foka *et al.*, 2019; Wang *et al.*, 2012).

The enterococci species *E. faecalis* and *E. faecium* pose risks to humans causing nosocomial infections and may also cause endocarditis, urinary tract infections and bacteraemia (Fernández-Guerrero *et al.*, 2002; Ratanasuwan *et al.*, 1999). These organisms pose risk to humans who are exposed to *E. faecalis* and *E. faecium* containing waters with serious infections. Possible sites that may be at health risk include the urban areas such as MU01, VA07 and GP08, and KW03 at a WWTP and informal settlement.

5.4.2 Identification of Clostridia isolates

Due to the anaerobic nature of *Clostridia*, they are commonly found in the intestine of humans and animals but are not limited to these environments. Twenty-seven of the 31 Clostridia isolates were identified to species level and included *Clostridium perfringens, C. baratii C. nitritogenes, C. bifermentans* and C. *sordellii.* These same species were isolated from the Schoonspruit River, Crocodile River and Groot Marico River by Fourie (2017). The presence of Clostridia is indicative of possible faecal contamination that may occur based on the surrounding land uses of the sample sites. These land uses include urban settings (MU01 and VA07), Agriculture (TS04 and KA05) and a WWTP (KW03).

Clostridium perfringens has been isolated from WWTPs, pigs and chicken farms as well as from plants (Abia, *et al.*, 2015a; Álvarez-Pérez *et al.*, 2018; Rimoldi *et al.*, 2015; Voidarou *et al.*, 2011; Watcharasukarn *et al.*, 2009). Clostridia were present at sample sites MU01, KW03, TS04, KD06, VA07 and GP08. Sample sites KD06, VA07 and GP08 are downstream of chicken farms. In a previous study*, C. baratii* and *C. sordellii* were isolated from chicken faeces (Rimoldi *et al.*, 2015) upstream of sites KW03, TS04, KA05, KD06 and VA07.

A common *Clostridium* pathogen, *Clostridium perfringens* is usually found in the intestinal tract of humans and animals. *C. perfringens'* pathogenicity ranges from gastroenteritis as a result of food poisoning to necrotising gas-gangrene (Irikura *et al.*, 2015).

C. perfringens was present at sites MU01, KW03, TS04, KD06, VA07 and GP08. Sites TS04, KD06, VA07 and GP08 are all downstream of a WWTP. Wastewater effluent can possibly introduce this pathogen into the aquatic environment. *Clostridium perfringens* produces endospores that are highly resistant to the treatment processes and environmental stressors (Ajonina *et al.*, 2015). This presents a cause for concern that this organism may cause health risks to both humans and animals.

5.4.3 Identification of presumptive *E. coli* isolates

The identified isolates included *Shewanella xiamenensis* (from MU01)*, Aeromonas hydrophila* (from MU01, TS04 and GP08)*, E. coli* (form MD02, KD03, KA05 and VA07)*, Serratia marcescens* (from MU01)*, Klebsiella aerogenes* (from KW03)*, Enterobacter cloacae* (from TS04, KD06 and GP08)*,* and *Citrobacter freundii* (from TS04). The expected outcome was to identify *E. coli*; however, various other isolates were identified. The reason to only isolate *E. coli* is that it serves as a faecal indicator. The *Escherichia, Citrobacter, Enterobacter, Serratia* and *Klebsiella* genera are all part of the *Enterobacteriaceae* taxonomic Family. *Shewanella* and *Aeromonas* both follow the same taxonomic classification of their genera but differ in the Order classification with *Alteromonadales* and *Aeromondales,* respectively. *E. coli* produce a yellow slant with a yellow butt, is positive for gas production and does not produce H_2S. *Enterobacter, Klebsiella, Shewanella* and *Aeromonas* all share these biochemical traits with *E. coli. Citrobacter* and *Serratia* tested negatively one parameter of the TSI test (black colour chance meaning hydrogen sulphide production). *Citrobacter* is positive for H_2S and *Serratia* do not produce gas. These discrepancies may be due to observational errors. 16S rRNA sequencing is therefore needed for definitive identification of the organism.

An important consideration is the possible presence of Verocytotoxin-producing *E. coli* known as Enterohemorrhagic *E. coli* (EHEC) such as *E. coli* O157. This strain has been isolated in the North West Provence by Ateba *et al.*, (2008), from cattle, pigs and human faeces. The *E. coli* O157 strain was found to be prevalent in cattle. Therefore, water sources that are frequented by grazing cattle could possibly contribute to the spread of *E. coli* O157. Hunter (2003), stated that *E. coli* O157:H7 may cause haemorrhagic enteritis or haemolytic uremic syndrome in humans.

5.4.4 Identification of HPC isolates

HPC isolates in the study were identified as *Flavobacterium* sp*., Sphingobacterium* sp., *Chryseobacterium indoltheticum*, *Arcicella rigui, Arthrobacter psychrochitiniphilus, Beta proteobacteria, Janthinobacterium lividum*, *Rheinheimera* sp., *Aeromonas* sp. and *Pseudomonas* sp. Which were similar HPC bacterial species found by Bezuidenhout *et al.* (2017); Carstens, (2012); Jordaan *et al.* (2019) in surrounding study areas. Opportunistic pathogens identified in the Loopspruit River from HPC bacteria were also observed in previous studies in the Mooi River comprising of *Pseudomonas, Acinetobacter, Aeromonas* and *Flavobacterium* (Horn *et al.*, 2016).

Flavobacterium are known for their industrially important compounds (Enisoglu-Atalay *et al.*, 2018) and enzymes. These include enzymes that can degrade agar, alginate, chitin, pectin, xylan, keratin and laminarin where chitin and xylan are important to note for this study. In the

environment, the hydrolysis of cellulose, xylan, and chitin is for the most part upheld by bacteria and fungi (Berlemont, 2017). *Sphingobacterium* sp. was isolated from soil in a rice paddy in Changzhou (Jiangsu Province, China) (Cai *et al.*, 2015). This organism may have originated from agricultural settings; however, the microorganisms were isolated from sample site MD02, which is an urban area and situated upstream of the agricultural farms.

Fortunately, there were no human gastrointestinal diseases associated with *Pseudomonas* (WHO, 2011). *Pseudomonas aeruginosa* is a waterborne opportunistic pathogen that poses a risk to immuno-compromised populations (Wang *et al.*, 2012). Increased levels of *Pseudomonas* may cause taste, odour and turbidity problems in water (WHO, 2011).

Aeromonas sp. and *Pseudomonas* sp. was present at all the sample sites of the Loopspruit River. In a study by Kivanc *et al.* (2011) the authors found *Aeromonas* sp. in drinking water, tap water and environmental water samples. They also found that *Aeromonas* sp. were more prevalent during the cold and dry months. *Pseudomonas* sp. are commonly found in groundwater and plants. *Pseudomonas* sp. are considered to be a plant and animal pathogen (Cui *et al.*, 2019).

5.5 Testing for antibiotic susceptibility and concentrations

5.5.1 MAR index

Van Boeckel *et al.* (2014) studied the use of antibiotics from 2000 to 2010 in 71 countries and found that antibiotic use increased by 36%. The study showed that antibiotics such as cephalosporins and broad-spectrum penicillin contributed to 55% of total antibiotic consumed in 2010. The antibiotic groups that were investigated (fluoroquinolones, macrolides and tetracyclines) showed no alarming resistance trends in this study. However, the frequent use of β-lactam antibiotics from the penicillin group (e.g. ampicillin), showed high resistances.

Antibiotic susceptibility testing for water quality is used to create an antibiotic resistance profile. The Multiple Antibiotic Resistance index refers to the antibiotic resistance profile to ampicillin, amoxicillin, streptomycin, oxy-tetracycline, vancomycin, penicillin G, neomycin, ciprofloxacin, trimethoprim, chloramphenicol, sulfamethoxazole and colistin. MAR index values greater than 0.2 are possible areas of concern. Table 4.6 indicates that the dry season had almost twice the antibiotic resistance bacteria compared with the wet season. During the dry season, all the sites had a MAR index value of ≥0.2 (0.38 – 0.75), only two sites (KD06 and GP08) had a MAR index value ≤0.2 during the wet season. The highest MAR values were observed at sites MU01 and KA05, with MU01 associated with mining activities and KA05 with agriculture. MU01 has mining

activities where for example lead contributes to bacterial gene upregulation. Perhaps these genes play dual roles as they help the bacteria survive harsh environments. This could be an interesting prospect that needs further investigation.

A study by Van Boeckel *et al.* (2014) showed a significant increase in antibiotic use in developing countries such as the BRICS (Brazil, Russia, India, China and South Africa) countries. Moreover, Laxminarayan *et al.* (2013), estimated that 100 000 – 200 000 tonnes of antibiotics are manufactured worldwide per annum, and are primarily used in the agricultural, aquacultural and veterinary sectors.

Since the Loopspruit River flows through areas with different land-use activities (see Section 3.1), including mining activities, WWTP, agriculture and urban activities, there are different MAR ranges throughout the Loopspruit River. Abia *et al*. (2015a) and Abia *et al.* (2015b) also reported higher MAR index values downstream of WWTP and agricultural land uses.

Antibiotics are absorbed in the sediment of river systems, decelerating its degradation, making the antibiotic compounds remain active for longer periods (Baquero *et al.*, 2008; Devarajan *et al.*, 2016). This may explain the increase in resistance in the environment to various antibiotics. There is a large antibiotic profile, in this study, where isolates showed resistance to. The MAR index of the Loopspruit River system represents a risk to both human and animal health that make use of the Loopspruit River as a water source. The HPC isolates from the Loopspruit River included possible opportunistic pathogens such as *Pseudomonas, Acinetobacter, Aeromonas* and *Flavobacterium.* Infections by antibiotic-resistant strains of these organisms would have reduced treatment options.

5.5.2 LC/MS analysis

Some antibiotics were quantified in the Loopspruit River, using LC/MS analysis (Table 4.7). The measured environmental concentrations (MEC) were compared to predict no-effect concentrations (PNEC). The MEC and PNEC were used to generate a risk selection (RQ) index. Only tetracycline was below the PNEC and had the lowest risk with an index value of 0.24. Trimethoprim, ciprofloxacin and erythromycin had varying ranges below and above the PNEC. Ampicillin PNEC is set at 75 ng/L and the MEC values in this study ranged from 2546.81 – 146679 ng/L. Ampicillin also had the highest RQ of 637.95. Also, almost all the isolates tested were resistant to Ampicillin (Appendix C Table C.1 and C.2). When the sites of the antibiotics are compared, it is clear that sites KW03, TS04 and KA05 contained the highest concentrations of the antibiotic compounds.

One of the possible reasons for the high levels of ampicillin is the high use of penicillin class antibiotics (Hutchings *et al.*, 2019), one of the first antibiotics used in clinical settings. Since 1940, the use of the antibiotics in the penicillin group, e.g. ampicillin has been used until the present day. The primary uses of tetracycline, trimethoprim, ampicillin, ciprofloxacin and erythromycin are for human, cattle, chicken and pig treatments in their food or water supply (Hoelzer *et al.*, 2017; Kim & Carlson, 2007). Without question, these antibiotics are the main reason for the increase in MAR because of the overuse of the antibiotics in the agricultural sector.

Tran *et al.* (2019) studied the incidence and risk of antibiotics in urban canals and lakes in Hanoi, Vietnam. Contrary to the findings in the present study, the authors rarely detected amoxicillin. All the antibiotics (except for tetracycline) may pose a risk to the ecological environments surrounding the Loopspruit River. The antibiotics trimethoprim, ampicillin, ciprofloxacin and erythromycin show risk (RQ>1.00) which could change the microbial diversity within the Loopspruit River.

The occurrence of antibiotic residues in urban canals might pose a possible risk to public health. The water from these urban canals could be used for irrigation. The antibiotic residues within these urban canals may accumulate in crops. This also implies that there is an ecological risk to aquatic ecosystems.

5.6 Detecting the presence of AmpC β-lactamase genes

5.6.1 Antibiotic-resistant genes

With the increase in antibiotic concentrations in the Loopspruit River, it becomes apparent why the MAR indices are so high. These MAR bacteria can react to a selective pressure for antibiotic-resistant strains. Bacteria can develop resistant genes to help them fight against antibiotics. The eDNA that was sequenced to detect the presence of antibiotic-resistant genes showed that bacteria at most sample sites had the resistant FOX genes and the presence of the integrase (*intI1*) genes (Figure 4.12 and 4.13).

The *intI1* gene is used as a marker for anthropogenic pollution, and when abundant in the environment, it is known for incorporating a diverse array of ARG's in the genome (Gillings *et al.*, 2015). The co-occurrence of *intI1*, together with a high copy number of AmpC β-lactamase, is an indicator of anthropogenic pollution. Even though there were few ARGs, the geographical location of the bacterial ARGs might be an indication of their detection frequency. The AmpC Heptaplex PCR melting curve analysis for the rapid detection of plasmid-mediated AmpC β-lactamase genes, may explain transference of plasmids to different bacterial genera (Liu *et al.*, 2015; Xu *et*

al., 2017). Activities such as direct pollution, spillages from WWTP runoff and urban runoff together with the impacts of agricultural runoff and recreational activity may create conditions for the increased exchange of resistant genes between resistant and non-resistant microorganisms (Jordaan & Bezuidenhout, 2016).

The African region, according to a 2014 WHO global surveillance report (WHO, 2014), stated that there might be an abundance of resistances as a result of the increase of β-lactamase genes in South African agricultural environments.

5.7 Bacterial diversity

Bacterial diversity is challenging to plot because of its hierarchical data. Through studying the bacterial community structure, it is possible to discern the potential bioindicators of environmental disturbances. This can be better explained through Alpha- and Beta-diversity indexes.

Bacterial alpha-diversity is one of the main driving forces behind multiple soil processes such as nutrient cycling, litter decomposition, degradation of toxins, gas emissions and plant productivity (Delgado-Baquerizo & Eldridge, 2019). Alpha-diversity is maintained by environmental factors such as pH, temperature, nutrient content, rainfall and climatic conditions (Delgado-Baquerizo & Eldridge, 2019).

Alpha-diversity indices reflect on consistency and abundance. The Cho1 and Shannon indices indicated significant differences ($p<0.05$). In this study, a great abundance of bacterial diversity was found at sites MU01, MD02 and KW03 (Figure 4.15). Although these sites have the highest diversity, with MU01 and KW03 showing similar diversity, MD02 had a different species abundance. Dominating at all the sites were *Proteobacteria*, followed by *Bacteroidetes, Cyanobacteria, Actinobacteria* and *Verrucomicrobia*. This agrees with the findings by Jordaan *et al.* (2019). The CCA plot (Figure 4.19) shows that *Proteobacteria* favours conditions with a high EC, whereas the *Bacteroidetes* favour areas with higher temperatures. Previous studies done on the effect of EC on the bacterial diversity suggested that *Bacteroidetes* were positively correlated with the EC values (Canfora *et al.*, 2014; Kim *et al.*, 2016). This is in direct contrast to the results of the present study. However, *Proteobacteria* and *Verrucomicrobia* results obtained here are similar to those found in a survey done by Kim *et al.* (2016) with a positive correlation to EC.

Beta-diversity differentiates between the various microbial composition at all the sample sites. A previous study showed that the land-use of an area actively shapes the bacterial community composition (Cai *et al.*, 2018). This phenomenon can be seen in Figure 4.16 where agricultural

land use (TS04 and KA05) grouped together and so did urban land-use (MU01, KW03, VA07 and GP08). The different land-use practices also showed unique plots where sample site MD02 is located downstream of mining activities, and KD06 at the Klipdrift Dam. A study by Keshri *et al.* (2015) showed that the bacterial communities isolated from mining activities in other parts of South Africa are similarly dominated by *Proteobacteria, Firmicutes, Bacteroidetes* and *Actinobacteria.* Abundant genera such as *Flavobacterium* and *Arcicella* from the *Bacteroidetes* group were found at the first sample site of the Loopspruit River.

5.8 Predicted metagenome analysis

5.8.1 Physico-chemical and microbiological correlations

The water quality of any body of water is dependent on the physico-chemical and microbial communities of the water body. Correlating the physico-chemical data with the microbiological data gives an overall idea of how these bacteria make use of specific nutrients provided by the physico-chemical environment. One drawback related to using a CCA plot is that it shows only the statistically significant ($p<0.05$) physico-chemical and microbiological data, whereas a predicted metagenome analysis provides a better holistic perspective.

The bacterial community in each environment is dependent on the relations of various factors such as pH, temperature, and the range of nutrients (Zhang *et al.*, 2010). These genera have an affinity for mesotrophic, eutrophic and hypertrophic water bodies rich in nutrients (De Figueiredo *et al.*, 2012). In contrast to the study done by De Figueiredo *et al.* (2012), there were no correlations to any of the nutrients

5.8.2 Metabolism of agrochemicals

Predicting the metabolic pathway at the sample sites may also help to predict the type of bacteria likely to be present in a geographical area. When there are increased levels of physico-chemical nutrients, the specific metabolic activities of the bacteria would also change, depending on the nutrients being metabolised. Figure 4.20 shows that most metabolic activities are unknown. The most likely metabolic pathways predicted were the ammonia oxidation, dehalogenation, nitrite reduction, sulphate reduction and sulphide oxidation. The remainder of the metabolic pathway activities of the sample sites can be referenced in Appendix D Figure D.7.

A study by Weigold *et al.* (2016) lists some bacterial taxa abundances that contribute to halogenation and dehalogenation. The authors list *Pseudomonas* and *Shewanella* genera from

the *Proteobacteria* phylum as organisms that contribute to dehalogenation. Also, the bacterial genes present for halogenase and dehalogenase are in the same order as the microbial nitrogen cycling. This suggests that these bacteria play an essential role in the cycling of halogens in soils in Figure D.8 (Appendix D) (Weigold *et al.*, 2016). Chitin is an abundant polysaccharide in terrestrial soils in ecosystems, and bacteria such as *Actinobacteria, Proteobacteria*, and *Firmicutes* are chitinolytic (Wieczorek *et al.*, 2019). Similar bacteria found in this study possibly indicates chitin degradation, modelled in the Loopspruit River.

Ammonia oxidation is the most frequently predicted metabolic activity. The metabolism of ammonia is interconnected with the nitrogen cycle, which also includes nitrite reducers and nitrogen fixation. A study Wang *et al.* (2019) indicated that phyla like *Chloroflexi* and *Chlorobi* are relatively abundant during the removal of nitrogen and refractory organics in landfill leachate. There were abundances of *Proteobacteria, Bacteroidetes*, C*yanobacteria* and *Chloroflexi* respectively, at sample site MD02 which is a downstream location of mining activities. Therefore, the results are supported by the findings Wang *et al.* (2019).

Sheng *et al.* (2013) stated that the increases in nitrogen and nitrogen-associated processes increase bacterial taxa such as *Proteobacteria.* An abundance of ammonia oxidising bacteria (AOB) communities typically includes *Nitrosospira, Nitrospira, Pseudomonas, Flavobacterium, Bacillus, Aquicella*, and *Bacillariophyta. Nitrosospira* and *Nitrospira* contribute to nitrogen cycling, whereas *Pseudomonas, Flavobacterium*, and *Bacillus* are linked to pathogen suppression (Eck *et al.*, 2019; Sheng *et al.*, 2013). This is in accordance with the present study, where the pathogen suppression bacterium *Flavobacterium* is in abundance at the first three sites (MU01 to KD03) resulting in fewer predicted pathogenic activities at the sample sites that follow.

In this study, the physico-chemical and microbiological parameters of the Loopspruit River were studied and analysed. The study revealed that modelling water quality and analysing the microbial diversities of the Loopspruit River, indicated that point and non-point pollutions are present. However, this study only focused on surface water. Many of the North West Province inhabits make use of groundwater. This creates a plethora of possible further studies that can be done on the Loopspruit River such as focusing on the physico-chemical and microbiological interactions between the surface water and the groundwater.

Finally, the integration of geospatial and microbiome analyses may be the new paradigm shift that is needed for better environmental and ecological management. This study predicted the metagenome analysis of the Loopspruit River and also investigated the water quality thereof. However, metagenomic data was not geospatially represented in this study, but this does warrant the need for future studies. The metagenomic geospatial visual representation was not done

because it was not the focus of this study. That being said, this does not mean it is impossible to do. A study by Afshinnekoo *et al.* (2015) did exactly that. The authors used metagenomic data to geospatially represent the density of three bacteria *Enterococcus faecium*, *Staphylococcus aureus* and *Pseudoalteromonas haloplanktis* associated with human body populace.

CHAPTER 6: CONCLUSION AND RECOMMENDATIONS

6.1 Conclusion

From the results obtained from this study, it can be concluded that there are point source and non-point source pollutions present within the Loopspruit River. With the aid of aerial photographs and the help of the GIS mapping software ArcMAP, sampling locations were identified. Sample locations were chosen based on three criteria i) public accessibility, ii) easily accessible and iii) they should include multiple land-use characteristics.

Choosing sampling sites with an in-depth desktop study of the area of interest is of paramount importance. This should make possible the inclusion of land use activities, geology, hydrology and geography. The sample sites chosen included agriculture areas, urban areas and informal settlements, mining areas and a WWTP to ensure site diversity.

The second objective was dependent on the season type. During the dry season, sampling had to take place when there were very few precipitation events to limit any possible surface runoff. However, during the wet season, sampling was done after frequent precipitation events. The physico-chemical results showed high levels of TDS, PO_4 and NO_2 for 2018–2019, exceeding their respective RWQO. This means that there was contamination from the agricultural and urban sectors surrounding the Loopspruit River.

The microbiological analysis was done by using the membrane filtration technique, Fung Double-tube technique and a dilution series for the HPC bacteria. *E. coli, Enterococcus* spp. and *Clostridium* spp. were used as faecal pollution indicators. An abundance of these bacteria indicates areas of gastrointestinal illnesses risk. During the dry season, the total and faecal coliforms and HPC bacteria exceeded the RWQR and during the wet season the total and faecal coliforms, HPC and Enterococci exceeded the RWQO. This indicated microbial contamination. The majority of the microbial contamination came from the WWTP and urban areas. Microbiological analysis helped to explain the likely origin of faecal pollution. Microbiological data for 2018 – 2019 showed that the WWTP contributed to faecal pollution in the wet seasons and urban land use contributed to faecal pollution during the dry season.

From among the HPC colonies, a myriad of unique colonies was chosen for antibiotic susceptibility testing with the Kirby-Bauer disk diffusion technique to create the MAR index for each site. The MAR index values were higher during the dry season. However, the MAR index showed that all the sample sites had ampicillin resistance and the majority of the sites showed resistance to ciprofloxacin. The antibiotic concentrations mirrored the ampicillin and ciprofloxacin

resistance shown in the MAR index. Both these compounds were higher than the PNEC. Ampicillin had an RQ index risk value of 637.97 posing a big environmental health risk. These high levels of antibiotics in the environment contribute to the increase of antibiotic resistance in bacterial consortia in the Loopspruit River. Antibiotic resistance genes such as the AmpC β-lactamase and *intI1* genes were detected. With continuous exposure to high levels of antibiotics worldwide, the expected antibiotic resistance and ARGs will also increase, posing dire risks for future generations.

Illumina MiSeq sequencing analysis listed some opportunistic pathogens. Physico-chemical parameters allow the prediction of likely bacteria and which metabolic pathway they use. This method indicates the abundant bacteria in areas where a certain physico-chemical compounds are abundant.

Geospatial models representing the physico-chemical water quality generated via the IDW interpolation in ArcMAP indicate where the most pollution occurs. It was observed that the WWTP and mining activities land uses had the highest point source pollution.

6.2 Recommendations

I. Water quality monitoring

Historical data from water monitoring stations and flow gauges serve a vital purpose to ensure that the water quality data remain up to date. Reactivation of these monitoring stations is crucial for continuous data generation. This will ensure more accurate and reliable models.

II. Education and monitoring

Education in urban, mining and agricultural sectors needs to be implemented. This should incorporate information regarding water quality and how to maintain the desired water quality levels. This might induce the mines to create a mine water treatment plant to ensure that there is minimal exposure to the contaminants produced by mining activities.

III. Agricultural activities

Where surface water from the Loopspruit River is being used for irrigation of crops and as drinking water for animals, this may have effects on the environment. It is necessary to determine how the water quality changes after the water was used and run off to flow back into the Loopspruit River.

IV. Hydrological groundwater survey

Some urban households and farms make use of groundwater for irrigation. The groundwater may be contaminated with agrichemicals in agricultural settings and the groundwater in urban settings may be contaminated with faecal material. It would be wise to study these groundwater sources to eliminate the possible spread of virulent faecal bacteria and to ensure that the soil chemistry is of the desired standard for optimal crop growth.

REFERENCES

Abia, A.L.K., Ubomba-Jaswa, E., du Preez, M., & Momba, M.N.B. 2015a. Riverbed sediments in the Apies River, South Africa: recommending the use of both *Clostridium perfringens* and *Escherichia coli* as indicators of faecal pollution. *Journal of Soils and Sediments*. 15(12):2412–2424.

Abia, A.L.K., Ubomba-Jaswa, E., & Momba, M.N.B. 2015b. High prevalence of multiple-antibiotic-resistant (MAR) *Escherichia coli* in river bed sediments of the Apies River, South Africa. *Environmental Monitoring and Assessment*. 187(10):652.

Adeola Fashae, O., Abiola Ayorinde, H., Oludapo Olusola, A., & Oluseyi Obateru, R. 2019. Landuse and surface water quality in an emerging urban city. *Applied Water Science*. 9(2):25.

Adeyemo, O.K., Adedokun, O.A., Yusuf, R.K., & Adeleye, E.A. 2013. Seasonal changes in physico-chemical parameters and nutrient load of river sediments in Ibadan City, Nigeria. *Global NEST Journal*. 10(3):326–336.

Adler, R.A., Claassen, M., Godfrey, L., & Turton, A.R. 2007. Water, mining, and waste: An historical and economic perspective on conflict management in South Africa. *The Economics of Peace and Security Journal*. 2(2):33–41.

Afshinnekoo, E., Meydan, C., Chowdhury, S., Jaroudi, D., Boyer, C., Bernstein, N., Maritz, J.M., Reeves, D., Gandara, J., Chhangawala, S., Ahsanuddin, S., Simmons, A., Nessel, T., Sundaresh, B., Pereira, E., Jorgensen, E., Kolokotronis, S.-O., Kirchberger, N., Garcia, I., Gandara, D., Dhanraj, S., Nawrin, T., Saletore, Y., Alexander, N., Vijay, P., Hénaff, E.M., Zumbo, P., Walsh, M., O'Mullan, G.D., Tighe, S., Dudley, J.T., Dunaif, A., Ennis, S., O'Halloran, E., Magalhaes, T.R., Boone, B., Jones, A.L., Muth, T.R., Paolantonio, K.S., Alter, E., Schadt, E.E., Garbarino, J., Prill, R.J., Carlton, J.M., Levy, S., & Mason, C.E. 2015. Geospatial resolution of human and bacterial diversity with city-scale metagenomics. *Cell Systems*. 1(1):72–87.

Aguado, D., Montoya, T., Ferrer, J., & Seco, A. 2006. Relating ions concentration variations to conductivity variations in a sequencing batch reactor operated for enhanced biological phosphorus removal. *Environmental Modelling & Software*. 21(6):845–851.

Ajonina, C., Buzie, C., Rubiandini, R.H., & Otterpohl, R. 2015. Microbial pathogens in Wastewater Treatment Plants (WWTP) in Hamburg. *Journal of Toxicology and Environmental Health - Part A: Current Issues*. 78(6):381–387.

Ali, L., Wang, Y.-Q., Zhang, J., Ajmal, M., Xiao, Z., Wu, J., Chen, J.-L., & Yu, D. 2016. Nutrient-induced antibiotic resistance in *Enterococcus faecalis* in the eutrophic environment. *Journal of Global Antimicrobial Resistance*. 7:78–83.

Allen, H.K., Donato, J., Wang, H.H., Cloud-Hansen, K.A., Davies, J., & Handelsman, J. 2010. Call of the wild: antibiotic resistance genes in natural environments. *Nature Reviews Microbiology*. 8(4):251–259.

Allen, M.J., Edberg, S.C., & Reasoner, D.J. 2004. Heterotrophic plate count bacteria—what is their significance in drinking water? *International Journal of Food Microbiology*. 92(3):265–274.

Allison, L.A. 2007. Fundamental Molecular Biology. Blackwell Publishing Ltd: Oxford.

Álvarez-Pérez, S., Blanco, J.L., Astorga, R.J., Gómez-Laguna, J., Barrero-Domínguez, B., Galán-Relaño, A., Harmanus, C., Kuijper, E., & García, M.E. 2018. Distribution and tracking of *Clostridium difficile* and *Clostridium perfringens* in a free-range pig abattoir and processing plant. *Food Research International*. 113(2018):456–464.

Alvarez-Romero, J.G., Devlin, M., Teixeira da Silva, E., Petus, C., Ban, N.C., Pressey, R.L., Kool, J., Roberts, J.J., Cerdeira-Estrada, S., Wenger, A.S., & Brodie, J. 2013. A novel approach to model exposure of coastal-marine ecosystems to riverine flood plumes based on remote sensing techniques. *Journal of Environmental Management*. 119:194–207.

Álvarez, X., Valero, E., Santos, R.M.B., Varandas, S.G.P., Sanches Fernandes, L.F., & Pacheco, F.A.L. 2017. Anthropogenic nutrients and eutrophication in multiple land use watersheds: Best management practices and policies for the protection of water resources. *Land Use Policy*. 69:1–11.

Andrews, J.E., Brimblecombe, P., Jickells, T.D., Liss, P.S., & Reid, B. 2004. An introduction to environmental chemistry. 2nd ed. Blackwell Publishing Ltd.

Ashton, P.J. 2002. Avoiding conflicts over Africa's water resources. *AMBIO: A Journal of the Human Environment*. 31(3):236–242.

Ateba, C.N., Mbewe, M., & Bezuidenhout, C.C. 2008. Prevalence of *Escherichia coli* O157 strains in cattle, pigs and humans in North West province, South Africa. *South African Journal of Science*. 104(1–2):7–8.

Awan, K.H. 2017. The therapeutic usage of botulinum toxin (Botox) in non-cosmetic head and neck conditions – An evidence based review. *Saudi Pharmaceutical Journal*. 25(1):18–24.

Bajpai, P. 2017. Basics of Anaerobic Digestion Process. 1st ed. in: Anaerobic Technology in Pulp and Paper Industry. SpringerBriefs in Applied Sciences and Technology, pp. 7–12.

Baquero, F., Martínez, J.L., & Cantón, R. 2008. Antibiotics and antibiotic resistance in water environments. *Current Opinion in Biotechnology*. 19(3):260–265.

Barrios, M.A., Saini, J.K., Rude, C.M., Beyer, R.S., Fung, D.Y.C., & Crozier-Dodson, B.A. 2013. Comparison of 3 agar media in Fung double tubes and petri plates to detect and enumerate *Clostridium* spp. in broiler chicken intestines. *Poultry Science*. 92(6):1498–1504.

Bashir, N., Saeed, R., Afzaal, M., Ahmad, A., Muhammad, N., Iqbal, J., Khan, A., Maqbool, Y., & Hameed, S. 2020. Water quality assessment of lower Jhelum canal in Pakistan by using geographic information system (GIS). *Groundwater for Sustainable Development*. 10(January):100357 (1–9).

Baudišová, D. 1997. Evaluation of *Escherichia coli* as the main indicator of faecal pollution. *Water Science and Technology*. 35(11–12):333–336.

Bauer, A.W., Kirby, W.M.M., Sherris, J.C., & Turck, M. 1966. Antibiotic susceptibility testing by a standardized single disk method. *American Journal of Clinical Pathology*. 45(4):493–496.

Ben, Y., Fu, C., Hu, M., Liu, L., Wong, M.H., & Zheng, C. 2019. Human health risk assessment of antibiotic resistance associated with antibiotic residues in the environment: A review. *Environmental Research*. 169:483–493.

Bengtsson-Palme, J. & Larsson, D.G.J. 2016. Concentrations of antibiotics predicted to select for resistant bacteria: Proposed limits for environmental regulation. *Environment International*. *The Authors*. 86:140–149.

Berg, M., Vanaerschot, M., Jankevics, A., Cuypers, B., Breitling, R., & Dujardin, J.-C. 2013. LC-MS metabolomics from study design to data-analysis - Usring a versitile pathogen as a test case. *Computational and Structural Biotechnology Journal*. 4(5):e201301002.

Berlemont, R. 2017. Distribution and diversity of enzymes for polysaccharide degradation in fungi. *Scientific Reports*. 7(1):1–11.

Beveridge, T. 2001. Use of the Gram stain in microbiology. *Biotechnic & Histochemistry*. 76(3):111–118.

Bezuidenhout, C., Mienie, C., De Klerk, T., & Molale, L. 2017. Geospatial analysis of microbial community structure and antimicrobial resistance analysis in the management of natural streams

and selected wetlands. Water Research Commission: WRC Report No. K5/2347//3.

Biemer, J.J. 1973. Antimicrobial susceptibility testing by the Kirby-Bauer disc diffusion method. *Annals of clinical laboratory science*. 3(2):135–40.

Biggs, J.S., Thorburn, P.J., Crimp, S., Masters, B., & Attard, S.J. 2013. Interactions between climate change and sugarcane management systems for improving water quality leaving farms in the Mackay Whitsunday region, Australia. *Agriculture, Ecosystems and Environment*. 180:79–89.

Binns, J.A., Illgner, P.M., & Nel, E.L. 2001. Water shortage, deforestation and development: South Africa's working for water programme. *Land Degradation & Development*. 12(4):341–355.

Boehm, A.B. & Sassoubre, L.M. 2014. Enterococci as indicators of environmental fecal contamination, in: Gilmore, M.S., Clewell, D.B., Ike, Y., Shankar, N. (Eds.), Enterococci from Commensals to Leading Causes of Drug Resistant Infection. Massachusetts Eye and Ear Infirmary: Boston. Massachusetts Eye and Ear Infirmary: Boston, pp. 101–122.

Borges, R.C., Mahler, C.F., Caldas, V.G., da Silva, A.P., & Bernedo, A.V.B. 2018. Mapping of the concentration of natural radionuclides in the Fundão Island, RJ, Brazil supported by geoprocessing and IDW interpolation. *Environmental Earth Sciences*. 77(17):1–13.

Brazier, J.S., Salmon, J.E., McLauchlin, J., Brett, M.M., Hall, V., Hood, J., Duerden, B.I., & George, R.C. 2002. Isolation and identification of Clostridium spp. from infections associated with the injection of drugs: experiences of a microbiological investigation team. *Journal of Medical Microbiology*. 51(11):985–989.

Breunig, M., Bradley, P.E., Jahn, M., Kuper, P., Mazroob, N., Rösch, N., Al-Doori, M., Stefanakis, E., & Jadidi, M. 2020. Geospatial data management research: Progress and future directions. *ISPRS International Journal of Geo-Information*. 9(2).

Bu, H., Meng, W., & Zhang, Y. 2014. Spatial and seasonal characteristics of river water chemistry in the Taizi River in Northeast China. *Environmental Monitoring and Assessment*. 186(6):3619–3632.

Bui, H.H., Ha, N.H., Nguyen, T.N.D., Nguyen, A.T., Pham, T.T.H., Kandasamy, J., & Nguyen, T.V. 2019. Integration of SWAT and QUAL2K for water quality modeling in a data scarce basin of Cau River basin in Vietnam. *Ecohydrology & Hydrobiology*. 19(2):210–223.

Cai, Z., Zhang, W., Li, S., Ma, J., Wang, J., & Zhao, X. 2015. Microbial degradation mechanism

and pathway of the novel insecticide Paichongding by a newly isolated *Sphingobacterium* sp. P1-3 from soil. *Journal of Agricultural and Food Chemistry*. 63(15):3823–3829.

Cai, Z., Zhang, Y., Yang, C., & Wang, S. 2018. Land-use type strongly shapes community composition, but not always diversity of soil microbes in tropical China. *CATENA*. 165(2018):369–380.

Campbell, J. & Shin, M. 2017. Essentials to Geographic Information Systems. 2nd ed. Flat World Knowledge, Inc.: San Francisco, California.

Canfora, L., Bacci, G., Pinzari, F., Lo Papa, G., Dazzi, C., & Benedetti, A. 2014. Salinity and bacterial diversity: To what extent does the concentration of salt affect the bacterial community in a saline soil? *PLoS ONE*. 9(9).

Cannarozzo, M., Noto, L.V., & Viola, F. 2006. Spatial distribution of rainfall trends in Sicily (1921–2000). *Physics and Chemistry of the Earth, Parts A/B/C*. 31(18):1201–1211.

Caraballo, M.A., Macías, F., Nieto, J.M., & Ayora, C. 2016. Long term fluctuations of groundwater mine pollution in a sulfide mining district with dry Mediterranean climate: Implications for water resources management and remediation. *Science of the Total Environment*. 539:427–435.

Carstens, A.J. 2012. Evaluation of microbiological and physico-chemical quality of water from aquifers in the North West Province, South Africa. North-West University (NWU) (MSc - Dissertation).

Carter, J.T., Rice, E.W., Buchberger, S.G., & Lee, Y. 2000. Relationships between levels of heterotrophic bacteria and water quality parameters in a drinking water distribution system. *Water Research*. 34(5):1492–1502.

Cazaudehore, G., Schraauwers, B., Peyrelasse, C., Lagnet, C., & Monlau, F. 2019. Determination of chemical oxygen demand of agricultural wastes by combining acid hydrolysis and commercial COD kit analysis. *Journal of Environmental Management*. 250:109464.

Chen, J., Seven, J., Zilla, T., Dippold, M.A., Blagodatskaya, E., & Kuzyakov, Y. 2019. Microbial C:N:P stoichiometry and turnover depend on nutrients availability in soil: A 14C, 15N and 33P triple labelling study. *Soil Biology and Biochemistry*. 131:206–216.

Chen, T., Ren, L., Yuan, F., Yang, X., Jiang, S., Tang, T., Liu, Y., Zhao, C., & Zhang, L. 2017. Comparison of spatial interpolation schemes for rainfall data and application in hydrological modeling. *Water*. 9(5):342.

Chen, Y., Cheng, J.J., & Creamer, K.S. 2008. Inhibition of anaerobic digestion process: A review. *Bioresource Technology*. 99(10):4044–4064.

Choi, D.-H., Beom, J.-A., Jeung, M.-H., Choi, W.-J., Her, Y.-G., & Yoon, K.-S. 2019. Characteristics of biochemical oxygen demand and chemical oxygen demand export from paddy fields during rainfall and non-rainfall periods. *Paddy and Water Environment*. 17(2):165–175.

Clarke, R., Peyton, D., Healy, M.G., Fenton, O., & Cummins, E. 2017. A quantitative microbial risk assessment model for total coliforms and *E. coli* in surface runoff following application of biosolids to grassland. *Environmental Pollution*. 224:739–750.

Clarridge, J.E. 2004. Impact of 16S rRNA gene sequence analysis for identification of bacteria on clinical microbiology and infectious diseases. *Clinical Microbiology Reviews*. 17(4):840–862.

Coffey, R., Cummins, E., Cormican, M., Flaherty, V.O., & Kelly, S. 2007. Microbial Exposure Assessment of Waterborne Pathogens. *Human and Ecological Risk Assessment: An International Journal*. 13(6):1313–1351.

Constancias, F., Terrat, S., Saby, N.P.A., Horrigue, W., Villerd, J., Guillemin, J.-P., Biju-Duval, L., Nowak, V., Dequiedt, S., Ranjard, L., & Chemidlin Prévost-Bouré, N. 2015. Mapping and determinism of soil microbial community distribution across an agricultural landscape. *MicrobiologyOpen*. 4(3):505–517.

Copatti, C.E., Baldisserotto, B., Souza, C. de F., & Garcia, L. 2019. Protective effect of high hardness in pacu juveniles (*Piaractus mesopotamicus*) under acidic or alkaline pH: Biochemical and haematological variables. *Aquaculture*. 502(September 2018):250–257.

Covington, B.C., McLean, J.A., & Bachmann, B.O. 2017. Comparative mass spectrometry-based metabolomics strategies for the investigation of microbial secondary metabolites. *Natural Product Reports*. 34(1):6–24.

Cui, Q., Huang, Y., Wang, H., & Fang, T. 2019. Diversity and abundance of bacterial pathogens in urban rivers impacted by domestic sewage. *Environmental Pollution*. 249:24–35.

Czekalski, N., Sigdel, R., Birtel, J., Matthews, B., & Bürgmann, H. 2015. Does human activity impact the natural antibiotic resistance background? Abundance of antibiotic resistance genes in 21 Swiss lakes. *Environment International*. 81:45–55.

Dallas, H.F. & Day, J. 2004. The Effect of Water Quality Variables on Aquatic Ecosystems : A review. Water Research Commission: WRC Report No. TT 224/04. Cape Town.

Dannhauser, H.P. 2016. Remediation of AMD through bentonitic clay adsorption. North-West University (NWU) (MEng - Dissertation).

Dass, C. 2008. Hyphenated Separations, in: Fundamentals of Contemporary Mass Spectrometry. pp. 16–18.

De Figueiredo, D.R., Ferreira, R. V., Cerqueira, M., De Melo, T.C., Pereira, M.J., Castro, B.B., & Correia, A. 2012. Impact of water quality on bacterioplankton assemblage along Cértima River Basin (central western Portugal) assessed by PCR-DGGE and multivariate analysis. *Environmental Monitoring and Assessment*. 184(1):471–485.

Delgado-Baquerizo, M. & Eldridge, D.J. 2019. Cross-Biome Drivers of Soil Bacterial Alpha Diversity on a Worldwide Scale. *Ecosystems*. 22(6):1220–1231.

Delpla, I., Jung, A. V., Baures, E., Clement, M., & Thomas, O. 2009. Impacts of climate change on surface water quality in relation to drinking water production. *Environment International*. 35(8):1225–1233.

Derakhshani, H., Tun, H.M., & Khafipour, E. 2016. An extended single-index multiplexed 16S rRNA sequencing for microbial community analysis on MiSeq illumina platforms. *Journal of Basic Microbiology*. 56(3):321–326.

DeSantis, T.Z., Hugenholtz, P., Larsen, N., Rojas, M., Brodie, E.L., Keller, K., Huber, T., Dalevi, D., Hu, P., & Andersen, G.L. 2006. Greengenes, a chimera-checked 16S rRNA gene database and workbench compatible with ARB. *Applied and Environmental Microbiology*. 72(7):5069–5072.

Desmarais, T.R., Solo-Gabriele, H.M., & Palmer, C.J. 2002. Influence of soil on fecal indicator organisms in a tidally influenced subtropical environment. *Applied and Environmental Microbiology*. 68(3):1165–1172.

Devarajan, N., Laffite, A., Mulaji, C.K., Otamonga, J.P., Mpiana, P.T., Mubedi, J.I., Prabakar, K., Ibelings, B.W., & Poté, J. 2016. Occurrence of antibiotic resistance genes and bacterial markers in a tropical river receiving hospital and urban wastewaters. *PLoS ONE*. 11(2):1–14.

Dhariwal, A., Chong, J., Habib, S., King, I.L., Agellon, L.B., & Xia, J. 2017. MicrobiomeAnalyst: a web-based tool for comprehensive statistical, visual and meta-analysis of microbiome data. *Nucleic Acids Research*. 45(1):180–188.

Dharmappa, H.B., Sivakumar, M., & Singh, R.N. 1998. Wastewater characteristics, management

and reuse in mining and mineral processing industries. *Wastewater Recycle, Reuse and Reclamation*. 1:10.

Di Cesare, A., Eckert, E.M., D'Urso, S., Bertoni, R., Gillan, D.C., Wattiez, R., & Corno, G. 2016. Co-occurrence of integrase 1, antibiotic and heavy metal resistance genes in municipal wastewater treatment plants. *Water Research*. 94:208–214.

Diaz, R.J. & Rosenberg, R. 2008. Spreading dead zones and consequences for marine ecosystems. *Science*. 321(5891):926–929.

Dolejska, M. & Papagiannitsis, C.C. 2018. Plasmid-mediated resistance is going wild. *Plasmid*. 99:99–111.

Doyle, C.J., O'Toole, P.W., & Cotter, P.D. 2018. Genomic characterization of sulphite reducing bacteria isolated from the dairy production chain. *Frontiers in Microbiology*. 9:1–9.

Dumur, C.I. 2015. Molecular Methodologies, in: Idowu, M.O., Dumur, C.I., Garrett, C.T. (Eds.), Molecular Oncology Testing for Solid Tumors. Springer International Publishing Switzerland, pp. 153–170.

DWAF: Department of Water Affairs and Forestry. 1996a. South African Water Quality Guidelines. Second ed. Volume 1: Domestic Use: Pretoria, South Africa.

DWAF: Department of Water Affairs and Forestry. 1996b. South African Water Quality Guidelines. Second ed. Volume 4: Agricultural Use: Irrigation: Pretoria, South Africa.

DWAF: Department of Water Affairs and Forestry. 1996c. South African Water Quality Guidelines. Second ed. Volume 2: Recreational Use: Pretoria, South Africa.

DWAF. 2004. Chapter 2 - South African water situation and strategies to balance supply and demand. National Water Resource Strategy. 1st edition. Pretoria, South Africa.

DWAF. 2009. Directorate National Water Resource Planning. Department of Water Affairs and Forestry, South Africa. Integrated Water Quality Management Plan For The Vaal River System: Task 2. Report No. P RSA C000/00/2305/1.

Eck, M., Sare, A., Massart, S., Schmautz, Z., Junge, R., Smits, T., & Jijakli, M. 2019. Exploring bacterial communities in aquaponic systems. *Water*. 11(2):260.

Edberg, S.C. & Allen, M.J. 2004. Virulence and risk from drinking water of heterotrophic plate count bacteria in human population groups. *Food Microbiology*. 92:255–263.

Elander, R.P. 2003. Industrial production of β-lactam antibiotics. *Applied Microbiology and Biotechnology*. 61(5–6):385–392.

Elliott, A.H., Semadeni-Davies, A.F., Shankar, U., Zeldis, J.R., Wheeler, D.M., Plew, D.R., Rys, G.J., & Harris, S.R. 2016. A national-scale GIS-based system for modelling impacts of land use on water quality. *Environmental Modelling and Software*. 86:131–144.

Enisoglu-Atalay, V., Atasever-Arslan, B., Yaman, B., Cebecioglu, R., Kul, A., Ozilhan, S., Ozen, F., & Cata, T. 2018. Chemical and molecular characterization of metabolites from Flavobacterium sp. *PLoS ONE*. 13(10):1–18.

Esselman, P.C., Jiang, S., Peller, H.A., Buck, D.G., & Wainwright, J.D. 2018. Landscape drivers and social dynamics shaping microbial contamination risk in three Maya communities in Southern Belize, Central America. *Water (Switzerland)*. 10(11):1–23.

EUCAST. 2017. The European Committee on Antimicrobial Susceptibility Testing. Breakpoint tables for interpretation of MICs and zone diameters. Version 7.1.

Fadiran, A.O. & Mamba, S.M. 2005. Analysis of nitrates and nitrites in some water and factory effluent samples from some cities in Swaziland. *Bulletin of the Chemical Society of Ethiopia*. 19(1):35–44.

Fattahi Mehraban, M., Ayatollahi, S., & Sharifi, M. 2019. Role of divalent ions, temperature, and crude oil during water injection into dolomitic carbonate oil reservoirs. *Oil & Gas Science and Technology – Revue d'IFP Energies nouvelles*. 74:36.

Fernández-Guerrero, M.L., Herrero, L., Bellver, M., Gadea, I., Roblas, R.F., & De Górgolas, M. 2002. Nosocomial enterococcal endocarditis: A serious hazard for hospitalized patients with enterococcal bacteraemia. *Journal of Internal Medicine*. 252(6):510–515.

Ferrer, I. & Thurman, E.M. 2012. Analysis of 100 pharmaceuticals and their degradates in water samples by liquid chromatography/quadrupole time-of-flight mass spectrometry. *Journal of Chromatography A*. 1259:148–157.

Fisher, K. & Phillips, C. 2009. The ecology, epidemiology and virulence of *Enterococcus*. *Microbiology*. 155(6):1749–1757.

Fourie, J.C.J. 2017. Characterization of *Clostridium* spp. isolated from selected surface water systems and aquatic sediment. North-West University (NWU) (Dissertation - MSc).

Francisque, A., Rodriguez, M.J., Miranda-Moreno, L.F., Sadiq, R., & Proulx, F. 2009. Modeling

of heterotrophic bacteria counts in a water distribution system. *Water Research*. 43(4):1075–1087.

Gajdács, M., Spengler, G., & Urbán, E. 2017. Identification and antimicrobial susceptibility testing of anaerobic bacteria: Rubik's cube of clinical microbiology? *Antibiotics*. 6(4):1–29.

Garner, E., Benitez, R., von Wagoner, E., Sawyer, R., Schaberg, E., Hession, W.C., Krometis, L.-A.H., Badgley, B.D., & Pruden, A. 2017. Stormwater loadings of antibiotic resistance genes in an urban stream. *Water Research*. 123:144–152.

Gelli, R., Scudero, M., Gigli, L., Severi, M., Bonini, M., Ridi, F., & Baglioni, P. 2018. Effect of pH and Mg2+ on Amorphous Magnesium-Calcium Phosphate (AMCP) stability. *Journal of Colloid and Interface Science*. 531:681–692.

Gemmer, M., Fischer, T., Jiang, T., Su, B., & Liu, L.L. 2011. Trends in Precipitation Extremes in the Zhujiang River Basin, South China. *Journal of Climate*. 24(3):750–761.

Gerten, D., Heinke, J., Hoff, H., Biemans, H., Fader, M., & Waha, K. 2011. Global water availability and requirements for future food production. *Journal of Hydrometeorology*. 12(5):885–899.

Ghaju Shrestha, R., Tanaka, Y., Malla, B., Bhandari, D., Tandukar, S., Inoue, D., Sei, K., Sherchand, J.B., & Haramoto, E. 2017. Next-generation sequencing identification of pathogenic bacterial genes and their relationship with fecal indicator bacteria in different water sources in the Kathmandu Valley, Nepal. *Science of The Total Environment*. 601–602:278–284.

Gidey, A. 2018. Geospatial distribution modeling and determining suitability of groundwater quality for irrigation purpose using geospatial methods and water quality index (WQI) in Northern Ethiopia. *Applied Water Science*. 8(3):82.

Gillings, M.R. 2014. Integrons: Past, Present, and Future. *Microbiology and Molecular Biology Reviews*. 78(2):257–277.

Gillings, M.R., Gaze, W.H., Pruden, A., Smalla, K., Tiedje, J.M., & Zhu, Y.G. 2015. Using the class 1 integron-integrase gene as a proxy for anthropogenic pollution. *ISME Journal*. *Nature Publishing Group*. 9(6):1269–1279.

Girlich, D., Naas, T., Bellais, S., Poirel, L., Karim, A., & Nordmann, P. 2000. Biochemical-genetic characterization and regulation of expression of an ACC-1-like chromosome-borne cephalosporinase from Hafnia alvei. *Antimicrobial Agents and Chemotherapy*. 44(6):1470–1478.

Goodchild, M.F. 2015. Geographic information systems, in: International Encyclopedia of the Social & Behavioral Sciences. pp. 58–63.

Gorde, S.P. & Jadhav, M. V. 2013. Assessment of water quality parameters : A review. *International Journal of Engineering Research and Applications*. 3(6):2029–2035.

Graham, D.W., Knapp, C.W., Christensen, B.T., McCluskey, S., & Dolfing, J. 2016. Appearance of β-lactam resistance genes in agricultural soils and clinical isolates over the 20th century. *Scientific Reports*. 6(1):21550.

Gregory, L.F., Karthikeyan, R., Aitkenhead-Peterson, J.A., Gentry, T.J., Wagner, K.L., & Harmel, R.D. 2017. Nutrient loading impacts on culturable *E. coli* and other heterotrophic bacteria fate in simulated stream mesocosms. *Water Research*. 126:442–449.

Gross, J.H. 2017. Mass Spectrometry. 3rd ed. Analytical Chemistry. Springer International Publishing: Cham.

Grueau, C. 2018. Applications of geographic information systems. *Journal of Geographical Systems*. *Springer Berlin Heidelberg*. 20(2):111–114.

Guenther, S., Ewers, C., & Wieler, L.H. 2011. Extended-spectrum beta-lactamases producing *E. coli* in wildlife, yet another form of environmental pollution? *Frontiers in Microbiology*. 2(DEC):1–13.

Hachich, E.M., Di Bari, M., Christ, A.P.G., Lamparelli, C.C., Ramos, S.S., & Sato, M.I.Z. 2012. Comparison of thermotolerant coliforms and *Escherichia coli* densities in freshwater bodies. *Brazilian Journal of Microbiology*. 43(2):675–681.

Hall, K.K., Evanshen, B.G., Maier, K.J., & Scheuerman, P.R. 2014. Application of multivariate statistical methodology to model factors influencing fate and transport of fecal pollution in surface waters. *Journal of Environment Quality*. 43(1):358.

Hamiwe, T., Kock, M.M., Magwira, C.A., Antiabong, J.F., & Ehlers, M.M. 2019. Occurrence of enterococci harbouring clinically important antibiotic resistance genes in the aquatic environment in Gauteng, South Africa. *Environmental Pollution*. 245:1041–1049.

Han, D. 2010. Concise hydrology. BookBoon: Bristol.

Han, D. 2015. Concise Environmental Engineering. BookBoon: Bristol.

Harley, J.P. & Prescott, L.M. 2002. Laboratory Exercises in Microbiology. 5th ed. The

McGraw−Hill Companies: New-York.

Harmon, S.M., Kautter, D.A., & Peeler, J.T. 1971. Improved medium for enumeration of *Clostridium perfringens*. *Applied microbiology*. 22(4):688–92.

Heaton, J.C. & Jones, K. 2008. Microbial contamination of fruit and vegetables and the behaviour of enteropathogens in the phyllosphere: A review. *Journal of Applied Microbiology*. 104(3):613–626.

Henry, R., Schang, C., Kolotelo, P., Coleman, R., Rooney, G., Schmidt, J., Deletic, A., & McCarthy, D.T. 2016. Effect of environmental parameters on pathogen and faecal indicator organism concentrations within an urban estuary. *Estuarine, Coastal and Shelf Science*. 174:18–26.

Henton, M.M., Eagar, H.A., Swan, G.E., & van Vuuren, M. 2011. Part VI. Antibiotic management and resistance in livestock production. *South African Medical Journal*. 101(8):583–586.

Herlemann, D.P.R., Labrenz, M., Jürgens, K., Bertilsson, S., Waniek, J.J., & Andersson, A.F. 2011. Transitions in bacterial communities along the 2000 km salinity gradient of the Baltic Sea. *The ISME Journal*. 5(10):1571–1579.

Hernández, F., Sancho, J. V., Ibáñez, M., & Guerrero, C. 2007. Antibiotic residue determination in environmental waters by LC-MS. *TrAC Trends in Analytical Chemistry*. 26(6):466–485.

Heydari, M.M. & Bidgoli, H.N. 2012. Chemical analysis of drinking water of Kashan District, Central Iran. *World Applied Sciences Journal*. 16(6):799–805.

Higuita Agudelo, Nelson I Huycke, M.M. 2014. Enterococcal disease, epidemiology, and implications for treatment, in: Michael Gilmore, B.S., Clewell, D.B., Ike, Y., Shankar, N. (Eds.), Enterococci : From Commensals to Leading Causes of Drug Resistant Infection. pp. 65–100.

HiMedia. 2019a. KF Streptococcal Agar Base.

HiMedia. 2019b. Reinforced Clostridial Agar.

Hoelzer, K., Wong, N., Thomas, J., Talkington, K., Jungman, E., & Coukell, A. 2017. Antimicrobial drug use in food-producing animals and associated human health risks: what, and how strong, is the evidence? *BMC Veterinary Research*. 13(1):211.

Holmatov, B., Lautze, J., Manthrithilake, H., & Makin, I. 2017. Water security for productive economies: Applying an assessment framework in southern Africa.

Horn, S., Pieters, R., & Bezuidenhout, C. 2016. Pathogenic features of heterotrophic plate count bacteria from drinking-water boreholes. *Journal of Water and Health*. 14(6):890–900.

Howard, I., Espigares, E., Lardelli, P., Martín, J.L., & Espigares, M. 2004. Evaluation of microbiological and physicochemical indicators for wastewater treatment. *Environmental Toxicology*. 19(3):241–249.

Huang, H., Zeng, S., Dong, X., Li, D., Zhang, Y., He, M., & Du, P. 2019. Diverse and abundant antibiotics and antibiotic resistance genes in an urban water system. *Journal of Environmental Management*. 231:494–503.

Hunter, P.R. 2003. Drinking water and diarrhoeal disease due to *Escherichia coli*. *Journal of Water and Health*. 1(2):65–72.

Hutchings, M., Truman, A., & Wilkinson, B. 2019. Antibiotics: past, present and future. *Current Opinion in Microbiology*. 51:72–80.

Irikura, D., Monma, C., Suzuki, Y., Nakama, A., Kai, A., Fukui-Miyazaki, A., Horiguchi, Y., Yoshinari, T., Sugita-Konishi, Y., & Kamata, Y. 2015. Identification and characterization of a new enterotoxin produced by *Clostridium perfringens* isolated from food poisoning outbreaks. *PLoS ONE*. 10(11):1–25.

Isiyaka, H.A., Mustapha, A., Juahir, H., & Phil-Eze, P. 2019. Water quality modelling using artificial neural network and multivariate statistical techniques. *Modeling Earth Systems and Environment*. 5(2):583–593.

Islam, A.R.M.T., Al Mamun, A., Rahman, M.M., & Zahid, A. 2020. Simultaneous comparison of modified-integrated water quality and entropy weighted indices: Implication for safe drinking water in the coastal region of Bangladesh. *Ecological Indicators*. 113(February):106229.

Iwase, T., Tajima, A., Sugimoto, S., Okuda, K., Hironaka, I., Kamata, Y., Takada, K., & Mizunoe, Y. 2013. A simple assay for measuring catalase activity: A visual approach. *Scientific Reports*. 3(1):3081.

Jahnen-Dechent, W. & Ketteler, M. 2012. Magnesium basics. *Clinical Kidney Journal*. 5(1):3–14.

Japoni, A., Gudarzi, M., Farshad, S., Basiri, E., Ziyaeyan, M., Alborzi, A., & Rafaatpour, N. 2008. Assay for integrons and pattern of antibiotic resistance in clinical *Escherichia coli* strains by PCR-RFLP in Southern Iran. *Japanese Journal of Infectious Diseases*. 61(1):85–88.

Jarvie, H.P., Neal, C., & Withers, P.J.A. 2006. Sewage-effluent phosphorus: A greater risk to river eutrophication than agricultural phosphorus? *Science of The Total Environment*. 360(1–3):246–253.

Jarvie, H.P., Withers, P.J.A., Hodgkinson, R., Bates, A., Neal, M., Wickham, H.D., Harman, S.A., & Armstrong, L. 2008. Influence of rural land use on streamwater nutrients and their ecological significance. *Journal of Hydrology*. 350(3–4):166–186.

Jennings, S.R., Blicker, S., Neuman, P., & Dennis, R. 2008. Acid mine drainage and effects on fish health and ecology: a review. *Reclamation Research Group*. 1(1):1–26.

Ji, Z.-G. 2008. Hydrodynamics and water quality: modelling rivers, lakes, and estuaries. John Wiley & Sons, inc.: Hoboken, New Jersey.

Jia, J., Guan, Y., Cheng, M., Chen, H., He, J., Wang, S., & Wang, Z. 2018. Occurrence and distribution of antibiotics and antibiotic resistance genes in Ba River, China. *Science of The Total Environment*. 642:1136–1144.

Jordaan, K. & Bezuidenhout, C.C. 2016. Bacterial community composition of an urban river in the North West Province, South Africa, in relation to physico-chemical water quality. *Environmental Science and Pollution Research*. 23(6):5868–5880.

Jordaan, K., Comeau, A.M., Khasa, D.P., & Bezuidenhout, C.C. 2019. An integrated insight into the response of bacterial communities to anthropogenic contaminants in a river: A case study of the Wonderfonteinspruit catchment area, South Africa. *PLoS ONE*. 14(5):1–24.

Joshi, M. & Deshpande, J.D. 2011. Polymerase chain reaction: methods, principles and application. *International Journal of Biomedical Research*. 2(1):81–97.

Kamleh, A., Barrett, M.P., Wildridge, D., Burchmore, R.J.S., Scheltema, R.A., & Watson, D.G. 2008. Metabolomic profiling using Orbitrap Fourier transform mass spectrometry with hydrophilic interaction chromatography: a method with wide applicability to analysis of biomolecules. *Rapid Communications in Mass Spectrometry*. 22(12):1912–1918.

Keshri, J., Mankazana, B.B.J.J., & Momba, M.N.B.B. 2015. Profile of bacterial communities in South African mine-water samples using Illumina next-generation sequencing platform. *Applied Microbiology and Biotechnology*. 99(7):3233–3242.

Khatri, N. & Tyagi, S. 2015. Influences of natural and anthropogenic factors on surface and groundwater quality in rural and urban areas. *Frontiers in Life Science*. 8(1):23–39.

Kim, J.M., Roh, A.-S., Choi, S.-C., Kim, E.-J., Choi, M.-T., Ahn, B.-K., Kim, S.-K., Lee, Y.-H., Joa, J.-H., Kang, S.-S., Lee, S.A., Ahn, J.-H., Song, J., & Weon, H.-Y. 2016. Soil pH and electrical conductivity are key edaphic factors shaping bacterial communities of greenhouse soils in Korea. *Journal of Microbiology*. 54(12):838–845.

Kim, K., Yoo, K., Ki, D., Son, I.S., Oh, K.J., & Park, J. 2011. Decision-Tree-based data mining and rule induction for predicting and mapping soil bacterial diversity. *Environmental Monitoring and Assessment*. 178(1–4):595–610.

Kim, M., Boithias, L., Cho, K.H., Silvera, N., Thammahacksa, C., Latsachack, K., Rochelle-Newall, E., Sengtaheuanghoung, O., Pierret, A., Pachepsky, Y.A., & Ribolzi, O. 2017. Hydrological modeling of fecal indicator bacteria in a tropical mountain catchment. *Water Research*. 119:102–113.

Kim, S.-C. & Carlson, K. 2007. Temporal and spatial trends in the occurrence of human and veterinary antibiotics in aqueous and river sediment matrices. *Environmental science & technology*. 41(1):50–7.

Kisakye, V. & Van der Bruggen, B. 2018. Effects of climate change on water savings and water security from rainwater harvesting systems. *Resources, Conservation and Recycling*. 138:49–63.

Kivanc, M., Yilmaz, M., & Demir, F. 2011. The occurrence of *Aeromonas* in drinking water, tap water and the Porsuk River. *Brazilian Journal of Microbiology*. 42(1):126–131.

Knapp, C.W., Dolfing, J., Ehlert, P.A.I., & Graham, D.W. 2010. Evidence of increasing antibiotic resistance gene abundances in archived soils since 1940. *Environmental Science & Technology*. 44(2):580–587.

Koczura, R., Mokracka, J., Taraszewska, A., & Łopacinska, N. 2016. Abundance of class 1 integron-integrase and sulfonamide resistance genes in river water and sediment is affected by anthropogenic pressure and environmental factors. *Microbial Ecology*. 72(4):909–916.

Kookana, R.S., Drechsel, P., Jamwal, P., & Vanderzalm, J. 2020. Urbanisation and emerging economies: Issues and potential solutions for water and food security. *Science of The Total Environment*. 732:139057.

Kora, A.J., Rastogi, L., Kumar, S.J., & Jagatap, B.N. 2017. Physico-chemical and bacteriological screening of Hussain Sagar lake: An urban wetland. *Water Science*. *National Water Research Center*. 31(1):24–33.

Korfmacher, W.A. 2005. Foundation review: Principles and applications of LC-MS in new drug discovery. *Drug Discovery Today*. 10(20):1357–1367.

Kostyla, C., Bain, R., Cronk, R., & Bartram, J. 2015. Seasonal variation of fecal contamination in drinking water sources in developing countries: A systematic review. *Science of the Total Environment*. 514:333–343.

Kristiana, I., Heitz, A., Joll, C., & Sathasivan, A. 2010. Analysis of polysulfides in drinking water distribution systems using headspace solid-phase microextraction and gas chromatography-mass spectrometry. *Journal of Chromatography A*. 1217(38):5995–6001.

Krumperman, P.H. 1983. Multiple antibiotic resistance indexing of *Escherichia coli* to identify high-risk sources of fecal contamination of foods. *Applied and environmental microbiology*. 46(1):165–70.

Kurenbach, B., Hill, A.M., Godsoe, W., van Hamelsveld, S., & Heinemann, J.A. 2018. Agrichemicals and antibiotics in combination increase antibiotic resistance evolution. *PeerJ*. 6(10):e5801.

Labbate, M., Chowdhury, P.R., & Stokes, H.W. 2008. A class 1 integron present in a human commensal has a hybrid transposition module compared to Tn402: Evidence of interaction with mobile DNA from natural environments. *Journal of Bacteriology*. 190(15):5318–5327.

Ladra, S., Paramá, J.R., & Silva-Coira, F. 2017. Scalable and queryable compressed storage structure for raster data. *Information Systems*. 72:179–204.

Langille, M.G.I., Zaneveld, J., Caporaso, J.G., McDonald, D., Knights, D., Reyes, J.A., Clemente, J.C., Burkepile, D.E., Vega Thurber, R.L., Knight, R., Beiko, R.G., & Huttenhower, C. 2013. Predictive functional profiling of microbial communities using 16S rRNA marker gene sequences. *Nature Biotechnology*. 31(9):814–821.

Laxminarayan, R., Duse, A., Wattal, C., Zaidi, A.K.M., Wertheim, H.F.L., Sumpradit, N., Vlieghe, E., Hara, G.L., Gould, I.M., Goossens, H., Greko, C., So, A.D., Bigdeli, M., Tomson, G., Woodhouse, W., Ombaka, E., Peralta, A.Q., Qamar, F.N., Mir, F., Kariuki, S., Bhutta, Z.A., Coates, A., Bergstrom, R., Wright, G.D., Brown, E.D., & Cars, O. 2013. Antibiotic resistance-the need for global solutions. *The Lancet Infectious Diseases*. 13(12):1057–1098.

Le, T.-H., Ng, C., Tran, N.H., Chen, H., & Gin, K.Y.-H. 2018. Removal of antibiotic residues, antibiotic resistant bacteria and antibiotic resistance genes in municipal wastewater by membrane bioreactor systems. *Water Research*. 145:498–508.

Lee, S.W., Kim, J.H., & Cha, S.M. 2020. Analysis of the relation between pollutant loading and water depth flowrate changes in a constructed wetland for agricultural nonpoint source pollution management. *Ecological Engineering*. 152(May):105841.

Legenza, L., Barnett, S., Lacy, J.P., See, C., Desotell, N., Eibergen, A., Piccirillo, J.F., & Rose, W.E. 2019. Geographic Mapping of Escherichia coli Susceptibility To Develop a Novel Clinical Decision Support Tool. *Antimicrobial Agents and Chemotherapy*. 63(6):1–4.

Li, J., Jiang, C., Lei, T., & Li, Y. 2016. Experimental study and simulation of water quality purification of urban surface runoff using non-vegetated bioswales. *Ecological Engineering*. 95:706–713.

Liang, Z., He, Z., Zhou, X., Powell, C.A., Yang, Y., He, L.M., & Stoffella, P.J. 2013. Impact of mixed land-use practices on the microbial water quality in a subtropical coastal watershed. *Science of the Total Environment*. 449:426–433.

Lim, J.S., Yang, S.H., Kim, B.S., & Lee, E.Y. 2018. Comparison of microbial communities in swine manure at various temperatures and storage times. *Asian-Australasian Journal of Animal Sciences*. 31(8):1373–1380.

Liu, J. 2019. Economic target of regional water resources based on bearing capacity. *Journal of Coastal Research*. 93:883.

Liu, L., Xing, X., Hu, C., & Wang, H. 2019. O3-BAC-Cl2: A multi-barrier process controlling the regrowth of opportunistic waterborne pathogens in drinking water distribution systems. *Journal of Environmental Sciences (China)*. 76:142–153.

Liu, Z., Zhang, J., Rao, S., Sun, L., Zhang, J., Liu, R., Zheng, G., Ma, X., Hou, S., Zhuang, X., Song, X., & Li, Q. 2015. Heptaplex PCR melting curve analysis for rapid detection of plasmid-mediated AmpC β-lactamase genes. *Journal of Microbiological Methods*. 110:1–6.

Long, S.C. & Plummer, J.D. 2004. Assessing land use impacts on water quality using microbial source tracking. *Journal of the American Water Resources Association*. 40(6):1433–1448.

Longley, P.A., Maguire, D.J., Goodchild, M.F., & Rhind, D.W. 2004. Geographical Information Systems. 2nd ed. John Wiley & Sons Ltd: Chichester.

Lu, G.Y. & Wong, D.W. 2008. An adaptive inverse-distance weighting spatial interpolation technique. *Computers & Geosciences*. 34(9):1044–1055.

Lucas, F.S., Therial, C., Gonçalves, A., Servais, P., Rocher, V., & Mouchel, J.M. 2014. Variation

of raw wastewater microbiological quality in dry and wet weather conditions. *Environmental Science and Pollution Research*. 21(8):5318–5328.

Lükenga, W. 2015. Water Resource Management. 1st ed. BookBoon.

Ma, X., Guo, N., Ren, S., Wang, S., & Wang, Y. 2019. Response of antibiotic resistance to the co-existence of chloramphenicol and copper during bio-electrochemical treatment of antibiotic-containing wastewater. *Environment International*. 126:127–133.

Madhloom, H., Al-Ansari, N., Laue, J., & Chabuk, A. 2017. Modeling spatial distribution of some contamination within the lower reaches of Diyala River using IDW interpolation. *Sustainability*. 10(2):22.

Mahmud, Z.H., Islam, M.S., Imran, K.M., Hakim, S.A.I., Worth, M., Ahmed, A., Hossan, S., Haider, M., Islam, M.R., Hossain, F., Johnston, D., & Ahmed, N. 2019. Occurrence of *Escherichia coli* and faecal coliforms in drinking water at source and household point-of-use in Rohingya camps, Bangladesh. *Gut Pathogens*. 11(1):1–11.

Malan, J.D. 2012. The impact of the gold mining industry on the water quality of the Kromdraai catchment. University of Johannesburg (UJ) (Dissertation - MSc)

Manzetti, S. & Ghisi, R. 2014. The environmental release and fate of antibiotics. *Marine Pollution Bulletin*. 79(1–2):7–15.

Martel, J.L., Tardy, F., Sanders, P., & Boisseau, J. 2001. New trends in regulatory rules and surveillance of antimicrobial resistance in bacteria of animal origin. *Veterinary Research*. 32(3–4):381–392.

Martinez, J.L. 2009. Environmental pollution by antibiotics and by antibiotic resistance determinants. *Environmental Pollution*. 157(11):2893–2902.

Masindi, V., Gitari, M.W., Tutu, H., & De Beer, M. 2015. Passive remediation of acid mine drainage using cryptocrystalline magnesite: A batch experimental and geochemical modelling approach. *Water SA*. 41(5):677.

Masson, V., Heldens, W., Bocher, E., Bonhomme, M., Bucher, B., Burmeister, C., de Munck, C., Esch, T., Hidalgo, J., Kanani-Sühring, F., Kwok, Y.T., Lemonsu, A., Lévy, J.P., Maronga, B., Pavlik, D., Petit, G., See, L., Schoetter, R., Tornay, N., Votsis, A., & Zeidler, J. 2020. City-descriptive input data for urban climate models: Model requirements, data sources and challenges. *Urban Climate*. 31(December 2018):100536.

Maurer, M. & Gujer, W. 1995. Monitoring of microbial phosphorus release in batch experiments using electric conductivity. *Water Research*. 29(11):2613–2617.

Mbuh, M.J., Mbih, R., & Wendi, C. 2019. Water quality modeling and sensitivity analysis using Water Quality Analysis Simulation Program (WASP) in the Shenandoah River watershed. *Physical Geography*. 40(2):127–148.

McCarthy, T.S. 2011. The impact of acid mine drainage in South Africa. *South African Journal of Science*. 107(5/6):1–7.

McGinnis, S., Spencer, S., Firnstahl, A., Stokdyk, J., Borchardt, M., McCarthy, D.T., & Murphy, H.M. 2018. Human Bacteroides and total coliforms as indicators of recent combined sewer overflows and rain events in urban creeks. *Science of the Total Environment*. 630:967–976.

Medema, G.J., Payment, P., Dufour, A., Robertson, W., Waite, M., Hunter, P., Kirby, R., & Andersson, Y. 2003. Introducing parameters for the assesment of drinking water quality. 1st ed. in: Assessing Microbial Safety of Drinking Water. IWA Publishing: London, pp. 47–77.

Merck. 2012. Microbiology Manual. 12th ed. http://www.scribd.com/doc%0A/94454909/ Merck-Microbiology-Manual-12th. Date of access: 15 Mar. 2020.

Merck. 2019. Tryptose Sulfite Cycloserine Agar, Perfringens Agar. https://www.sigmaaldrich.com/content/dam/sigma-aldrich/docs/Sigma-Aldrich/Datasheet/1/93745dat.pdf. Date of access: 12 Mar. 2020.

Mhlongo, S., Mativenga, P.T., & Marnewick, A. 2018. Water quality in a mining and water-stressed region. *Journal of Cleaner Production*. 171:446–456.

Milly, P.C.D., Dunne, K.A., & Vecchia, A. V. 2005. Global pattern of trends in streamflow and water availability in a changing climate. *Nature*. 438(7066):347–350.

Molale, L. 2016. Characterization of enterococci isolates from water sources in the North West Province. North-West University (NWU) (Thesis - PhD).

Molale, L.G. & Bezuidenhout, C.C. 2016. Virulence determinants and production of extracellular enzymes in *Enterococcus* spp. from surface water sources. *Water Science and Technology*. 73(8):1817–1824.

Mueller-Spitz, S.R., Stewart, L.B., Val Klump, J., & McLellan, S.L. 2010. Freshwater suspended sediments and sewage are reservoirs for enterotoxin-positive *Clostridium perfringens*. *Applied and Environmental Microbiology*. 76(16):5556–5562.

Muraleedharan, C., Talreja, D., Kanwar, M., Kumar, A., & Walia, S.K. 2019. Occurrence of extended-spectrum β-lactamase-producing bacteria in urban Clinton River habitat. *Journal of Global Antimicrobial Resistance*. *Taibah University*. 16:225–235.

Muyzer, G., De Waal, E.C., & Uitterlinden, A.G. 1993. Profiling of complex microbial populations by denaturing gradient gel electrophoresis analysis of polymerase chain reaction-amplified genes coding for 16S rRNA. *Applied and Environmental Microbiology*. 59(3):695–700.

Naicker, K., Cukrowska, E., & McCarthy, T.. 2003. Acid mine drainage arising from gold mining activity in Johannesburg, South Africa and environs. *Environmental Pollution*. 122(1):29–40.

Ngoye, E. & Machiwa, J.F. 2004. The influence of land-use patterns in the Ruvu river watershed on water quality in the river system. *Physics and Chemistry of the Earth*. 29(15–18):1161–1166.

Njage, P.M.K. & Buys, E.M. 2015. Pathogenic and commensal *Escherichia coli* from irrigation water show potential in transmission of extended spectrum and AmpC β-lactamases determinants to isolates from lettuce. *Microbial Biotechnology*. 8(3):462–473.

NWREAD: North West Department of Rural Environment and Agricultural Development. 2014. North West Environment Outlook Report 2013. North West Provincial Government. Mahikeng.

Ogbozige, F.J., Adie, D.B., & Abubakar, U.A. 2018. Water quality assessment and mapping using inverse distance weighted interpolation: a case of River Kaduna, Nigeria. *Nigerian Journal of Technology*. 37(1):249.

Olad, A., Zebhi, H., Salari, D., Mirmohseni, A., & Reyhani Tabar, A. 2018. Slow-release NPK fertilizer encapsulated by carboxymethyl cellulose-based nanocomposite with the function of water retention in soil. *Materials Science and Engineering C*. 90(July 2017):333–340.

Oliver, D.M., Porter, K.D.H., Pachepsky, Y.A., Muirhead, R.W., Reaney, S.M., Coffey, R., Kay, D., Milledge, D.G., Hong, E., Anthony, S.G., Page, T., Bloodworth, J.W., Mellander, P.-E., Carbonneau, P.E., McGrane, S.J., & Quilliam, R.S. 2016. Predicting microbial water quality with models: Over-arching questions for managing risk in agricultural catchments. *Science of The Total Environment*. 544:39–47.

Oxoid Limited. 2012. Oxoid microbiology products. Membrane Lactose Glucuronide Agar (MLGA). http://www.oxoid.com/UK/blue/prod_detail/prod_detail.asp?pr=CM1031&%0Aorg=71&c=UK&lang. Date of access: 12 Mar. 2020.

Painter, K.L., Hall, A., Ha, K.P., & Edwards, A.M. 2017. The electron transport chain sensitizes *Staphylococcus aureus* and *Enterococcus faecalis* to the oxidative burst. *Infection and Immunity*. 85(12):1–13.

Panigrahi, A., Saranya, C., Sundaram, M., Vinoth Kannan, S.R.R., Das, R.R., Satish Kumar, R., Rajesh, P., & Otta, S.K.K. 2018. Carbon: Nitrogen (C:N) ratio level variation influences microbial community of the system and growth as well as immunity of shrimp (*Litopenaeus vannamei*) in biofloc based culture system. *Fish and Shellfish Immunology*. 81(June):329–337.

Panwar, A., Bartwal, S., Dangwal, S., Aswal, A., Bhandari, A., & Rawat, S. 2015. Water Quality Assessment of River Ganga using Remote Sensing and GIS Technique. *International Journal of Advanced Remote Sensing and GIS*. 4(1):1253–1261.

Parry, R. 1998. Agricultural phosphorus and water quality: A U.S. Environmental Protection Agency perspective. *Journal of Environment Quality*. 27(2):258.

Paruch, A.M. & Mæhlum, T. 2012. Specific features of *Escherichia coli* that distinguish it from coliform and thermotolerant coliform bacteria and define it as the most accurate indicator of faecal contamination in the environment. *Ecological Indicators*. 23:140–142.

Pascual-Benito, M., Nadal-Sala, D., Tobella, M., Ballesté, E., García-Aljaro, C., Sabaté, S., Sabater, F., Martí, E., Gracia, C.A., Blanch, A.R., & Lucena, F. 2020. Modelling the seasonal impacts of a wastewater treatment plant on water quality in a Mediterranean stream using microbial indicators. *Journal of Environmental Management*. 261(January).

Patil, P., Sawant, D., & Deshmukh, R. 2012. Physico-chemical parameters for testing of water-A review. *International Journal of Environmental Sciences*. 3(3):1194–1207.

Paulse, A., Jackson, V., & Khan, W. 2009. Comparison of microbial contamination at various sites along the Plankenburg- and Diep Rivers, Western Cape, South Africa. *Water SA*. 35(4):469–478.

Pavlov, D., de Wet, C.M.., Grabow, W.O.., & Ehlers, M.. 2004. Potentially pathogenic features of heterotrophic plate count bacteria isolated from treated and untreated drinking water. *International Journal of Food Microbiology*. 92(3):275–287.

Payment, P., Waite, M., & Dufour, A. 2003. Introducing parameters for the assessment of drinking water quality, in: Assessing Microbial Safety of Drinking Water: Improving Approaches and Methods. pp. 47–77.

Pei, R., Kim, S.-C., Carlson, K.H., & Pruden, A. 2006. Effect of river landscape on the sediment concentrations of antibiotics and corresponding antibiotic resistance genes (ARG). *Water Research*. 40(12):2427–2435.

Perez-Perez, F.J. & Hanson, N.D. 2002. Detection of plasmid-mediated AmpC β-lactamase genes in clinical isolates by using multiplex PCR. *Journal of Clinical Microbiology*. 40(6):2153–2162.

Petit, L., Gibert, M., & Popoff, M.R. 1999. *Clostridium perfringens*: Toxinotype and genotype. *Trends in Microbiology*. 7(3):104–110.

Pullanikkatil, D., Palamuleni, L., & Ruhiiga, T. 2015. Impact of land use on water quality in the Likangala catchment, southern Malawi. *African Journal of Aquatic Science*. 40(3):277–286.

Radhouani, H., Silva, N., Poeta, P., Torres, C., Correia, S., & Igrejas, G. 2014. Potential impact of antimicrobial resistance in wildlife, environment and human health. *Frontiers in Microbiology*. 5(32):1–12.

Rajaei, B., Siadat, S.D., Razavi, M.R., Aghasadeghi, M.R., Rad, N.S., Badmasti, F., Jafroodi, S.K., Rajaei, T., Moshiri, A., & Javadian, S. 2011. Expanding drug resistance through integron acquisition in *Salmonella* spp. isolates obtained in Iran. *African Journal of Microbiology Research*. 5(16):2249–2253.

Raju, P.L.N. 2004. Fundamentals of Geographical Information System, in: Satellite Remote Sensing and GIS Applications in Meteorology. World Meteorological Organisation: Geneva, Switzerland, pp. 175–194.

Ramos, M.C., Quinton, J.N., & Tyrrel, S.F. 2006. Effects of cattle manure on erosion rates and runoff water pollution by faecal coliforms. *Journal of Environmental Management*. 78(1):97–101.

Ratanasuwan, W., Iwen, P.C., Hinrichs, S.H., & Rupp, M.E. 1999. Bacteremia due to motile *Enterococcus* species: clinical features and outcomes. *Clinical Infectious Diseases*. 28(5):1175–1177.

Rijsberman, F.R. 2006. Water scarcity: Fact or fiction? *Agricultural Water Management*. 80(1–3):5–22.

Rimoldi, G., Uzal, F., Chin, R.P., Palombo, E.A., Awad, M., Lyras, D., & Shivaprasad, H.L. 2015. Necrotic Enteritis in chickens associated with *Clostridium sordellii*. *Avian Diseases*. 59(3):447–451.

Rolfe, R.D., Hentges, D.J., Campbell, B.J., & Barrett, J.T. 1978. Factors related to the oxygen tolerance of anaerobic bacteria. *Applied and Environmental Microbiology*. 36(2):306–313.

Romanazzi, V., Bonetta, S., Fornasero, S., De Ceglia, M., Gilli, G., & Traversi, D. 2016. Assessing *Methanobrevibacter smithii* and *Clostridium difficile* as not conventional faecal indicators in effluents of a wastewater treatment plant integrated with sludge anaerobic digestion. *Journal of Environmental Management*. 184:170–177.

Rothenheber, D. & Jones, S. 2018. Enterococcal concentrations in a coastal ecosystem are a function of fecal source input, environmental conditions, and environmental sources. *Applied and Environmental Microbiology*. 84(17):1–18.

Sagar, S.S., Chavan, R.P., Patil, C.L., Shinde, D.N., & Kekane, S.. 2015. Physico-chemical parameters for testing of water-A review. *International Journal of Chemical Studies*. 3(4):24–28.

Sanchez Ramos, L. & Rodloff, A.C. 2018. Identification of *Clostridium* species using the VITEK® MS. *Anaerobe*. 54:217–223.

Sangavai, C. & Chellapandi, P. 2017. Amino acid catabolism-directed biofuel production in *Clostridium sticklandii*: An insight into model-driven systems engineering. *Biotechnology Reports*. 16:32–43.

Sankararamakrishnan, N. & Guo, Q. 2005. Chemical tracers as indicator of human fecal coliforms at storm water outfalls. *Environment International*. 31(8):1133–1140.

SANS. 2015. Drinking water for SANS 241 : 2015. Pretoria, South Africa.

Schleifer, K.H. & Kilpper-Balz, R. 1984. Transfer of *Streptococcus faecalis* and *Streptococcus faecium* to the genus *Enterococcus* nom. rev. as *Enterococcus faecalis* comb. nov. and *Enterococcus faecium* comb. nov. *International Journal of Systematic Bacteriology*. 34(1):31–34.

Schoeman, C., Mashiane, M., Dlamini, M., & Okonkwo, O. 2015. Quantification of selected antiretroviral drugs in a wastewater treatment works in South Africa using GC-TOFMS. *Journal of Chromatography & Separation Techniques*. 06:1–7.

Schwartz, T., Kohnen, W., Jansen, B., & Obst, U. 2003. Detection of antibiotic-resistant bacteria and their resistance genes in wastewater, surface water, and drinking water biofilms. *FEMS Microbiology Ecology*. 43(3):325–335.

Scorciapino, M.A., Acosta-Gutierrez, S., Benkerrou, D., D'Agostino, T., Malloci, G., Samanta, S.,

Bodrenko, I., & Ceccarelli, M. 2017. Rationalizing the permeation of polar antibiotics into Gram-negative bacteria. *Journal of Physics: Condensed Matter*. 29(11):113001.

Şener, Ş., Şener, E., & Davraz, A. 2017. Evaluation of water quality using water quality index (WQI) method and GIS in Aksu River (SW-Turkey). *Science of the Total Environment*. 584–585:131–144.

Senna, A.M. & Botaro, V.R. 2017. Biodegradable hydrogel derived from cellulose acetate and EDTA as a reduction substrate of leaching NPK compound fertilizer and water retention in soil. *Journal of Controlled Release*. 260(June):194–201.

Serumaga-Zake, P.A.E. & Arnab, R. 2012. The dynamics of poverty, migration and changes in the demographics of household structure: an exploratory case study of the North West Province of South Africa. *International Journal of Economics and Business Studies*. 2(1):58–79.

Sheng, R., Meng, D., Wu, M., Di, H., Qin, H., & Wei, W. 2013. Effect of agricultural land use change on community composition of bacteria and ammonia oxidizers. *Journal of Soils and Sediments*. 13(7):1246–1256.

Shil, S. & Singh, U.K. 2019. Health risk assessment and spatial variations of dissolved heavy metals and metalloids in a tropical river basin system. *Ecological Indicators*. 106(June):105455.

Shirzadi, A., Solaimani, K., Roshan, M.H., Kavian, A., Chapi, K., Shahabi, H., Keesstra, S., Ahmad, B. Bin, & Bui, D.T. 2019. Uncertainties of prediction accuracy in shallow landslide modeling: Sample size and raster resolution. *Catena*. 178(May 2018):172–188.

Sibanda, T., Chigor, V.N., & Okoh, A.I. 2013. Seasonal and spatio-temporal distribution of faecal-indicator bacteria in Tyume River in the Eastern Cape Province, South Africa. *Environmental Monitoring and Assessment*. 185(8):6579–6590.

Sinclair, L., Osman, O.A., Bertilsson, S., & Eiler, A. 2015. Microbial community composition and diversity via 16S rRNA gene amplicons: Evaluating the illumina platform. *PLOS ONE*. 10(2):1–19.

Socolofsky, S.A. & Jirka, G.H. 2002. Environmental fluid mechanics part I: Mass transfer and diffusion. 2nd ed. Universität Karlsruhe: Karlsruhe.

Sophocleous, M. 2002. Interactions between groundwater and surface water: the state of the science. *Hydrogeology Journal*. 10(1):52–67.

Sophocleous, M., Atkinson, J.K., Smethurst, J.A., Espindola-Garcia, G., & Ingenito, A. 2020. The

use of novel thick-film sensors in the estimation of soil structural changes through the correlation of soil electrical conductivity and soil water content. *Sensors and Actuators, A: Physical*. 301:111773.

Sówka, I., Grzelka, A., Pawnuk, M., & Pielichowska, A. 2020. The use of ordinary kriging and inverse distance weighted interpolation to assess the odour impact of a poultry farming. *Przegląd Naukowy Inżynieria i Kształtowanie Środowiska*. 29(1):17–26.

Staedtke, V., Roberts, N.J., Bai, R.-Y., & Zhou, S. 2016. *Clostridium novyi*-NT in cancer therapy. *Genes & Diseases*. 3(2):144–152.

StatsSA. 2010. Water Management Areas in South Africa. *Discussion document: D0405.8*. *Statistics South Africa*.

Steele, M. & Odumeru, J. 2004. Irrigation water as source of foodborne pathogens on fruit and vegetables. *Journal of Food Protection*. 67(12):2839–2849.

Stoner, D.L., Geary, M.C., White, L.J., Lee, R.D., Brizzee, J.A., Rodman, A.C., & Rope, R.C. 2001. Mapping microbial biodiversity. *Applied and Environmental Microbiology*. 67(9):4324–4328.

Sundsfjord, A., Simonsen, G., Haldorsen, B., Haaheim, H., Hjelmevoll, S., Littauer, P., & Dahl, K. 2004. Genetic methods for detection of antimicrobial resistance. *APMIS*. 112(11–12):815–837.

Switala, J. & Loewen, P.C. 2002. Diversity of properties among catalases. *Archives of Biochemistry and Biophysics*. 401(2):145–154.

Tallon, P., Magajna, B., Lofranco, C., & Kam, T.L. 2005. Microbial indicators of faecal contamination in water: A current perspective. *Water, Air, and Soil Pollution*. 166(1–4):139–166.

Tatsing Foka, F.E., Ateba, C.N., & Lourenco, A. 2019. Detection of virulence genes in multidrug resistant enterococci isolated from feedlots dairy and beef cattle: Implications for human health and food safety. *BioMed Research International*. 2019.

Tawfik, S.A., Azab, M.M., Ahmed, A.A.A., & Fayyad, D.M. 2018. Illumina MiSeq sequencing for preliminary analysis of microbiome causing primary endodontic infections in egypt. *International Journal of Microbiology*. 2018:1–15.

Thairu, Y., Usman, Y., & Nasir, I. 2014. Laboratory perspective of gram staining and its significance in investigations of infectious diseases. *Sub-Saharan African Journal of Medicine*. 1(4):168.

Tian, S., Cui, X., & Gong, Y. 2015. An approach to generate spatial Voronoi Treemaps for points, lines, and polygons. *Journal of Electrical and Computer Engineering*. 2015.

Tran, N.H., Hoang, L., Nghiem, L.D., Nguyen, N.M.H., Ngo, H.H., Guo, W., Trinh, Q.T., Mai, N.H., Chen, H., Nguyen, D.D., Ta, T.T., & Gin, K.Y.-H. 2019. Occurrence and risk assessment of multiple classes of antibiotics in urban canals and lakes in Hanoi, Vietnam. *Science of The Total Environment*. 692:157–174.

Tranmer, A.W., Marti, C.L., Tonina, D., Benjankar, R., Weigel, D., Vilhena, L., McGrath, C., Goodwin, P., Tiedemann, M., Mckean, J., & Imberger, J. 2018. A hierarchical modelling framework for assessing physical and biochemical characteristics of a regulated river. *Ecological Modelling*. 368:78–93.

Van Boeckel, T.P., Gandra, S., Ashok, A., Caudron, Q., Grenfell, B.T., Levin, S.A., & Laxminarayan, R. 2014. Global antibiotic consumption 2000 to 2010: An analysis of national pharmaceutical sales data. *The Lancet Infectious Diseases*. 14(8):742–750.

van der Walt, J., Nell, B., & Winde, F. 2002. Integrated catchment management: The Mooi River (Northwest Province, South Africa) as a case study. *Cuadernos de Investigación Geográfica*. 28:109.

van Ginkel, C.E. 2011. Eutrophication: Present reality and future challenges for South Africa. *Water SA*. 37(5):693–702.

Vaz-Moreira, I., Nunes, O.C., & Manaia, C.M. 2014. Bacterial diversity and antibiotic resistance in water habitats: Searching the links with the human microbiome. *FEMS Microbiology Reviews*. 38(4):761–778.

Vereen, E., Lowrance, R.R., Jenkins, M.B., Adams, P., Rajeev, S., & Lipp, E.K. 2013. Landscape and seasonal factors influence *Salmonella* and *Campylobacter* prevalence in a rural mixed use watershed. *Water Research*. 47(16):6075–6085.

Viau, E.J., Goodwin, K.D., Yamahara, K.M., Layton, B.A., Sassoubre, L.M., Burns, S.L., Tong, H.I., Wong, S.H.C., Lu, Y., & Boehm, A.B. 2011. Bacterial pathogens in Hawaiian coastal streams-Associations with fecal indicators, land cover, and water quality. *Water Research*. 45(11):3279–3290.

Vierheilig, J., Frick, C., Mayer, R.E., Kirschner, A.K.T., Reischer, G.H., Derx, J., Mach, R.L., Sommer, R., & Farnleitner, A.H. 2013. *Clostridium perfringens* is not suitable for the indication of fecal pollution from ruminant wildlife but is associated with excreta from nonherbivorous

animals and human sewage. *Applied and Environmental Microbiology*. 79(16):5089–5092.

Vijayavel, K., Fung, D.Y.C., & Fujioka, R.S. 2009. Modification of fung double tube and CP anaselect oxyplate methods to improve their performance in enumerating *Clostridium perfringens* from sewage and environmental waters. *Journal of Rapid Methods & Automation in Microbiology*. 17(4):535–549.

Voidarou, C., Bezirtzoglou, E., Alexopoulos, A., Plessas, S., Stefanis, C., Papadopoulos, I., Vavias, S., Stavropoulou, E., Fotou, K., Tzora, A., & Skoufos, I. 2011. Occurrence of *Clostridium perfringens* from different cultivated soils. *Anaerobe*. 17(6):320–324.

von Bormann, T. & Gulati, M. 2016. Food, Water, and Energy: Lessons From the South African Experience. *Environment*. 58(4):4–17.

Walmsley, R.D. 2000. Perspectives on eutrophication of surface waters : Policy / research needs in South Africa. Water Research Commission: WRC Report No. KV129/00.

Wang, H., Masters, S., Hong, Y., Stallings, J., Falkinham, J.O., Edwards, M.A., & Pruden, A. 2012. Effect of disinfectant, water age, and pipe material on occurrence and persistence of Legionella, Mycobacteria, Pseudomonas aeruginosa, and two amoebas. *Environmental Science and Technology*. 46(21):11566–11574.

Wang, Y., Lin, Z., He, L., Huang, W., Zhou, J., & He, Q. 2019. Simultaneous partial nitrification, anammox and denitrification (SNAD) process for nitrogen and refractory organic compounds removal from mature landfill leachate: Performance and metagenome-based microbial ecology. *Bioresource Technology*. 294(August):122166.

Watcharasukarn, M., Kaparaju, P., Steyer, J.-P., Krogfelt, K.A., & Angelidaki, I. 2009. Screening *Escherichia coli, Enterococcus faecalis*, and *Clostridium perfringens* as indicator organisms in evaluating pathogen-reducing capacity in biogas plants. *Microbial Ecology*. 58(2):221–230.

Watson-Craik, I.A. & Stams, A.J. 1995. Anaerobic digestion. *Antonie van Leeuwenhoek*. 67(1):1–2.

Weigold, P., El-Hadidi, M., Ruecker, A., Huson, D.H., Scholten, T., Jochmann, M., Kappler, A., & Behrens, S. 2016. A metagenomic-based survey of microbial (de)halogenation potential in a German forest soil. *Scientific Reports*. 6:1–13.

White, A.S., Godard, R.D., Belling, C., Kasza, V., & Beach, R.L. 2010. Beverages obtained from soda fountain machines in the U.S. contain microorganisms, including coliform bacteria.

International Journal of Food Microbiology. 137(1):61–66.

WHO. 2006. Guidelines for Drinking-water Quality. Geneva: Switzerland.

WHO. 2011. Guidelines for Drinking-water Quality. 4th ed. World Health Organization publications: Geneva.

WHO. 2014. Antimicrobial Resistance Global Report on Surveillance. World Health Organization. Geneva: Switzerland.

Wieczorek, A.S., Schmidt, O., Chatzinotas, A., von Bergen, M., Gorissen, A., & Kolb, S. 2019. Ecological functions of agricultural soil bacteria and microeukaryotes in chitin degradation: A case study. *Frontiers in Microbiology*. 10(JUN):1–13.

Wijesiri, B., Liu, A., Deilami, K., He, B., Hong, N., Yang, B., Zhao, X., Ayoko, G., & Goonetilleke, A. 2019. Nutrients and metals interactions between water and sediment phases: An urban river case study. *Environmental Pollution*. 251:354–362.

Willey, J.M., Sherwood, L.M., & Woolverton, C.J. 2011a. Prescott's Microbiology. 9th ed. McGraw-Hill Companies.

Willey, J.M., Sherwood, L.M., & Woolverton, C.J. 2011b. Prescott, Harley, and Klein's microbiology. 7th ed. McGraw-Hill: New York.

Woo, P.C.Y., Lau, S.K.P., Teng, J.L.L., Tse, H., & Yuen, K.-Y. 2008. Then and now: use of 16S rDNA gene sequencing for bacterial identification and discovery of novel bacteria in clinical microbiology laboratories. *Clinical Microbiology and Infection*. 14(10):908–934.

Wright, G.D. 2010. Antibiotic resistance in the environment: A link to the clinic? *Current Opinion in Microbiology*. 13(5):589–594.

Wrublack, S.C., Mercante, E., Boas, M.A.V., Prudente, V.H.R., & Silva, J.L.G. 2018. Variation of water quality along a river in agricultural watershed with support of geographic information systems and multivariate analysis. *Engenharia Agricola*. 38(1):74–81.

Wu, J. 2019. Linking landscape patterns to sources of water contamination: Implications for tracking fecal contaminants with geospatial and Bayesian approaches. *Science of the Total Environment*. 650:1149–1157.

Wu, J., Yunus, M., Islam, M.S., & Emch, M. 2016. Influence of climate extremes and land use on fecal contamination of shallow tubewells in Bangladesh. *Environmental Science and*

Technology. 50(5):2669–2676.

Xu, Y.-B., Hou, M.-Y., Li, Y.-F., Huang, L., Ruan, J.-J., Zheng, L., Qiao, Q.-X., & Du, Q.-P. 2017. Distribution of tetracycline resistance genes and AmpC β-lactamase genes in representative non-urban sewage plants and correlations with treatment processes and heavy metals. *Chemosphere*. 170(100):274–281.

Xue, F., Tang, J., Dong, Z., Shen, D., Liu, H., Zhang, X., & Holden, N.M. 2018. Tempo-spatial controls of total coliform and *E. coli* contamination in a subtropical hilly agricultural catchment. *Agricultural Water Management*. 200:10–18.

Yang, K., Yu, Z., Luo, Y., Yang, Y., Zhao, L., & Zhou, X. 2018. Spatial and temporal variations in the relationship between lake water surface temperatures and water quality - A case study of Dianchi Lake. *Science of The Total Environment*. 624:859–871.

Yang, Y., Gao, Y., Huang, X., Ni, P., Wu, Y., Deng, Y., & Zhan, A. 2019. Adaptive shifts of bacterioplankton communities in response to nitrogen enrichment in a highly polluted river. *Environmental Pollution*. 245:290–299.

Ye, Q., Wu, Q., Zhang, S., Zhang, J., Yang, G., Wang, H., Huang, J., Chen, M., Xue, L., & Wang, J. 2017. Antibiotic-resistant extended spectrum ß-lactamase- and plasmid-mediated AmpC-producing *Enterobacteriaceae* isolated from retail food products and the Pearl River in Guangzhou, China. *Frontiers in Microbiology*. 8:1–12.

Zhang, R., El-Mashad, H.M., Hartman, K., Wang, F., Liu, G., Choate, C., & Gamble, P. 2007. Characterization of food waste as feedstock for anaerobic digestion. *Bioresource Technology*. 98(4):929–935.

Zhang, S., Yang, G., Hou, S., & Wang, Y. 2010. Abundance and diversity of glacial bacteria on the tibetan plateau with environment. *Geomicrobiology Journal*. 27(8):649–655.

Zhang, X.-X., Zhang, T., & Fang, H.H.P. 2009. Antibiotic resistance genes in water environment. *Applied Microbiology and Biotechnology*. 82(3):397–414.

Zhou, Z.-C., Feng, W.-Q., Han, Y., Zheng, J., Chen, T., Wei, Y.-Y., Gillings, M., Zhu, Y.-G., & Chen, H. 2018. Prevalence and transmission of antibiotic resistance and microbiota between humans and water environments. *Environment International*. 121:1155–1161.

Zhu, G., Yuan, C., Di, G., Zhang, M., Ni, L., Cao, T., Fang, R., & Wu, G. 2018. Morphological and biomechanical response to eutrophication and hydrodynamic stresses. *Science of The Total*

Environment. 622–623:421–435.

APPENDIX A

Table A.1: List of bacterial cultivation medias with their related metabolic activity and selective processes

Growth media	Used for	Metabolic activity and selection process
m-Endo agar	Total coliforms	Various nutrients which promote the growth of coliforms. It contains lauryl sulphate and deoxycholate which inhibits the growth of other organisms The reaction of lactose positive colonies with fuchsin-sulfite releases fuchsin which induces the red colour of the colonies. The metallic green sheen of the colonies develops due to the formation of aldehydes during lactose fermentation (Merck, 2012).
m-Fc	Faecal coliforms	Faecal coliforms produce blue colonies on m-FC agar. m-Fc agar contains bile salts which inhibit the growth of Gram-positive bacteria. Peptone and yeast serve as nutrients for the growth of faecal coliforms. The blue colour of the colonies is induced by lactose fermentation at elevated temperatures (Merck, 2012)
Membrane Lactose Glucuronide (MLG) agar	Distinguish between total coliforms and Escherichia coli	Membrane Lactose Glucuronide agar contains lauryl sulphate which inhibits the growth of Gram-positive organisms. The identification of coliforms and E. coli on MLG agar is based on two principles: 1) lactose fermentation induces the yellow colour of the colonies when acid is produced; 2) the enzyme glucuronidase cleaves the chromogenic substrate 5-bromo-4-chloro-3-indolyl-β-D-glucuronide (BCIG) and produces a blue chromophore which builds up in the bacterial cells. Coliforms ferment lactose so colonies will appear yellow on MLG agar, whereas E. coli ferments lactose and possesses the glucuronidase enzyme,

		therefore, colonies will appear green (Oxoid Limited, 2012)
Reasoner - 2A agar	Heterotrophic Plate Counts	Pigmented colonies can be useful indicators for changes in the microbiological quality of drinking water (Carter *et al.*, 2000)
KF strep	Faecal Streptococci	Peptone with yeast extract provides nitrogen, carbon, sulphur, amino acids, vitamins and trace ingredients to the faecal Streptococci. Lactose and maltose are the fermentable carbohydrates and therefore serve as energy sources. Sodium azide is a selective agent, which inhibits the growth of Gram-negative bacteria. 2,3,5-Triphenyl Tetrazolium Chloride (TTC) is reduced to insoluble formazan by actively metabolizing cells, resulting in the formation of pink or red colonies. Bacteria resistant to azide, utilize lactose and / or maltose. The acidity so produced changes the colour of the indicator dyes to yellow. Bacterial cells reduce TTC to insoluble formazan, resulting in the formation of pink to red colonies (HiMedia, 2019a)
Tryptose sulphite cycloserine (TSC) Agar	Selective for sulphite-reducing indicators Clostridium sp.	Tryptose, yeast extract and soya peptone provide the essential vitamins and nutrients for SRC species to develop. Furthermore, sulphite-reducing indicators such as ferric ammonium citrate and sodium metabisulphite result in distinct black SRC colonies (Merck, 2019)
Reinforced Clostridia agar	Cultivation and enumeration of clostridia and other anaerobes	Reinforced Clostridial Agar contains casein enzymic hydrolysate and beef extract as sources of carbon, nitrogen, vitamins and minerals. Yeast extract supplies B-complex vitamins which stimulate bacterial growth. Dextrose is the carbohydrate source. Sodium chloride maintains the osmotic balance. In low concentrations, soluble starch detoxifies metabolic byproducts. Cysteine hydrochloride is the reducing

	agent. Sodium acetate acts as a buffer (HiMedia, 2019b)

Table A.2: The generated work methods protocol for the physico-chemical and microbiological analysis

	Media and equipment	**Quantity**	**Preparation steps**	**Results**
Clostridium	1) Clostridium perfringens agar base 2) Fung tubes 3) TSC supplement containing D-cycloserine	1) 23 g Clostridium perfringens agar base premix 2) 500 mL dH2O 3) ± 24 fung tubes	1) Dispense 7 mL of Clostridium perfringens agar base 2) Autoclave	1) When liquid media is at ~50°C; add 500 mL of sample into fung tube 2) When liquid media is at ~50°C; add 32 µL of the TSC supplement containing D-cycloserine 3) Insert autoclaved inserter into fung tube and seal with the cap 4) Incubate @ 44°C for 6 h 5) Count black colonies (≤ 300)
Membrane	1) KF-Streptococcus 2) TTC Supplement 3) Agar plates 4) 0.45 µm membrane filters	1) 76 g KFS premix 2) 1 L dH2O 3) 1 mL to every 100 mL agar 4) 24 Membrane filters	1) Add components to dH2O and bring final value to 1 L 2) Mix thoroughly 3) Autoclave 4) Add supplement when agar is 60°C 5) Pour agar into Petri dishes	1) Filter 100 mL of sample through membrane with Merc filter machine (Triplicate) 2) Place filter on KFS Agar plate 3) Incubate @ 35°C for 48h 4) Count light pink or flat dark red colonies

	1) m-FC Agar 2) Agar plates 3) 0.45 µm membrane filters	1) 50 g mFC premix 2) 1L dH2O	1) Add components to dH2O and bring final value to 1 L 2) Mix thoroughly 3) Autoclave 4) Pour agar into Petri dishes	1) Filter 100 mL of sample through membrane with Merc filter machine (Triplicate) 2) Place filter on mFC Agar plate 3) Incubate @ 44.5°C for 24h 4) Count blue colonies
	1. MLG Agar 2. Agar plates 3. 0.45 µm membrane filters	1) 88 g MLG premix 2) 1 L dH2O	1) Add components to dH2O and bring final value to 1 L 2) Mix thoroughly 3) Autoclave 4) Pour agar into Petri dishes	1) Filter 100 mL of sample through membrane with Merc filter machine (Triplicate) 2) Place filter on MLG Agar plate 3) Incubate @ 37°C for 24 h 4) Count green colonies (*E. coli*)
HPC	1) McCartney bottles 2) dH2O	1) **1** L dH2O 2) McCartney bottles	1) Dispense 9 mL(dH2O) in McCartney bottles samples 2) Mix thoroughly 3) Autoclave	1) Inoculate McCartney broth bottles with samples 2) Incubate @ 35°C for 24 h
			1) Dispense 9 mL (dH2O) in McCartney bottles	1) Make dilution series 10^{-10} for each sample (8x) by diluting with 1 mL 2) Incubate @ 35°C for 24h

	1. R2A 2. Agar plates 3. Bunsen burner 4. Streaker 5. McCartney bottles	1. 18 g R2A premix 2. 1L dH2O	1) Add components to dH2O and bring final value to 1 L 2) Mix thoroughly 3) Autoclave 4) Pour agar into Petri dishes	1) Take dilution series and pipet 100 µL to R2A plates 2) Make a spread plate 3) Incubate @ room Temp for 7d $Coliformcolonies/100mL = \frac{coliform\ colonies\ counted}{mL\ water\ filtered}$
	Test	**Media and reagents**	**Quantity and preparation**	**Result**
Hach	Phosphate (PO4) 8048	1) Sample 2) PO4 reagent packet	1) 10 mL sample in sample cell 2) 10 mL dH2O in another sample cell 3) Add PO4 packet contents in sample cell 4) Wait for reaction 2 minutes	1) Insert programme no. 490 2) Insert dH2O sample cell in the machine to blank 3) Insert Sample cell to measure PO4 levels 4) Do in triplicate
	Nitrite (NO2) 8153	1) Sample 2) NO2 reagent packet	1) 10 mL sample in sample cell 2) 10 mL dH2O in another sample cell 3) Add NO2 packet contents in sample cell	1) Insert programme no. 373 2) Insert dH2O sample cell in the machine to blank 3) Insert Sample cell to measure NO2 levels 4) Do in triplicate

			4) Wait for reaction 10 minutes	
	Nitrate (NO3) 8039	1) Sample 2) NO3 reagent packet	1) 10 mL sample in sample cell 2) 10 mL dH2O in sample cell 3) Add NO3 packet contents in sample cell and shake for one minute 4) Wait for reaction 5 minutes	1) Insert programme no. 355 2) Insert dH2O sample cell in the machine to blank 3) Insert Sample cell to measure NO3 levels 4) Do in triplicate
	Sulphide (SO3) 8131	1) Sample 2) Sulphite solution 1 3) Sulphite solution 2	1) 10 mL sample in sample cell 2) 10 mL dH2O in sample cell 3) Add 0.5 mL of sulphide 1 in both sample cells 4) Add 0.5 mL of sulphide 2 in both sample cells 5) Wait for reaction 5 minutes	1) Insert programme no. 690 2) Insert dH2O sample cell in the machine to blank 3) Insert Sample cell to measure SO3 levels 4) Do in triplicate

	Sulphate (SO4) 8051	1) Sample 2) SO4 reagent packet	1) 10 mL sample in sample cell 2) 10 mL dH2O in sample cell 3) Add PO4 packet contents in sample cell 4) Wait for reaction 5 minutes	1) Insert programme no. 480 2) Insert dH2O sample cell in the machine to blank 3) Insert Sample cell to measure SO4 levels 4) Do in triplicate
	COD 8000	3) Sample 4) COD vials	1) 2 mL sample in sample vile 2) 2 mL dH2O in sample vile (Blank) 3) Tilt vile to mix 4) Heat for 2h	1) Insert programme no. 430 2) Invert hot vile 3) Let cool to room Temp 4) Insert blank vile to blank 5) Insert sample vile to measure COD levels 6) Do in triplicate

APPENDIX B

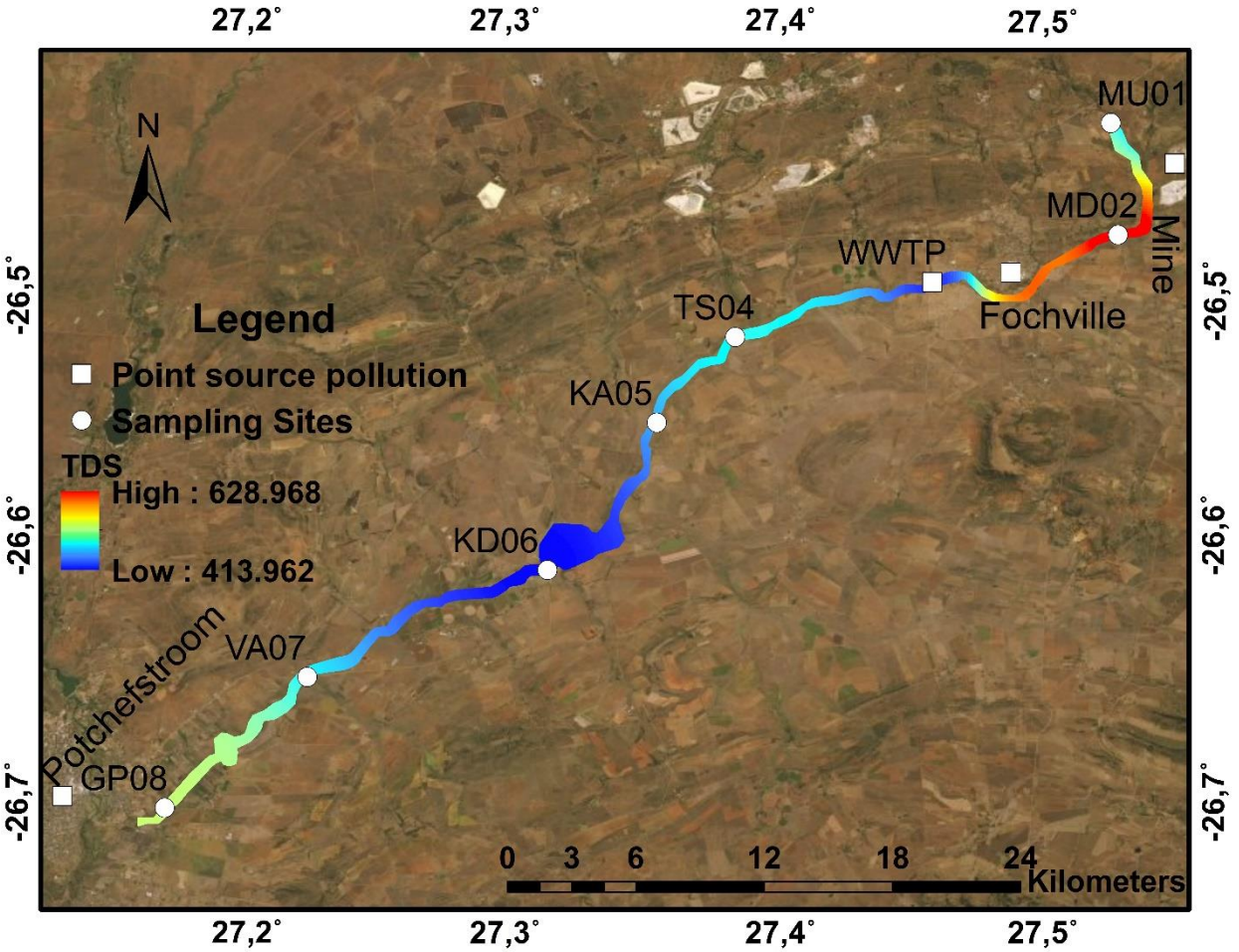

Figure B.1: A geospatial representation of the Loopspruit River with Total Dissolved Solids (TDS).

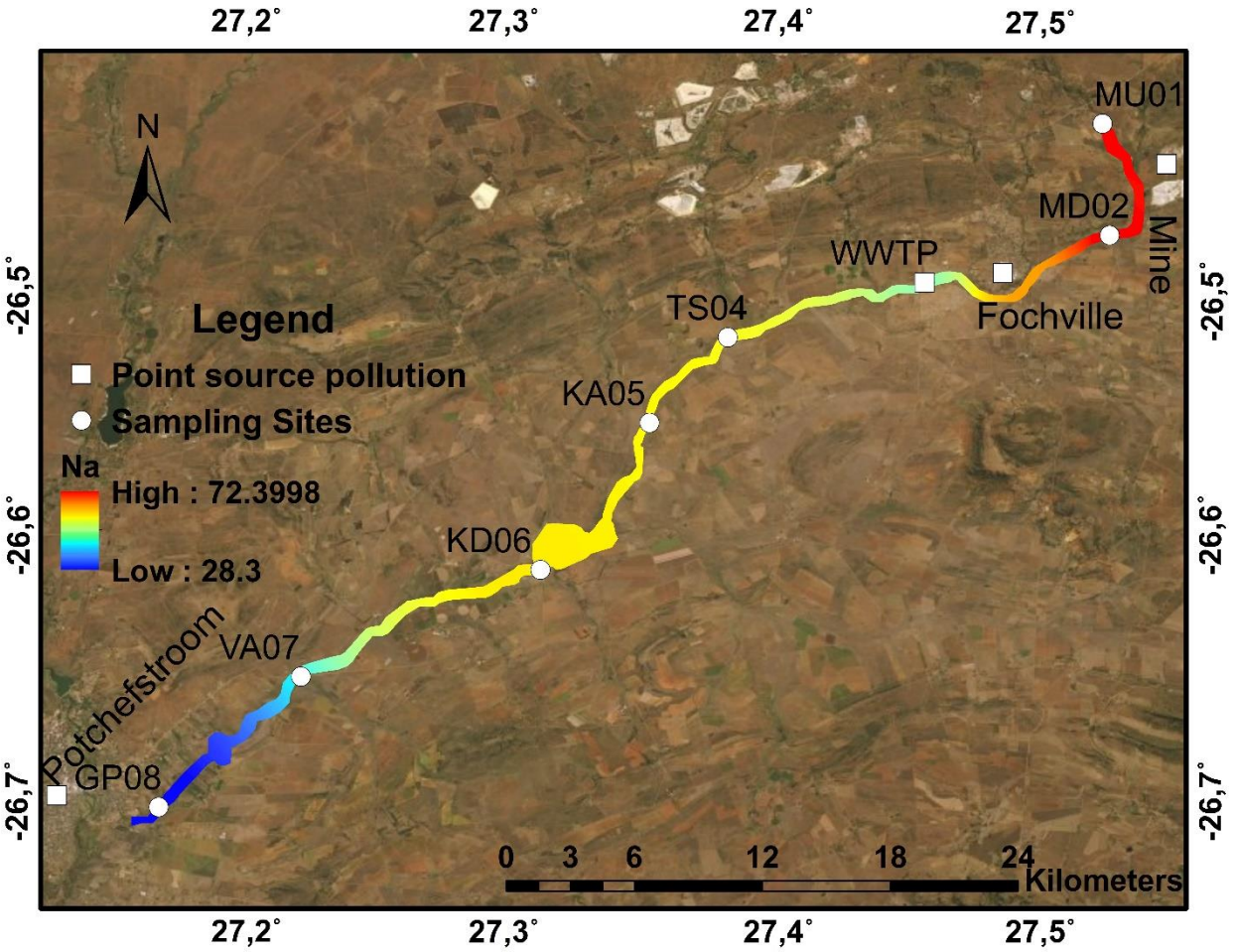

Figure B.2: A geospatial representation of the Loopspruit River with Sodium (Na).

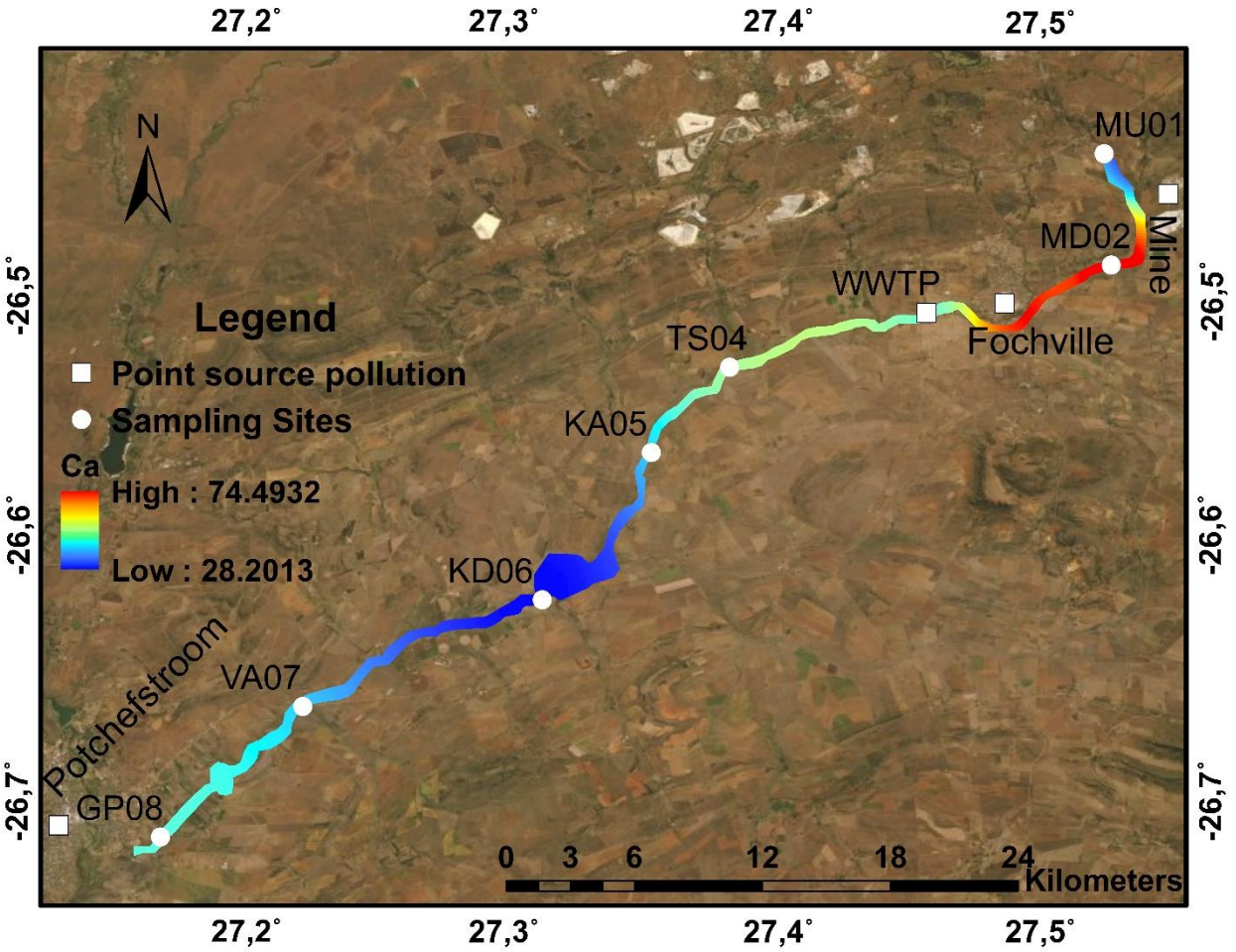

Figure B.3: A geospatial representation of the Loopspruit River with Calcium (Ca)

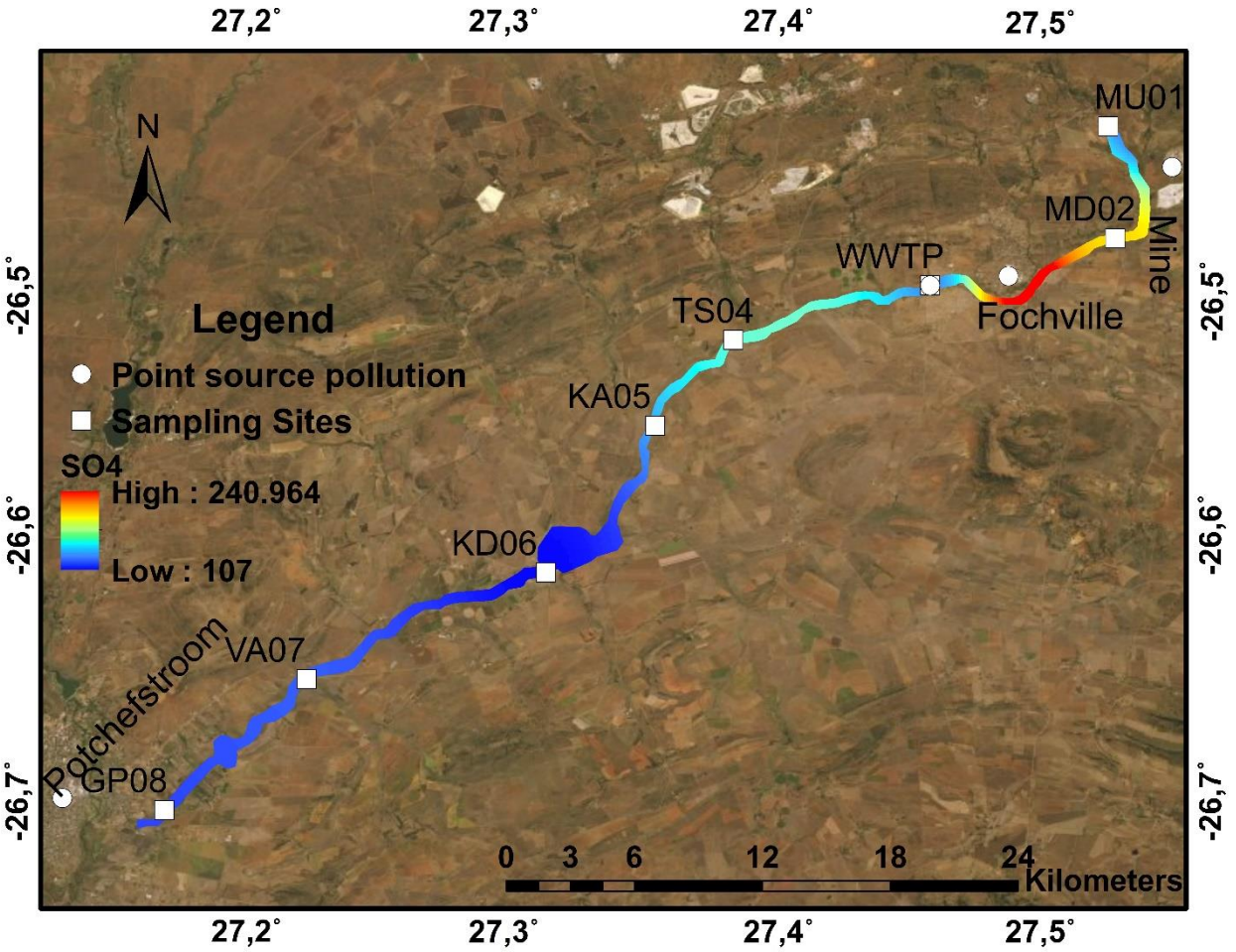

Figure B.4: A geospatial representation of the Loopspruit River with Sulphates (SO_4)

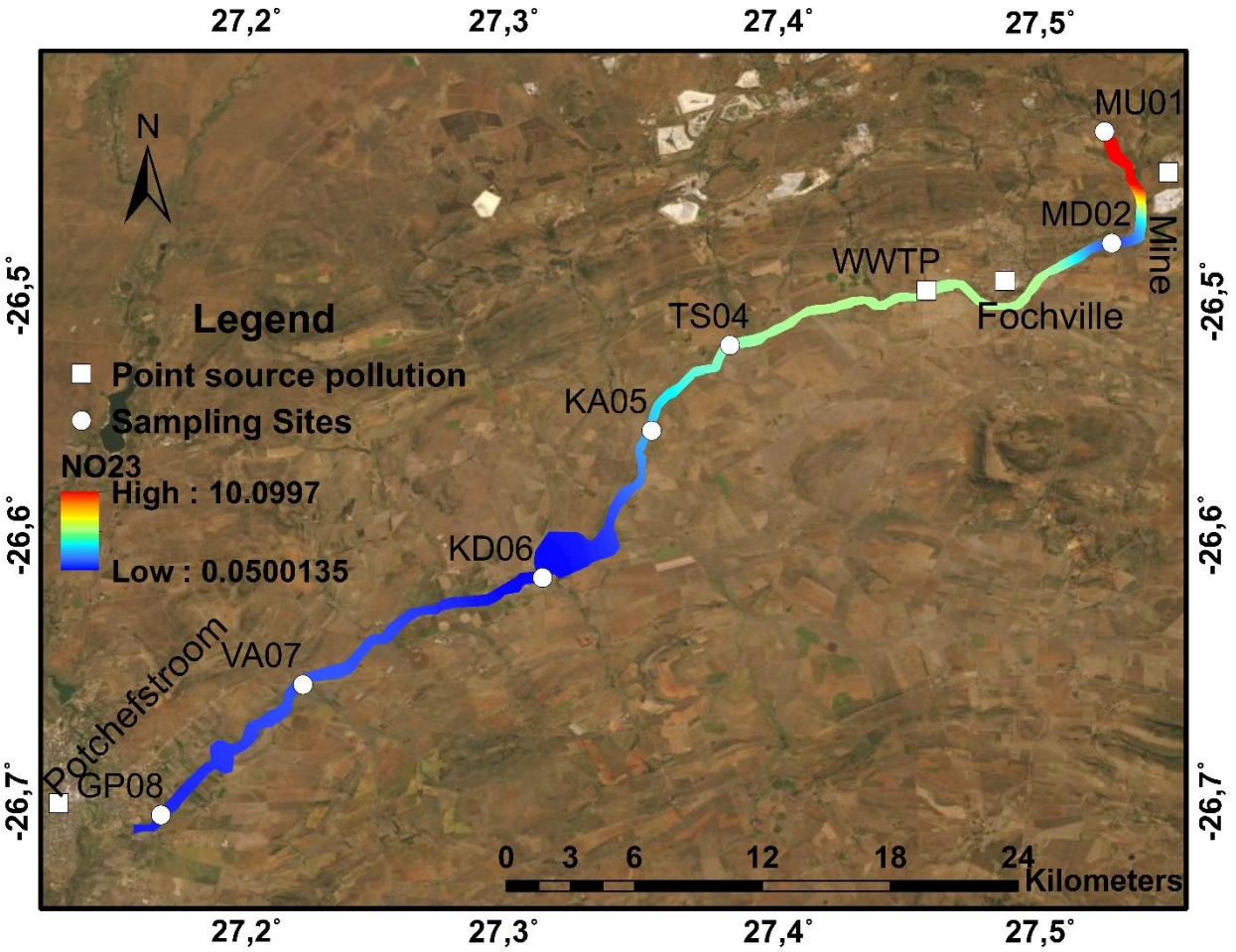

Figure B.5: A geospatial representation of the Loopspruit River with Nitrites (NO_2) and Nitrates (NO_3) as nitrogen (N)

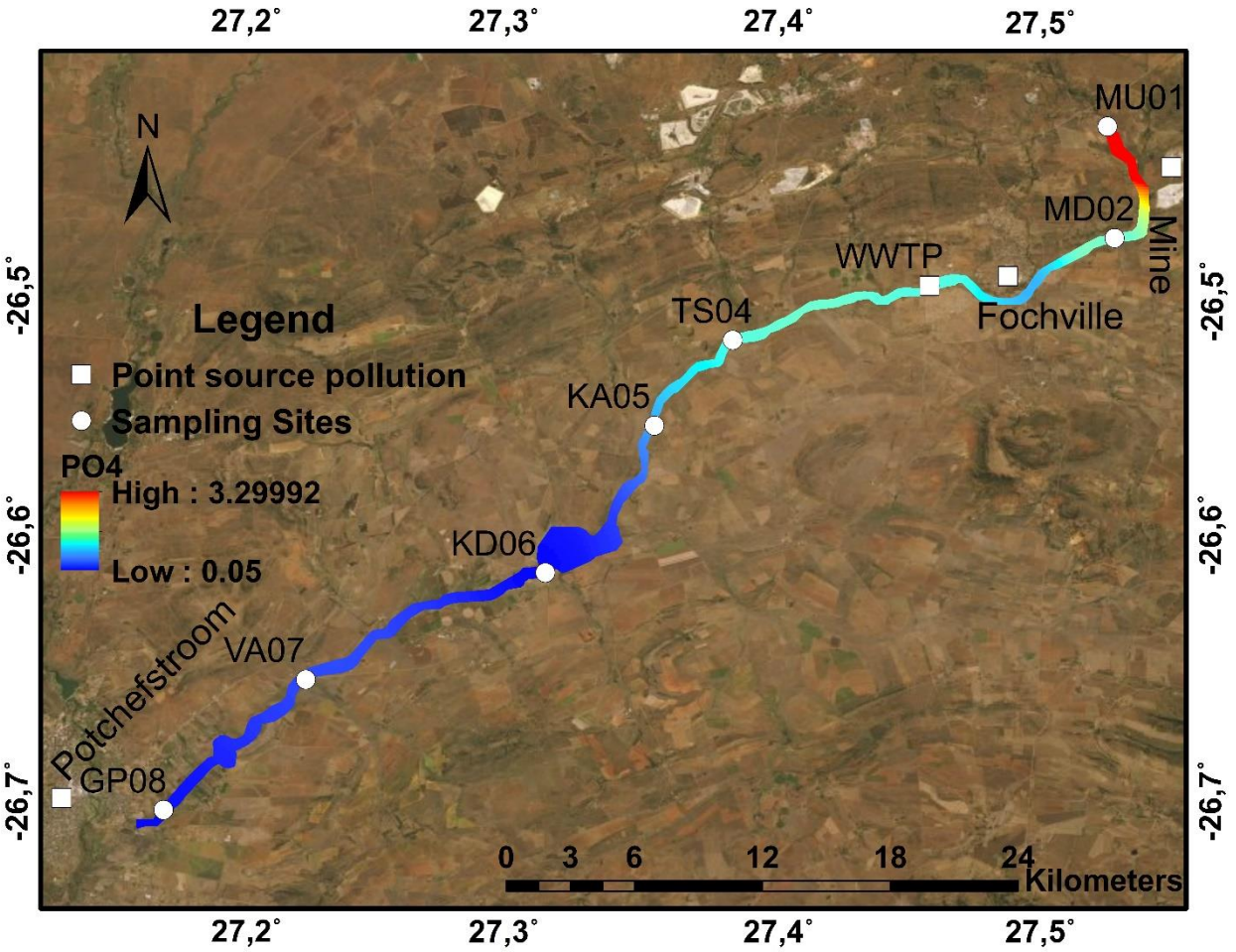

Figure B.6: A geospatial representation of the Loopspruit River with Phosphates (PO_4)

APPENDIX C

Table C.3: The antibiotic resistance profiling during the wet season.

Sample	Trimethoprim (W)	Ciprofloxacin (CIP)	Neomycin (N)	Streptomycin (S)	Chloramphenicol ©	Amoxicillin (AML)	Oxy-Tetracycline (OT)	Penicillin G (P)	Vancomycin (VA)
1.4.A	R	I	R	I	I	R	S		
1.5.A	R	S	S	S	S	S	S	I	S
1.6.A	R	S	R	S	S	S	S		
2.5.A	R	S	S	S	S	R	S		
2.5.B	S	S	S	S	S	S	S	I	R
3.4.A	S	S	S	S	S	S	S		
3.5.A	R	I	I	S	S	R	S		
3.6.A	S	S	S	S	S	R	S		
4.2.A	R	S	S	S	S	S	S		
4.3.B	R	S	I	S	S	S	S		
5.6.A	S	S	S	S	S	I	S	I	R
5.6.B	S	S	S	S	S	S	S	I	R
5.7.A	R	I	S	S	S	R	S		
6.5.A	S	S	S	S	S	S	S	S	S
6.5.B	S	R	S	S	S	S	S		
7.2.A	R	I	I	S	S	I	S	I	S
7.2.B	S	S	I	S	S	S	S		
7.2.C	R	S	S	S	S	I	S		
7.5.A	R	I	S	S	S	R	S		
7.5.B	S	S	S	S	S	R	S	R	R
8.2.A	S	S	S	S	S	R	S		
8.2.B	S	S	S	S	S	S	S		

R= Resistant; S= Susceptible; I= Intermediate

Table C.4: The antibiotic profiling during the dry season

Sites	Ciprofloxacin (CIP)	Neomycin (N)	Sulphamethoxazole (RL)	Trimethoprim (W)	Colistin (CT)	Chloramphenicol ©	Amoxicillin (AML)	Oxy-Tetracycline (OT)	Streptomycin (S)	Ampicillin (AMP)	Penicillin G (P)	Vancomycin (VA)
1.2.A	S	R	S	R	R	S	S	S	R	R		
1.2.B	S	R	R	R	R	I	R	R	R	R		
1.2.C	S	I	R	R	R	R	R	R	R	R		
1.2.D	S	S	S	S	S	S	S	S	S	R		
1.2.E	R	S	R	R	S	S	R	S	S	R		
1.2.F	S	S	R	R	I	R	R	R	S	R		
1.2.H	S	S	S	S	R	R	R	I	S	R		
1.2.K	S	R	R	R	R	S	R	S	R	R		
1.3.A	S	R	R	R	R	R	R	R	R	R		
1.3.B	S	R	R	R	R	S	R	S	S	S		
2.2.C	S	R	R	R	R	R	R	S	R	R		
2.2.D	S	S	R	R	I	R	R	S	S	R		
2.2.E	S	S	S	R	S	R	R	S	S	R		
2.2.F	S	R	S	S	R	R	R	R	R	R		
2.3.A	S	S	R	R	I	R	R	S	S	R		
2.3.C	S	R	R	R	R	I	R	S	R	R		
2.4.A	R	S	R	S	R	S	S	S	S	R		
3.3.A	S	S	R	R	R	R	R	I	R	R		
3.3.B	S	S	R	S	S	S	R	S	S	R		
3.4.A	S	S	R	S	S	S	R	S	S	R		
4.2.A	S	R	I	R	R	I	R	S	R	R		
4.2.B	S	R	R	R	I	S	S	S	I	R		
4.3.C	S	S	S	R	I	R	S	S	S	R		
5.2.A	S	I	R	R	R	R	R	R	R	R		
5.3.B	S	R	I	R	I	S	S	S	I	R		
6.2.C	S	R	R	R	R	S	R	S	I	R		
6.2.D	S	S	I	I	S	R	R	S	S	R		
6.2.E	S	S	S	S	R	S	S	S	S	S	S	R
6.2.I	S	R	5	R	R	S	S	S	I	R		
6.3.C	S	S	S	S	S	S	R	S	S	R		
7.2.A	S	S	R	R	S	S	R	S	S	R		
7.2.C	S	S	S	S	S	S	S	S	S	R		
7.3.C	S	I	R	R	S	S	R	S	S	R		
7.3.E	S	S	R	R	R	S	R	S	S	R		
8.2.A	S	R	R	R	R	I	R	S	I	R		
8.2.E	S	R	R	R	R	R	S	R	R	R		
8.3.A	S	I	R	R	I	S	S	S	S	R		
8.3.C	S	S	S	S	S	S	R	S	I	S		

8.3.D	S	R	S	S	S	R	R	R	R	R

R= Resistant; S= Susceptible; I= Intermediate

APPENDIX D

Appendix D

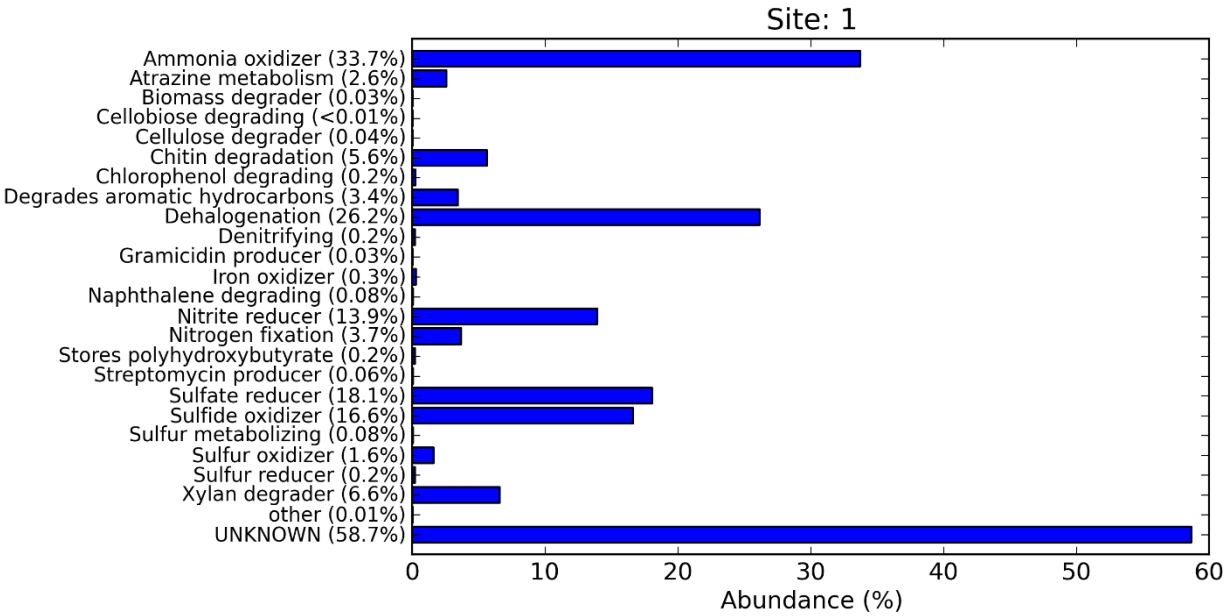

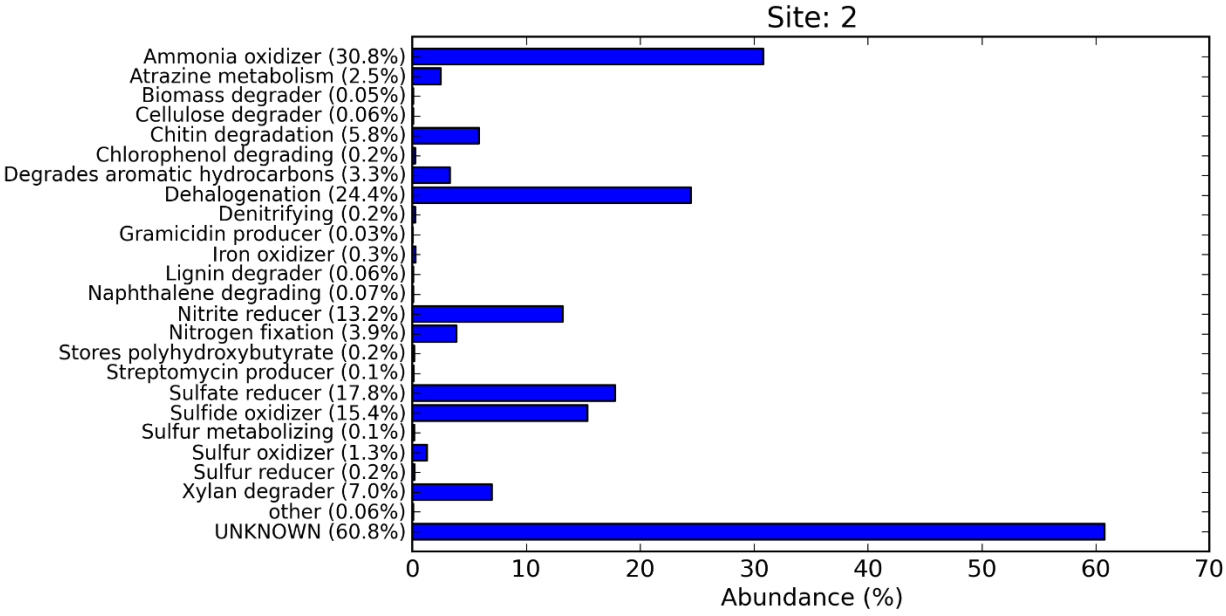

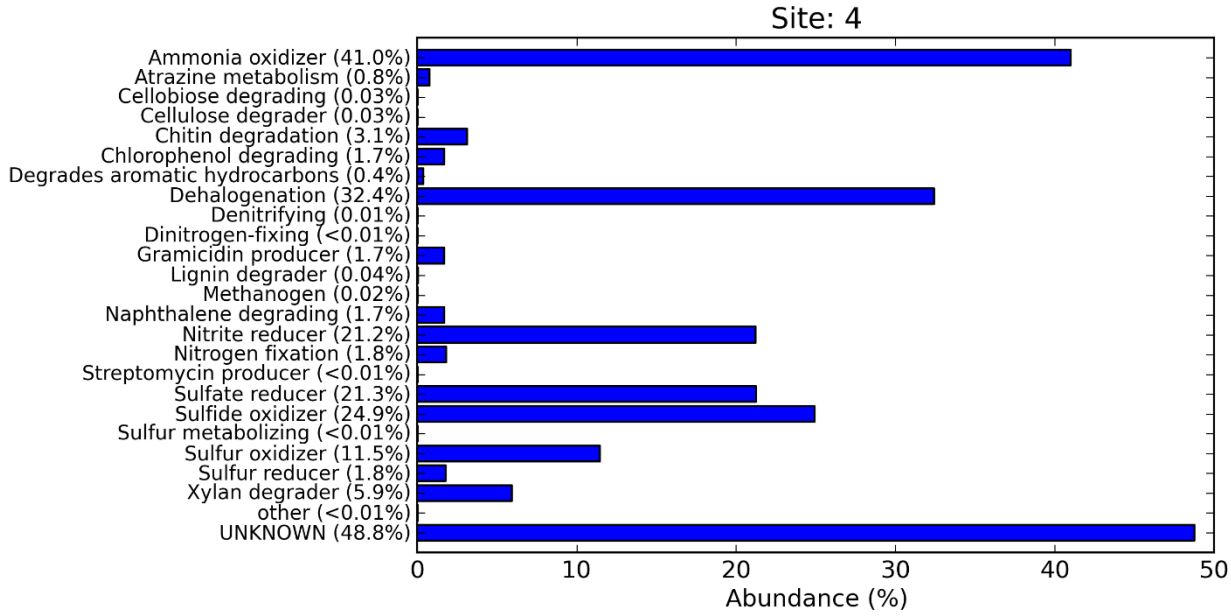
Site: 4
Ammonia oxidizer (41.0%)
Atrazine metabolism (0.8%)
Cellobiose degrading (0.03%)
Cellulose degrader (0.03%)
Chitin degradation (3.1%)
Chlorophenol degrading (1.7%)
Degrades aromatic hydrocarbons (0.4%)
Dehalogenation (32.4%)
Denitrifying (0.01%)
Dinitrogen-fixing (<0.01%)
Gramicidin producer (1.7%)
Lignin degrader (0.04%)
Methanogen (0.02%)
Naphthalene degrading (1.7%)
Nitrite reducer (21.2%)
Nitrogen fixation (1.8%)
Streptomycin producer (<0.01%)
Sulfate reducer (21.3%)
Sulfide oxidizer (24.9%)
Sulfur metabolizing (<0.01%)
Sulfur oxidizer (11.5%)
Sulfur reducer (1.8%)
Xylan degrader (5.9%)
other (<0.01%)
UNKNOWN (48.8%)
0
10
20
30
40
50
Abundance (%)

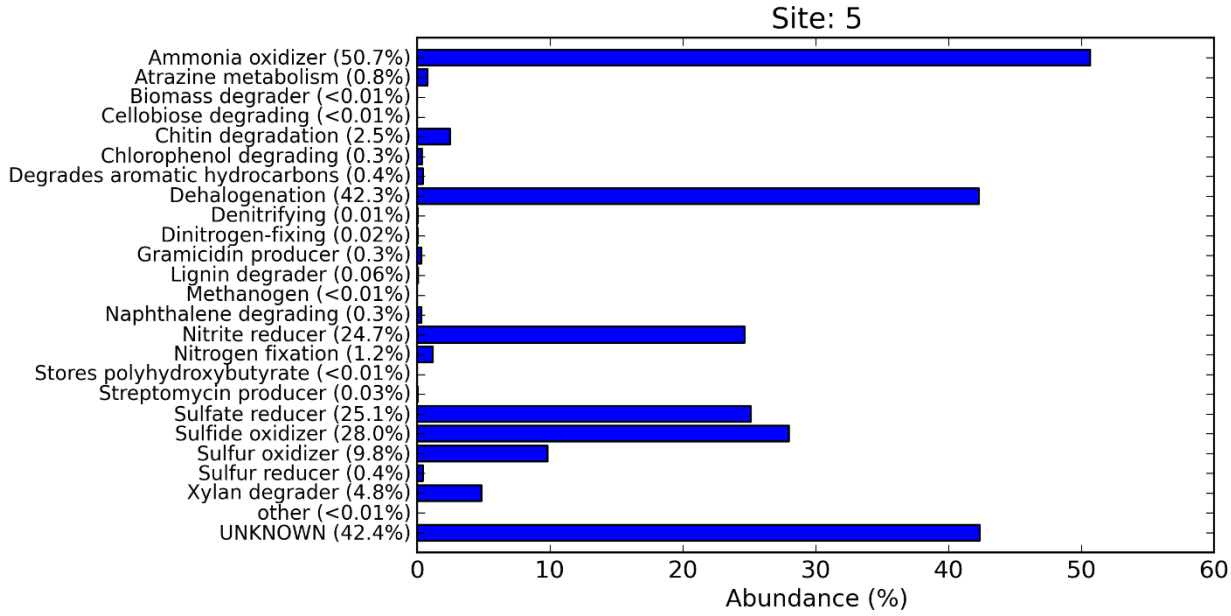
Site: 5
Ammonia oxidizer (50.7%)
Atrazine metabolism (0.8%)
Biomass degrader (<0.01%)
Cellobiose degrading (<0.01%)
Chitin degradation (2.5%)
Chlorophenol degrading (0.3%)
Degrades aromatic hydrocarbons (0.4%)
Dehalogenation (42.3%)
Denitrifying (0.01%)
Dinitrogen-fixing (0.02%)
Gramicidin producer (0.3%)
Lignin degrader (0.06%)
Methanogen (<0.01%)
Naphthalene degrading (0.3%)
Nitrite reducer (24.7%)
Nitrogen fixation (1.2%)
Stores polyhydroxybutyrate (<0.01%)
Streptomycin producer (0.03%)
Sulfate reducer (25.1%)
Sulfide oxidizer (28.0%)
Sulfur oxidizer (9.8%)
Sulfur reducer (0.4%)
Xylan degrader (4.8%)
other (<0.01%)
UNKNOWN (42.4%)
0
10
20
30
40
50
60
Abundance (%)

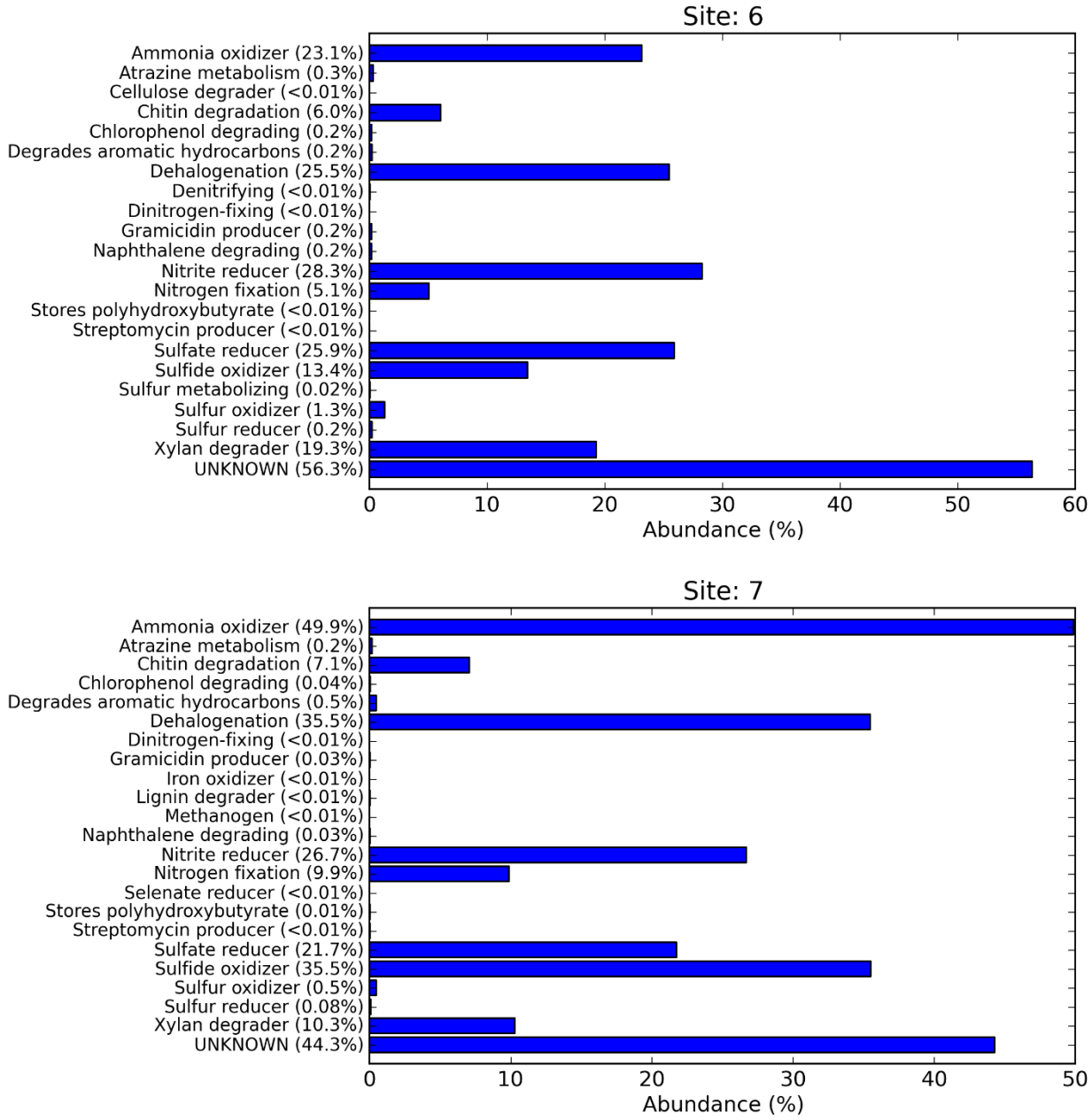

Figure D.7: The taxonomic to phenotype mapping of OTUs at Site 1 (MU01), Site 2 (MD02), Site 4 (TS04), Site 5 (KA05), Site 6 (KD06) and Site 7 (VA07) that shows the predicted metabolic activities

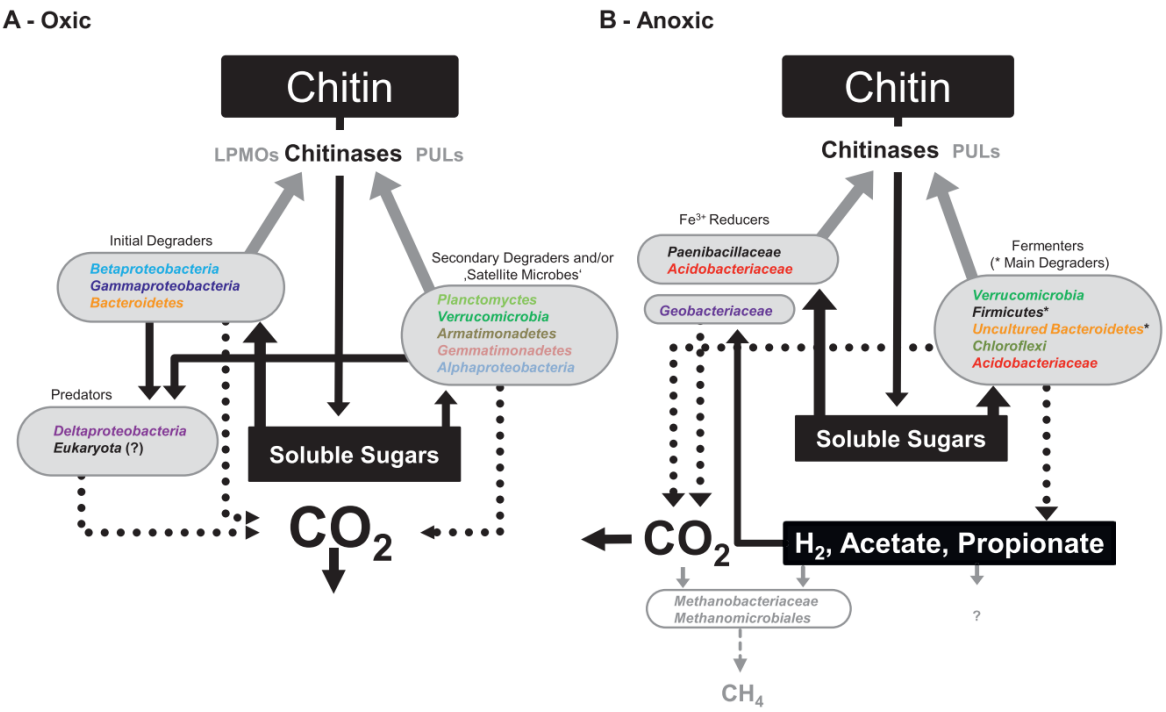

Figure D.8: A conceptual model of the soil microbiome that carries out chitin degradation during its metabolic processes (Wieczorek *et al.*, 2019)